

Hydrate Phase Transition-Risk, Energy Potential and CO₂ Storage Possibilities

Solomon Aforkoghene Aromada

Thesis for the degree of Philosophiae Doctor (PhD)
University of Bergen, Norway
2022

UNIVERSITY OF BERGEN



Hydrate Phase Transition-Risk, Energy Potential and CO₂ Storage Possibilities

Solomon Aforkoghene Aromada



Thesis for the degree of Philosophiae Doctor (PhD)
at the University of Bergen

Date of defense: 11.02.2022

© Copyright Solomon Aforkoghene Aromada

The material in this publication is covered by the provisions of the Copyright Act.

Year: 2022

Title: Hydrate Phase Transition-Risk, Energy Potential and CO2 Storage Possibilities

Name: Solomon Aforkoghene Aromada

Print: Skipnes Kommunikasjon / University of Bergen

DEDICATION

This work is dedicated to my lovely wife, Blessing Ijeoma Aromada; my amazing sons, Favour Oghale Aromada, Victor Orezioghene Aromada, Emmanuel Uvieoghenena Aromada; and to my wonderful mother, Madam Josephine Hossana Edoghor who made it possible for me to start my university education and ensured that I do not lack finance during my bachelor days.

ACKNOWLEDGEMENT

Several individuals contributed in one way or the other in the studies documented in this dissertation. I am sincerely grateful to everyone for every effort and time invested into this project.

I would like to specially express my heartfelt appreciation to my first supervisor, Professor Bjørn Kvamme. This PhD study opportunity became possible because he believed in me. His support and contribution towards the success of my studies is invaluable. Thank you, Professor Bjørn, Kvamme for your mentorship. I am sincerely grateful for his time, inspiration, guidance and feedbacks. Even after his resignation, he was still fully available to help, this is not common. I learnt so much from him.

I am also grateful to Professor Tatiana Kuznetsova for stepping in to become my only supervisor after Professor Bjørn Kvamme resigned. I am thankful for all her contribution and support.

I want to recognise the time and efforts of everyone that we collaborated with and everyone that we worked together as a team during this PhD project. Particularly, Petter Berge Gjerstad and Mojdeh Zarifi at the University of Bergen, Navid Saeidi at the University of California. I would also like to thank Hanne Israelsen for her support during my studies.

My profound appreciation also goes to my wife, Blessing Ijeoma Aromada and our sons, Favour Oghale Aromada, Victor Orezioghene Aromada and Emmanuel Uvieoghena Aromada especially for their understanding, invaluable sacrifice, encouragement and support. I am grateful to my mother, Madam Josephine Hossana Edoghor Edeh who did everything within her power to ensure that my dream of being educated is realised. I want to thank Mr. Stephen Neba-Fuh, Mr. Otobong Ezekiel Ubengama and Enobong Ezekiel Ubengama, Mr. Samuel Egbona and his family, Mr. Akeno Oriomah and Mrs. Oluyemi Oriomah, Mr. Collins Ajiri Enuwe, Mrs. Keziah Chiedozie, Timothy Aideloje, Pastor Placid Ugochukwu Eboh, Gabriel Taiwo Ohiare, Olubusayo Ohiare, John Augustine and family, Pastor Gabriel Epah, Jonathan Adra for their encouragement and support.

I want to thank my brothers Lucky Aromada, Robinson Aromada, Emmanuel Okemena Barnabas, Philemon Aromada, Morgan Aromada, Ofegor Aromada; and my sisters, Zino Mada and Gladys Imaboyo for their encouragement.

I am very grateful for the love and great support I received from the English Cell Group of Kristent Felleskap in Bergen. I am grateful to DMC Norway AS and Quality Renhold AS for the opportunity given to me to work during my studies.

Abstract

Natural gas hydrate (NGH) can cause crucial flow assurance problems to the oil and gas industry. It is being considered as a potential vast energy resource for the world in the future. It could also potentially provide a long-term offshore storage possibility for carbon dioxide. Therefore, the risk of hydrate formation during processing and pipeline transport of natural gas and CO₂, thermodynamics and kinetics of hydrate formation, and simultaneous CH₄ production from in-situ hydrate and CO₂ long-term offshore storage in form of CO₂ hydrate are important research concerns. The main scientific method used in this project is classical thermodynamics based on thermodynamic properties calculated using methods in Quantum Mechanics and Classical Mechanics. Classical thermodynamics was used together with residual thermodynamics description for every phase; this includes the hydrate phase, to analyse different routes to hydrate formation between hydrate formers (or guest molecules) and water.

NGHs are formed from water and natural gas at high pressures and low temperatures conditions under the constraints of mass and heat transport. The problem is that natural gas is usually produced together with water and operations are usually at elevated pressures and low temperatures. Current industrial approach for evaluating the risk of hydrate formation is based on liquid water condensing out of the bulk gas at dewpoint and at a specific pressure-temperature (P-T) condition. In this method, the maximum allowable water content will be kept below the projected dew-point mole-fractions during transport, considering the operational P-T conditions. However, a previous study in our research group suggested that solid surface, particularly rust (Hematite) is another precursor to hydrate formation; rust provides another route for liquid water to drop out through the mechanism of adsorption. And pipelines are generally rusty before they are mounted in place for operations.

The two approaches have been applied to study the risk of water dropping out from natural gas from different real gas fields. The approach of adsorption of water onto Hematite (rusty surfaces) completely dominates. The dew-point method over-estimates the safe limit (maximum mole-fraction) of water that should be permitted to flow with bulk gas about 18 – 20 times greater than when the effect of hematite is considered,

depending on the specific gas composition. That suggests that hydrate may still form when we base our hydrate risk analysis on dew-point technique. The presence of higher hydrocarbon (C_{2+}) hydrate formers causes a decrease in allowable water content with increasing concentration of ethane, propane and isobutane for the temperature range of 273 – 280 K. As their concentrations increase in the bulk gas, these C_{2+} act to draw down the water tolerance of the gas mixture to a point where they completely dominate or dictate the trends.

For the inorganic components, CO_2 has little or no significant impact on the allowable upper-limit of water when its concentration increases. While the presence of H_2S causes a consideration reduction in water tolerance of the system as its concentration in the mixture increases. The presence of 1 mol% of H_2S in the bulk gas may cause about 1 % reduction in water tolerance. The reduction in maximum content of water could be up to about 2 – 3 % and up to about 4 – 5 % if the concentration increases to 5 mol% and 10 mol% respectively.

It is not appropriate to interpret hydrate stability entirely based on equilibrium P–T curves as often done in literature. The hydrate stability curve of CO_2 hydrate has lower pressures (thus more stable) compared to that of CH_4 hydrate but only to a certain temperature. That is the quadruple-point where phase-split occurs causing the pressures of CO_2 hydrate going above that of CH_4 hydrate due to the increase in density caused by the CO_2 liquid phase. A free energy analysis revealed that CO_2 hydrate has lower free energy across the entire temperature range, thus more stable at all the temperatures. Therefore, hydrate stability should rather be based on free energy analysis since in real situations hydrate cannot reach equilibrium. Consequently, the most stable hydrate is the hydrate with the minimum free energy. The hydrate with the least or most negative free energy will first form under constraints of mass and heat transport, then followed by the subsequent most stable hydrate. Among the hydrocarbon guest molecules studied, the most stable hydrate is hydrate of isobutane, followed by that of propane, and then by ethane.

Induction times are sometimes mistaken as hydrate nucleation times, which is why some works report nucleation times of hours. Hydrate formation is a nano-scale process,

and the hydrate nucleation times computed for both heterogeneous and homogeneous hydrate formation in this project are in nano-seconds. The long times experienced before hydrates are detected are caused by mass transport limitations due to the initial thin hydrate film formed at the interface between water and the hydrate former interface. Another misunderstanding about hydrate nucleation is that only one uniform-phase hydrate is formed from either a single guest or a multicomponent mixtures of hydrate formers. Based on the combined first and second laws of thermodynamics, nucleation will commence with the most stable hydrates, under the constraints of heat and mass transport. Nucleation can happen via different routes: hydrate formation will originate at the interface between the guest molecule phase and water. A range of hydrates with different compositions of the original hydrate former(s), different densities and different free energies will form from aqueous solution (dissolve hydrate formers). Theoretically, hydrate can also nucleate from water dissolved in the guest molecules phase. Such hydrate cannot be stable because of the little mass of water that will dissolved in the guest molecule phase as well as limitation of heat transport, especially in the case of hydrocarbon guests like methane which is a poor heat conductor.

The thermodynamics of simultaneous natural gas production from in-situ CH₄ hydrate and CO₂ long-term offshore storage was studied. Two processes were studied: mixing of nitrogen with the CO₂ and injecting the mixture into the hydrate reservoir and the implication of the enthalpies of hydrate phase transitions. The study indicated that the proportion of CO₂ needed in the CO₂/N₂ mixture is only about 5 – 12 % without H₂S in the gas stream. While it is about 4 – 5 % and 2 – 3 % with the presence of 0.5 % and 1 % of H₂S respectively. Virtually, direct solid-state CO₂-CH₄ swap will be extremely kinetically restricted, and it is not significant.

Enthalpy changes of hydrate phase transition in literature obtained from experiment, Clausius-Clapeyron and Clapeyron models are limited and often lack some vital information needed for proper understanding and interpretation. Information on thermodynamic properties such as pressure, temperature (or both), hydrate composition, and hydration number are often missing. The equation of state utilised is

also not stated in certain literature. Several experimental data also lack any measured filling fractions, and frequently, they apply a constant value which suggests that the values may be merely guessed. In addition, older data based on Clapeyron equation lack appropriate volume corrections. The calculations of both Clausius-Clapeyron and Clapeyron equations are based on hydrate equilibrium data of pressure and temperature from experiments or calculated data. But hydrate formation is a non-equilibrium process. Information about superheating above the hydrate equilibrium conditions to totally dissociate the gas hydrate to liquid water and gas is normally lacking. The values vary considerably in such a way that some of them decided to base their results on average values over a range of temperatures. For example, Gupta et al. (2008) conducted a study with experiment, Clausius-Clapeyron and Clapeyron equations but all the results varied substantially. We therefore propose a method based on residual thermodynamics which does not have the limitations of the current methods. We do not expect much agreement of our results with a lot of the literature, firstly, because of the limitations of the other methods, especially, the simplicity of both the Clapeyron and Clausius-Clapeyron equations. Secondly, the remarkable disagreement among current data reported in literature.

The residual thermodynamics scheme used in this project is based on the unique and straight forward thermodynamic relationship between change in free energy and enthalpy change, with thermodynamic properties evaluated from residual thermodynamics. Such properties are change in free energy as the thermodynamic driving force in kinetic theories, equilibrium curves, and enthalpy changes of hydrate phase transition. With residual thermodynamics, real gas behaviour taking into account thermodynamic deviations from ideal gas behaviour can be evaluated.

The results of enthalpy changes of carbon dioxide hydrate phase transitions using residual thermodynamics in this project are around 10 – 11 kJ/mol guest molecule greater than the ones of methane hydrate phase transition for 273 – 280 K range of temperatures. Calculations based on kJ/mol hydrate within the same temperature range gave 0.5 – 0.6 kJ/mol hydrate. Anderson's results using Clapeyron equation are a little close to the results obtained in this work, precisely 10 kJ/mol and 7 kJ/mol guest

molecule at 274 K and at 278 K respectively. While Kang et al. (2001) in their experiment put this difference at 8.4 kJ/mol guest molecule at 273.65 K.

However, in replacement of in-situ CH₄ hydrate with CO₂, it is not the temperature-pressure curve that is most essential, but what is most important is the difference in free energies of both hydrates, CH₄ hydrate and CO₂ hydrate, and the enthalpies of CO₂ hydrate formation relative to the enthalpies of CH₄ hydrate dissociation. The free energy of CO₂ hydrate is around 1.8 – 2.0 kJ/mol more negative or lower than the free energy of CH₄ hydrate within a temperature range of 273.15 – 283.15 K (0 – 10 °C). That confirms that hydrate of CO₂ is more stable thermodynamically than hydrate of CH₄.

It is pertinent to state that this proposition is still under investigation, and it is still under development. In addition, there are constraints that are also under study. Hydrate formation at the interface between CO₂ gas and liquid water is very rapid, forming a hydrate film which will quickly block the pore spaces thereby limiting further CO₂ supply. Studies also need to be done on finding the most efficient and effective way to reduce the thermodynamic driving force, either by using any thermodynamic inhibitor or other substances.

List of papers

Peer-reviewed publications in scientific journals

Aromada, S. A.; Kvamme, B. New approach for evaluating the risk of hydrate formation during transport of hydrocarbon hydrate formers of sl and slI. *AIChE Journal*, 2019, 65(3): 1097-1110.

Kvamme, B.; Aromada, S. A. Risk of hydrate formation during the processing and transport of Troll gas from the North Sea. *Journal of Chemical & Engineering Data*, 2017, 62(7): 2163-2177.

Kvamme, B.; Aromada S. A. Alternative routes to hydrate formation during processing and transport of natural gas with a significant amount of CO₂: Sleipner gas as a case study. *Journal of Chemical & Engineering Data*, 2018, 63(3): 832-844.

Kvamme, B.; Aromada, S. A.; Kuznetsova, T.; Gjerstad, P. B.; Canonge, P. C.; Zarifi, M. Maximum tolerance for water content at various stages of a Natuna production. *Heat and Mass Transfer*, 2019, 55(4): 1059-79.

Aromada, S. A.; Kvamme, B. Impacts of CO₂ and H₂S on the risk of hydrate formation during pipeline transport of natural gas. *Frontiers of Chemical Science and Engineering*, 2019, 13(3): 616-627.

Kvamme, B.; Aromada, S. A.; Saeidi, N. Heterogeneous and homogeneous hydrate nucleation in CO₂/water systems. *Journal of Crystal Growth*, 2019, 522: 160-174

Kvamme, B.; Aromada, S.A.; Saeidi N.; Hustache-Marmou, T.; Gjerstad, P.B. Hydrate nucleation, growth and induction. *ACS Omega*, 2020, 5(6): 2603-2619.

Kvamme, B.; Aromada, S. A., Gjerstad, P. B. Consistent Enthalpies of the Hydrate Formation and Dissociation Using Residual Thermodynamics. *Journal of Chemical & Engineering Data*, 2019, 64(8): 3493-3504

Aromada, S. A.; Kvamme, B.; Wei, N.; Saeidi, N. Enthalpies of hydrate formation and dissociation from residual thermodynamics. *Energies*, 2019, 12(24): 4726.

Aromada, S. A.; Kvamme, B. Modelling of Methane Hydrate Formation and Dissociation using Residual Thermodynamics. *Simulation Notes Europe Journal*, SNE 31(3), 2021, 143-150. DOI: 10.11128/sne.31.tn.10575

Aromada, S. A.; Kvamme, B. Simulation of Hydrate Plug Prevention in Natural Gas Pipeline from Bohai Bay to Onshore Facilities in China. *Simulation Notes Europe Journal*, SNE 31(3), 2021, 151-157, DOI: 10.11128/sne.31.tn.10576

Peer-reviewed publications in conference proceedings

Zarifi, M.; Kvamme, B.; Gjerstad, P.; Aromada, S. A. Dynamics of heat and mass transport during hydrate dissociation and reformation in sediments. The 14th International Conference on Heat Transfer, Fluid Mechanics and Thermodynamics. Wicklow, Ireland, July 21–24, 2019

Aromada, S. A.; Kvamme, B. Production of methane from hydrate and CO₂ zero-emission concept. Proceedings in: The 10th EUROSIM Conference, Logroño (La Rioja), Spain, July 1– 5, 2019. EasyChair Preprint No. 1546.

Oral and postal presentations in international conferences

Zarifi, M.; Kvamme, B.; Gjerstad, P.; Aromada, S. A. Dynamics of heat and mass transport during hydrate dissociation and reformation in sediments. The 14th International Conference on Heat Transfer, Fluid Mechanics and Thermodynamics. July 21–24, 2019.

Aromada, S. A.; Kvamme, B. Simulation of hydrate plug prevention in natural gas pipeline from Bohai Bay to onshore facilities in China. Oral presentation at The 10th EUROSIM Conference, La Rioja, Spain, July 1– 5, 2019.

Aromada, S. A.; Kvamme, B. Modelling of methane hydrate formation and dissociation using residual thermodynamics. Oral presentation at The 10th EUROSIM Conference, Logroño (La Rioja), Spain, July 1– 5, 2019.

Aromada, S. A.; Kvamme, B. Production of methane from hydrate and CO₂ zero-emission concept. Oral presentation at The 10th EUROSIM Conference, Logroño (La Rioja), Spain, July 1– 5, 2019.

Aromada, S. A.; Kvamme, B. Consistent enthalpies of the hydrate formation and dissociation using residual thermodynamics. Poster presentation at The 12th International Methane Hydrate Research and Development Conference, October 31 – November 3, 2018.

Kvamme, B.; Aromada, S. A.; Kuznetsova, T.; Gjerstad, P. B.; Canonge, P. C.; Zarifi, M. Maximum limitations of adding N₂ to CO₂ during combined CO₂ storage and CH₄ production with examples from offshore Indonesia. Oral presentation at Fiery Ice 2017 in Corpus Christie, Texas, U.S.A., December 6 – 8, 2017.

Publications included in this thesis

Paper 1:

Aromada, S. A.; Kvamme, B. New approach for evaluating the risk of hydrate formation during transport of hydrocarbon hydrate formers of sl and slI. *AIChE Journal*, 2019, 65(3):1097-1110.

Paper 2:

Kvamme, B.; Aromada S. A. Risk of hydrate formation during the processing and transport of Troll gas from the North Sea. *Journal of Chemical & Engineering Data*, 2017, 62(7):2163-2177.

Paper 3:

Kvamme, B.; Aromada, S. A. Alternative routes to hydrate formation during processing and transport of natural gas with a significant amount of CO₂: Sleipner gas as a case study. *Journal of Chemical & Engineering Data*, 2018, 63(3):832-844.

Paper 4:

Kvamme, B.; Aromada, S. A.; Kuznetsova, T.; Gjerstad, P. B.; Canonge, P. C.; Zarifi, M. Maximum tolerance for water content at various stages of a Natuna production. *Heat and Mass Transfer*, 2019, 55(4):1059-1079.

Paper 5:

Aromada, S. A.; Kvamme, B. Impacts of CO₂ and H₂S on the risk of hydrate formation during pipeline transport of natural gas. *Frontiers of Chemical Science and Engineering*, 2019, 13(3):616-627.

Paper 6:

Aromada, S. A.; Kvamme, B. Simulation of Hydrate Plug Prevention in Natural Gas Pipeline from Bohai Bay to Onshore Facilities in China. *Simulation Notes Europe Journal*, SNE 31(3), 2021, 151-157, DOI: 10.11128/sne.31.tn.10576

Paper 7:

Kvamme, B.; Aromada, S. A.; Saeidi, N. Heterogeneous and homogeneous hydrate nucleation in CO₂/water systems. *Journal of Crystal Growth*, 2019, 522: 160-174.

Paper 8:

Kvamme, B.; Aromada, S.A.; Saeidi N.; Hustache-Marmou, T.; Gjerstad, P.B. Hydrate nucleation, growth and induction. *ACS Omega*, 2020, 5(6): 2603-2619.

Paper 9:

Kvamme B.; Aromada S. A.; Gjerstad, P. B. Consistent enthalpies of the hydrate formation and dissociation using residual thermodynamics. *Journal of Chemical & Engineering Data*, 2019, 2019, 64(8):3493-3504.

Paper 10:

Aromada, S. A.; Kvamme, B. Modelling of Methane Hydrate Formation and Dissociation using Residual Thermodynamics. *Simulation Notes Europe Journal*, SNE 31(3), 2021, 143-150. DOI: 10.11128/sne.31.tn.10575

Paper 11:

Aromada, S. A.; Kvamme, B. Production of methane from hydrate and CO₂ zero-emission concept. The 10th EUROSIM Conference, Logroño (La Rioja), Spain, July 1– 5, 2019. EasyChair Preprint No. 1546.

Paper 12:

Aromada, S. A.; Kvamme, B.; Wei, N.; Saeidi, N. Enthalpies of hydrate formation and dissociation from residual thermodynamics. *Energies*, 2019, 12, 24, 4726.

List of tables

TABLE 2.1: <i>SUMMARY OF HYDRATE CRYSTAL STRUCTURES [112]</i>	17
TABLE 2.2: <i>FACTORS OF WATER CAVITIES (EMPTY-HYDRATE) STABILIZATION</i>	18
TABLE 4.1: <i>LIST OF DRIVING FORCES FOR FORMATION AND DISSOCIATION OF HYDRATE [223]</i>	45

List of figures

FIGURE 1.1: NETWORK OF PIPELINES IN THE NORWEGIAN CONTINENTAL SHELF, SHOWING EUROPIPE I, EUROPIPE II AND OTHERS [30]	4
FIGURE 1.2: PIPELINE PLUGGED BY HYDRATE [36].....	5
FIGURE 1.3: PIPELINES ALREADY COVERED WITH RUST [37]	6
FIGURE 1.4: MAP SHOWING LOCATIONS WHERE GAS HYDRATE HAS BEEN RECOVERED, WHERE GAS HYDRATE IS INFERRED TO BE PRESENT ON THE BASIS OF SEISMIC DATA, AND WHERE GAS HYDRATE DRILLING EXPEDITIONS HAVE BEEN COMPLETED IN PERMAFROST OR DEEP MARINE ENVIRONMENTS, ALSO LEADING TO RECOVERY OF GAS HYDRATE [58].	8
FIGURE 2.1: TYPICAL ILLUSTRATION OF GAS HYDRATE STRUCTURE WITH WATER MOLECULES LINKED TOGETHER TO FORM CAGES AND TRAP GAS MOLECULES (LIKE METHANE, PROPANE AND SO ON) [110]	16
FIGURE 2.2: SCHEMATIC ILLUSTRATION OF STRUCTURE OF GAS HYDRATE [111]	16
FIGURE 2.3: ILLUSTRATION OF THE RELATIONSHIP BETWEEN HYDRATE FORMING GUEST MOLECULES SIZE AND THE HYDRATE STRUCTURE TYPE THAT WOULD BE FORMED [115].	19
FIGURE 3.1: ILLUSTRATION OF HYDRATE NUCLEATION AT THE INTERFACE BETWEEN GAS PHASE AND LIQUID WATER PHASE. ..	29
FIGURE 3.2: ILLUSTRATION OF HYDRATE NUCLEATION FROM DISSOLVED HYDRATE FORMER IN LIQUID WATER PHASE.	30
FIGURE 3.3: ILLUSTRATION OF HYDRATE NUCLEATION FROM DISSOLVED WATER IN HYDRATE FORMER PHASE.	31
FIGURE 3.4: EXPERIMENTAL RESULTS OF CH ₄ HYDRATE FORMATION FROM WATER AND CH ₄ AT 1200 PSIA (83 BAR) AND 3 °C [206]	35
FIGURE 4.1: PHASE DIAGRAM FOR ICE, WATER, HYDRATE FORMERS AND HYDRATE.....	41
FIGURE 4.2: HYDRATE EQUILIBRIUM CURVES FOR METHANE, ETHANE, PROPANE, ISOBUTENE, CARBON DIOXIDE AND HYDROGEN SULPHIDE.	42
FIGURE 4.3: METHANE HYDRATE EQUILIBRIUM CURVE COMPARED WITH LITERATURE [215, 216]	43
FIGURE 4.4: CARBON DIOXIDE HYDRATE EQUILIBRIUM CURVE COMPARED WITH LITERATURE [213, 214].....	44
FIGURE 5.1: THE PH. D. PROJECT AND PUBLICATIONS. ARROW CONNECTS EACH PAPER TO THE PART OF THE PROJECT IT FULFILS	53

Table of contents

Dedication.....	II
Acknowledgement.....	III
Abstract.....	V
List of papers.....	X
Publications included in this thesis.....	XIII
List of tables.....	XV
List of figures.....	XVI
Table of contents.....	XVII
1 Introduction	1
1.1 Motivation.....	1
1.2 Objective	10
1.3 Scope.....	11
2 Hydrate	12
2.1 History of hydrate	12
2.2 Hydrate structures	14
2.3 Water cavities stabilization.....	17
2.4 Applications of gas hydrates	19
2.4.1 Storage and transport of natural gas.....	19
2.4.2 Marine CO ₂ sequestration.....	20
2.4.3 Cool storage application	21
2.4.4 Separation processes	22
3 Kinetics of hydrate formation	24
3.1 Hydrate nucleation.....	25
3.1.1 Theories of hydrate nucleation.....	27
3.2 The hydrate core stable growth stage	32
3.2.1 Modelling approaches of hydrate stable growth	34
3.3 Induction time.....	34
4 Thermodynamics.....	37
4.1 Thermodynamics and hydrate formation.....	37

4.2	Gibbs phase rule	38
4.3	Hydrate stability from phase diagram	40
4.4	Hydrate formation driving forces	44
4.5	Hydrate thermodynamics	45
5	Procedure, project and publications	49
5.1	Scientific method	49
5.2	The PhD project and publications	51
6	Summary of papers	54
6.1	New approach for evaluating the risk of hydrate formation during transport of hydrocarbon hydrate formers of SI and SII	54
6.2	Risk of hydrate formation during the processing and transport of Troll gas from the North Sea.	56
6.3	Alternative routes to hydrate formation during processing and transport of natural gas with a significant amount of CO ₂ : Sleipner gas as a case study	58
6.4	Maximum tolerance for water content at various stages of a Natuna production.....	60
6.5	Impacts of CO ₂ and H ₂ S on the risk of hydrate formation during pipeline transport of natural gas.	62
6.6	Simulation of hydrate plug prevention in natural gas pipeline from Bohai Bay to onshore facilities in China.....	63
6.7	Heterogeneous and homogeneous hydrate nucleation in CO ₂ /water systems. Journal of Crystal Growth	65
6.8	Hydrate nucleation, growth and induction.	68
6.9	Consistent enthalpies of the hydrate formation and dissociation using residual thermodynamics	70
6.10	Modelling of methane hydrate formation and dissociation using residual thermodynamics.	72
6.11	Production of methane from hydrate and CO ₂ zero-emission concept	73
6.12	Enthalpies of hydrate formation and dissociation from residual thermodynamics	74

7	General discussion, conclusion and further works	75
7.1	General discussion	75
7.1.1	Risk of hydrate formation and the impact of rust in pipeline transport of natural gas and CO ₂	75
7.1.2	Kinetics of hydrate formation	80
7.1.3	Simultaneous production of energy and long-term CO ₂ offshore storage	82
7.2	Conclusion	86
7.3	Further works	90
7.3.1	Comparative cost of dehydration to dewpoint and hematite demands.....	90
7.3.2	Experimentation of impact of rusty surfaces on the risk of hydrate formation in gas transport pipelines.....	91
7.3.3	Impacts of the presence of other gases that cannot form hydrate but can affect hydrate formation	91
7.3.4	More experimental works involving carbon dioxide and structure II hydrate formers.....	91
7.3.5	Injection gas mixture of choice	92
7.3.6	Calculations outside hydrate equilibrium pressure and temperature	92

Part 1

1 Introduction

This thesis contains the report of the studies done in the Ph.D. project. The project is aimed at studying the risk of hydrate formation during pipeline transport of natural gas and CO₂ with emphasis on the impact of solid surfaces; thermodynamics and kinetics of hydrate formation; and enthalpy changes of hydrate phase transition with focus on simultaneous production of in-situ methane hydrate and long-term CO₂ offshore storage. The main part of this thesis is the attached articles (papers). The motivation for the project which forms the background of all the studies, objectives and scope of the project are written in chapter one. Chapter two contains information about natural gas hydrate: history of hydrate, hydrate structures, and applications of gas hydrate. Kinetics of hydrate formation and related theories are discussed in chapter three. Important thermodynamic concepts of gas hydrate are briefly discussed in chapter four. Chapter five has brief explanation of the scientific method, how the project was executed and results disseminated in publications. The summary of every paper that make up this thesis is presented in chapter six. Chapter seven contains general discussion, conclusion and suggested further works.

1.1 Motivation

Natural gas hydrate (NGH) is a problem, a crucial one [1, 2] to the energy industry, a potential vast source of low-carbon energy for the world in the future [3-8], and it could also potentially provide a long-term storage possibility for carbon dioxide [9-11]. Several studies and pilot tests have been performed, and much research efforts are still being invested in this subject. Nevertheless, there is still a poor understanding of the thermodynamics and even the kinetics of these complex natural systems [9, 12-14].

The entire world depends on energy to function. Even with the concerted efforts made so far in development and utilization of renewable energy sources like hydro, solar, geothermal, wind and biomass/biofuel, it will take decades for them to be able to entirely substitute the fossil fuels. Fossil fuels include coal, oil, and natural gas. Natural gas is a very low carbon source of energy; thus, it would continue to be accepted as an

environmentally friendly energy resource and a good source for producing hydrogen [15]. Among the fossil fuels, natural gas consumption [16] will increase the most from 2010 to 2040. Natural gas accounted for about 22 per cent [17] of the world energy consumption in 1990, and it is projected to be around 26 per cent by 2030.

However, natural gas operations, that is production, processing and transport involve thermodynamic conditions that are necessary for hydrate to form. These operations are usually carried out at high pressures and low temperatures [18-20]. Water is also usually produced together with natural gas [1, 21]. The major components in natural gas form hydrate with (free) water when the aforementioned thermodynamic conditions exist with favourable mass and heat transport. Natural gas is predominantly methane (CH_4) but often consists of other higher hydrocarbons like ethane (C_2H_6), propane (C_3H_8), iso-butane ($\text{i-C}_4\text{H}_{10}$), normal-butane ($\text{n-C}_4\text{H}_{10}$), and sometimes, inorganics like carbon dioxide (CO_2), hydrogen sulphide (H_2S) and nitrogen (N_2) are also present.

Natural gas is typically produced in places (like offshore, swamps, and hinterland forest) that are far from its end-users or markets. Therefore, it must be transported from production sites to its processing facilities and finally to its market. Thus, transport is a vital aspect of natural gas operations.

Transport of natural gas from production sites (reservoir) offshore [18, 22, 23] and onshore to processing facilities and to supply delivery terminals is mostly done using pipelines. An overall pipeline network length of about two million kilometres [24] were already in operation in the world in 2010 to transport natural gas, crude petroleum, and other petroleum products. As at 2009, about 8000 kilometres [25] long pipeline networks (see Figure 1.1) were in use for transporting about 96 billion standard cubic metres [19, 26] of natural gas in the North Sea. These pipelines are mostly laid on the seafloor thereby exposing them to low temperatures of about 272 –279 K (-1 to +6 °C). An example of such pipelines is the Europipe II (EP II) [22, 23] in the North Sea (Figure 1.1). The temperature of the gas at the receiving terminal is expected to be as low as -5°C [22]. The gas is sent at 190 bar from Norway and it is received at 90 bar in Germany. These operations pressure-temperature conditions are favourable for hydrate to form

if water drops out from the gas. The Europipe II is an export gas pipeline having a length of approximately 660 km [22, 23], with 627 km of the pipeline offshore and it passes through the Norwegian-Danish-German parts of the North Sea. This pipeline transports 65.9 Mega Standard Cubic Metres of gas per day [22, 23] from Kårstø gas processing plant in Norway to the Europipe II Receiving Facilities (ERF) reception centre at Dornum in Germany. Another example is the 58 km subsea wet gas pipeline [18] that transports natural gas from Platform QK18-1 in southwest of Bohai Bay to the gas processing plant onshore in Northeast China at elevated pressures and low temperatures. This pipeline is occasionally plugged by hydrate.

In addition, the strong international attention on CO₂ emissions reduction to mitigate global warming involves situations in which water can condense out of the CO₂ streams in pipelines and eventually leads to hydrate formation from the dropped-out water and the CO₂. Transport of carbon dioxide in pipelines to offshore storage sites classically involves elevated pressures and low temperatures beneficial for hydrate to form.

Norway is a pioneer country in carbon capture, transport, and storage. The country recently celebrated 20 years of storing a million ton of CO₂ separated from the Sleipner gas field per year in the Utsira formation since 1996. From 1996 till now, the amount of CO₂ that have been injected and stored in Utsira Formation is well over 16 million tonnes [27]. In the Snøhvit project, a slightly smaller amount, 700000 tons CO₂ per year, is stored in deep aquifer formations. The CO₂ stream contains water which can also drop out and can eventually form hydrate at high pressures and low temperatures, which are the usual operations conditions. An example of a CO₂ transport pipeline is the planned huge pipeline for transport of separated CO₂ from the continent, mainly Germany (Europipe I) [28, 29] to use for enhanced oil recovery (see *Figure 1.1*). Though it is currently put on hold due to changes in German CO₂ handling policy, the project has sponsored a hydrate study project at the University of Bergen.



Figure 1.1: Network of pipelines in the Norwegian Continental Shelf, showing Europipe I, Europipe II and others [30]

Hydrate formation during pipeline transport of natural gas or CO₂ is a critical problem. Hydrate can eventually plug pipelines (see Figure 1.2), destroy pipelines and equipment [1, 31, 32], and lives can also be lost [32, 33]. When this happens, operations will stop or be suspended, and by implication, there will be economic losses due to non-operation. Additional cost will be incurred to safely dissociate the hydrate for operations to commence again. The petroleum industry spends about a billion dollars (USD) [31] every year to prevent hydrate formation in wells, gas processing equipment and transport pipelines. According to Jassim & Abdi (2008) [34], offshore operations cost

additionally approximately 1.6 million dollars (USD) per kilometre on the insulation of subsea pipelines to prevent hydrates. Sloan [35] puts this insulation cost per kilometre of pipeline at 1 million dollars (USD).

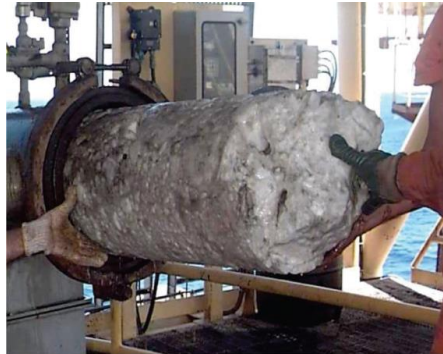


Figure 1.2: Pipeline plugged by hydrate [36]

The classical method currently used by the industry for evaluating the risk of hydrate nucleation and growth is based on estimating water dew-point [2] for the specific gas. If the pipeline or processing equipment's condition of pressure-temperature is more than or above water dewpoint such that water drops out, then the amount of water that will condense out is evaluated. Evaluation of hydrate formation will follow. This includes evaluation of the maximum amount of hydrate that would form from the dropped-out water. The dew-point method is used to evaluate the upper-limit of water (in vapour form), that is the maximum mole-fraction of water that can be allowed to flow with the bulk gas without the risk of water condensing out as liquid droplets and eventually leading to hydrate formation.

The problem with the current approach is that before pipelines are mounted in place for gas transport operations, they are already rusty (see Figure 1.3). These rusty surfaces have hydrate formation implications: they provide water adsorption sites which can cause hydrate to form in the pipeline or equipment. These surfaces can make free liquid water available through the mechanism of adsorption. The current approach used

by the industry does not consider the impact of hematite (rusty surfaces). The implication of this other means of water dropping out from the bulk gas stream needs to be investigated as it would have an impact on the maximum mole-fraction of water that can be permitted to follow the bulk gas during pipeline transport, thus, it could also have an impact on gas dehydration systems design. Hence, it is beneficial to enhance the understanding of the risk of hydrate formation during pipeline transport and processing. For comprehensiveness, impacts of the important components in natural gas on safe transport of the bulk gas also need to be investigated.



Figure 1.3: Pipelines already covered with rust [37]

Natural gas hydrate could also be a potential solution to the challenge of the world's ever-increasing energy demand [38] as the world's population continues to grow. Natural gas (methane) hydrates are vastly distributed worldwide in the permafrost and in the sediments of continental margins of oceans [9, 39]. The abundant amount of methane gas trapped in the naturally occurring hydrates promises to serve the world for many centuries when produced or extracted [39-41]. Figure 1.3 shows where in the world NGHs have been recovered and inferred to exist. NGHs in the world have been conservatively estimated to hold organic carbon in the amount of over two times the over-all quantities of carbon in the fossil fuels on the earth [38, 39, 42-47]. Therefore, the reason for the great international attention and research.

For example, Japan imports the highest amount [48] of liquefied natural gas (LNG) in the world and the second largest net importer [48, 49] of other fossil fuels in the world, due to no significant resources of gas, is actively exploiting other energy resources like wind, solar and naturally occurring gas hydrates available to her [50]. Results of Bottom Simulating Reflectors (BSR) showed that Japan has a vast amount of gas hydrate reserves, mostly distributed in the Southwestern Islands trench, Boso Peninsula East, Nankai Trough, the Kuril Trench, Tatar Trough, Japan sea east edge, and Okhotsk region [20]. The hydrate spreads across around 44 thousand square kilometres with an estimated over-all reserve of 40-63 times the gas consumption of Japan [50, 51]. The first phase of production of natural gas from methane hydrate applying depressurization technique has been carried out by the Japan, Oil, Gas, and Metal National Corporation (JOGMEC) off the coast off Shima peninsula and Atsumi peninsula. They produced 120 thousand cubic metres of methane gas from the hydrate [20].

Taiwan also, due to having limited energy resources, about 98 % [52] of their energy requirements are imported (Taiwan consumes around 10 billion cubic metres of natural gas yearly). However, it has gas hydrate reserves of about 2.7 trillion cubic metres in the coast of Tainan-Pingtung, which implies Taiwan can be self-sufficient if the methane in these hydrates are mined [53] and their energy need can be met for 270 years.

It is important to mention China, the highest importer [54] of fossil fuel in the world. The good news is that China has about 108 trillion cubic metres of natural gas resources trapped in hydrate both in land and offshore. It can take China about 750 years [20] to consume these natural gas resources in those hydrate deposits. Therefore, their immense investment in gas hydrate research to help them exploit their huge hydrate reserves.

India, the second most populated country in the world, will experience a growth in primary energy demand from 2017 to 2040 of over 25 % [55] of the net primary energy demand of the entire world, and they import huge amount of natural gas. However, India has the second largest [56] natural gas hydrate deposit in the world. The Kerala, Cauvery and Krishna-Godavari (KG) basins only are estimated to have about 2.83 – 3.68

trillion cubic metres [57] of natural gas hydrate reserves. Thus, India is committing much research efforts towards mining the hydrate reserves.

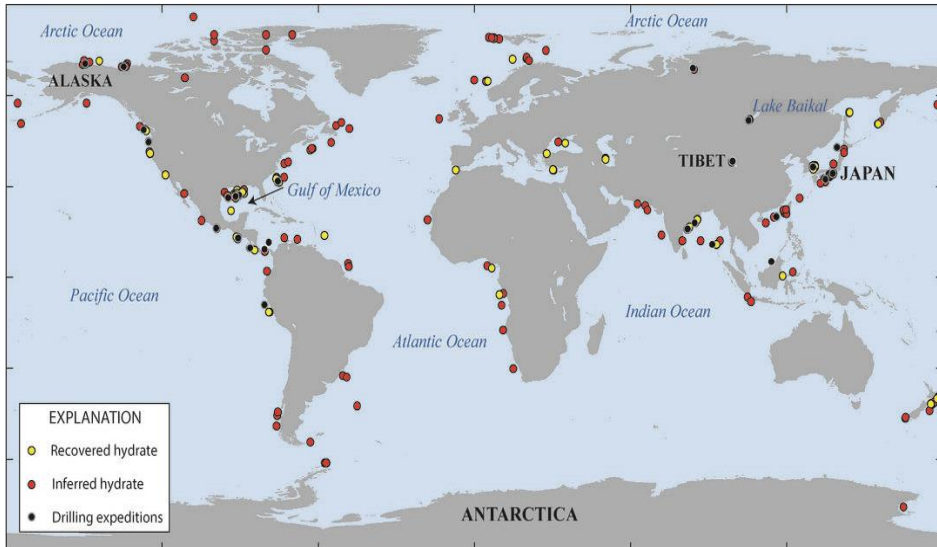


Figure 1.4: Map showing locations where gas hydrate has been recovered, where gas hydrate is inferred to be present on the basis of seismic data, and where gas hydrate drilling expeditions have been completed in permafrost or deep marine environments, also leading to recovery of gas hydrate [58].

Several methods have been proposed for production of methane from the naturally occurring gas hydrates: depressurization or pressure reduction [3, 38, 59], thermal stimulation [60-62], chemical inhibitor injection (i.e., thermodynamic hydrate inhibitors and kinetic hydrate inhibitors) [63-67], and simultaneous CH_4 production and CO_2 storage (CH_4 replacement by CO_2) [10, 68]. Effectiveness and economic implications must be considered before choosing any specific method or before combining methods. Li et al. (2016) [38] suggest a combination of all the methods. Reduction of the hydrate deposits pressure below the hydrate stability pressure will create a thermodynamic driving force of course, but the heat of dissociation is required to be supplied. Applying the fourth technique promises to potentially provide a solution for reducing CO_2 emission into the atmosphere: it could provide a possibility for long-term storage of CO_2

(CO₂ sink) in form of CO₂ hydrate in the place of the in-situ methane hydrate. Whichever way, to produce the natural gas trapped in hydrates, heat is required to be supplied [69] for the dissociation of the methane hydrate to continue. Therefore, there is need to study the heat of hydrate phase transitions.

To supply or add heat for dissociation of the trapped natural gas in the hydrate, information on heat of dissociation is obviously needed. It is vital to know the amount of heat required for dissociation of the hydrate, and the superheating involved. Some pilot tests have been performed which confirmed the importance of heat supply. Examples are the two tests [69] carried out in Japan (offshore) some years ago where they encountered the problem of freezing down (they also produce sand and water) in the first case just after 6 days. The second test was planned to last for 6 months continuous production of methane but was shut down just 24 days into the operation due to the same freezing down problem. Thermal stimulation method using steam or hot water is a solution, but it has been assessed [69] to be excessively costly if used as the only technique. Therefore, injection of carbon dioxide into the methane hydrate deposit (4th method) is a more attractive approach. Lee et al. [70] and Falenty et al. [71] have demonstrated a solid-state process of CO₂-CH₄ swap in hydrate for the ice region of water. When CO₂ is injected into a reservoir of CH₄ hydrate, a new CO₂ hydrate will be formed.

Based on these discussions, this project was undertaken through rigorous scientific research and collaborations. The results obtained have been published the in journals and some have been presented at international conferences (oral presentations, poster presentation and as proceedings) which form the main report documented in this thesis.

1.2 Objective

Hydrate formation or dissociation is a very complex process where both thermodynamics and kinetics play a very major role. A clear investigation into how hydrate nucleation and growth occur in industrial systems and nature is vital to provide the right and important information that would help to prevent the problem of hydrate, and to provide valuable information for production of natural gas from the abundant in-situ methane hydrate in the earth, and for effective and efficient simultaneous storing of CO₂ in the place of the original CH₄ as CO₂ hydrate. And for dissociating hydrate plugs, a reliable and simple method for calculating enthalpies of dissociation is important.

Prior to this projects several hydrate formation and dissociation modelling works have been carried at the University of Bergen using especially Phase-Field Theory (PFT) and Multicomponent Diffuse Interface Theory (MDIT). Therefore, this work is primarily aimed at application of our novel but already developed thermodynamic scheme, but (in this project) based on Classical Nucleation Theory (CNT). The application involves comprehensive validation of the scheme with experimental data from systems involving different single components and multicomponent gas streams; evaluation of upper limit of water in different gas systems; illustration of kinetics of hydrate formation and evaluation of enthalpies of hydrate formation and their implications.

The specific objectives of the project are:

- to evaluate the impact of solid surfaces on maximum limits of water that should be permitted in pipeline transport streams (hydrocarbon streams and carbon dioxide streams). This involves investigation of different gas systems and the impacts of different hydrate formers.
- to enhance the understanding of the thermodynamics and kinetics of hydrate phase transitions in industrial systems and nature.
- to evaluate the process of combined storage of CO₂ and release of CH₄ from in-situ hydrates: the consequences of adding nitrogen to CO₂ for combined storage of CO₂ and release of CH₄ from natural gas hydrates; and implication of enthalpies of hydrate formation. And to establish a reliable and simple scheme for evaluating enthalpies of hydrate dissociation.

1.3 Scope

The Ph.D. project entails the following works in order to achieve the above objectives.

- Investigation of the impact of solid surfaces (rusty surfaces) on the risk of hydrate formation during processing and pipeline transport of natural gas (multicomponent gas) and CO₂ streams.
- Non-uniform hydrate formation and free energy analysis for evaluation of hydrate distributions during transport of hydrate forming mixtures.
- Risk of hydrate formation in hydrate forming systems which exhibit phase split during transport and hydrate forming conditions during processing.
- Study of kinetics of hydrate nucleation using classical nucleation theory (CNT).
- Implications of adding nitrogen to CO₂ for combined CO₂ storage as hydrate and release of in situ methane from hydrate. Free energy analysis and simplified kinetic modelling based on classical nucleation theory.
- Implications of enthalpies of hydrate formation or dissociation on combined CO₂ storage as hydrate and release of in situ methane from hydrate. Free energy analysis and simplified kinetic modelling based on classical nucleation theory.
- Establishment of a reliable and simple scheme for evaluating enthalpies of hydrate dissociation.

2 Hydrate

Natural gas hydrates (NGH) are non-stoichiometric crystalline inclusion compounds that are formed at high pressure and low temperature. They are formed when hydrogen-bonded water molecules form three-dimensional solid cage-like structures with cavities that entrap suitably small sized molecules of certain gases and volatile liquids [26, 72] known as guest molecules. The hydrogen-bonded water molecules are known as “hosts” to the “guest molecules”. The guest molecules stabilize the hydrate. Examples of guest molecules are methane, ethane, propane, iso-butane, carbon dioxide and hydrogen sulphide. The empty clathrate (without any guest molecule) is not thermodynamically stable [72]. Thus, guest molecules having diameter lesser than that of the water cavities need to occupy the cavities at typically elevated pressures and low temperatures to obtain a thermodynamically stable hydrate.

2.1 History of hydrate

The discovery of hydrate is credited to Sir Humphrey Davy [73-75] in 1810 for his discovery of chlorine hydrate, that is hydrate formation from chlorine and water - the first gas hydrate. Several other scientists began to engage in experimental research on hydrate. It is noteworthy to mention some of them. Chlorine hydrate was confirmed by Faraday [76] in 1823. And in 1840 hydrate formed from H_2S was made known by Woehler [77]. Hydrate formation from CO_2 was studied by Wroblewski [78-80] in 1882. While Ditte's work in 1882 [81], Maumene's publication of 1883 [82], and Roozeboom's study in 1884 [83] re-examined Faraday's [76] proposed water-chlorine ratio. The work of Cailletet and Bordet [84] published in 1882 is the first to record measurement of hydrate formation involving mixture of two hydrate formers [33]. However, it is after 78 years (that is in 1888) from Davy's discovery of chlorine hydrate that hydrates formed from hydrocarbons were discovered by Villard [85]. Hydrates formed from methane, ethane, ethene, ethyne and nitrogen dioxide were first studied by him. Before entering the 20th century, 40 hydrate guest molecules had already been identified and hydrate science was seen as a developing field with particular focus on thermodynamic studies [86].

The problem of natural gas pipeline plugging by hydrate was made known in the 1930's by Hammerschmidt [1] in his work published in 1934. Thus, prevention of hydration formation and many other hydrate science areas began to attract extensive research efforts. The targets of the researches were on calculation of hydrate composition as well as the effects of various hydrate inhibitors on the process of hydrate formation up to initial correlations used for evaluation of hydrate phase equilibrium [74]. Yet, before the 1930s, information about structures of hydrate was still a puzzle. But the description of a hydrogen-bonded water lattice which have cavities that can entrap the guest molecules having van der Waals type of interactions between both the guest and host was already propounded. These concepts were authenticated between 1951 and 1952 when modelling and X-ray crystallography were used to discover the first two structures of hydrate structures, (structure I and structure II) [87-91]. Hydrates became recognized as clathrates. This was founded on Powell's nomenclature for inclusion compounds which have molecules of guests enclosed in cavities of the lattice of a host [92]. Then, van der Waals and Platteeuw [93] developed statistical mechanical model, followed by Barrer and Stuart [94]. The model took into account the stability of hydrate lattices and a number of unique properties of hydrate; like non-stoichiometry, based on the information of structures of hydrate and other thermodynamic information available then. It became possible to evaluate macro-scale thermodynamic properties such as gas hydrate's temperature and pressure, with the use of micro-scale properties such as intermolecular potentials. And after 1970, it became possible to estimate different hydrate properties using physical methods. That included ability to evaluate the distribution of guests over the cavities of hydrate and composition of hydrates [86]. Likewise, a new structure of hydrate with larger guest molecules became acknowledged as structure H [95].

A new period in the history of hydrate studies brought about the discovery of in-situ natural gas hydrates (naturally existing gas hydrate). Makogon and his group drilled the first well [96] (Markhinskaya well) in 1963. The well showed evidence of possible existence of in-situ methane hydrate in Siberia. Makogon then hypothesize [31, 97] the occurrence of abundant in-situ methane gas hydrate in cold layers. However, he was

greatly doubted by experts. They insisted that the idea must be validated experimentally. In 1965, Makogon was able to finally use experiment to authenticate his claim (hypothesis) [97] that gas hydrates could amass as large natural deposits (in-situ hydrate) in porous rock. Subsequently, the Soviet Union discovered the first main gas hydrate naturally existing as deposit in permafrost [98]. The discovery Makogon was formally approved and documented in 1969 in the Soviet Union. Therefore, the discovery of in-situ gas hydrate is credited to Makogon. The first discovery of substantial deposit of gas hydrate in permafrost was in Masssayokha field in the Soviet Union. After Masssayokha, more proofs of in-situ gas hydrate reservoirs were found in some other parts of the world. Natural occurring gas hydrate discovered at Alaska in the United States [99] and at MacKenzie Delta in Canada [100]. Well log responses in the Arctic Archipelago area have been shown by Weaver and Stewart [101] in 1982 and Franklin [102] in 1983. Both [103] and [104] did a summary of in-situ gas hydrate in 1982 and 1995 respectively. The sum of 23 hydrate cores [33] have already been discovered as at 2008 in the ocean; Gulf of Mexico and three Soviet Union water bodies.

2.2 Hydrate structures

Many different hydrate structures have been identified. But the most common types are structure I (sI) and structure II (sII) proposed by Clausen [87-89]. Structure H (sH) is acknowledged to be the third hydrate structure type [95], even though the sI and sII are more common. Yet, sH is more common compared to all other unusual hydrate structure types which are formed from other compounds other than natural gas hydrate formers (including Jeffrey's structures III to VII [105]). Each of the three different structure type has different composition. The unit cell is the smallest symmetrical unit crystal that is repeated in all cubic dimensions into macro-size crystals [75]. A brief detail of the three major or recognized hydrate structures are presented below.

Every unit cell of sI hydrate is made up of 46 water molecules; it consists of 2 small cages and 6 large cages. The two types of cavities are referred to as dodecahedron (small cages) and tetrakaidecahedron (large cages). The dodecahedron cavity has twelve-sided polyhedron with pentagonal faces is depicted as 5^{12} as proposed by [105]. The "5"

signifies pentagonal face and “12” represents the number of faces. The tetrakaidecahedron cavity has fourteen-sided polyhedron having twelve pentagonal faces and two hexagonal faces and it is similarly described with $5^{12}6^2$ [105]. The cubic unit cell also referred to as cell constant of structure I hydrate is around 12.01 Å at a temperature of 273.15 K. methane, ethane, hydrogen sulphide and carbon dioxide will typically form SI hydrate. These guest molecules are the main focus of [Paper 4 – Paper 8, Paper 10, Paper 11].

Hydrate Structure II was first studied by piston cores in water depth of 530 to 560 m on the Gulf slope offshore of Louisiana [106]. The hydrate was recognised as SII hydrate [106] based on the relative high amount of both propane and isobutane (as guest molecules) in it. This was confirmed using solid-state nuclear magnetic resonance (NMR) [107]. Structure II hydrates also comprise two types of cavities, the dodecahedron (small cage) and hexakaidecahedron (large cage), also depicted as 5^{12} and $5^{12}6^4$ respectively. The unit cell consists of 136 molecules of water, having 16 small and 8 large cavities with a cell constant of 17.36 Å at 273.15 K. Our studies involving SII guest molecules are presented in [Paper 1 – Paper 3 and Paper 6].

Structure H hydrates have been found in Gulf of Mexico [108]. Mehta and Sloan [109] proposed that structure H hydrate could exist in nature as the common occurrence of petroleum. Structure H hydrate consists of three sizes of cavity: three pentagonal dodecahedrals in the small cavity depicted as 5^{12} , the medium cavity with two irregular dodecahedron represented as $4^35^66^3$, and the large cavity with one icosahedron denoted by $5^{12}6^8$. The smallest cavity of structure H hydrate is like the small cavities in SI and SII, but the largest cavity is larger than the large cavity of both hydrate types SI and SII. When a smaller “help” molecule, for example methane is present, larger guest molecules such as benzene, cyclopentane and cyclohexane can occupy the SH largest cavity.

Figure 2.1 illustrates a typical gas hydrate structure showing water molecules linked together to form cavities and showing a guest molecule entrapped in the cavity. The three main structures of hydrate are presented in Figure 2.2. The structural properties of the three hydrate structure types are summarized in

Table 2.1. In subsequent sections and chapters, we will only mention sI and sII hydrate since they are the hydrate structure type that we come across in industrial processes during processing and pipeline transport of hydrocarbons. Thus, sH hydrate will neither be mentioned or investigated.

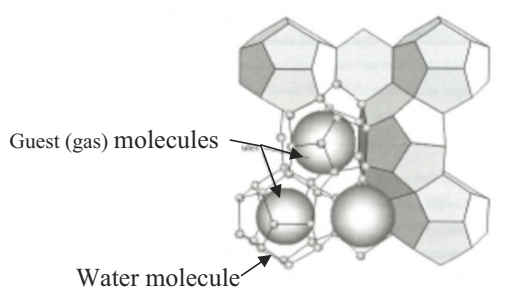


Figure 2.1: Typical illustration of gas hydrate structure with water molecules linked together to form cages and trap gas molecules (like methane, propane and so on) [110]

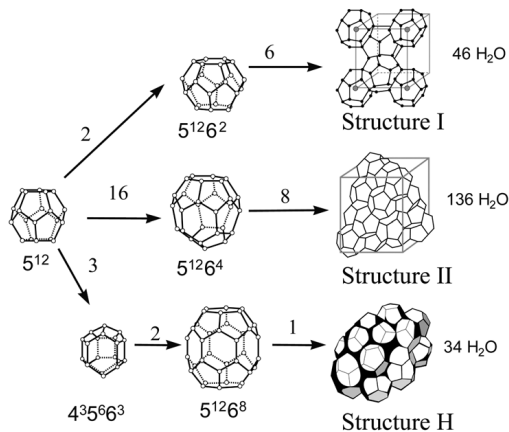


Figure 2.2: Schematic illustration of structure of gas hydrate [111]

Table 2.1: Summary of hydrate crystal structures [112]

Hydrate crystal structure	I		II		H		
	Small	Large	Small	Large	Small	Medium	Large
Description	5 ¹²	5 ¹² 6 ²	5 ¹²	5 ¹² 6 ⁴	5 ¹²	4 ³ 5 ⁶ 6 ³	5 ¹² 6 ⁸
Number of cavities per unit cell	2	6	16	8	3	2	1
Number of water molecule per unit cell	46		136		34		
Average cavity radius (Å)	3.95	33	3.91	4.73	3.91*	4.06*	5.71*
Coordination number [^]	20	24	20	28	20	20	36

*Estimates of structure H cavities from geometric models

[^]Number of oxygens at the periphery of each cavity

2.3 Water cavities stabilization

Figure 2.3 illustrates the relationship between hydrate formers molecules sizes and the type of hydrate structure that can be formed. Guest molecules within the range of 4.4 – 6.0 Å in diameter commonly form structure I hydrate. These are molecules like methane, ethane, carbon dioxide, and hydrogen sulphide. Structure II hydrate would be formed from guest molecules of propane and isobutane having molecules diameter between 6.0 – 7.0 Å. While hydrate formation will not occur from molecules with diameter either below 4.2 or 7.0 Å. Based on this illustration, we may conclude that the type of hydrate structure that will be formed mostly depends on the size of the guest molecule. That illustration implies the structure of hydrate that will form depends on the available space in the cavities relative to the hydrate former molecule's diameter.

However, the actual stabilization is dependent on the short-range interactions referred to as van der Waal type of interactions. And in certain situations, such as the case of H₂S (it is a slightly polar molecule), it is coulombic interactions [26] between partial charges on the hydrogen and oxygen atoms in the water molecule in the cavities and the hydrate former's molecule without chemical bonding. The explanation is that the water cavities (inside) have average inward negative charges (i.e., from the oxygen

atom) oppositely facing average positive field on the H₂S molecule's hydrogen atom (ion). Therefore, H₂S is a better and strong hydrate former because of the effect of its polarity [113]. H₂S is a better hydrate former than expected due to the impact of its polarity [113]. More details on H₂S and CO₂ have been presented in [26, 113, 114] and [Paper 5]. Table 2.2 tabulates cavities stabilization factors as summarized in [26].

Table 2.2: Factors of water cavities (empty-hydrate) stabilization

What stabilizes cavities	Reasons
Size and shape	Water lattice cannot collapse because the size and shape prevent it from collapsing.
Water-guest attraction	Helps in holding the water molecule together.
Coulombic interactions	Average extra attraction by reason of some coulombic interactions: in certain situation, like H ₂ S, it gives extra stabilizations in addition to hydrogen bonds as empty hydrate.

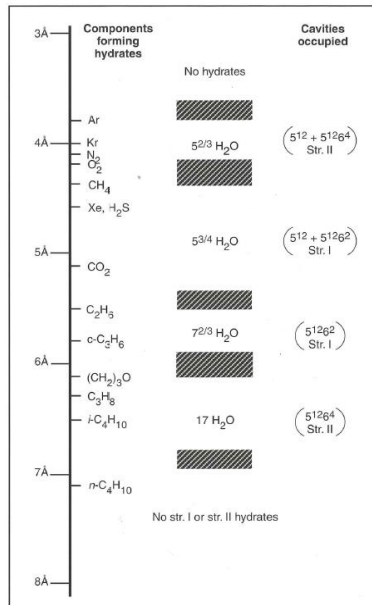


Figure 2.3: Illustration of the relationship between hydrate forming guest molecules size and the hydrate structure type that would be formed [115].

2.4 Applications of gas hydrates

In Section 1.1, that is motivation, gas hydrate is discussed as a problem and as a potential solution to some of man's needs. This section then focuses on some other applications of hydrate in a beneficial way which are discussed in the following subsections. Information in this section was mainly taken from [116].

2.4.1 Storage and transport of natural gas

Storage and transport of natural gas in form of gas hydrates has been demonstrated and considered a good means of natural gas transportation, partly because of gas hydrates being able to have a high concentration of gas [117]. Three steps are involved in this process: producing the hydrate from methane and water, transporting the hydrate to where the gas is needed, and lastly hydrate dissociation to methane and water to recover the natural gas (methane) [118]. To produce the natural gas hydrate, the gas and water are mixed at thermodynamic conditions appropriate for hydrate to form. According to [118], a pressure range of 80 – 100 bar, and temperature range of 2–100 °C are typical. In our publications, [Paper 1 – Paper 6], a temperature range of 0 –7 °C was mostly used based on the expected temperatures of the North Sea. A pressure range of 50 – 250 bar was used because our work focused on pipeline transport of the gas, and these are the usual operations pressures in such situations.

Introduction of surfactant into the solution can speed up the rate of hydrate formation [119-121]. A novel approach for the natural gas hydrate production involves adding heat to a mixture of natural gas and melting ice which will result in formation of hydrate crystals [122]. To keep the hydrates stable during transportation, that is to avoid hydrate dissociation, they are cooled to and maintained at -15 °C at atmospheric pressure, and the carriers are usually insulated [123]. The natural gas is then finally recovered by dissociating (melting) the hydrate, thereby releasing the stored-up gas. The metastability of CH₄ hydrate [122] makes the entire process of storage and transportation possible. Shirota et al. [124] stated that CH₄ hydrate will likely show

metastable characteristic at temperatures between -80 and 75 °C and atmospheric pressure. As long as the pressures are lower and temperature higher than those for liquefaction and compression processes respectively, transport of natural gas by means of hydrates appears to be as feasible as these classical processes. Utilization of surfactant promoters and sH hydrate [125] are now being looked at as a way to increase the gas storage capacity [120, 121, 126].

2.4.2 Marine CO₂ sequestration

Carbon dioxide is responsible for around sixty-four per cent (64 %) of the greenhouse gas effect [127], and anthropogenic activities are responsible for over 6 gigatonnes per year (Gt/yr) [128]. Greenhouse gas effect is irrefutably the cause of global warming [129], thus, there is a key environmental challenge to reduce the amount of CO₂ emission into the atmosphere. Much proportion of CO₂ from several sources can be captured by several techniques for example chemical absorption in amines [128, 130, 131], and then sequestered in geological media and oceans [116, 132, 133]. The sequestration can be accomplished by discharging the CO₂ in water utilizing a procedure adapted to the injection depth [116, 134, 135]. For depth of around 400 metres, CO₂ gas is injected into the water, then it will dissolve in the water [136]. For depths of 1000 – 2000 metres in the ocean, liquid CO₂ will diffuse and dissolve as well [137]. Also, hydrates of CO₂ can form in depths of 500 – 900 metres in seawater rich in CO₂ [135]. Due to the density of the CO₂ hydrates [138] being higher than that of seawater, they will sink towards the bottom of the deep sea where long term stability can be realised [139, 140]. However, marine sequestration of CO₂ is currently is still being experimented [116], which means there is need for more research on CO₂ solubility [135, 141-143], kinetics of CO₂ hydrate formation [138, 139, 144, 145] and the stability of CO₂ hydrate [140, 145, 146]. In [Paper 7], kinetics of CO₂ homogeneous and heterogeneous hydrate formation was studied.

2.4.3 Cool storage application

After the ratification of the Montreal Protocol in 1987 and the signing of the Kyoto Protocol ten years later in 1997, it is now vital for increased research efforts focused on refrigeration systems having less negative effect on the environment. Secondary refrigeration is considered as an auspicious option to tackle the challenge by the control of a lessened load of primary refrigerant (HFCs) in engine room [116]. The capacity of refrigeration transferred to the secondary refrigerant is thus conveyed towards where it is used [147-150]. Applying a phase change material in the secondary refrigerant [151-153] can partly improve the system's exergy [116]. Certainly, the phase change material mostly adds to the heat transport due to the latent heat associated with melting. The secondary refrigerants formed which are in two phase could either be slurries of ice [151, 154-156] or slurries of hydrate [147, 152, 157], where the carrier fluid is an aqueous solution and the phase change material is ice or crystals of hydrate. The first indication of gas hydrates in refrigeration processes was associated with refrigerant (CFC) hydrate formation, which sadly transpired in expansion valves [158]. Nevertheless, gas hydrates were well reconsidered at a later date, particularly for cold storage, having established in different literature that they have high heat of melting [152, 154, 159-162]. Also, because the temperature of the phase transition is more than the freezing point of water [152, 159, 161, 163, 164], utilizing the hydrate energy is obviously important in air conditioning processes.

In addition, slurries of hydrates are able to flow effortlessly through secondary refrigerant loop [147, 152, 157, 159, 165]. Currently, advanced research is being carried out with focused on slurries of hydrates from hydrate formers, for example hydrates formed from TBAB which are better environmentally compared to CFC refrigerant [152]. Efforts are also being invested in applications of hydrate formed from CO₂ at pressures that are moderate [153]. Sloan [166] stated that the enthalpy of hydrate dissociation may be associated with just the structure of its host (and not the kind of hydrate former's molecule), which comprises molecules of water bonded together by hydrogen bonds. But this cannot be so based on our works published in [Paper 8; Paper 10; Paper 11] and other literature that use even Clapeyron and Clausius-Clapeyron equations. The

heat of hydrate dissociation of CO₂ is about 9-10 kJ/mol of guest molecule higher than that of CH₄ according to [Paper 8; Paper 11] which are based on residual thermodynamics. Kang et al. [167] put this difference at 8.4 kJ/ mol of guest molecule and Anderson [9, 168] at 5.1 – 9.6 kJ/ mol of guest molecule.

Kang and Lee [146] have written that there is a possibility of shifting hydrate formed from carbon dioxide and nitrogen from sl to slI if THF is added to the aqueous solution. A Cemagref group is presently studying this property for a further utilization of carbon dioxide hydrate slurry energy [169].

2.4.4 Separation processes

Gas hydrates also find valuable usefulness in desalination or gas-liquid fractionation. The practicability of seawater desalination using gas hydrates has been proven in the 1960s and in the beginning of the 1970s. However, the process was not found to be economically reasonable, thus, there was no advancement to industrial level [43]. The process involves production of hydrate by means of injecting refrigerant into seawater. When the crystals of gas hydrate have been separated from the residual concentrated solution of brine, the hydrate can then be heated to obtain pure water. Some literature [159] have indicated that the hydrate desalination process could be hard to carry out due to the slurry texture of the gas hydrates.

A number of researchers are investigating the potential of gas hydrates in a gas separation process towards capture of CO₂ from flue gas produced from large power plants [170]. The United States Department of Energy (DOE) is working on a CO₂ separation process that uses high pressure [171]. This process pays particular attention to the low temperature SIMTECHE process [116], and it involves mixing of a stream of a shifted synthesis gas (that is carbon dioxide, hydrogen and other gases) and nucleated water (which has been pre-cooled) inside a reactor of carbon dioxide hydrate slurry. Then, the resulting mixture which comprises slurry of carbon dioxide hydrate, hydrogen and other gases enters a hydrate slurry gas separator which splits the stream into two: a stream of slurry of carbon dioxide hydrate and a product gas that is rich in hydrogen.

One more process referred to as hydrate based gas separation has been studied with tetrahydrofuran (THF) as a promoter of hydrate formation [116, 146]. THF helps to lower the hydrate equilibrium pressure and by implication it acts to increase the stability zone of the gas hydrate. The authors stated that the hydrate-based gas separation process helps to ensure a separation of over ninety-nine mole per cent (99 mol%) of carbon dioxide from a flue gas stream. There are many benefits of this process, for example, continuous operations can be done at moderate temperature range of 0 – 100 °C, thus, a possibility of processing higher flows of gas stream.

3 Kinetics of hydrate formation

Hydrate nuclei will not attain thermodynamic stability until they grow up to a certain minimum size known as critical core radius or critical nuclei radius or size. This is usually a random process in respect of movement of molecules and diffusion of heat. Hydrate phase transition is chiefly governed by Gibbs free energy under the constraint of heat and mass transport. The Gibbs free energy change of hydrate phase transition depends on two contrary contributions that competes for dominance. One of the contributions is the “benefit” of a new phase (hydrate) being formed due to phase transition to hydrate being favourable (having the least free energy). This is expressed as $\underline{\Delta G}^{Phase\ transition}$ in equation (3.1). It is free energy per unit volume. The second contribution is the “push work penalty” which is required to push away the old phase (the surroundings) to make space for the hydrate core (the new phase). It is expressed as $\underline{\Delta G}^{Push\ work}$ in equation (3.1) and it is the interface free energy per unit area in Joules/m². The net free energy for these two competing processes at a specific pressure and temperature is given as:

$$\underline{\Delta G}^{Total} = \underline{\Delta G}^{Phase\ transition} + \underline{\Delta G}^{Push\ work} \quad (3.1)$$

Considering the simplest possible crystal geometry, a sphere, having radius R, we will have:

$$\underline{\Delta G}^{Total} = \frac{4}{3}\pi R^3 \rho_N^H \Delta G^{Phase\ transition} + 4\pi R^2 \gamma \quad (3.2)$$

where ρ_N^H denotes the molar density of the hydrate and γ signifies the interface free energy between the hydrate and the surrounding phase. Partial differentiation of (3.1) with respect to R and calculating for the free energy maximum radius (the critical core radius) gives us the usual result:

$$R^* = -\frac{2\gamma}{\rho_N^H \Delta G^{Phasetransition}} \quad (3.3)$$

the superscript * signifies critical nuclei radius or critical core radius. This is the minimum size a hydrate core or nucleus must attain before a steady growth can commence. Classical nucleation theory (CNT) of crystallization or crystal formation can be used to describe the process of hydrate nucleation and growth. This theory was developed in the 1930s. The works of Volmer and Weber [172] and Becker and Döring [173] are acknowledged as the first works. The works of [174] and [175] are also notable in this field. Based on CNT, the kinetics of hydrate phase transitions comprises two physically well-defined stages: nucleation stage and stable growth stage. There is a stage that is normally referred to as a third stage of hydrate formation. It is known as the induction stage, or “onset of massive growth” and it is a result of many different effects [26]. Some literature misinterprets induction times as nucleation times. We have comprehensively discussed this in [Paper 7, Paper 8]. Nucleation is the first stage of hydrate formation when the thermodynamic benefits of hydrate phase transition competes with the penalty of the push work to make space for the new phase. The subsequent transition over to stable growth when the benefits are much more than the penalties occurs after attainment of critical size. Theories of hydrate formation are reviewed in the subsequent sections.

3.1 Hydrate nucleation

Nucleation is a nano-scale process which involves tens to hundreds of molecules gathering and spreading to reach the critical size [33]. Thus, it is difficult to observe. The critical core radius can be about one to five nanometres [26]. Therefore, it is likely that it cannot be measured [176]. The randomness is about the building blocks’ directions and momentum of movement. Transfer of energy also involves random elements though heat transfer will be chiefly be in the fastest directions. The system’s rate of local heat transport dictates the amount of heat that can be transferred from the system in hydrate formation process. This rate is not fast in areas where the concentrations of hydrate guest molecules are high. However, it is fast through water and hydrate [26, 177].

Based on the on the theory of nucleation in crystallization in Mullen [178] and Kashchiev and Firoozabadi [179], two types of nucleation are known: homogenous and heterogeneous nucleation. Homogenous nucleation of hydrate core happens in a single (uniform) phase. This can only usually be observed or achieved in the laboratory. This is not to say it cannot occur, however the solubility of hydrocarbons in water is limited.

CO₂ is more soluble in water compare to hydrocarbons, but it does not adsorb well [26] on rusty surfaces (Hematite) directly. Yet, it can concentrate in structured-adsorbed water on rust/Hematite [26]. Its solubility in a water film outside the layer of water adsorbed on solid surface (Hematite) will also be higher. Hydrate nucleation from CO₂ phase outside the water film can ensue homogeneously in the water film, and heterogeneously from CO₂ adsorbed on the initial hydrate film from below. Thus, it is hard to happen in practice. Nevertheless, it is possible for hydrate nucleation to occur in a homogenous system with a guest molecule dissolved in water [180]. We have a discussion of this in [Paper 7, Paper 8]. An example of homogeneous hydrate nucleation is a situation where hydrate nucleates right in the aqueous phase from guest molecules dissolved in water.

Heterogeneous hydrate nucleation can ensue in the presence of a foreign like a solid surface (e.g., internal walls of pipeline or container). In a situation where the solid surface has some effects on guest molecule and/or water, nucleation can heterogeneously occur at smaller supercoolings than that needed by homogeneous nucleation [33]. Kaolinite (a clay mineral), Hematite (a thermodynamic stable form of rust), and Calcite are characteristic examples of solid surfaces which are active in water adsorption. Guest molecules can be trapped in water absorbed onto solid surfaces. In some situations, they can be directly adsorbed on the mineral surfaces. An example is CO₂ adsorption on Calcite. For materials made of plastic, hydrocarbon wetting will occur and can result in accumulation of guest molecules on the surface of plastic. This will aid hydrate induction as observed by Buanes [181] experimentally. In porous media two types of heterogeneous hydrate may occur; nucleation towards surfaces of mineral will compete nucleation ensuing on the interface between the hydrate former phase and liquid water. This is what we referred to as hydrate I in [Paper 7 – Paper 8]. We do not

imply hydrate structure I (sl) but the first hydrate that will likely form. Stainless steel and other atomistic metals [26] having no charge distributions naturally will be neutral. In our studies we focused on the impacts of internal walls of pipeline which are normally rusty (covered with Hematite) as a route to hydrate formation as presented in [Paper 1-Paper 8]. In pipeline transport of bulk gas (hydrate former phase), it is Hematite (rusty pipeline surfaces) [182] [Paper 1-3, 5-7] that will promote water drop out from the gas stream because the chemical potential of the water adsorbed on Hematite is very low. This is the type of nucleation that we frequently come across in nature and industrial applications.

3.1.1 Theories of hydrate nucleation

Hydrate nucleation is basically modelled in two different viewpoints as documented in literature [183]. What is different with these two perspectives is where nucleation originates from. That is if it is in the liquid water interface or towards the hydrate former side of the interface [183].

Based on these two viewpoints, there are two foremost theories of nucleation of hydrates. The first is presented in [33] and the second is propounded by Kvamme [183] and Long [184]. In the first theory, hydrate nucleation starts with dissolved hydrate formers in liquid water. Water molecules form clusters around the hydrate guest molecule. The clusters will subsequently transform to unit cells, leading to either sl or sII hydrate being form, depending on the type of hydrate former molecule present. This will be followed by eventual amalgamation of the hydrate cores or clusters to reach the critical nuclei radius for stable growth of the hydrate to commence.

However, according to the second theory, hydrate nucleation begins from the hydrate former side of the interface between the gas and water. This is due to the high number of the guest molecules that are needed (maximum of 15 %) inside the hydrate [177]. And it is rare to see a high concentration of gas dissolved in the liquid phase as this. Kvamme in his works [185-187] originally introduced the hypothesis of this second theory. And recent studies using Nuclear Magnetic Resonance (NMR) spectroscopy [188, 189] are in agreement with Kvamme's proposal. Kvamme's [183] studies on

methane hydrate formation showed that nucleation commences from the gas side of the interface and might be most influential in the hydrate formation from the gas (methane) and liquid water with the same conditions studied by [190]. According to [183], this is the only theory that is associated with the initiation of nucleation of hydrate as a surface adsorption process, the studies of Kobayashi [189] from NMR measurements at Rice University in Houston also agree with this theory. The input parameters of the model needed are pressure, temperature, composition of guest molecule, and active interface surface area [183].

This theory which all our works are based on shows that not only one hydrate having uniform composition of the hydrate former, uniform density and uniform chemical potentials is formed at the end, but a variety of hydrate phases will finally form. This is because each of the hydrate phase will have unique density and unique composition of the hydrate former which makes each a unique phase. Figures 3.1 – 3.3 illustrate this theory, showing that heterogeneous hydrate nucleation will commence at the interface (forming hydrate 1, represented as H_1) due to the high concentration of guest molecules at the interface. The blue arrows pointing upward show molecules of water leaving the liquid water phase to the gas phase, and the black arrows pointing downward represent equal number of molecules but of the gas going (dissolving) into the liquid water phase at equilibrium. Hydrate 2 (H_2) will form from the hydrate former dissolved in the liquid water. Homogeneous hydrate formation can occur from the dissolved hydrate former. Thermodynamically, hydrate 3 (H_3) can form from water dissolved in gas phase, but it is highly unlikely to occur due to limited amount of water in the gas phase and heat limitation of the gas phase.

Since hydrate nucleation in real systems are non-equilibrium systems (as explained in Section 4.2), we will analyse these routes of hydrate nucleation based on free energy changes of phase transition. Using a system of only a single hydrate guest molecule (for example methane) and liquid water under conditions beneficial for hydrate formation, and disregarding the impacts of the solid-surface (like rust), we can express the free energy change of the hydrate phase transition (of the first hydrate being formed) at the interface as illustrated in *Figure 3.1* as:

$$\Delta G^{H_1} = \left[x_{H_2O}^{H_1} \left(\mu_{H_2O}^{H_1} (T, P, \bar{x}^{H_1}) - \mu_{H_2O}^{water} (T, P, \bar{x}) \right) + \sum_j x_j^{H_1} \left(\mu_j^{H_1} (T, P, \bar{x}^{H_1}) - \mu_j^{gas} (T, P, \bar{y}^{gas}) \right) \right] \quad (3.4)$$

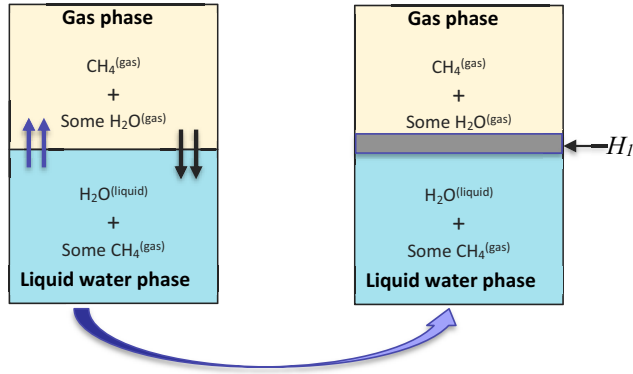


Figure 3.1: Illustration of hydrate nucleation at the interface between gas phase and liquid water phase.

where ΔG is the change in free energy associated with hydrate phase transition. Superscript H_1 implies the specific hydrate phase, superscript *water* denotes the water phase which goes into hydrate formation, and superscript *gas* symbolises the hydrate former's phase x stands for mole-fraction (liquid water phase or hydrate), and y means mole-fraction in hydrate former phase (gas or liquid). The vector (arrow) sign signifies the mole-fraction of every component in its actual phase. Subscript j refers to guest molecules, while subscript H_2O is water. The water phase is normally liquid or ice, but only liquid water is relevant in the systems under investigation. Factors like mass transport of building blocks and heat play vital roles in the formation process. As the initial thin film of hydrate on the water surface develop and closes in, the transport of mass for hydrate formation turns out to be very slow (transport limitation).

The mass transport limitation restricting transport of mass across the interface for the nucleation to continue therefore opens up another route to hydrate nucleation. In this second route, the guest molecule already dissolved in the liquid water will be used for hydrate nucleation. Hydrate nucleation through this H_2 route will be restricted by the

concentration of guest molecule (methane in this case) in the liquid water. However, it is more probable for the nucleation to be heterogeneous at the hydrate/water interface (interface at the water side) because of higher concentrations of the hydrate former (CH_4) at this interface compared to other parts of the water. Nevertheless, homogeneous hydrate nucleation in the water solution is likewise possible. Remembering that we are dealing with non-equilibrium system, the chemical potential of CH_4 dissolved in liquid water will not essentially be equal to the chemical potential of CH_4 of methane in the gas phase (they will be different). Consequently, the composition of hydrate (H_2) formed in this case will be different from that of H_1 . The free energy change related to this hydrate formation (H_2) illustrated in

Figure 3.2 can be expressed as:

$$\Delta G^{H_2} = \left[x_{\text{H}_2\text{O}}^{H_2} \left(\mu_{\text{H}_2\text{O}}^{H_2}(T, P, \bar{x}^{H_2}) - \mu_{\text{H}_2\text{O}}^{\text{water}}(T, P, \bar{x}) \right) + \sum_j x_j^{H_2} \left(\mu_j^{H_2}(T, P, \bar{x}^{H_2}) - \mu_j^{\text{water}}(T, P, \bar{x}) \right) \right] \quad (3.5)$$

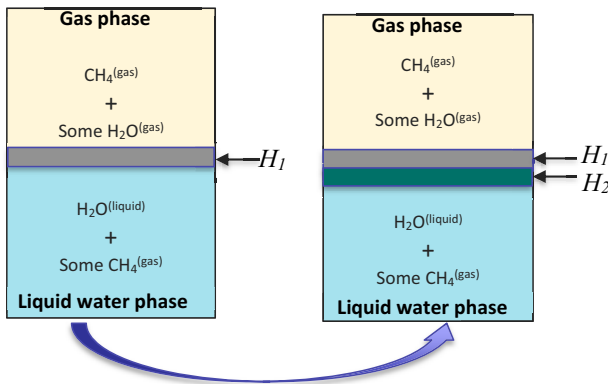


Figure 3.2: Illustration of hydrate nucleation from dissolved hydrate former in liquid water phase.

As already explained above, there is a thermodynamically possible third route to hydrate formation (H_3), but it is not feasible due to the limited amount of water dissolved in the hydrate former's phase. Besides the mass transport limitation, heat transport limitation will also work against hydrate formation in this case since methane is very poor in heat transport (it acts as a heat insulator). And if the exothermic heat of hydrate formation is not transported away from the system, any hydrate formed will dissociate. Although, if water in the hydrate former phase condenses on the initial hydrate film at the interface, then hydrate formation can occur but in limited amount. This H_3 is represented in Figure 3.3 and the associated free energy change is formulated as given in equation (3.6):

$$\Delta G^{H_3} = x_{H_2O}^{H_3} \left(\mu_{H_2O}^{H_3}(T, P, \vec{x}^{H_3}) - \mu_{H_2O}^{gas}(T, P, \vec{y}^{gas}) \right) + \sum_j x_j^{H_3} \left(\mu_j^{H_3}(T, P, \vec{x}^{H_3}) - \mu_j^{gas}(T, P, \vec{y}^{gas}) \right) \quad (3.6)$$

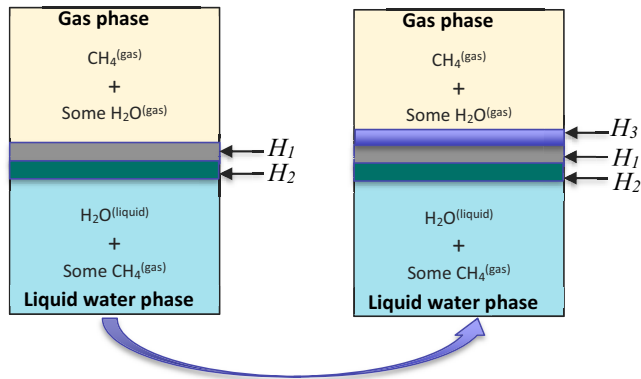


Figure 3.3: Illustration of hydrate nucleation from dissolved water in hydrate former phase.

Besides the two foremost approaches, other modelling perspectives exist. In 1991, Sloan and Fleyfel [191] proposed a model for nucleation of hydrate which they referred to as the Labile Cluster Hypothesis. They hypothesised that nucleation of hydrate occurs in three steps:

- (i) Spontaneous appearance or formation of hydrate cores or clusters from a hydrophobic solute that is dissolved in water in a favourable thermodynamic condition of temperature, pressure and chemical potential for formation of hydrate.
- (ii) Several of the hydrate cores or cluster aggregate and form a hydrate nucleus, where every cluster comprise one gas molecule and 20-24 water molecules.
- (iii) A number of different configurations of hydrate nuclei are formed, though, only a single stable hydrate structure that will be formed and continue to grow.

However, this Labile Cluster Hypothesis has faced severe criticism, it has been faulted [192] based on the high amount of available molecular dynamics and Monte Carlo simulations results. Furthermore, data from experiment using Neutron Diffraction and Differential Scanning Calorimetry [193] showed that the methane hydrated shell enclosing the molecule of methane in hydrate phase is around 1 Å bigger than in solution. Also, the data showed that during formation of hydrate, there is more disorderliness in the shell when compared to in both solution and the hydrate phase, thus typifying significant changes to the hydration shell. Labile clusters are consequently considered to form basically only in dilute solutions and that the energy barrier the clusters need to agglomerate to a critical core radius is high [194].

Christiansen and Sloan [195] also have another approach. In their model, there is no assumption made regarding where the process of nucleation originates or is initiated. They modelled hydrate formation using thermodynamic cycle as a standard chemical reaction, and also used classical thermodynamic relations to model the free energies changes in the cycle leaving from water (liquid) and hydrate formers [183]. Skovborg [196] proposed other macroscopic models based on the ideas of Yousif [197] and Natarajan [198] established on different formulations of the driving forces.

3.2 The hydrate core stable growth stage

This is the second stage of hydrate formation. When the critical nucleus size (and shape) is attained, the stage where the hydrate core undergoes continuous growth

commences. The rate of growth is controlled by accessibility of hydrate formers (the supply of guest molecules) and water, and a coupling of both mass and heat transport [176]. In this stage, the consequence of mass and heat transport is essentially crucial. Based on the simple classical nucleation theory, the mass transport flux is given by:

$$J = J_0 e^{-\beta \Delta G^{Total}} \quad (3.4)$$

$$\text{And } \beta = \frac{1}{R.T} \quad (3.5)$$

where J represents the classical nucleation rate owing to mass transport. J_0 is the mass transport flux supplying building blocks for hydrate growth. And it is either three dimensional (3-D) for homogeneous flux in homogeneous hydrate growth, or it is two dimensional (2-D) in case of heterogeneous formation of hydrate. We have discussed this in [Paper 7, Paper 8]. The consistent heat of hydrate formation released which is coupled to equation (3.4) is given by:

$$\frac{\partial \left[\frac{\Delta G^{Total}}{RT} \right]_{P, \vec{N}}}{\partial T} = - \left[\frac{\Delta H^{Total}}{RT^2} \right] \quad (3.6)$$

where ΔH^{Total} refers to the enthalpy change owing to the phase transition and the related push work penalty. T is temperature in Kelvin, \vec{N} stands for the vector of mole numbers in the system, and R is the universal gas constant which is equal to 8.3143 J/mol·K

The mass transfer of gas (hydrate former) to the hydrate surface will likely dominate in the process of stable growth. Hydrate stable growth can also be controlled by the heat of formation of hydrate. Instead of formation, dissociation can happen if this exothermic heat of hydrate formation is not transported from the system.

3.2.1 Modelling approaches of hydrate stable growth

Englezos et al. and Englezos and Bishnoi [199, 200] have modelled the stable growth stage as a process of crystal growth. It basically assumed that the gas (hydrate former) will move from the vapour phase to the liquid phase. Afterwards, the gas is transported to a reaction site at the surface of the already formed nuclei by diffusion. Then the gas is converted at a specific rate. The rate at which the hydrate former is transported depends on the rate of gas transport and transport of the dissolved gas in the liquid phase like in a 2-film theory. Assuming that the crystals are covered by water (liquid) in this model is a theoretical ambiguity [183]. Skovborg and Rasmussen [201] have simplified this approach and they suggested the use of one rate constant related to the liquid water/hydrate interface region, as well as the differences in mole fraction of the hydrate former both at the bulk and at the interface. Another approach for modelling hydrate stable growth using the classical nucleation theory (CNT) is suggested in [185-187, 202, 203]. In CNT, water chemical potentials in the different phases are computed from the TIP4P [204] model, being aware that simulations of water (liquid) as well as hydrate [205] show that this model is capable to correctly recreate important dynamic features and also chemical potentials.

3.3 Induction time

Induction time is often discussed as the third stage of hydrate formation in literature [176]. This can be viewed as the time for the onset of massive growth of hydrate. Nucleation time or lag time are other terms used in some literatures [33] for induction time. From a physical viewpoint, and based on previous discussion above, induction time is not the same with nucleation time. We have comprehensively discussed this in [Paper 7, Paper 8]. Induction time is rather the time required to establish a stable cluster of hydrate for continuous growth to ensue unconditionally under favourable mass (access to mass) and heat transport in the system (exothermic heat of formation must be transported away). Onset of massive growth is often delayed by some factors, most frequently, mass transport limitations. An example of hydrate formation experiment is presented in Figure 3.2. In this experimental, the resolution was

300 microns, therefore, both nucleation stage and first stages of growth could not be detected. We can observe from Figure 3.2 that the time for onset of massive growth of hydrate is 100 hours or 360000 seconds. This duration cannot be reasonable for hydrate nucleation time. Kvamme et al. [206] and the Ph.D works of Svandal [207] and Buanes [181] are in agreement with this experimental results. While nucleation is a micro-scale phenomenon, induction time is a macro-scale occurrence which can be observed visually. Induction time is the time elapse until a noticeable volume of hydrate phase can be detected.

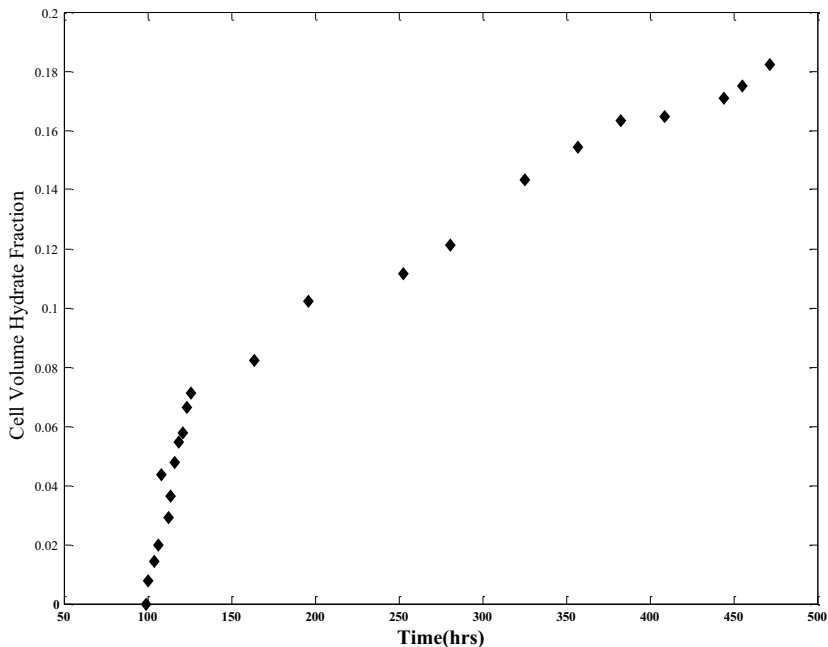


Figure 3.4: Experimental results of CH₄ hydrate formation from water and CH₄ at 1200 psia (83 bar) and 3 °C [206]

Induction time can be detected by measuring the gas consumption in an experiment at controlled pressure and temperature, or reduction of pressure in an experimental cell having where the volume is constant. Various possible techniques exist to detect solid hydrate particles, and therefore, the accuracy of detecting induction time will also vary.

Accuracy of detection depends on the resolution of the monitoring system, whether MRI, laser, or pressure change etc. is used. The work of Haymet and Barlow [208] presented induction times for very similar freezing water that stochastically vary. Therefore, it will be more complicated to predict systems that are more complex like hydrate systems with two or more components, involving two or more different phases. It is only increasing the driving force (subcooling to a higher degree) that could make the system more predictable [166].

Typically, this period occurs due to limited access to mass needed for the hydrate clusters to grow further. Why the induction time could be long sometimes is that when a hydrate film is formed on the interface between water and the gas phase (hydrate former), the hydrate film then acts like a sealing membrane having very slow mass transport (of water and guest molecules) through it. If the system is not stirred to break the hydrate film a number of processes will ensue. One of such processes will be hydrate growing from guest molecules dissolved in water. On the gas side, little amount of hydrate is able to form on the initial hydrate because of water that will be dissolved in the hydrate former phase. Thus, a uniform hydrate film is not expected regarding in respect of free energy. The hydrate regions that are most stable in the hydrate film will consume those that are less stable. Solid surfaces and effects of adsorption are also factors that affects induction time. So, induction period is not one physical process but several of processes controlled by thermodynamics together with mass and heat transport. Induction time can be regarded as the time for “onset of massive growth” of hydrate. Hydrate critical core size is around of 2.5 – 3.5 nanometres [207], that is around 100 – 200 molecules of water, which depends on thermodynamic driving forces and favourable mass transport of building blocks. The transport of heat is fast for the initial hydrate at the interface. The heat transport is over two times [Paper 2] more rapid than transport of mass through the liquid water.

4 Thermodynamics

The focus in this chapter is not to repeat the thermodynamic models used in the project. These have already been comprehensively discussed in each of the papers which form the main part of this thesis. Therefore, this chapter focuses on emphasizing why hydrate formation in industrial systems as well as in nature is a non-equilibrium process, hydrate stability, systems involving phase split and hydrate driving forces.

4.1 Thermodynamics and hydrate formation

Natural gas hydrate is formed from water and hydrate formers under the conditions of low temperature and elevated pressure. Nevertheless, it is Gibbs free energy [26, 209] that dictates the formation process even though other factors such as mass transport of building blocks and transport of the exothermic heat of formation out of the system play very significant roles. For hydrate to form, the new phase free energy, that is the hydrate phase needs to be lower than the free energies of the original hydrate formers phase and the separate water phase, since thermodynamics [Paper 1] favours the process with the least or minimum free energy. Systems will always strive towards or move in the direction of the lowest or minimum Gibbs free energy possible based on the fact that not all systems can reach equilibrium. And hydrate formation in industrial processes and in nature are examples of such processes. Apart from in the laboratory, hydrate formation in real systems (industry and nature) like the ones investigated in this project are non-equilibrium processes. If we look at a very simple scenario of a system which involves only one guest molecule, CH₄ or CO₂ for instance and separate water phase, the free energies of the guest molecule and water in the hydrate phase have to be lower than both of their free energies in their original phases, that is CH₄ or CO₂ in their original phase and water in the separate water phase. In our first paper [Paper 1], we performed a free energy analysis on various hydrocarbon guest molecules based on the combined first and second laws of thermodynamics to show which molecule will preferentially form hydrate first among them. This is however subject to mass transport constraint [Paper 1].

4.2 Gibbs phase rule

A phase can be described as an ensemble of molecules which have unique composition and unique density at a specific thermodynamic condition of temperature and volume. Based on canonical ensemble in statistical mechanics, a phase will also have a unique free energy and other thermodynamic properties as mathematical functions of that coupled to macroscopical thermodynamics [26]. A single phase is uniform, but any phase controlled by fluids having contact with solid surfaces is non-uniform. Water adsorbed on surfaces of mineral will be structured, this is caused by the interactions with surfaces of mineral in one direction (z) and will like to retain strong hydrogen bonding as much as possible in the plane parallel to the surface of the mineral.

Hydrate formation in industrial systems and nature considered in this project cannot successfully reach equilibrium because of the restriction imposed by Gibbs phase rule. To attain thermodynamic equilibrium, the temperature, pressure and chemical potential of every component will be equal in all co-existing phases in the system. Gibbs phase rule is used to determine thermodynamic equilibrium for heterogeneous systems having non-reactive multicomponent. Josiah Willard Gibbs [210, 211] proposed this rule in his revolutionary work. This rule is aimed at evaluating the number of independent thermodynamic properties that are needed to be defined or specified for a thermodynamic system to attain equilibrium. It is simply the balance between independent thermodynamic variables in all coexisting phases minus conservation laws and equilibrium conditions [Paper 1]. It is just a balance between independent variables and governing equations [Paper 1]. The expression for the Gibbs phase rule is:

$$F = C - P_h + 2 \quad (4.1)$$

“ F ” is the degrees of freedom; the defined or specified independent thermodynamic variables in the system. “ P_h ” is the number of actively coexisting phases, and “ C ” is the number of active components in respect of hydrate phase transitions. Any thermodynamic system is under-determined if F is greater than the defined

independent thermodynamic variables. It is over-determined if F is lower than the specified independent thermodynamic variables [212].

To exemplify how to use the Gibbs phase rule, we can begin by using a simple case of only one hydrate former in a system with bulk gas and liquid water. For example, CH₄ and liquid water. If we have a hydrate cluster, we will have three actively coexisting phases, that is P_h is 3, and two active components, C is 2. Using Gibbs phase rule, there will be only one degree of freedom, $F = 1$, for equilibrium to be attained by the system. The system will certainly never get to equilibrium because in real systems like the industrial situations and nature that involve flowing stream, hydrodynamics and hydrostatics, and phase transitions involving exchange of heat, the local temperature and pressure are generally defined. Thus, the simplest system with only one guest molecule will not reach equilibrium.

If we consider a system that involves several hydrate formers, for example CH₄, C₂H₆, C₃H₈, *i*-C₄H₁₀ and water, with no hydrate cluster, that is before nucleation takes place in the system, C will be 5. If we assume no adsorbed phase, then P_h is then 2. Thus, the independent thermodynamic variables required to be defined for the system to reach equilibrium is 5, $F = 5 - 2 + 2 = 5$. This means we have an over-determined system. Likewise, the degrees of freedom will be 4 if we have a hydrate phase ($P_h = 3$) and the same number of active components. Equally, we will end up with an over-determined system which cannot reach equilibrium because the maximum independent variables we can specify are the local pressure and temperature. Consequently, hydrate formation in real industrial systems and nature cannot attain equilibrium. That is the complexity of the system increases when the system in consideration involves a multicomponent bulk gas. Nevertheless, it is imperative to remember that the combined first and second laws of thermodynamics will always direct the system towards the possible least or minimum free energy. Based on the first and second law of thermodynamics, hydrate formation will begin with the most stable hydrate from the best hydrate former in terms of free energy. After the best hydrate former is used up to form hydrate, the inferior guest molecules will afterward form less stable hydrates. At the end we will have a range of different hydrates having gradually increasing free

energies, consequently, will be less stable [176]. The different hydrates are acknowledged as separate or different phases [176] because each of them has a unique composition, density and free energy. Besides, effect of solid surfaces such as water absorbed onto Hematite is also regarded as a separate phase. Consequently, hydrate formation in a real system will never attain thermodynamic equilibrium. Thermodynamic equilibrium is only possible if the number of thermodynamic variables specified are equal to the degrees of freedom, F .

However, we only use Gibbs phase rule to find out the maximum possible number of phases (P_h) when the degrees of freedom are defined. The possibility of these phases existing under any given thermodynamic conditions is not stated by this rule. Gibbs phase rule is merely mass conservation under the constraints of thermodynamic equilibrium [176].

4.3 Hydrate stability from phase diagram

Phase diagrams of hydrate, water (liquid or ice), and guest molecule (gas or liquid) illustrate hydrate stability region in respect of temperature and pressure. These are usually referred to as equilibrium diagrams or curves. In Figure 4.1, the straight-line phase boundaries are merely used to illustrate phase transition behaviours of water and hydrate formers. That is from ice to liquid water, and from gas (or vapour) to liquid hydrate formers. Real phase boundaries are not necessarily straight lines as can be seen in Figure 4.1 and Figure 4.2, they are typically curved as we can observe in Figure 4.3 and Figure 4.4. However, we can obtain straight phase boundary lines or nearly straight phase boundary lines are from logarithm plots [33] as presented in Figure 4.1 and Figure 4.2.

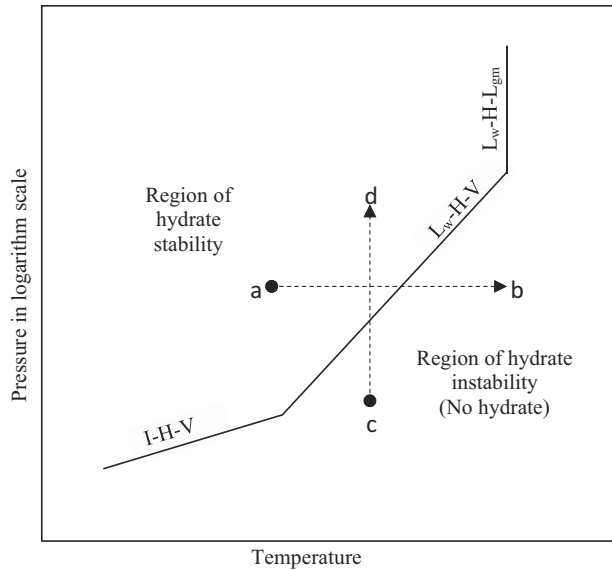


Figure 4.1: Phase diagram for ice, water, hydrate formers and hydrate

In Figure 4.1, “I” refers to water in ice (solid) phase, “L_w” represents liquid water, “H” denotes hydrate phase, “V” signifies hydrate guest molecule (hydrate former) in vapour phase, while “L_{gm}” stands for hydrate guest molecule in liquid phase. Frequently, we read about quadruple points in literatures [33]. They are points of coexistence of four phases and are generally signified by Q_n, where “n” denotes numbers (for example, 1 or 2, for Q₁ or Q₂) to distinguish one quadruple point from the other. Based on the fact that natural gas is mostly methane (CH₄), the phase boundary line of liquid water-hydrate-gas (L_w-H-V) is the most significant pressure-temperature conditions in natural gas operations [33]. The L_w-H-L_{gm} line is vertical and that indicates that the guest molecule experiences phase transition from gas phase to liquid phase at the point where the line turns vertical. These points are represented by A, B, C, D for CO₂, C₂H₆, C₃H₈, and

iC_4H_{10} respectively in Figure 4.2. These are pressure-temperature points where phase split occurs, thus, four phases coexist at these points which are referred to as quadruple points as already explained. In several literature, these points are smoothed out, some stop their experiments or calculations at that point. Smoothing out the point of phase split does not give a true representation of the real system. The slope of the phase boundary line denoted by I-H-V is less than that of the L_w -H-V phase boundary line.

In Figure 4.1, hydrates are stable at the left-hand-side of the I-H-V + L_w -H-V + L_w -H- L_{gm} phase boundary line, but unstable at the right-hand-side. Therefore, the broken line with an arrow from point “a” to “b” illustrates hydrate dissociation by means of increase in temperature (the constant pressure is just for simple illustration). Similarly, broken line “c” to “d” shows hydrate formation due to increase in pressure (constant temperature assumed just for illustration).

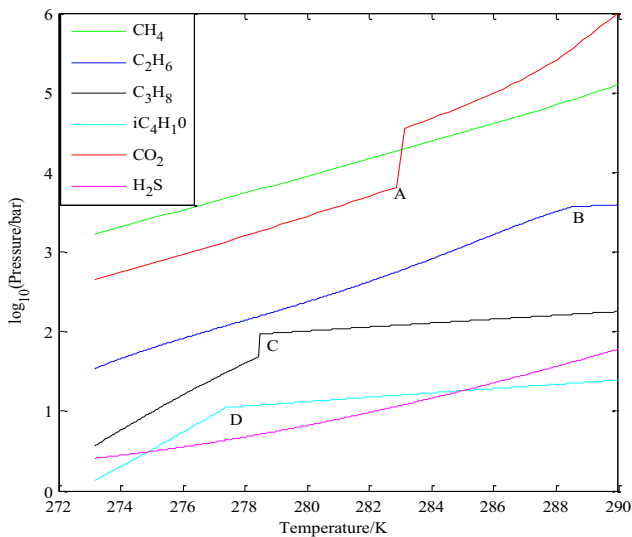


Figure 4.2: Hydrate equilibrium curves for methane, ethane, propane, isobutene, carbon dioxide and hydrogen sulphide.

The main significance of Figure 4.2 is to show and compare different hydrate formers hydrate stability P-T conditions and occurrence of phase split (from gas to liquid). The pressure is in logarithm to base 10 to enable us to observe a clearer picture

of the difference. All the important hydrate formers involved in our publications are represented in Figure 4.2. They are methane, ethane, propane, isobutane, carbon dioxide and hydrogen sulphide. The two most important hydrate formers in this project are methane and carbon dioxide. Thus, we have plotted their P-T equilibrium curves using our thermodynamic scheme and compared our estimations with literature in Figure 4.3 for methane and Figure 4.4 for carbon dioxide. In Figure 4.4, the experimental work of Ohgaki et al. [213] also show a change to liquid CO₂ but it occurred about 1 K (1°C) less than our estimate. Anderson [214] calculation probably indicates an assumption of gas phase beyond the point of phase split. A comprehensive explanation of this occurrence is given in [Paper 3]. We also observe it in the works published [Paper 9, Paper 11, Paper 12].

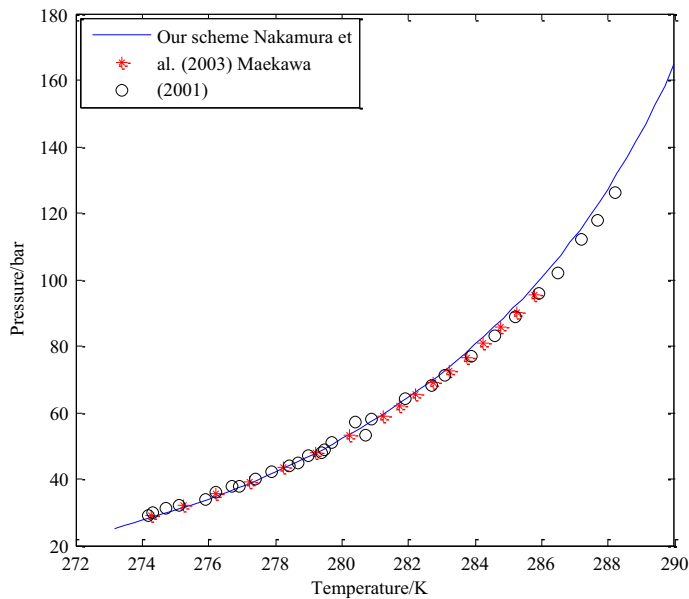


Figure 4.3: Methane hydrate equilibrium curve compared with literature [215, 216]

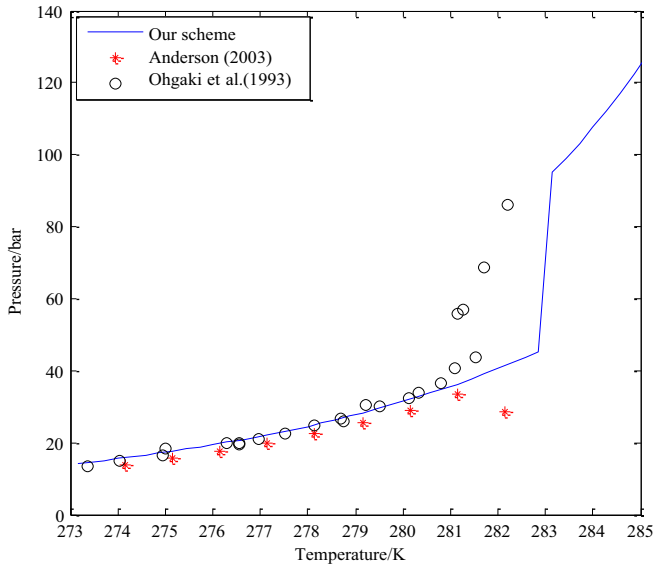


Figure 4.4: Carbon dioxide hydrate equilibrium curve compared with literature [213, 214]

4.4 Hydrate formation driving forces

Pressure and temperature are not just the only hydrate formation driving forces, kinetics of the process as well poses a limitation during formation of hydrate [176, 177]. Sufficient mass necessary for hydrate to grow must be available and be transported from other existing phases into the hydrate. A number of hydrate formation driving forces are recorded in literature [201, 217-222]. Nevertheless, not much of them give satisfactory justifications [33] for these driving forces based on equilibrium or non-equilibrium thermodynamics. Qorbani et al. [223] have presented a lists of hydrate formation driving forces for alternative routes to formation and dissociation of hydrates useful for gas pipeline transport situations in respect of their associated free energy changes in *Table 4.1* *Table 4.1: List of driving forces for formation and dissociation of hydrate* [223].

Table 4.1: List of driving forces for formation and dissociation of hydrate [223].

i	δ	Initial phase(s)	Driving force	Final phase(s)
1	-1	Hydrate	Outside stability in terms of local P and/or T	Gas, water, Liquid water
2	-1	Hydrate	Sublimation (gas under saturated with water)	Gas
3	-1	Hydrate	Outside liquid water under saturated with respect to Methane and/or other enclathrated impurities originating from the methane phase	Liquid water, (Gas)
4	-1	Hydrate	Hydrate gets in contact with solid walls at which adsorbed water have lower chemical potential than hydrate water	Liquid water, Gas
5	1	Gas/fluid	Hydrate more stable than water and hydrate formers in the fluid phase	Hydrate
6	1	Gas + Liquid water	Hydrate more stable than condensed water and hydrate formers from gas/fluid	Hydrate
7	1	Surface reformation	Non-uniform hydrate rearranges due to mass limitations (lower free energy hydrate particles consumes mass from hydrates of higher free energy)	Hydrate
8	1	Aqueous Phase	Liquid water super saturated with methane and/or other hydrate formers, with reference to hydrate free energy	Hydrate
9	1	Adsorbed	Adsorbed water on rust forms hydrate with adsorbed hydrate formers.	Hydrate
10	1	Adsorbed +fluid	Water and hydrate formers from gas/fluid forms hydrate	Hydrate

4.5 Hydrate thermodynamics

The chemical potential of water in hydrate is usually evaluated applying the statistical mechanical model. This is a typical Langmuir type of adsorption model. van der Waals and Platteeuw [93] were the first to develop a thermodynamic model from statistical mechanics in 1958, with the aim evaluating or predicting gas hydrate phase equilibria. It is typically a Langmuir type of adsorption model (as mentioned above) generally applied for the description of ideal localised adsorption. The developed their model based mainly on the following assumptions:

- a) a cavity can be occupied merely by one hydrate former molecule.

- b) the movement of a hydrate former's molecule in its cavity is not dependent on the number and types of the hydrate formers' molecules that are available.
- c) interactions between water cavities (the hosts) and molecules of entrapped hydrate formers (the guests) are weak van der Waals forces, that they only extend to the initial shell of water molecules surrounding each molecule of a hydrate former (guest to guest interactions between different cavities are also not considered).
- d) the molecule of hydrate former does not distort the hydrate.

The model is given in equation (4.2) and (4.3)

$$y_{k_i} = \frac{C_{k_i} f_k}{1 + \sum_J C_{J_i} f_J} \quad (4.2)$$

$$\mu_Q = \mu_Q^\beta + mT \sum_i v_i \ln(1 - \sum_k y_{k_i}) \quad (4.3)$$

Where f_k denotes the fugacity of solute k , y_{k_i} refers to composition, that is occupancy by guest molecule k or the probability of a solute (gas) molecule k occupying a host (water) cavity of type i , and μ_Q stands for the chemical potential of water in hydrate. μ_Q^β signifies the chemical potential of the empty hydrate (that is without guest molecule occupation). And C_{k_i} refers to an equilibrium constant for the k th type of hydrate former (guest) or the J th type of hydrate former for C_{J_i} in the i th cavity type. While v_i denotes the number of type i cavities per water molecule in the lattice of the hydrate.

This model works well near the ice point of water; however, substantial deviations occur going far beyond the ice point. Regardless of the limitations and simplicity of the model, other newer models developed are still based on it [43]. In 1972, Parrish and Prausnitz [224] extended the van der Waals and Platteeuw model to multi-component gas mixtures. Klauda and Sandler [225] formulated a classical thermodynamic method in 2000 to evaluate hydrate phase behaviour. This model increases accuracy because the reference energy parameters required in the model of van der Waals and Platteeuw is eliminated [226]. An approach founded on the phonon properties of crystals applied

for direct estimation of water lattice's free energy, eliminating van der Waals and Platteeuw's assumption of no lattice relaxation was formulated by Westacott and Rodger [227]. This model can be applied to evaluate phase diagrams of hydrate when used with an equation of state. Another thermodynamic formulation that considers the impact of lattice stretching as a consequence of the size of guest molecule on the reference chemical potential difference between the lattice of empty hydrate and water (ice or liquid water) has also been done by Zele et al. [228]. Molecular dynamics (MD) simulations at constant pressure was utilized to evaluate the new reference chemical potential difference for prediction of the hydrate equilibrium conditions for one component and multi-components gas. The MD simulations indicated a slight expansion of the hydrate lattice when hydrate formers with larger molecules are present. This agrees with some experiments [226], for example, the findings indicate that the lattice constant for a hydrate formed from krypton, a structure II hydrate is 1.69 nanometres, which increases to 1.76 nanometres in the case of another hydrate structure II formed from isobutane.

In this project, all our studies documented in [Paper 1– Paper 11] used the Kvamme & Tanaka's model [186] given in equation (4.4). This formulation considers movements of the lattice and corresponding impacts of different guest molecules; it considers collisions between molecules of hydrate formers and water which are adequately strong to have effect on water motions. We need to remember that the more general van der Waal and Platteeuw's model [93] assumes "rigid lattice"- the assumption is that water movements in the lattice are not affected by the molecule of hydrate former, represented as j .

$$\mu_{H_2O}^{(H)} = \mu_{H_2O}^{(0,H)} - R.T \sum_{i=1}^2 v_i \ln \left(1 + \sum_{j=1}^{n_{guest}} h_{ij} \right) \quad (4.4)$$

Where superscript H represents the hydrate phase. Thus, $\mu_{H_2O}^{(H)}$ is chemical potential of water in hydrate, and $\mu_{H_2O}^{(0,H)}$ is chemical potential of water in empty hydrate structure. v_i denotes fraction of cavity type i per water molecule, h_{ij} stand for canonical cavity

partition function of component j in cavity type i , and n_{guest} is number of guest molecules in the system.

The unit cell of sl hydrate has 46 molecules of water. The sl hydrate has 2 small and 6 large cages, thus, $v_{small} = 1/23$ and $v_{large} = 3/23$. The canonical partition function is evaluated from the relation in equation (4.3):

$$h_{ij} = e^{-\beta(\mu_i^H - \Delta g_{ij}^{inc})} \quad (4.5)$$

And
$$\beta = \frac{1}{R.T} \quad (4.6)$$

R is universal gas constant, and T is temperature. Δg_{ij}^{inc} represents the impacts on hydrate water from inclusion of the molecules j of the hydrate former in the cavity i [112, 186].

5 Procedure, project and publications

5.1 Scientific method

Comprehensive details of the scheme used in this project are given in each of the papers presented in this thesis. Therefore, only a brief description of and explanation of why we used the method used is necessary. The main scientific method used in this project is classical thermodynamics but based on thermodynamic properties calculated using methods in Quantum Mechanics and Classical Mechanics. We used classical thermodynamics together with residual thermodynamics description for every phase; this includes the hydrate phase, to analyse different routes to hydrate formation between hydrate formers (or guest molecules) and water.

The systems investigated in this project, that is hydrate formation or dissociation in pipelines and nature (in-situ hydrates) comprise adsorbed phase, water phase, gas (or vapour) phase and hydrate phase. Based on restriction by the Gibbs phase rule, these systems cannot reach equilibrium. Which implies these systems are not governed by equilibrium. More details can be found in the papers, especially [Paper 1]. Consequently, free energy minimization method in classical thermodynamics is the right choice of scientific method for this project. Since we are talking about non-equilibrium systems, a primary tool for comparison must be minimization of free energy. Rigorous free energy minimization technique entails programming fairly extensive computer code. Nonetheless, a simplified approximation to this kind of approach is to compare possible phase transitions and analyse each in terms of changes in free energy, and qualitatively there will possibly be some heat and mass transport challenges. Using the same reference state for analysis is also necessary. We do this by using chemical potential of liquid water and that of empty hydrate structures. This is based on the molecular dynamics simulation works of Kvamme and Tanaka [186]. The gas/fluid phase analysis is implemented based on residual thermodynamics, applying Soave-Redlich-Kwong (SRK) equation of state [229] and ideal gas as a reference state. Residual thermodynamics helps to evaluate the real gas behaviour based on thermodynamic deviations from ideal gas behaviour [207]. Additional merit of a discrete evaluation of

possible routes to hydrate formation based on free energy gain (for formation of hydrate), and consideration of related heat and mass transport aspects is that these kinds of evaluations will be uncomplicated and easy to implement in industrial hydrate risk evaluation tools in the thermodynamic software (that is as extensions).

Classical nucleation theory (CNT) has been used for the hydrate formation/dissociation kinetics analysis in this project. It enables us to separate the thermodynamic impact and the mass transport. Therefore, the possibility to construct mass transport models that are based on theoretical work and molecular (MD) simulations, yet end up as numerically simple models which can simply be implemented as extensions of previously existing codes or software for hydrate risk evaluation. See [Paper 7, Paper 8], especially the discussion sections.

Non-equilibrium systems can be effectively evaluated using more advance theoretical concepts like the Multicomponent Diffuse Interface Theory (MDIT) [230, 231], which is based on changes in structure for determination of kinetic rate; or the Phase Field Theory (PFT) [232-235] that is based on both structure and free energy (canonical ensemble). Nevertheless, CNT presents a more perceptible or visible distinction between the various contributions and gives better illustration of hydrate nucleation as indeed a nano-scale phenomenon. Also, that the usual long induction times observed during hydrate formation is principally due to mass transport limitations through hydrate films and/or a non-equilibrium process which results in hydrate dissociation when there is contact with under saturated phases. CNT makes it easier to illustrate the variation of hydrates that can possibly form in a real system, in addition to seeing a better picture of critical nuclei sizes and nucleation times. The CNT is an easy scheme to illustrate the coupled mass transport and thermodynamic control of the kinetics of hydrate phase transition. With CNT, it is more easy to illustrate to people who are not well versed in statistical mechanics. The equations are simple enough to be extended into hydrate risk evaluation software and in reservoir simulators (already implemented into the group's in-house simulator). Moreover, previous hydrate kinetics works in this group have used MDIT [230] and PFT [20, 207, 209, 232-235].

5.2 The PhD project and publications

The focus of this project is application of the group's already developed thermodynamic scheme to study hydrate risk in industrial systems, thermodynamics and kinetics of hydrate formation, and simultaneous production of CH₄ from in-situ hydrate and CO₂ long-term storage as hydrate.

The first study in the first part of the PhD project, hydrate risk analysis with focus on the impact of solid surfaces (rust) was carried out based on a gas mixture containing CH₄, C₂H₆, C₃H₈, i-C₄H₁₀. The results are published in [Paper 1]. Aromada and Kvamme [Paper 1] also presents information about non-uniform hydrate formation and free energy analysis for evaluation of hydrate distributions during transport of hydrate forming mixtures. The compositions used in [Paper 1] were not based on any real gas field data. A new study was conducted using a real gas field data. Composition data of Troll gas [236] from the North Sea, which consist of mainly hydrocarbon hydrate formers of sl and sII, with a very high concentration of CH₄ were used for the study published in [Paper 2].

Natural gas sometimes contains inorganics like CO₂. Thus, there was a need to investigate the impact of having inorganic gas in the bulk gas. Sleipner gas was selected as a case study for this, and the results are published in [Paper 3]. Analysis of systems which exhibit phase split during transport and hydrate forming conditions during processing was also done in [Paper 3]. Some literature [237-241] assume uniform phase at all thermodynamic conditions or stop their analysis just at the point of phase-split (quadruple point). Analysis involving phase-split, that is quadruple points and beyond were also done in some of the subsequent studies.

Natuna gas field also contains CO₂ but over 70 per cent (70 %) which makes it very different from Sleipner gas, thus, a hydrate prevention study was conducted on it and the results are published in [Paper 4]. Carbon dioxide and hydrogen sulphide are very good hydrate formers, more aggressive hydrate formers than the hydrocarbons, and they could be present in natural gas streams. So, investigation of the impacts of these two inorganic gases was also done. The results are published in [Paper 5].

Another hydrate risk analysis was conducted on a wet-gas subsea pipeline that occasionally experience plugging by hydrate in China [18]. The results were presented at the 10th EUROSIM2019 congress in Spain. The full paper which is [Paper 6] will be published in the proceedings. Even though [Papers 7, Paper 8] are mainly works in the second part of the project, which focus on the kinetics of hydrate formation (nucleation, growth and induction time), we also highlighted the impacts of solid surface (rust) on the upper limit of water that can be permitted in both the CO₂ stream and natural gas stream respectively in these papers. Europipe I [28, 29] and Europipe II [22, 23] in the North Sea were used for the hydrate risk studies presented in [Paper 7, Paper 8] respectively.

In the second part of this project we focused on the second main objective, kinetics of hydrate formation. That is hydrate nucleation times, growth and induction period. The studies were done for CO₂ [Paper 7] and methane [Paper 8]. Nucleation times of hydrate are very fast, they happen in the nanoseconds range.

The third part of the project focuses on enthalpies of hydrate phase transition, as a potential means for simultaneous production of CH₄ from in-situ CH₄ hydrate and long-term CO₂ storage. We found out that in several literature, enthalpies data obtained directly or indirectly for hydrate formation and dissociation are limited. And relevant information needed for proper interpretation are often lacking. Owing to the limitations associated with current methods, we propose a solution by using residual thermodynamics for evaluation of enthalpy changes of hydrate phase transitions in [Paper 9]. Part of the work which involved only methane hydrate formation was presented at the 10th EUROSIM2019 congress in Spain, and it is published in Simulation Notes Europe Journal [Paper 10]. A study focused on the implication of enthalpies of methane and CO₂ hydrate phase transitions, and their free energies (to show the more stable hydrate) in simultaneous CH₄ production from in-situ CH₄ hydrate and long-term CO₂ hydrate was conducted. The results were also presented at the 10th EUROSIM2019 Congress in Spain [Paper 11]. In the final paper, that is [Paper 12], we re-emphasize the use of residual thermodynamics for evaluating enthalpy changes of hydrate phase transitions and we did a more comprehensive analysis of applications of these enthalpy

changes in CH₄ – CO₂ swap. These twelve papers are summarized in Section 6, and how the publications fulfil each part of the Ph.D. project is illustrated in Figure 5.1.

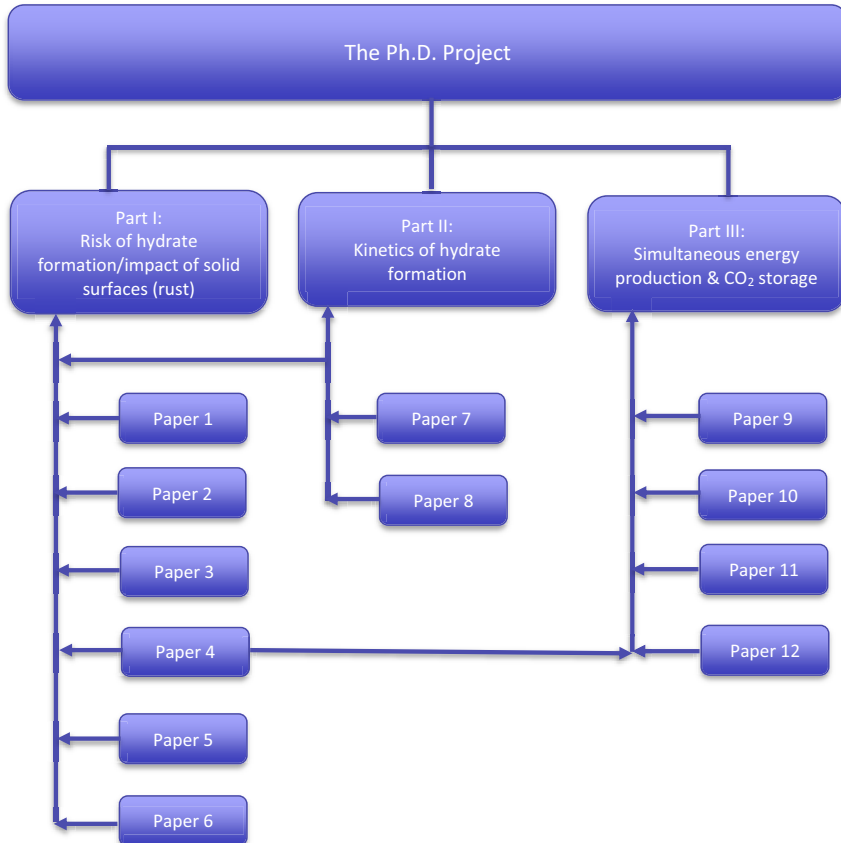


Figure 5.1: The Ph.D. project and publications. Arrow connects each paper to the part of the project it fulfils

6 Summary of papers

This chapter contains a summary of each paper in this project. The reason each paper was written (the objective it fulfils), what was done, and the outcome are stated in the summary of each paper. The summary is arranged according to paper numbers, such that Paper 1 is Section 6.1. The summary of Paper is Section 6.2 and so on.

6.1 New approach for evaluating the risk of hydrate formation during transport of hydrocarbon hydrate formers of SI and SII

The primary focus of this first work is to evaluate the impact of rusty surfaces on maximum limits of water that can be permitted to flow with hydrocarbons during processing and pipeline transport without the risk of water dropping out of the bulk gas and eventually leading to hydrate formation. This is because currently the industry evaluates the risk of hydrate formation using water dew point calculations, without acknowledging the effects of the presence of rust on the surfaces of the internal walls of gas pipelines and gas process equipment. Even before pipelines are mounted in place for natural gas transport operations, they are already rusty. When we talk about rust in all the studies, we refer to Hematite which is one of the most thermodynamically stable form of iron oxide. In this study, we refer to the dew point approach as “Route 1” for hydrate formation, while we call the second method which involves water dropping out on rusty surfaces through the mechanism of adsorption “Route 2” for hydrate formation. The rusty surfaces work as a catalyst to pull-out water from the bulk gas stream, thereby making water available for hydrate to form. Hence, a new approach for evaluation of the risk of hydrate formation based on water adsorbing on hematite.

The investigations of upper limits of water were based on only hydrocarbon guest molecules; pure and mixtures of hydrate Structures I and structure II hydrocarbon, namely, methane, ethane, propane, and isobutane. The study indicates that the safe limit of water mole fractions in pure hydrocarbons based on Route 1 is about 19 times higher than that estimated using the new approach of Route 2 at 274 K. The value

obtained applying Route 1 is approximately 18 times higher than that with Route 2 at 280 K. The results clearly show that water will choose to drop out more easily through the process of adsorption onto rusty surfaces than dropping out below dew-point conditions. Similar values were estimated for a mixture of the four hydrocarbon components. A sensitivity analysis revealed the effects of the Structure II hydrocarbon guest molecules in binary mixtures with methane. The allowable maximum mole-fraction of water in the gas mixture decreases with increasing concentrations of propane and isobutane with the heavier isobutane having more impact. These suggest that the presence of Structure II hydrate guest molecules in considerable amounts in natural gas may cause a decrease in the safe-limit of water compared to that of pure methane of methane highly dominated gas mixture.

Another major objective of this work was to conduct a free energy analysis to qualitatively give insight into the selectivity of the different hydrocarbons during hydrate formation. With this analysis, we able to visualize the nonuniform hydrate formation characteristic in real situations. That is to show which hydrate former will form hydrate first based on the combined first and second laws of thermodynamics in terms of Gibbs free energy. Based on the first and second laws of thermodynamics, the most stable hydrate will form first from a multicomponent mixture, under constraints of mass and heat transport. That is the one with the least or minimum free energy. Thermodynamic systems proceed in the direction of the least free energy as function of pressure, temperature, and distribution of masses in the system over possible phases, under the constraints of mass and heat transport. The structure II hydrate formers will therefore go into hydrate first and they form more stable hydrate compared to particularly methane.

This study simply suggests that the new route to hydrate formation involving adsorption of water onto the internal walls of pipelines covered by rust (Hematite) totally dominates. Consequently, this route of liquid water adsorption onto rusty surfaces could have a considerable impact on the design parameters in natural gas dehydration systems.

6.2 Risk of hydrate formation during the processing and transport of Troll gas from the North Sea.

The main objective of the work documented in this paper is also to investigate the impact of rusty surfaces on the upper-limits of water (in vapour phase) that can be allowed in natural gas streams during processing and pipeline transport to avoid the risk of condensation of liquid water from the bulk gas, as that would lead to hydrate formation. In this study, we used real natural gas field molar composition data, data of Troll gas field in the North Sea of Norway. We used the molar composition data of Troll gas well-head fluid and of Separator 1 from Statoil (Norway). Troll gas is very rich in methane, having about 96 per cent of methane and negligible amount of all hydrate formers and no CO₂ or H₂S.

Like in other publications, we gave a detailed description of the equations that make up the thermodynamic scheme. We also extensively and systematically performed model verification on pure hydrocarbon hydrate guest molecules and multicomponent mixtures of hydrocarbon hydrate formers by comparing the estimates of equilibrium pressures (equilibrium curves) with experimental data. And we observed a very good agreement without any form of data fitting. Molar free energy was also computed for the hydrate and water chemical potential as a function of temperature for the equilibrium pressures to show their thermodynamic stability along the equilibrium curve in non-equilibrium perspective. This is important because the systems under investigation cannot attain equilibrium. A discussion of the three thermodynamically possible routes to hydrate formation was also done: water condensation at or below dew point conditions, adsorption of water onto hematite (rust-solid surface) and direct hydrate formation from water vapour dissolved or dispersed in the gas phase. The direct route is only thermodynamically possible, in real situation it is highly unlikely due to especially mass transport limitation. Heat transport will also pose a barrier. Therefore, this third route is not investigated in this work and most of the other studies that are parts of this project. Our investigations cover a pressure range of 5000 – 25000 kPa and

temperature range of 273-280 K because they represent the operation conditions in the North Sea of Norway.

The trends from our investigations based on the dew point water drop out which is the current industrial hydrate risk evaluation approach compared with those based on the new approach of adsorption of water on Hematite are very clear. The latter clearly dominates. Results of the dew point calculations of the maximum mole-fractions of water vapour that can be permitted in the troll gas are about 18 to 19 times higher than the estimates using the approach of water onto solid surfaces (rust), depending on the pressure-temperature conditions and composition. This can be explained from chemical potential perspective. Earlier work suggested that absorbed water on Hematite may have a chemical potential of 3.4 kJ/mol more negative than that of liquid water. And thermodynamic systems strive towards the least or minimum free energy as function of pressure, temperature, and distribution of masses in the system over possible phases, under the constraints of mass and heat transport according to the combined first and second laws of thermodynamics. Despite that hematite routes dominates water drop out process, and thus very significant in hydrate nucleation, the very low chemical potential of the first three to four layers of the water absorbed on the solid surface (Hematite) makes it impossible for initial hydrate nuclei to attach directly to the hematite, but on absorbed water above the first 3 – 4 layers.

The solubility of water in hydrocarbons is sensitive to the system's density and composition. Thus, the solubility of water in the heavier hydrocarbon (C₂₊) increases, therefore, the safe-limit of water increases accordingly, in contrast to the light systems of methane where the upper-limit of water decrease with increasing pressure. The reverse is the case for the higher hydrocarbons. In addition to the solubility explanation, the opposite trends observed for the C₂₊ compared to CH₄ is also because of the high-density nonpolar phase of the higher hydrocarbons at higher pressures. This is revealed in a sensitivity analysis of the C₂₊. The sensitivity analysis also shows that the dew-point method over-estimates safe-limit of water in the gas in the order of 20. This calls for a concern if we must operate without the risk of hydrate formation.

6.3 Alternative routes to hydrate formation during processing and transport of natural gas with a significant amount of CO₂: Sleipner gas as a case study

In this study, the main aim is to study another gas system that has substantial amount of higher hydrocarbon hydrate formers (propane and isobutane) and an inorganic gas, CO₂ in this case. We found Sleipner gas to be appropriate for the analysis of the impacts of higher hydrocarbons and CO₂ (an inorganic gas) on water tolerance during processing and pipeline transport of natural gas. What is unique is that Sleipner gas has CO₂, less methane and significant concentration of higher hydrocarbons (C₂₊) compared to the Troll gas. In production and processing of Sleipner gas, over one million tons of CO₂ are transported and injected into Utsira formation in the North Sea every year. And since 1996, more than 16 million tons have been injected into Utsira Formation.

Our finding is that no remarkable differences in water tolerance between the Sleipner gas with CO₂ and without CO₂. The water tolerance in Sleipner gas without CO₂ compared with that with CO₂ is very negligible, it is not up to 0.1 %. The explanation is based on the fact that both cases are methane-dominated. The mole-fraction of CO₂ used is just around 0.035, and both CH₄ and CO₂ exhibit similar trends within the pressure range of 5000 – 25000 kPa investigated. The water tolerance of pure methane and pure carbon dioxide were also investigated and comparing the estimates, only a very insignificant shift in the absolute values is observed, methane having the very slightly higher values.

The trends of water tolerance of the pure components of hydrate structure I hydrate formers (methane and CO₂), the safe limit of water decreases with increase in pressure. Same results are obtained for the Sleipner gas studied showing its methane-dominance. The heavier structure II hydrate formers (propane and isobutane) cause the water tolerance of the Sleipner gas stream to become relatively insensitive to further increase in pressure from 13000 to 25000 kPa, in contrast with the case of the pure CH₄ and CO₂. The C₂₊ (C₃H₈ and iC₄H₁₀ in this case), also exhibit opposite trends due to

solubility implication and resistance to pressure because of the high-density nonpolar phase at higher pressures. This can also be seen in both [Paper 1, Paper 2]. The presence of the heavier hydrocarbons also results in a slight shift in the absolute values of the upper limit of the allowable mole fractions of water even at 5000 and 9000 kPa. A sensitivity analysis of the mole fractions of water that can be permitted at varying concentrations of the higher hydrocarbons of propane and isobutane (structure II guest molecules) are also examined. The nonpolar heavier hydrocarbons act to draw down the water tolerance of the gas mixture to a point where they completely dominate or dictate the trends. This can also be observed in [Paper 2], especially in the sensitivity analysis section.

We applied both the dew point method and the technique of adsorption of water onto Hematite. From the alternative approach of adsorption of water onto Hematite, the dew point methods over-estimates the maximum concentration of water allowable in the Sleipner gas system in the order of more than 18 times.

In this study, we also show that hydrate forming systems can exhibit phase split. That is the hydrate former originally in gas phase can split into two phase, gas and liquid phase at higher pressure-temperature condition, unlike the uniform phase that is reported in several literature. We observed this using our inhouse software and other commercial software. This means different hydrate phases are expected to form from this kind of system, since the hydrate that will form from each phase will have different composition of the original hydrate former and different densities. By definition, a phase can be described as an ensemble of molecules which have unique composition and unique density at a specific thermodynamic condition of temperature and volume.

6.4 Maximum tolerance for water content at various stages of a Natuna production.

This study was conducted because of the uniqueness of the composition of Natuna gas and the area the gas field is located, which are very relevant to this project. The Natuna gas contains over 70 per cent of CO₂. Therefore, we considered separation of the gas into two streams: methane-rich stream and CO₂-rich stream. We performed hydrate risk analysis on the original reservoir stream containing about 71 % CO₂, the methane-rich stream and the CO₂-rich stream. Like the three previous studies, the analysis was based on the maximum amount of water that can be permitted to flow with the gas streams without the risk of liquid water either dropping out at or below dew-point and by mechanism of adsorption of water onto rusty internal walls of gas transmission pipelines. The hydrate risk estimates for the three gas similarly indicate that the application of the dew-point criterion over-estimates the safe-limit of water in all the gas streams over 18 times when compared to using the approach of adsorption of water onto Hematite (rusty surfaces).

One of the challenges we have to look at is, “how to utilise the large amount of CO₂ produced together with the Natuna natural gas”. Indonesia is fortunate because significant amount of naturally occurring gas hydrate has been found at around 1127 km (700 miles) from Natuna gas field. This makes gas transmission pipeline economically feasible. Therefore, we can consider utilisation of the CO₂ for production of the methane as source of energy while storing the CO₂ for long term in form of hydrate. The data collected by Jackson (2004) indicates that the hydrates occurs at a depth of 2.45 km spreading to area of 8000 m². With information about the properties of seafloor and crust, we are able to estimate the pressure and temperature gradients of the reservoir. This led us to a pressure range of 200 – 250 bar and a temperature range of 274 – 282 K. Direct solid-state CO₂-CH₄ exchange (swap) has been demonstrated, but practically, it will be tremendously restricted kinetically and is not significant. Pilot tests have been conducted in Alaska (U.S.A.) where nitrogen gas has been mixed with CO₂ to reduce the thermodynamic driving force, in order to avoid the normal rapid CO₂ hydrate formation. We evaluated the proportion of CO₂ in the CO₂/N₂ mixture that will ensure successful

conversion of CH₄ hydrate to CO₂ hydrate without the risk of rapid formation of CO₂ hydrate that can eventually block further supply of CO₂. Even though Natuna gas may not have H₂S or significant H₂S, the impact of H₂S, a very vigorous hydrate former was also investigated. The amount of CO₂ that will be needed in mixture with N₂ required by the solid-state swap mechanism is around 5 – 12 % when H₂S is not present in the gas stream. However, introducing only 0.5 % of H₂S into the gas mixture will cause the required composition of CO₂ to reduce to only 4 – 5 %, and 2 – 3 % when 1 % of H₂S is considered.

6.5 Impacts of CO₂ and H₂S on the risk of hydrate formation during pipeline transport of natural gas.

One of the objectives of this PhD project is to evaluate the impacts different hydrate guest molecules will have on the upper limit of water to prevent the risk of hydrate formation. This has been evaluated for the hydrocarbon hydrate forming molecules in [Paper 1]. Natural gas in most cases includes some inorganic components that form hydrate like CO₂ and H₂S. CO₂ and H₂S are more soluble in water compared to the hydrocarbons and are also better hydrate formers. Therefore, it is important to evaluate impacts of their presence in a natural gas stream during pipeline transport. To do this, Troll gas from the North Sea of Norway was selected because it does not contain H₂S and very negligible amount of CO₂.

We performed our calculations on varying concentration of these two inorganic components. The water tolerance of the systems was evaluated. We observed that the introduction of CO₂ in varying amount does not show any distinguishable effect on water tolerance of the system. The presence of H₂S causes a considerable reduction in the water tolerance of the system. With H₂S, the maximum content of water that can be tolerated in the gas stream decreases with increasing mole-fraction of H₂S. We also studied the impacts of varying (increasing) the concentration of ethane in the Troll gas, that is without CO₂ and H₂S. The maximum allowable content of water in the Troll gas stream without the risk of hydrate formation also decreases with increasing mole-fraction of ethane, just like H₂S. However, the presence of H₂S showed the least water tolerance among the three components investigated.

6.6 Simulation of hydrate plug prevention in natural gas pipeline from Bohai Bay to onshore facilities in China

Since conference presentation(s) is a requirement needed to be fulfilled in this PhD programme, it is important to present a work on risk of hydrate formation during pipeline transport which forms a major objective of this PhD project. We found a natural gas transmission pipeline case in China which is very relevant for the study. That is the 58 kilometres subsea pipeline used for transmission of natural gas from Platform QK18-1 in southwest of Bohai Bay to the onshore natural gas processing plant in Northeast China. This is a wet gas subsea pipeline which is occasionally blocked or plugged by gas hydrates. This happens for the reason that the operational conditions are favourable for gas hydrates to form; a wet gas transported through a subsea pipeline at elevated pressures and low temperatures.

Li et al. (2013) conducted an experimental study on how to prevent the occurrence of the gas hydrate formation in this pipeline and suggested three ways that could help. They are reduction of operational pressure (that should be below hydrate formation pressure at a given local temperature) or increasing the temperature by means of heating or dehydrating the gas (that should be through subsea processing), or by adding chemicals (e.g., thermodynamic hydrate inhibitors) that can sufficiently shift the hydrate zone backward and upward. The study in this paper focuses on the second suggestion, which Li et al (2013) stated that is the best solution. Their study did not state how much water is safe to follow the gas or any method that can be used to evaluate that. We therefore responded through this study, with emphasis on the impact of solid surfaces (rusty surfaces of internal walls of gas transport pipelines) as another precursor for hydrate formation in pipelines. We evaluated the maximum content of water that should be allowed in the bulk gas transported through the subsea pipeline to prevent the risk of water dropping out to eventually lead to hydrate formation.

For this gas composition, the current industrial method based on water dew-point analysis over-estimates the maximum allowable water contents 18 to 19 times higher if the criterion for calculation is based on the mechanism of adsorption of water onto Hematite (rusty pipeline walls). This suggests that with the effect of rusty surfaces in

gas transmission pipelines, it may still be risky basing our hydrate risk evaluation on the current industrial approach based on water dewpoint calculations. Sensitivity analysis of pressure was also conducted which indicate that the safe limit of water in the bulk gas reduces with increase pressure.

6.7 Heterogeneous and homogeneous hydrate nucleation in CO₂/water systems. *Journal of Crystal Growth*

The emphasis in this work is to show that different ranges of hydrate can homogeneously form from CO₂ dissolved in water; to show the difference between hydrate nucleation and induction; to show that nucleation times are very fast and that they are in nanoseconds; to show why induction time can be very long, which is because of the slow transport of hydrate building blocks through the initial hydrate films. Chapter 4 dealt with the focus of this paper, but since this is a summary of a paper, it has to be reviewed again.

Hydrate formation process is typically divided into two physically well-defined stages: nucleation stage and stable growth stage. The first stage which is the nucleation stage is an unstable crystallisation phase where the thermodynamic benefit of the hydrate phase transition competes with the thermodynamic penalty of pushing away the existing phases towards attainment of the hydrate critical core radius. The second stage starts after the attainment of the critical radius, when the growth of the hydrate can be stable. This second process is a function of the size and shape of the growing hydrate nuclei. Another stage is normally identified as third stage, though not uniquely physically defined. This is known as induction time. This is the stage where the hydrate growth is massive and visible by several detection techniques such as laser detection of crystals, change in pressure, or other imaging methods.

Hydrate nucleation times are often mistaken as induction times. This may be because of the small size of the initial thin stable hydrate film, which is formed at the interface between water and the guest molecule phase. This thin initial hydrate film causes a restriction to transport of water and hydrate building blocks required for the stable growth of hydrate. This could cause a delay by several hours before a detectable hydrate core can be observed (onset of massive growth), which depends on the situation and likely effects of solid surface. Solid surfaces, for example, rusty surfaces of internal walls of pipelines frequently have effect on the hydrate phase transition process-transitions to induction. In the previous articles, we have explained the role of solid surfaces (Hematite) as a precursor to hydrate formation.

The nucleation times calculated for heterogeneous hydrate nucleation on water/CO₂ interface are in nanoseconds. It is the same for homogeneous hydrate nucleation from CO₂ dissolved in water. The delayed observed during induction time is because of the slow mass transport through the initial hydrate films formed at the interface between water and the hydrate former. Simple estimates show that induction times could be many hours when there are no hydrodynamic shear forces to break the hydrate films, for example in the absence of stirring. The slow mass transport limited growth towards a detectable hydrate is for that reason commonly misconstrued as absence of hydrate.

In addition, contrary to the assumption that only one structure and only one hydrate composition could form during hydrate formation, a variety of hydrates will form. We have discussed that hydrate formation will commenced at the interface between the hydrate former phase and water due to the higher concentration of both original phases at the interface. This we usually denote as H_1 . Then several hydrates having different hydrate composition and densities can be form from dissolved hydrate former in water, which we also refer to as H_2 . Another hydrate can thermodynamically be formed from dissolved water in hydrate former phase, but this will be challenged by too little mass of water in the hydrate former phase and heat transport limitation. We designate this as H_3 .

Hydrate formation in industrial systems and in nature will never reach equilibrium. Local chemical potential of H₂O and guest molecules are consequently subject to local minimum free energy under the constraints of heat and mass transport. This means that the cavity partition functions in the statistical mechanical theory for hydrate will vary with local chemical potentials for hydrate formers. Hydrate formation from dissolved hydrate formers in water can form several hydrates with different compositions and densities as the concentration of guest molecules in the surrounding water changes.

We used a simple nucleation theory, the classical nucleation theory (CNT). Thermodynamic properties associated with the hydrate phase transitions in this model are evaluated from classical thermodynamics. Hydrate properties are derived from data

obtainable from molecular dynamic (MD) simulations to get a consistent and transparent reference level for every component in every phase.

It is important to discuss upper limit of water allowable in CO₂ stream when discussing kinetics of hydrate nucleation since CO₂ and water can form hydrate. Therefore, we considered a pipeline situation for transport of CO₂, the Europipe I for transporting CO₂ from Germany to the North Sea of Norway for offshore long-term storage. We applied the same approaches used in the previous articles. The water dew-point method calculated about 20 times higher water tolerance in the CO₂ stream compared to the approach based on water adsorption on solid surface (Hematite).

6.8 Hydrate nucleation, growth and induction.

This study follows the same procedure of [Paper 7], but our component of interest here is methane. The main objective is also to clarify some misconceptions about kinetics and thermodynamics of hydrate formation. Nucleation time is different from induction. Nucleation times are nanoscale processes. The dynamics of hydrate stable growth can be very slow because of mass transport limitations; limitation of transporting water and hydrate-forming molecules across initial hydrate films. Diffusivity decreases, thus, the time for stable growth to attain a point of detection by any instrument or technique will increase because of the mass transport limitation posed by the initial hydrate film formed at the interface.

Hydrate formation in industrial systems and nature cannot reach thermodynamic equilibrium since both temperature and pressure are always specified, and we will end up with only one degree of freedom for a simple case involving one hydrate-forming component. It is not only one but a number of different hydrates with different densities, different compositions and different free energies will form. It depends on the phases the hydrate forming molecule and water come from. A variety of different hydrates can also form from a mixture of methane and carbon dioxide based on the impact of the combined first and second laws of thermodynamics. This implies hydrate nucleation will begin first with the most stable hydrates, under the constraints of heat and mass transport. Nucleation can occur through a variety of routes.

Several misunderstandings about hydrate stability also exist. Discussions on hydrate stability are mainly based on pressure-temperature stability limit projection, which is not proper. It could be reasoned that hydrate of methane is more stable above a specific pressure-temperature condition based on P-T equilibrium curve, that is above the quadruple-point where CO₂ gas splits into two phases (gas and liquid). But plotting the free energies of both CH₄ and CO₂ hydrates along the hydrate formation curves indicates that CO₂ hydrate is more stable compared to CH₄ hydrate over the entire P-T range for both hydrates. These features are not directly observable in the old-fashion hydrate formation P-T or stability curves because they are founded on semi-empirical fitting of the chemical potential of liquid water minus the chemical potential of empty hydrate.

A pipeline hydrate risk analysis was also conducted to discuss the different routes water can be made available for hydrate to form thermodynamically. Our study was based on Europipe II which transports export natural gas from the Kårstø processing facility in Norway to the Europipe receiving facilities (ERF) reception centre at Dornum in Germany. The results show that rusty surfaces in pipelines will make it about 20 times riskier for liquid water to drop out through the process of adsorption compared to the route of condensation via water dewpoint.

6.9 Consistent enthalpies of the hydrate formation and dissociation using residual thermodynamics

This article contains some of the works done in the third and last part of the project. Enthalpy of hydrate formation or dissociation is one of the most vital properties of gas hydrates. The experimental data obtainable for gas hydrate formation and dissociation enthalpies are limited and commonly contain various types of bias. A characteristic reason for bias is the applied conditions. Even if the temperature is specified, with missing pressure information, it will still be impossible to define the degree of superheating required for total dissociation of hydrate relative to hydrate equilibrium pressure at the given temperature. For example, Kang et al. (2001) state: “...was kept above the equilibrium dissociation pressure”. However, the degree of superheating (temperature above the equilibrium temperature) is necessary to understand how much heat is used in heating the hydrate sample and how much heat is actually being consumed for dissociation of the sample. This is very imperative because it is clearly not possible to dissociate a sample of hydrate precisely at the hydrate equilibrium conditions because it will take infinite time.

Indirectly, models used for evaluating enthalpies of hydrate formation and dissociation have been based generally on both the Clapeyron and Clausius–Clapeyron equations. In several articles, the simplified Clausius–Clapeyron equation is used together with hydrate equilibrium data obtained by experiment or by calculation. However, these methods fail for conditions where condensed phase volumes become significant. These approaches have a number of limitations. For instance, Clapeyron and Clausius–Clapeyron equations cannot be applied directly to conditions outside of the hydrate equilibrium curve. Clausius–Clapeyron equation will fail at higher pressures.

Therefore, we propose a consistent thermodynamic scheme, which is based on using residual thermodynamics for evaluating every property such as change in free energy as the thermodynamic driving force in kinetic theories, equilibrium curves, and enthalpy changes of hydrate dissociation and formation. Unlike the Clapeyron method, this approach can easily be extended to thermodynamic conditions outside of equilibrium, and to other hydrate phase transitions. Applicable cases are enthalpy

changes associated with hydrate forming from dissolved guest molecules in water, and the reverse process of dissociation of hydrate towards water undersaturated with hydrate former. Other applicable hydrate phase transitions are hydrate formation toward solid (mineral) surfaces. This residual thermodynamic approach can simply be applied to any mixtures of hydrates that will be formed in a free-energy analysis of hydrate formation from mixture of guest molecules.

In this work, data of enthalpy changes of hydrate formation/dissociation from experiments and from both Clausius–Clapeyron and Clapeyron equations were plotted, as well as the results we obtained using our proposed scheme. There is a wide disagreement with most of the available data, even the ones obtained from the same approach. This may be due to the over-simplifications involved in Clausius–Clapeyron and Clapeyron and the obvious limitations in some of the experiments. We are to evaluate real gas behaviour taking into account thermodynamic deviations from ideal gas behaviour by use of residual thermodynamics.

6.10 Modelling of methane hydrate formation and dissociation using residual thermodynamics.

It was also important to us to present the work in the third part of the PhD project in an international conference since we are the only research group who have used our proposed approach. In this paper, we show how the data of enthalpies of hydrate formation or dissociation that are currently available are not consistent, thus unreliable. That is because they usually lack relevant information that are essential for proper interpretation, like the hydrate composition, hydration number, the pressure condition at which they were estimated. In addition, the level of superheating needed for total dissociation of hydrate usually captured. Yet, it is very important because expecting hydrate to dissociate at equilibrium conditions is not feasible, because it will take infinite time. The Clausius-Clayperon and the Clapeyron modelling approaches are usually based on equilibrium pressure-temperature conditions (they cannot directly be applied for non-equilibrium situations which is the normal industrial systems and nature). They involve oversimplification that affects their results. The limitations of the current methods used for evaluation of enthalpy changes of hydrate phase transitions are discussed. Some of the current data are plotted as well as the estimates from our proposed approach based on residual thermodynamics. This study is based on only methane as we have done a more comprehensive study in [Paper 9].

6.11 Production of methane from hydrate and CO₂ zero-emission concept

We stated in [Paper 9, Paper 10] that enthalpy is one of the most important properties of gas hydrates. One of the reasons is its practical implication to greenhouse gas control and production of a cleaner source of fossil fuel, natural gas; simultaneous CH₄ production and CO₂ offshore long-term storage. We evaluated the enthalpy changes of hydrate formation and dissociation for methane and carbon dioxide using residual thermodynamics approach. We also performed a free energy analysis for both components. According to our study, the exothermic heat of CO₂ hydration formation may be 9 – 10 kJ/mol of guest molecule greater than the heat needed for dissociation of a CH₄ hydrate to CH₄ gas and liquid water. The implication is that the released heat is available to help to dissociate the surrounding CH₄ hydrate to liquid water and CH₄ gas. The dissociation of CH₄ hydrate will make additional free water available added to the free pore water for new CO₂ hydrate to form in place of the originally existing in-situ CH₄ hydrate. Based on the combined first and second laws of thermodynamics, which helps us to analyse non-equilibrium thermodynamic processes based on free energy analysis, we found out that the change in free energy of CO₂ hydrate could be 1.8 – 2.0 kJ/mol more negative (that is less) than that of CH₄ hydrate. And consequently, since the systems under consideration cannot attain equilibrium, we concluded that the free energy change difference between CO₂ and CH₄ hydrates as well as the relative heat of formation or dissociation are the most important factors to consider in replacing in-situ CH₄ hydrate with CO₂ as CO₂ hydrate and eventual mining of the natural gas.

6.12 Enthalpies of hydrate formation and dissociation from residual thermodynamics

A poster of this work was presented at the 12th International Methane Hydrate Research and Development Conference and China Engineering Technology Forum (12th IMHRD) which was held in Chengdu-China between 31st of October to 3rd of November 2018. The presentation is among the seven selected for special issue journal publication in *Energies*. It is in this presentation that we first proposed using residual thermodynamics for calculation of enthalpies of hydrate formation and dissociation.

What is new in this article? We emphasise the approach of residual thermodynamics because of the obvious limitations of the current approaches, and also reported the important implication of the heats of hydrate formation and dissociation in in-situ CH₄-CO₂ swap. We did a more rigorous review of available experimental data and calculated data from Clapeyron and Clausius-Clapeyron modelling approaches for enthalpy changes of hydrate formation and dissociation. We calculated and plotted enthalpy changes of hydrate formation and dissociation in kJ/mol of guest molecule in terms of temperature and also as a function of pressure to give overview of the currently available data. We did the same in the case of hydration number. We also calculated enthalpy changes of hydrate formation or dissociation in kJ/mol of hydrate, considering the hydration number. In addition, we used both Clausius-Clapeyron and Clapeyron equations to calculate enthalpy of hydrate formation or dissociation, which were also plotted together with extensive data from literature and our proposed residual thermodynamics approach.

The implication of enthalpy changes of hydrate phase transitions to environmentally friendly mining of natural gas from in-situ methane hydrate and simultaneous long-term carbon dioxide offshore storage in form of gas hydrate is also documented in this paper. We evaluated CO₂ enthalpy changes of hydrate phase transition to be 10 – 11 kJ/mol of guest molecule much more than that of CH₄ hydrate for 273 – 280 K range of temperature. Thus, our inference of this implication is the same for [Paper 11], that is, the heat of CO₂ hydrate formation is available, and more than the

7 General discussion, conclusion and further works

This chapter presents the general discussion of the studies conducted in this project, which fulfil the objectives of the project. Relevant conclusions drawn from the studies follows the general discussion, which is finally followed by suggested further works. All the papers are discussed together in each of the three main objectives. Therefore, a repetition of some of the information especially in Chapter 6 (Summary of papers) should be expected.

7.1 General discussion

This PhD project is meant to extensively validate the thermodynamic scheme with experimental data (including calculated data from very good literature) and to apply it to comprehensively study the risk of hydrate formation during processing and pipeline transport of natural gas, thermodynamics and kinetics of hydrate formation, and simultaneous CH₄ production from in-situ hydrate and CO₂ long-term offshore storage in form of CO₂ hydrate.

Equilibrium or stability pressures estimated from the thermodynamic scheme used in this project were compared with several experimental data for validation. The agreements were satisfactory for all the systems investigated. Model validation was done for hydrates formed from single component, binary and multicomponent mixtures of guest molecules.

7.1.1 Risk of hydrate formation and the impact of rust in pipeline transport of natural gas and CO₂

Water is always produced together with oil and natural gas. This water gives the petroleum industry a great concern [1] since it can form hydrate with the light components in natural gas (methane, ethane, propane and isobutane in their pure form) at high pressures and low temperatures. Hydrates can plug pipelines [1, 18] which can lead to severe economic losses [31].

The typical techniques proposed and used for prevention of hydrate formation in gas transport pipelines are pressure reduction, thermal means (increasing the temperature above hydrate stability temperature), injection of chemicals, or dehydration of the gas [2, 18, 32, 226, 242-244].

The first three methods are very costly especially for long pipelines like the ones studied in this project, particularly [18, 23, 245-247]. Therefore, dehydration of the gas is the best option [18], especially for export gas. The vital question is then, “how much water should be removed from the gas, or how much water vapour should be allowed to follow the gas without the risk of liquid water dropping out to eventually lead to hydrate formation”?

The current industrial practice for estimating the maximum mole-fraction of water that can be permitted without the risk of liquid water dropping out has been based on if the gas is either at or below water dew-point [2]. This classical approach [2] presently used for hydrate risk evaluation during transport of natural gas and CO₂ is based on condensation of water from the bulk gas at dew point (as stated above). Which means the mole-fraction of water that should be permitted in the bulk gas must be below the water dewpoint mole-fraction of the least operation P-T conditions.

Previous works [248-250] in our research group indicated that the rusty surfaces of the internal walls of gas transport pipelines and equipment could provide another route (besides dewpoint condensation) for liquid water to drop out of the bulk gas and ultimately leads to hydrate formation. This is ignored in the current hydrate risk approach. However, before pipelines are mounted and laid on the sea floor for hydrocarbon operations, they are already rusty as discussed in Section 1.1 and shown in Figure 1.3. [37]. These rusty surfaces have hydrate formation implications: they provide water adsorption sites, thus, a precursor to hydrate formation in the pipeline or equipment. These rusty surfaces can make free liquid water available through the mechanism of adsorption. Rust [19, 26] is a mixture of several different oxides of iron like iron oxide (FeO), hematite (Fe₂O₃), and magnetite (Fe₃O₄). Magnetite generally forms very quickly or early, but the most dominant oxide is hematite, and it is one of the most thermodynamically stable forms of the ordinary rust. By ordinary rust we imply

different oxides of iron that are formed by exposing iron to oxygen and water. Therefore, discussions are based on impact of Hematite in this project.

Hydrate nucleation and growth cannot occur directly on hematite [19] because of incompatibility between the distribution of partial charges of hydrogen and oxygen in the lattice and atom charges in the hematite (rusty) surface. Nevertheless, the hematite works as a catalyst for pulling out the water from the gas by means of adsorption. Then, hydrate can form slightly outside of the first 2-3 layers of water of about 1 nm.

A third route for hydrate nucleation and growth, where water dissolved in the guest molecule can lead to hydrate nucleation is theoretically or thermodynamically possible, but it is not feasible. This is due to the very low concentration of water in the hydrate former's phase and poor heat transfer out of the system: mass and heat transport limitations. During hydrate formation from water and guest molecule at the interface between them, a hydrate film will subsequently and rapidly be formed at that interface. This will block further transport of mass through the hydrate film (very low coefficient of diffusivity) very quickly, thereby preventing continuous growth or cause a delay in the growth of the hydrate. Nevertheless, in the absence of effects of surface stress from flow on the water/hydrate former system (just like a system without stirring), hydrate formation will happen from the water dissolved in gas. This will also benefit from hydrate nucleation on the hydrate surface from water condensed on it and hydrate guest molecules. When a flowing situation with turbulent shear forces is considered, hydrate formation from water dissolved in gas phase cannot be realised. Hence, this route to hydrate formation is not considered in most of the studies.

The results of the hydrate risk analysis of all the systems investigated in this project [Paper 1 – Paper 8] indicate that the approach of adsorption of water onto Hematite (rusty surfaces) completely dominates. The dewpoint method over-estimates the safe limit (maximum mole-fraction) of water that should be permitted to flow with the bulk gas about 18–20 times greater than when the effect of hematite is considered, depending on the specific gas composition. This can also be explained based on the combined first and second laws of thermodynamics, from which we understand that thermodynamic systems will move or proceed towards the minimum or least free

energy possible as a function of temperature, pressure, and distribution of masses in the system over possible phases, under the constraints of mass and heat transport. Water adsorbed on Hematite (rusty surface) has an average chemical potential of approximately -3.4 kJ/mol [176, 182] less than or more negative than the chemical potential of liquid water. It means that it is more likely for liquid water to adsorb on rusty surfaces for subsequent hydrate formation to occur than for water to drop out through water dewpoint condensation. This implies gas transmission pipelines could still encounter hydrate plugging if the hydrate risk evaluation done is entirely based on dewpoint technique.

Almost all the systems investigated involved hydrate formers of structures I and II since real natural gas usually contain more than methane and other structure I hydrate forming guest molecules. Therefore, real natural gas compositions were used in most of the studies. Natural gas fields data of Troll gas [Paper 2, Paper 5], Sleipner gas [Paper 3], Natuna gas [Paper 4], a wet gas from Bohai Bay in China [Paper 6], export gas from Norway to Germany through Europipe II [Paper 7], and that of the CO₂ pipeline from Germany to Norway through Europipe I [Paper 8] were used. Few years before this project, Kvamme et al. [19] obtained a similar result, precisely 20 times higher but for pure methane and pure CO₂. Kvamme and Sapate [251] also calculated the dewpoint analysis 18 times greater than analysis based on the mechanism of adsorption of water onto Hematite, but it is also based on a binary gas system of only structure I hydrate former, precisely, methane and ethane.

Other research groups do not discuss calculation of the maximum limit of water, but they usually discuss that the gas needs to be dehydrated [18, 252]. However, it is important to know to what extent should the gas be dehydrated. This will have impact in the design of gas dehydration systems. What a lot of the other research groups focus on is mainly injection of chemicals which is quite more expensive [69, 226, 253, 254].

The effect of the presence of higher hydrocarbon hydrate formers which we referred to as C₂₊ in this project were investigated [Paper 1 – Paper 3]. The trends demonstrate a decline in allowable water content with increasing concentration of ethane, propane and isobutane for the temperature range of 273 – 280 K. As their

concentrations increase in the bulk gas, these C₂₊ act to draw down the water tolerance of the gas mixture to a point where they completely dominate or dictate the trends.

The effects of the presence of inorganic gases of CO₂ [Paper 3 – Paper 5] and H₂S [Paper 5] in the bulk gas on water tolerance were also studied. CO₂ has little or no significant impact on the maximum mole-fraction of water that can be permitted to flow with the bulk gas as its concentration increases. While H₂S, like ethane, propane and isobutane show a consideration reduction in water tolerance of the system as its concentration in the mixture increases. Its impact is slightly greater than that of ethane according to the dewpoint analysis. But based on the approach of water on Hematite, it has a well greater effect on the safe-limit of water compared to ethane. The presence of 1 % of H₂S in the bulk gas may cause about 1 % reduction in water tolerance. The reduction in maximum content of water could be up to about 2 – 3 % and up to about 4 – 5 % if the concentration increases to 5 % and 10 % respectively [Paper 5].

In the literature [255], discussion of hydrate stability is often based on equilibrium pressure-temperature curves. This is not proper because industrial system and even in nature hydrate systems can never attain equilibrium. They are non-equilibrium systems. In equilibrium situation, the chemical potentials of different guest molecules in a multicomponent gas mixture in different phases are equal. However, in a nonequilibrium systems, the chemical potentials of different hydrate formers are not equal, they are distinct in value across all the phase boundaries. Therefore, free energy analysis based on the combined first and second laws of thermodynamics under the constraints of conservation of mass and energy is appropriate. Based on this, the results obtained explained why in a multicomponent mixture of hydrocarbon gases the most stable hydrates will form first, under the constraints of mass and heat transport, followed by the subsequent most stable hydrates according to each stability. The most stable hydrate is then the hydrate with the minimum free energy. The most stable hydrate is therefore hydrate of isobutane, followed by that of propane, and then by ethane [Paper 1]. Consequently, i-C₄H₁₀ followed by and C₃H₈ will first fill the large cavities of all hydrate but under the constraints of distribution of masses. Then C₂H₆ will

occupy the large cavities of sl hydrate before CH₄ will enter and occupy the small cages of sl hydrate.

This explanation may be seen as the same with hydrate stability analysis based on hydrate equilibrium or hydrate stability curves, but it is not so. For instance, the hydrate stability curve of CO₂ hydrate has lower pressures (thus more stable) compared to that of methane hydrate, but only to a certain temperature. That temperature is the point where the gas guest molecule experiences a phase-split, were CO₂ hydrate, liquid water, liquid CO₂ and CO₂ gas coexist (quadruple-point). Beyond this temperature, the pressures of CO₂ hydrate stability curve become higher than those of CH₄ due to the density change caused by the additional (liquid) phase of CO₂. This can mistakenly be interpreted as CH₄ hydrate becoming more stable than CO₂ hydrate beyond this point if we base our interpretation only on stability curves. Conducting a free energy analysis revealed that CO₂ hydrate has lower free energy across the entire temperature range. Thus, CO₂ hydrate is more at all the temperature even beyond the quadruple-point were phase-split occurs [Paper 8].

7.1.2 Kinetics of hydrate formation

Kinetics of hydrate formation is not well understood, certain misinterpretations or misunderstanding exist [9, 12, 14, 256]. Hydrate formation just like the process of crystallisation is generally divided into two well defined phases or stages: hydrate nucleation and hydrate stable growth stage [199, 200, 218, 257]. Kinetics of hydrate formation has been extensively discussed in Section 3.1. The first stage involves random formation and shrinking of hydrate nuclei under beneficial thermodynamic conditions and favourable heat and mass transport [258] to attain the critical nuclei size from which stable hydrate growth (second stage) can commence. Another stage which is physically not well defined is often referred to as a third stage known as induction. Induction time is the time elapse before hydrate becomes detectable. While hydrate nucleation time is the time it takes for hydrate core or nuclei to form.

Nucleation times are sometimes mistaken as induction times. This is not correct because nucleation is a nano-scale process. That hydrate cannot be detected before

induction does not imply hydrate does not exist. That several hours may elapse before hydrate can be detected does not mean hydrate nucleation took several minutes or hours. For example, Davies et al. [259] calculated a nucleation time of over five hours in the isothermal experiment they conducted at 268 K. The hydrate nucleation times computed for both heterogeneous and homogeneous hydrate formation in this project are in nano-seconds [Paper 7, Paper 8]. The works of [14, 260] are also in agreement with the results obtained in this project. The long times experienced before hydrates are detected are caused by mass transport limitations due to the initial thin hydrate film formed at the interface between water and the hydrate former interface [Paper 7, Paper 8]. This has been comprehensively discussed in Section 3.1.1. There is a limitation in the transport of guest molecules and water across thin initial hydrate film. This implies a decrease of diffusivity coefficient, thereby resulting in increase in the time for continuous growth to reach a detectable size.

Another misunderstanding about hydrate nucleation is that only one uniform-phase hydrate is formed from either a single guest or a multicomponent mixture of hydrate formers. This analysis has also been presented in Section 3.1.1. Based on the combined first and second laws of thermodynamics, nucleation will commence with the most stable hydrates, under the constraints of heat and mass transport. Nucleation can happen via different routes [Paper 7, Paper 8]. Even in a system with a single guest molecule and water, a variety of hydrate with distinct density, distinct chemical potential and distinct composition will finally form. While a system with multicomponent guest molecules and water, the final hydrate will be a mixture of different hydrates, different hydrate structures (when guest of more than one structure exist), different chemical potential, different densities and different composition. Hydrate formation will commence at the interface between the guest molecule phase and water [Paper 7, Paper 8] and [258]. The experimental work of [261] gives a good illustration of this in page 4166. A range of hydrates with different compositions of the original hydrate former(s), different densities and different will form from aqueous solution (dissolve hydrate formers). Theoretically, hydrate can also nucleate from water dissolved in the guest molecules phase. Such hydrate cannot be stable because of the

little mass of water dissolved in the guest molecule phase as well as limitation of heat transport, especially in the case of hydrocarbon guests like methane-poor heat conduction.

In Section 4.2, non-equilibrium nature of hydrate formation in industrial systems and nature has been comprehensively discussed. Hydrate stability for different hydrate formers has also been discussed in the previous section, Section 4.3.

7.1.3 Simultaneous production of energy and long-term CO₂ offshore storage

Natural gas hydrates (NGHs) are widely distributed all over the world, in the permafrost and in the oceans [9]. They are being considered as possible unconventional energy resource for the world in the future [262, 263]. NGHs have been estimated to hold a huge amount of relatively cleaner energy resource (natural gas) [10], as much as twice the amount of the entire reserves of all the fossil fuels in the world [264, 265]. Some of the great economies of the world like Japan and India have significant deposits of natural gas hydrate but are currently largely depended on import of fuels for their energy needs [263, 266-269]. This explains the increase interest in hydrate research.

Several methods have been proposed to mine these energy resources for the benefit of man. Though, attention has been given to mostly pressure reduction and thermal stimulation (for example, use of steam or hot water). A more innovative approach is utilisation of CO₂. This approach is attractive because it combines both mining of the natural gas stored up in the NGHs and simultaneously storing of CO₂ in form of hydrate, and in place of the original CH₄ hydrate. One of the techniques which has been tested in a Pilot test conducted at Alaska (U.S.A.) [270] involved mixing nitrogen gas with CO₂ to reduce the thermodynamic driving force, to avoid the typical rapid formation of CO₂ hydrate. This is based on a solid-state swap mechanism. Lee et al. [70] and Falenty et al. [271] have verified the solid-state process for the ice region of water. The amount (%) of CO₂ needed in the CO₂/N₂ mixture to successfully convert the CH₄ hydrate to CO₂ hydrate to avoid the risk of rapid CO₂ hydrate formation which can eventually block further supply of CO₂ was studied in this project [Paper 4]. Natuna gas

in offshore Indonesia is the case study. The study indicated that the required proportion of CO₂ about is around 5 – 12 mol% without H₂S in the gas stream. While it is about 4 – 5 mol% and 2 – 3 mol% with the presence of 0.5 mol% and 1 mol% of H₂S respectively. Direct solid-state CO₂-CH₄ swap will be extremely kinetically restricted and is not significant.

Just as discussed in Section 1.1 (Motivation), Offshore of Japan two pilot tests were also performed some years ago [3]. In both Pilot tests, a major problem they encountered was freezing down as a result of inadequate heat supply capacity from the surroundings [69]. Even though thermal stimulation offers solution to this challenge, it is however considered too costly as the only means. Nevertheless, any technique that will be applied to produce CH₄ from CH₄ gas hydrates successfully will involve heat transfer. Therefore, it is imperative to investigate the heats of these hydrate formation and dissociation. Thus, it is vital to obtain accurate values of these heat of hydrate phase transitions.

In this project, we proposed a residual thermodynamic approach for computing consistent enthalpy changes of hydrate phase transitions. This is because there are different limitations and sources of biases in the current approaches. Experimental data of enthalpy changes of hydrate phase transitions available in literature lack significant information essential for right interpretation. They are also filled with various sources of bias. A lot of calorimetric experimental data does not also have any measured filling fractions. They often apply a constant value, which indicates the constant values could be merely guessed. Information about superheating above the hydrate equilibrium conditions to completely dissociate the gas hydrate to liquid water and gas is normally not lacking. Other relevant information needed for good understanding and appropriate interpretation are normally missing. Generally missing information are composition of hydrate, hydration (occupation) number, temperature and/or pressure data, and degree of super heating involved in total hydrate dissociation.

Clausius-Clapeyron model used with either measured or calculated pressure-temperature equilibrium data is the simplest indirect methods used for evaluating enthalpy changes associated with hydrate phase transition. However, this approach

involves over-simplifications. These over-simplifications make all the data based on Clausius-Clapeyron to be unreliable. Therefore, the ordinary Clapeyron equation is favoured by most recent works applying different modifications, especially models for the change in volume associated with the hydrate phase transitions [168, 214]. However, older data obtained from the Clapeyron approach do not have appropriate volume corrections. In addition, both Clausius-Clapeyron and Clapeyron are based on equilibrium P-T data obtained by experiment or by calculation. But hydrate cannot attain equilibrium in industrial systems and nature. In non-equilibrium systems, we apply free energy analysis (minimisation).

Enthalpy change is uniquely but trivially related thermodynamically to change in free energy. Therefore, thermodynamic models used for description of change in free energy related to phase transition of hydrate (formation or dissociation) will have a consistent change in enthalpy on the basis of the specific models. This is why we recommend the method based on using residual thermodynamics scheme for all properties like equilibrium (pressure-temperature) curves, free energy changes as thermodynamic driving force in kinetic theories and enthalpies of hydrate formation and dissociation. With residual thermodynamics we calculate real and not just ideal thermodynamic properties. We can calculate values outside of equilibrium. We can obtain the degree of superheating needed for dissociation of hydrates to liquid water and guest molecule back to its original phase (this is not included in this study but in a subsequent work to this). Calculations based on residual thermodynamics enable us to evaluate real gas behaviour with consideration of the thermodynamic deviations from ideal gas behaviour.

Enthalpy changes of hydrate phase transition and hydration number in literature obtained from experimental studies as well as Clausius-Clapeyron and Clapeyron models have been studied in this project. The values vary significantly in such a way that some of them decided to base their results on average values over a range of temperatures [272]. Gupta et al. [273] obtained dissimilar values for enthalpies of hydrate dissociation from experimental study, Clausius-Clapeyron and Clapeyron equation. We do not expect much agreement with our results based on the limitations of the other methods,

especially, the simplicity of both the Clapeyron and Clausius-Clapeyron equations. Nevertheless, for methane hydrate, the results of Nakamura et al. [215] are closed to our results, and also the experimental results of Gupta et al. [273] but only between 280 and 286 K. The single point value of Kang et al. [167] and Sloan and Fleyfel [274] are close to our results.

The results of enthalpy changes of carbon dioxide hydrate phase transitions using residual thermodynamics in this project are around 10 – 11 kJ/mol of guest molecule greater than the ones of methane hydrate phase transition for 273 – 280 K range of temperatures. Calculations based on kJ/mol hydrate within the same temperature range give 0.5–0.6 kJ/mol hydrate. Anderson's results [168, 214] using Clapeyron equation are a little close to the results obtained in this work, precisely 10 kJ/mol and 7 kJ/mol of guest molecule at 274 K and at 278 K respectively. While Kang et al. [167] in their experiment put this difference at 8.4 kJ/mol of guest molecule at 273.65 K.

These results suggest that the exothermic heat released per guest molecule or per hydrate during CO₂ hydrate formation, especially from the available free water (pore water inclusive) and also directly via solid-state mechanism is more than that required for dissociation of CH₄ hydrate. The implication is that if CO₂ is injected into CH₄ hydrate deposits, the heat supply requirement from the surroundings for dissociation of CH₄ hydrate to continue and to avoid the problem of freezing down will be met by the exothermic heat of CO₂ hydrate formation. The exothermic heat of CO₂ hydrate formation will help to dissociate the CH₄ hydrate to CH₄ gas and liquid water. The CH₄ gas can then be produced, and the liquid water will be used for further CO₂ hydrate formation. However, it is pertinent to state that this proposition is still under investigation, and it is still under development. In addition, there are constraints that are also under study. Hydrate formation at the interface between CO₂ gas and liquid water is very rapid, forming a hydrate film which will quickly block the pore spaces thereby limiting further CO₂ supply.

In replacement of in-situ CH₄ hydrate with CO₂, it is not the temperature-pressure that is essential, but what is important is the difference in free energies of both hydrates, CH₄ hydrate and CO₂ hydrate, and the enthalpies of CO₂ hydrate formation relative to

the enthalpies of CH₄ hydrate dissociation. The free energy of CO₂ hydrate is around 1.8 – 2.0 kJ/mol more negative or lower the free energy of CH₄ hydrate within a temperature range of 273.15 – 283.15 K (0 – 15 °C). That confirms that hydrate of CO₂ is more stable thermodynamically than hydrate of CH₄.

We also studied enthalpies of hydrate phase transitions involving mixtures. The mixtures are limited to our components of interest (CH₄, CO₂ and N₂) for “simultaneous production of natural gas from CH₄ hydrate and CO₂ long-term offshore storage in form of CO₂ hydrate. The limits of N₂ in possible injection gas mixtures has been studied in [275, 276] and in [Paper 4]. Hydrate formation from the mixtures of these components will result in a better stabilization of both cavities, with CO₂ filling the large cavities and CH₄ and N₂ stabilising the small cavities, so, we expect higher absolute values of enthalpies. Excess enthalpies available for dissociation of the in-situ CH₄ hydrate were also calculated. For example, even at a N₂ concentration as high as 30 mole per cent with 70 mole per cent of CO₂, excess heat of around 6 kJ/mol was computed.

7.2 Conclusion

Current industrial approach for evaluating the risk of hydrate formation is based on liquid water dropping out of the bulk gas at dewpoint at a given pressure-temperature (P-T) condition. In this method, the maximum allowable water content will be kept below the projected dew-point mole-fractions during transport, considering the operational P-T conditions. Solid surfaces, in this project, rust (Hematite) is another precursor to hydrate formation. Rust provides another route for liquid water to drop out through the mechanism of adsorption. And pipelines are generally rusty before they are mounted in place for operations.

The approach of adsorption of water onto Hematite (rusty surfaces) completely dominates. The dew-point method over-estimates the maximum mole-fraction of water that can be permitted to flow with bulk gas about 18 – 20 times greater than when the impact of hematite is considered, depending on the specific gas composition. Thus, hydrate may still form when we base our hydrate risk analysis entirely on dew-point method.

The presence of higher hydrocarbon (C₂₊) guest molecules causes a decrease in the safe-limit of water with increasing concentration of ethane, propane and isobutane for the temperature range of 273 – 280 K. These C₂₊ act to draw down the water tolerance of the gas mixture to a point where they completely dominate or dictate the trends as their concentrations increase in the bulk gas.

For the inorganic components, CO₂ has little or no significant impact on the allowable upper-limit of water when its concentration increases. While the presence of H₂S causes a consideration reduction in water tolerance of the system as its concentration in the mixture increases. The presence of 1 % of H₂S in the bulk gas may cause about 1 % reduction in water tolerance. The reduction in maximum content of water could be up to about 2 – 3 % and up to about 4 – 5 % if the concentration increases to 5 % and 10 % respectively.

It is not proper to interpret hydrate stability completely based on equilibrium P-T curves as frequently done in literature. The hydrate stability curve of CO₂ hydrate has lower pressures (thus more stable) compared to that of CH₄ hydrate but only to a certain temperature. That is the quadruple-point where phase-split occurs causing the pressures of CO₂ hydrate going above that of CH₄ hydrate due to the increase in density caused by the CO₂ liquid phase. A free energy analysis revealed that CO₂ hydrate has lower free energy across the entire temperature range, thus more stable at all the temperatures. Therefore, hydrate stability should rather be based on free energy analysis since in real situations hydrate cannot reach equilibrium. Consequently, the most stable hydrate is the hydrate with the minimum free energy. The hydrate with the least or most negative free energy will first form under constraints of mass and heat transport, then followed by the subsequent most stable hydrate. Among the hydrocarbon guest molecules studied, the most stable hydrate is hydrate of isobutane, followed by that of propane, and then by ethane.

Induction times are sometimes mistaken as hydrate nucleation times, which is why some works report nucleation times of hours. Hydrate formation is a nano-scale process and the hydrate nucleation times computed for both heterogeneous and homogeneous hydrate formation in this project are in nano-seconds. The long times experienced

before hydrates are detected are caused by mass transport limitations due to the initial thin hydrate film formed at the interface between water and the hydrate former interface.

Another misunderstanding about hydrate nucleation is that only one uniform-phase hydrate is formed from either a single guest or a multicomponent mixtures of hydrate formers. Based on the combined first and second laws of thermodynamics, nucleation will commence with the most stable hydrates, under the constraints of heat and mass transport. Nucleation can happen via different routes: hydrate formation will originate at the interface between the guest molecule phase and water. A range of hydrates with different compositions of the original hydrate former(s), different densities and different free energies will form from aqueous solution (dissolve hydrate formers). Theoretically, hydrate can also nucleate from water dissolved in the guest molecules phase. Such hydrate cannot be stable because of the little mass of water that will dissolve in the guest molecule phase as well as limitation of heat transport, especially in the case of hydrocarbon guests like methane which is a poor heat conductor.

For injection of CO₂ into in-situ CH₄ for simultaneous mining of the CH₄ and storage of the CO₂ in form of hydrate, the amount of CO₂ needed in the CO₂/N₂ mixture is only about 5 – 12 % without H₂S in the gas stream. While it is about 4 – 5 % and 2 – 3 % with the presence of 0.5 % and 1 % of H₂S respectively. Direct solid-state CO₂–CH₄ swap will be extremely kinetically restricted, and it is not significant.

To successfully produce CH₄ from the in-situ CH₄ hydrates, whichever method or combination of methods chosen, heat is required to be supplied from the surroundings. To know how much heat is needed, that has to be calculated. However, enthalpy changes of hydrate phase transition in literature obtained from experiment, Clausius-Clapeyron and Clapeyron models are limited and often lack some vital information needed for proper understanding and interpretation. These are the current approaches for evaluating these enthalpies. Information on thermodynamic properties such as pressure, temperature (or both), hydrate composition, and hydration number are often missing. The equation of state utilised is also not stated in certain literature. A number of experimental data also lack any measured filling fractions, and frequently, they apply

a constant value which suggests that the values may be merely guessed. In addition, older data based on Clapeyron equation lack appropriate volume corrections. The calculations of both Clausius- Clapeyron and Clapeyron equations are based on hydrate equilibrium data of pressure and temperature from experiments or calculated data. But hydrate formation is a non-equilibrium process. Information about superheating above the hydrate equilibrium conditions to totally dissociate the gas hydrate to liquid water and gas is normally lacking. However, enthalpy change of any phase transition is trivially coupled to the free energy change of the phase transition.

We therefore propose a consistent scheme for calculating free energy change, as well as the associated enthalpy change, using residual thermodynamics was proposed. This scheme is feasible due to results from Molecular Dynamics simulations, which provides chemical potential for water in liquid state, ice and empty clathrates of structures I and II. With residual thermodynamics, real gas behaviour taking into account thermodynamic deviations from ideal gas behaviour can be evaluated. Residual thermodynamic (equation of state) description of the hydrate former phase gives a complete scheme for residual thermodynamic description of each component in all co-existing phases.

Injecting CO₂ into naturally occurring CH₄ reservoir, a new CO₂ hydrate is expected to form especially from the available pore water. The enthalpies of the resulting CO₂ hydrate formation are well higher than that required for dissociation of in-situ CH₄ hydrate. The free energy of CO₂ hydrate is also more negative or lower than the free energy of CH₄ hydrate within a temperature range of 273.15 – 283.15 K (0 – 15 °C). That confirms that hydrate of CO₂ is more stable thermodynamically than hydrate of CH₄. In replacement of in-situ CH₄ hydrate with CO₂, what is important is the difference in free energies of both hydrates, CH₄ hydrate and CO₂ hydrate, and the enthalpies of CO₂ hydrate formation relative to the enthalpies of CH₄ hydrate dissociation. However, it is appropriate to state that this proposition is still under investigation and it is still under development. In addition, there are constraints that are also under study. Hydrate formation at the interface between CO₂ gas and liquid water is very rapid, forming a hydrate film which will quickly block the pore spaces thereby limiting further CO₂ supply.

Studies also need to be done on finding the most efficient and effective way to reduce the thermodynamic driving force, either by using any thermodynamic inhibitor or other substances.

7.3 Further works

Having completed this project, it will be interesting to study the following suggested areas/topics in Section 7.3.1 – Section 7.3.6.

7.3.1 Comparative cost of dehydration to dewpoint and hematite demands

It will be interesting to perform a cost analysis of dehydration of an export natural gas to the level required by dew-point technique and by the approach of water absorption onto Hematite (rusty surfaces). The studies in this thesis have provided useful information for this. In this work, natural gas dehydration plant(s) need(s) to be design and simulated using Aspen HYSYS, Aspen Plus, UniSim Design or any other relevant process simulation software. This will be followed by equipment dimensioning/sizing. The equipment sizing should preferably be done using the Spreadsheet in the process simulation software (for example Aspen HYSYS). Microsoft Excel, Matlab or Python can also be used. Equipment cost data can preferably be obtained from the recent version of Aspen In-Plant Cost Estimator (A.I.C.E.). Cost data can also be obtained from some chemical engineering websites, articles, or books. Detailed factor or other methods can be applied, and the cost can be escalated to the year of study. The cost of processes of chemicals injection like thermodynamic inhibitors and/or kinetic inhibitor can similarly be evaluated. Then, they can be compared. The advantages and disadvantages of each process can also be evaluated, especially environmental impact of each process.

7.3.2 Experimentation of impact of rusty surfaces on the risk of hydrate formation in gas transport pipelines

The studies on impact of solid surfaces on the risk of water dropping out from natural gas streams and eventually forming hydrate have been based on the thermodynamic properties obtained from Molecular Dynamic simulations. Several reviewers were interested in seeing a follow up work where the process of adsorption of water onto Hematite could be experimented.

7.3.3 Impacts of the presence of other gases that cannot form hydrate but can affect hydrate formation

In this project, our focus was on only hydrate formers that can form hydrate in their pure form. These are methane, ethane, propane, isobutane, carbon dioxide and hydrogen sulphide. However, natural gas often contains some components that cannot form hydrate in their pure form for example normal butane and nitrogen. They can however form hydrate in the presence of a help molecule like methane. Normal-butane and nitrogen generally have dilution effect on hydrate formation process of the main guest molecules. There is need to evaluate the effects of these other gases (e.g., n-C₄H₁₀ and N₂) will have on the maximum content of water that can be permitted to flow with the bulk gas without the risk of hydrate formation.

7.3.4 More experimental works involving carbon dioxide and structure II hydrate formers

One major challenge encountered in this project was that experimental data for hydrate equilibrium for mixtures of carbon dioxide and propane or isobutane are very limited. In actual fact, for any given mixture composition of these components, there is a lack of pressure-temperature (P-T) data sets having more than two or three P-T points. Adisasmito and Sloan (1992) [165] also observed this since 1992. Therefore, it will be meaningful to perform more experiments to obtain adequate P-T data set for such mixtures. Propane and isobutane can exist in considerable amount in natural gas from certain gas fields. In addition, the system of mixture propane and carbon dioxide in te

work of Adisasmito and Sloan [165] seem to be more complicated in terms of quadruple points or phase-split. This same system has been evaluated in this project applying different equations of state and commercial software as well as in-house PVT tool.

From our studies, these systems at certain P-T condition undergo phase-split, where part of the gas becomes liquid (quadruple-point). Therefore, it would also be worthwhile to experimentally re-examine these systems.

7.3.5 Injection gas mixture of choice

There is a need to carry out a study to find out the best substance to combine with CO₂ during injection into in-situ methane hydrate reservoir to simultaneously produce methane and store CO₂ in form of hydrate. Substances that can reduce the driving force of CO₂ hydrate formation but can allow much amount of CO₂ in the mixture are needed for this operation.

7.3.6 Calculations outside hydrate equilibrium pressure and temperature

At equilibrium, all phases, that is hydrate phase, water and hydrate former phase will co-exist. Thus, it will take some amount of superheating above equilibrium temperature to achieve complete dissociation. It will take infinite time to completely dissociate hydrate at equilibrium. It is important to evaluate the excess enthalpy (superheating) needed for total dissociation of hydrates. This is possible with the residual thermodynamic scheme. Thermodynamic properties outside of equilibrium can be evaluated. Clapeyron and Clausius-Clapeyron approaches are based on hydrate pressure-temperature equilibrium data and thus cannot be used for determining the required superheating to achieve complete dissociation of a required hydrate like in-situ methane hydrate for efficient production of methane or complete dissociation of hydrates in industrial systems in pipelines and equipment. It will be interesting to evaluate the enthalpies required for complete dissociation of hydrates using residual thermodynamic scheme.

References

1. Hammerschmidt, E., *Formation of gas hydrates in natural gas transmission lines*. Industrial & Engineering Chemistry, 1934. **26**(8): p. 851-855.
2. Mokhtab, S., R. Wilkens, and K. Leontaritis, *A review of strategies for solving gas-hydrate problems in subsea pipelines*. Energy Sources, Part A, 2007. **29**(1): p. 39-45.
3. Collett, T.S. and V.A. Kuuskraa, *Hydrates contain vast store of world gas resources*. Oil and Gas Journal, 1998. **96**(19): p. 90-94.
4. Kvenvolden, K.A., *Methane hydrate—a major reservoir of carbon in the shallow geosphere?* Chemical geology, 1988. **71**(1-3): p. 41-51.
5. Kvenvolden, K.A., *Potential effects of gas hydrate on human welfare*. Proceedings of the National Academy of Sciences, 1999. **96**(7): p. 3420-3426.
6. Kvenvolden, K.A., *Gas hydrate and humans*. Annals of the New York Academy of Sciences, 2000. **912**(1): p. 17-22.
7. Bacher, P., *Meeting the energy challenges of the 21st century*. International Journal of Energy Technology and Policy, 2002. **1**(1-2): p. 1-26.
8. Sloan, E., *Gas hydrates of natural gases.—2nd ed.* 1998, Marcel Dekker: New York.
9. Anderson, R., et al., *Experimental measurement of methane and carbon dioxide clathrate hydrate equilibria in mesoporous silica*. The Journal of Physical Chemistry B, 2003. **107**(15): p. 3507-3514.
10. Ohgaki, K., et al., *Methane Exploitation by Carbon Dioxide from Gas Hydrates—Phase Equilibria for CO₂-CH₄ Mixed Hydrate System—*. Journal of chemical engineering of Japan, 1996. **29**(3): p. 478-483.
11. Nakano, S., K. Yamamoto, and K. Ohgaki, *Natural gas exploitation by carbon dioxide from gas hydrate fields—high-pressure phase equilibrium for an ethane hydrate system*. Proceedings of the Institution of Mechanical Engineers, Part A: Journal of Power and Energy, 1998. **212**(3): p. 159-163.
12. Clennell, M.B., et al., *Formation of natural gas hydrates in marine sediments: 1. Conceptual model of gas hydrate growth conditioned by host sediment properties*. Journal of Geophysical Research: Solid Earth, 1999. **104**(B10): p. 22985-23003.
13. Henry, P., M. Thomas, and M.B. Clennell, *Formation of natural gas hydrates in marine sediments: 2. Thermodynamic calculations of stability conditions in porous sediments*. Journal of Geophysical Research: Solid Earth, 1999. **104**(B10): p. 23005-23022.
14. Hawtin, R.W., D. Quigley, and P.M. Rodger, *Gas hydrate nucleation and cage formation at a water/methane interface*. Physical Chemistry Chemical Physics, 2008. **10**(32): p. 4853-4864.
15. Englezos, P. and J.D. Lee, *Gas hydrates: A cleaner source of energy and opportunity for innovative technologies*. Korean Journal of Chemical Engineering, 2005. **22**(5): p. 671-681.
16. Sieminski, A., (U.S. Senate Briefing), *International energy outlook 2013*. US Energy Information Administration, 2013.
17. Energy, B., *Energy outlook 2030*. 2012: BP Publishers: London.
18. Li, W., et al., *A study of hydrate plug formation in a subsea natural gas pipeline using a novel high-pressure flow loop*. Petroleum science, 2013. **10**(1): p. 97-105.
19. Kvamme, B., et al., *Hydrate Formation during Transport of Natural Gas Containing Water and Impurities*. Journal of Chemical & Engineering Data, 2016. **61**(2): p. 936-949.
20. Baig, K., *Nano to Micro Scale Modeling of Hydrate Phase Transition Kinetics*. 2017, University of Bergen.

21. Naseer, M. and W. Brandstatter, *Hydrate formation in natural gas pipelines*. WIT Transactions on Engineering Sciences, 2011. **70**: p. 261-270.
22. Schuchardt, D., D.-G.G. Krause, and D. Kulp, *Environmental Impact Assessment Europipe II in Germany: Offshore and Onshore Section*. 1998: Bioconsult Schuchardt & Scholle. Bremen, Germany.
23. Gassco. *Europipe II*. [cited 2019 July 29]; Available from: <https://www.gassco.no/en/our-activities/pipelines-and-platforms/europipe-ii/>.
24. ChartsBin. *Total Length of Pipelines for Transportation by Country*. [cited 2019 July 29, 2019]; Available from: <http://chartsbin.com/view/1322>.
25. Rømo, F., et al., *Optimizing the Norwegian natural gas production and transport*. Interfaces, 2009. **39**(1): p. 46-56.
26. Aromada, S.A., *New Concept for Evaluating the Risk of Hydrate Formation during Processing and Transport of Hydrocarbons*. 2017, Master's Thesis, The University of Bergen, Norway.
27. Equinor. *Sleipner area*. [cited 2019 July 29, 2019]; Available from: <https://www.equinor.com/en/what-we-do/norwegian-continental-shelf-platforms/sleipner.html>.
28. Kaarstad, O. and C.-W. Hustad, *Delivery of CO₂ to Gullfaks/Tampen Area. A report by Elsam A/S-Denmark, Kinder Morgan CO₂ Company L.P.-USA, New Energy (Statoil)-Norway*. 2003.
29. Jakobsen, J., et al., *Developing a Pilot Case and Modelling the Development of a Large European CO₂ Transport Infrastructure-The GATEWAY H2020 Project*. Energy Procedia, 2017. **114**: p. 6835-6843.
30. Gassco AS, N.P. *Production and exports: The oil and gas pipeline system 2008* [cited 2019 18.12.2019]; Available from: <https://www.norskpetroleum.no/en/production-and-exports/the-oil-and-gas-pipeline-system/>.
31. Makogon, Y.F., *Natural gas hydrates—A promising source of energy*. Journal of Natural Gas Science and Engineering, 2010. **2**(1): p. 49-59.
32. McMullen, N., *Chapter Four - How Hydrate Plugs Are Remediated*, in *Natural Gas Hydrates in Flow Assurance*, D. Sloan, et al., Editors. 2011, Gulf Professional Publishing: Boston. p. 49-86.
33. Sloan Jr, E.D. and C.A. Koh, *Clathrate hydrates of natural gases*. 2007: CRC press.
34. Jassim, E.I., M.A. Abdi, and Y. Muzychka. *A CFD-Based Model to Locate Flow-Restriction Induced Hydrate Deposition in Pipelines*. in *Offshore Technology Conference*. 2008. Offshore Technology Conference.
35. Sloan, E.D., *A changing hydrate paradigm—from apprehension to avoidance to risk management*. Fluid Phase Equilibria, 2005. **228**: p. 67-74.
36. Koh, C.A., et al., *Fundamentals and applications of gas hydrates*. The Annual Review of Chemical and Biomolecular Engineering, 2011. **2**: p. 237–257.
37. Pixabay. *Free images of Rusted Pipes*. [cited 2019 18.12.2019]; Available from: <https://pixabay.com/images/search/rusted%20pipes/>.
38. Li, X.-S., et al., *Investigation into gas production from natural gas hydrate: A review*. Applied Energy, 2016. **172**: p. 286-322.
39. Demirbas, A., *Methane hydrates as potential energy resource: Part 1—Importance, resource and recovery facilities*. Energy Conversion and Management, 2010. **51**(7): p. 1547-1561.
40. Nakicenovic, N., *Methane as an energy source for the 21st century*. International Journal of Global Energy Issues, 2002. **18**(1): p. 6-22.

41. Desa, E. *Submarine methane hydrates-potential fuel resource of the 21st century*. in *Proceedings of Andhra Pradesh Akademi of Sciences*, . 2001.
42. Makogon, I.U.r.F., *Hydrates of natural gas*. 1981: PennWell Books Tulsa, OK.
43. Englezos, P., *Clathrate hydrates*. *Industrial & engineering chemistry research*, 1993. **32**(7): p. 1251-1274.
44. Collett, T.S., *Energy resource potential of natural gas hydrates*. *AAPG bulletin*, 2002. **86**(11): p. 1971-1992.
45. Hacısalihoglu, B., A.H. Demirbas, and S. Hacısalihoglu, *Hydrogen from gas hydrate and hydrogen sulfide in the Black Sea*. *Energy Education Science and Technology*, 2008. **21**(1-2): p. 109-115.
46. Mazzini, A., et al., *Methane-related authigenic carbonates from the Black Sea: geochemical characterisation and relation to seeping fluids*. *Marine Geology*, 2004. **212**(1-4): p. 153-181.
47. Kvenvolden, K., *A primer on the geological occurrence of gas hydrate*. Geological Society, London, Special Publications, 1998. **137**(1): p. 9-30.
48. CICEP. *Japan*. [cited 2019 July 29, 2019]; Available from: <http://www.cicep.no/japan>.
49. U.S. Energy Information Administration. *Today in energy*. [cited 2019 July 29, 2019]; Available from: <https://www.eia.gov/todayinenergy/detail.php?id=13711>.
50. Okuda, Y., *Natural gas hydrate as a future resource*. *Journal of the Japan Institute of Energy*, 1993. **6**: p. 425-435.
51. Satoh, M., *Estimation of amount of methane and resources of natural gas hydrates in the world and around Japan*. *Journal Geological Society of Japan*, 1996. **102**: p. 959.
52. U.S. Energy Information Administration. *Taiwan: Analysis - Energy Sector Highlights*. 2016 [cited 2019 July 29, 2019]; Available from: <https://www.eia.gov/beta/international/country.php?iso=TWN>.
53. Weng, T., et al., *The general situation of the distribution and potential volume of gas hydrate in the south China*. *Min Metall*, 2013. **57**(2): p. 56-70.
54. U.S. Energy Information Administration. *Today in energy: China surpassed the United States as the world's largest crude oil importer in 2017 (February 5, 2018)*. 2018 [cited 2019 July 2019]; Available from: <https://www.eia.gov/todayinenergy/detail.php?id=34812>.
55. BP Energy Outlook – 2019, *Insights from the Evolving transition scenario – India*.
56. Digitally Learn. *Natural Gas Hydrates in India | UPSC – IAS*. [cited 2019 July 2019]; Available from: <https://digitallylearn.com/natural-gas-hydrates-in-india-upsc-ias/>.
57. Dutta, S., *US Geological Survey confirms ONGC's mega gas find* Read more at: http://timesofindia.indiatimes.com/articleshow/53400640.cms?utm_source=contentofinterest&utm_medium=text&utm_campaign=cppst, in *The Times of India*. 2016 (July 26).
58. (USGS), U.S.G.S. *Map of Gas Hydrates*. [cited 2019 18.12.2019]; Available from: <https://www.usgs.gov/media/images/map-gas-hydrates>.
59. Collett, T.S. and G.D. Ginsburg, *Gas hydrates in the Messoyakha gas field of the West Siberian Basin-a re-examination of the geologic evidence*. *International Journal of Offshore and Polar Engineering*, 1998. **8**(01).
60. Feng, J.-C., et al., *Evolution of hydrate dissociation by warm brine stimulation combined depressurization in the South China Sea*. *Energies*, 2013. **6**(10): p. 5402-5425.
61. Feng, J.-C., et al., *Numerical investigation of hydrate dissociation performance in the South China Sea with different horizontal well configurations*. *Energies*, 2014. **7**(8): p. 4813-4834.

62. Li, B., et al., *The use of heat-assisted antigravity drainage method in the two horizontal wells in gas production from the Qilian Mountain permafrost hydrate deposits*. Journal of Petroleum Science and Engineering, 2014. **120**: p. 141-153.
63. Li, G., et al., *Experimental investigation of production behavior of methane hydrate under ethylene glycol injection in unconsolidated sediment*. Energy Fuels 2007. **21**: p. 3388–3393.
64. Kawamura, T., et al., *Dissociation behavior of hydrate core sample using thermodynamic inhibitor*. International Journal of Offshore and Polar Engineering, 2006. **16**: p. 5–9.
65. Ross, M.J. and L.S. Toczykin, *Hydrate dissociation pressures for methane or ethane in the presence of aqueous solutions of triethylene glycol*. Journal of Chemical and Engineering Data, 1992. **37**(4): p. 488-491.
66. Afzal, W., A.H. Mohammadi, and D. Richon, *Experimental measurements and predictions of dissociation conditions for methane, ethane, propane, and carbon dioxide simple hydrates in the presence of diethylene glycol aqueous solutions*. Journal of Chemical & Engineering Data, 2008. **53**(3): p. 663-666.
67. Babae, S., et al., *Thermodynamic model for prediction of phase equilibria of clathrate hydrates of hydrogen with different alkanes, alkenes, alkynes, cycloalkanes or cycloalkene*. Fluid Phase Equilibria, 2012. **336**: p. 71-78.
68. Ohgaki, K., *Proposal for gas storage on the ocean floor using gas hydrate*. Kagaku Kogaku Ronbunshu, 1991. **17**: p. 1053-1055.
69. Kvamme, B., *Environmentally Friendly Production of Methane from Natural Gas Hydrate Using Carbon Dioxide*. Sustainability, 2019. **11**(7): p. 1964.
70. Lee, H., et al., *Recovering methane from solid methane hydrate with carbon dioxide*. Angewandte Chemie International Edition, 2003. **42**(41): p. 5048-5051.
71. Falenty, A., A. Salamatın, and W. Kuhs, *Kinetics of CO₂-hydrate formation from ice powders: Data summary and modeling extended to low temperatures*. The Journal of Physical Chemistry C, 2013. **117**(16): p. 8443-8457.
72. Englezos, P. and Y.T. Ngan, *Incipient equilibrium data for propane hydrate formation in aqueous solutions of sodium chloride, potassium chloride and calcium chloride*. Journal of Chemical and Engineering Data, 1993. **38**(2): p. 250-253.
73. Schroeder, W., *In Ahren's Sammlung Chemischer und Chemisch-Technik Vortrage, pp.21-71, Cross referenced from Hammerschmidt (1934)*. 1926-28.
74. Vafaei, M.T., *Reactive transport modelling of hydrate phase transition dynamics in porous media*. 2015, University of Bergen, Norway.
75. Campbell, J.M., *Gas Conditioning and Processing, Volume 1. Basic Principles. Pp 157-200*. 2003.
76. Faraday, M. and H. Davy, *On Fluid Chlorine*. Philosophical Transactions Royal Society London, 1823, **113**: p. 160-165.
77. Woehler, F., *Krystallisirtes Schwefelwasserstoff-Hydrat*. Justus Liebig's Annalen der Chemie, 1840. **33**(1): p. 125-126 Cross referenced from Hammerschmidt (1934).
78. Wroblewski, S., *On the laws of solubility of carbonic acid in water at high pressures (in French)*. Acad. Sci. Paris, *ibid.*, 1882c: p. 1355–1357.
79. Wroblewski, S., *On the composition of the hydrate of carbonic acid (in French)*. Acad. Sci. Paris, *ibid*, 1882b: p. 954–958.
80. Wroblewski, S., *On the combination of carbonic acid and water (in French)* Acad. Sci. Paris, *Comptes rendus*, 1882a. **94**: p. 212–213.
81. Ditte, A., *Crystallisation of Chlorine Hydrate* *Compt. rend.*, 1882. **95**: p. 1283-1284.
82. Maumene, E., *Chem. N*, 1883. **47**.

83. Roozeboom, H.W.B., *Sur l'hydrate de l'acide sulfureux* Rec. Trav. Chim. Pays-Bas., 1884. **3** p. 29-58. Cross referenced from: Ripmeester, J. A.; Alavia, S. (2016), <https://doi.org/10.1016/j.cossms.2016.03.005>.
84. Cailletet, L.P. and R. Bordet, *Sur divers hydrates qui se forment par la pression et la détente*. Compt. Rend. , 1882. **95**: p. 58–61.
85. Villard, P., *Sur quelques nouveaux hydrates de gaz*. Compt. rend, 1888. **106**: p. 1602-1603.
86. Ripmeester, J.A. and S. Alavi, *Some current challenges in clathrate hydrate science: Nucleation, decomposition and the memory effect*. Current Opinion in Solid State and Materials Science, 2016. **20**(6): p. 344-351.
87. Claussen, W.F., *Suggested structures of water in inert gas hydrates*. The Journal of Chemical Physics, 1951. **19**(2): p. 259-260.
88. Claussen, W.F., *Erratum: Suggested Structures of Water in Inert Gas Hydrates*. . The Journal of Chemical Physics, 1951. **19**(5): p. 662-662.
89. Claussen, W., *A second water structure for inert gas hydrates*. The Journal of Chemical Physics, 1951. **19**(11): p. 1425-1426.
90. Stackelberg, M.v. and H.R. Muller, *On the structure gas hydrate*. J. Chem. Phys., 1951. **19**.
91. Muller, H.R. and M.v. Stackelberg, *Zur Struktur de Gashydrate* Naturwissensch, 1952. **39**.
92. Pauling, L. and R.E. Marsh, *The structure of chlorine hydrate*. Proceedings of the National Academy of Sciences, 1952. **38**(2): p. 112-118.
93. Van der Waals, J.H. and J.C. Platteeuw, *Clathrate solutions*. Advances in Chemical Physics, 1959. **2**: p. 1-57.
94. Barrer, R.M. and W.I. Stuart. *Non-stoichiometric clathrate compounds of water*. in *Proceedings of the Royal Society of London A: Mathematical, Physical and Engineering Sciences*. 1957. The Royal Society.
95. Ripmeester, J.A., et al., *A new clathrate hydrate structure*. Nature, 1987. **325**(6100): p. 135-136.
96. Amundsen, L. and M. Landrø. *Gas Hydrates - Part I: Burning Ice*. 2012 June 3, 2017]; Available from: <http://www.geoexpro.com/articles/2012/12/gas-hydrates-part-i-burning-ice>.
97. Makogon, Y., *A gas hydrate formation in the gas saturated layers under low temperature*. Gas Industry, 1965. **5**: p. 14-15.
98. Makogon, Y., *Les hydrates de gaz: de l'énergie congelée*. La Recherche, 1987. **18**(192): p. 1192-1200.
99. Collett, T.S., *Detection and Evaluation of Natural Gas Hydrates from Wall Logs, Prudhoe Bay, Alaska*. 1983, University of Alaska, Fairbanks, Alaska.
100. Bily, C. and J.W.L. Dick, Bull. Can. Petr. Geol., 1974. **22**.
101. Weaver, J. and J. Stewart. *In situ hydrates under the Beaufort Sea shelf*. in *Proceedings, Fourth Canadian Permafrost Conference, March*. 1982.
102. Franklin, L., *In Natural Gas Hydrates: Properties, Occurrence and Recovery*, ed. e. Cox. J. L. Vol. 115. 1983, Butterworth, Boston, MA
103. Judge, A.S. *Natural gas hydrates in Canada*. in *Proceedings of the 4th Canadian Permafrost Conference*. 1982.
104. Collett, T.S., *National Assessment of United States Oil and Gas Resources on CD-ROM*, D.L. Gautier, Dolton, G. L., Takahashi, K. I., ed., Editor. 1995: USGS Digital Data Series 30, Washington DC.

105. Jeffrey, G.A., *Inclusion Compounds*, (Atwood, J.L., Davies, J.E.D., MacNichol, D.D., eds.). 1984, Academic Press: London. p. 135.
106. Brooks, J., et al., *Thermogenic gas hydrates in the Gulf of Mexico*. Science, 1984. **225**(4660): p. 409-411.
107. Davidson, D., et al., *Laboratory analysis of a naturally occurring gas hydrate from sediment of the Gulf of Mexico*. Geochimica et Cosmochimica Acta, 1986. **50**(4): p. 619-623.
108. Sassen, R. and I.R. MacDonald, *Evidence of structure H hydrate, Gulf of Mexico continental slope*. Organic Geochemistry, 1994. **22**(6): p. 1029-1032.
109. Mehta, A.P. and E.D. Sloan Jr, *Structure H hydrate phase equilibria of methane+ liquid hydrocarbon mixtures*. Journal of Chemical and Engineering Data, 1993. **38**(4): p. 580-582.
110. Maslin, M., et al., *Gas hydrates: past and future geohazard?* Philosophical Transactions of the Royal Society of London A: Mathematical, Physical and Engineering Sciences, 2010. **368**(1919): p. 2369-2393.
111. Aman, Z.M., et al., *Interfacial mechanisms governing cyclopentane clathrate hydrate adhesion/cohesion*. Physical Chemistry Chemical Physics, 2011. **13**(44): p. 19796-19806.
112. Sloan, E.D., *Fundamental principles and applications of natural gas hydrates*. Nature, 2003. **426**(6964): p. 353.
113. Kvamme, B. and O.K. Førrisdahl, *Polar guest-molecules in natural gas hydrates. Effects of polarity and guest-guest-interactions on the Langmuir-constants*. Fluid phase equilibria, 1993. **83**: p. 427-435.
114. Kvamme, B. and A. Lund, *The influence of gas-gas interactions on the Langmuir constants for some natural gas hydrates*. Fluid phase equilibria, 1993. **90**(1): p. 15-44.
115. Sloan Jr, E. *Hydrate nucleation from ice*. in *69th Annual Gas Proceedings Conference, Phoenix, Ariz.* 1990b.
116. Chatti, I., et al., *Benefits and drawbacks of clathrate hydrates: a review of their areas of interest*. Energy conversion and management, 2005. **46**(9-10): p. 1333-1343.
117. Davidson, D. *Natural gas hydrates in northern Canada*. in *Proc. 3rd Int. Conf. on Permafrost*. 1978. National Research Council of Canada.
118. Thomas, S. and R.A. Dawe, *Review of ways to transport natural gas energy from countries which do not need the gas for domestic use*. Energy, 2003. **28**(14): p. 1461-1477.
119. Zhong, Y. and R. Rogers, *Surfactant effects on gas hydrate formation*. Chemical Engineering Science, 2000. **55**(19): p. 4175-4187.
120. Sun, Z.-G., et al., *Experimental studying of additives effects on gas storage in hydrates*. Energy & Fuels, 2003. **17**(5): p. 1180-1185.
121. Sun, Z.-g., et al., *Natural gas storage in hydrates with the presence of promoters*. Energy Conversion and Management, 2003. **44**(17): p. 2733-2742.
122. Stern, L.A., et al., *Anomalous preservation of pure methane hydrate at 1 atm*. The Journal of Physical Chemistry B, 2001. **105**(9): p. 1756-1762.
123. Taylor, M., R.A. Dawe, and S. Thomas. *Fire and Ice: Gas hydrate transportation-A possibility for the Caribbean region*. in *SPE Latin American and Caribbean Petroleum Engineering Conference*. 2003. Society of Petroleum Engineers.
124. Shirota, H., et al. *Measurement of methane hydrate dissociation for application to natural gas storage and transportation*. in *Proceedings of the 4th International Conference on Gas Hydrates, Yokohama, Japan*. 2002.
125. Khokhar, A., J. Gudmundsson, and E. Sloan, *Gas storage in structure H hydrates*. Fluid Phase Equilibria, 1998. **150**: p. 383-392.

126. Gnanendran, N. and R. Amin, *The effect of hydrotropes on gas hydrate formation*. Journal of Petroleum Science and Engineering, 2003. **40**(1-2): p. 37-46.
127. Bryant, E. and E.A. Bryant, *Climate process and change*. 1997: Cambridge University Press.
128. Desideri, U. and A. Paolucci, *Performance modelling of a carbon dioxide removal system for power plants*. Energy Conversion and Management, 1999. **40**(18): p. 1899-915.
129. Smith, I. and K. Thambimuthu, *Greenhouse gas emissions, abatement and control: the role of coal*. Energy & fuels, 1993. **7**(1): p. 7-13.
130. Chakma, A., *CO₂ capture processes—opportunities for improved energy efficiencies*. Energy conversion and management, 1997. **38**: p. S51-S56.
131. Gray, M., et al., *CO₂ capture by amine-enriched fly ash carbon sorbents*. Separation and Purification Technology, 2004. **35**(1): p. 31-36.
132. Hendriks, C. and K. Blok, *Underground storage of carbon dioxide*. Energy Conversion and Management, 1993. **34**(9-11): p. 949-957.
133. Bachu, S., *Sequestration of CO₂ in geological media in response to climate change: road map for site selection using the transform of the geological space into the CO₂ phase space*. Energy Conversion and management, 2002. **43**(1): p. 87-102.
134. Brewer, P.G., et al., *Direct experiments on the ocean disposal of fossil fuel CO₂*. Science, 1999. **284**(5416): p. 943-945.
135. Kojima, R., K. Yamane, and I. Aya. *Dual nature of CO₂ solubility in hydrate forming region*. in *Greenhouse Gas Control Technologies-6th International Conference*. 2003. Elsevier.
136. Bachu, S. and J. Adams, *Sequestration of CO₂ in geological media in response to climate change: capacity of deep saline aquifers to sequester CO₂ in solution*. Energy Conversion and management, 2003. **44**(20): p. 3151-3175.
137. Liro, C.R., E.E. Adams, and H.J. Herzog, *Modeling the release of CO₂ in the deep ocean*. Energy Conversion and Management, 1992. **33**(5-8): p. 667-674.
138. Holder, G.D., A.V. Cugini, and R.P. Warzinski, *Modeling clathrate hydrate formation during carbon dioxide injection into the ocean*. Environmental science & technology, 1995. **29**(1): p. 276-278.
139. Lee, S., et al., *CO₂ hydrate composite for ocean carbon sequestration*. Environmental science & technology, 2003. **37**(16): p. 3701-3708.
140. Harrison, W.J., R.F. Wendlandt, and E.D. Sloan, *Geochemical interactions resulting from carbon dioxide disposal on the seafloor*. Applied Geochemistry, 1995. **10**(4): p. 461-475.
141. Aya, I., K. Yamane, and H. Nariai, *Solubility of CO₂ and density of CO₂ hydrate at 30 MPa*. Energy, 1997. **22**(2-3): p. 263-271.
142. Uchida, T., et al., *Dissolution mechanisms of CO₂ molecules in water containing CO₂ hydrates*. Energy Conversion and Management, 1997. **38**: p. S307-S312.
143. Yang, S., et al., *Measurement and prediction of phase equilibria for water+ CO₂ in hydrate forming conditions*. Fluid Phase Equilibria, 2000. **175**(1-2): p. 75-89.
144. Englezos, P., *Computation of the incipient equilibrium carbon dioxide hydrate formation conditions in aqueous electrolyte solutions*. Industrial & engineering chemistry research, 1992. **31**(9): p. 2232-2237.
145. Circone, S., et al., *CO₂ hydrate: synthesis, composition, structure, dissociation behavior, and a comparison to structure I CH₄ hydrate*. The Journal of Physical Chemistry B, 2003. **107**(23): p. 5529-5539.
146. Kang, S.-P. and H. Lee, *Recovery of CO₂ from flue gas using gas hydrate: thermodynamic verification through phase equilibrium measurements*. Environmental science & technology, 2000. **34**(20): p. 4397-4400.

147. Inaba, H., *New challenge in advanced thermal energy transportation using functionally thermal fluids*. International journal of thermal sciences, 2000. **39**(9-11): p. 991-1003.
148. Aittomäki, A. and A. Lahti, *Potassium formate as a secondary refrigerant*. International journal of refrigeration, 1997. **20**(4): p. 276-282.
149. Lugo, R., et al., *An excess function method to model the thermophysical properties of one-phase secondary refrigerants*. International Journal of Refrigeration, 2002. **25**(7): p. 916-923.
150. Saito, A., *Recent advances in research on cold thermal energy storage*. International Journal of Refrigeration, 2002. **25**(2): p. 177-189.
151. Bel, O. and A. Lallemand, *Study of a two phase secondary refrigerant 1: intrinsic thermophysical properties of an ice slurry*. 1999, ELSEVIER SCI LTD THE BOULEVARD, LANGFORD LANE, KIDLINGTON, OXFORD OX5 1GB
152. Tanasawa, I. and S. Takao. *Low-temperature storage using clathrate hydrate slurries of tetra-n-butylammonium bromide: thermophysical properties and morphology of clathrate hydrate crystals*. in *Fourth international conference on gas hydrates*. Yokohama, Japan. 2002.
153. Fournaison, L., et al., *CO₂ hydrates in refrigeration processes*. Industrial & engineering chemistry research, 2004. **43**(20): p. 6521-6526.
154. Tanino, M. and Y. Kozawa, *Ice-water two-phase flow behavior in ice heat storage systems*. International journal of refrigeration, 2001. **24**(7): p. 639-651.
155. Ayel, V., O. Lottin, and H. Peerhossaini, *Rheology, flow behaviour and heat transfer of ice slurries: a review of the state of the art*. International Journal of Refrigeration, 2003. **26**(1): p. 95-107.
156. Matsumoto, K., et al., *Continuous ice slurry formation using a functional fluid for ice storage*. International journal of refrigeration, 2004. **27**(1): p. 73-81.
157. Bi, Y., et al., *Influence of volumetric-flow rate in the crystallizer on the gas-hydrate cool-storage process in a new gas-hydrate cool-storage system*. Applied energy, 2004. **78**(1): p. 111-121.
158. WITTSTRUCK, T.A., et al., *Solid hydrates of some halomethanes*. Journal of Chemical and Engineering Data, 1961. **6**(3): p. 343-346.
159. Mori, T. and Y. Mori, *Characterization of gas hydrate formation in direct-contact cool storage process*. International journal of refrigeration, 1989. **12**(5): p. 259-265.
160. Tomlinson, J., *Clathrates: a storage alternative to ice for residential cooling*. 1983, Oak Ridge National Lab., TN (USA).
161. Carbajo, J.J., *A direct-contact-charged direct-contact-discharged cool storage system using gas hydrate*. ASHRAE Trans.:(United States), 1985. **91**(CONF-850606-).
162. Akiya, T., *Cool storage using gas hydrate*. 17th Int. Cong. of Refrigeration Proc., 1987: p. 160-170.
163. Mori, Y.H. and T. Mori, *Formation of gas hydrate with CFC alternative R-134a*. AI Ch. E. Journal (American Institute of Chemical Engineers);(USA), 1989. **35**(7).
164. Mori, Y.H. and F. Isobe, *A model for gas hydrate formation accompanying direct-contact evaporation of refrigerant drops in water*. International communications in heat and mass transfer, 1991. **18**(5): p. 599-608.
165. Lubert-Martin, M., M. Darbouret, and J.-M. Herri. *Rheological study of two-phase secondary fluids for refrigeration and air conditioning*. 2003.
166. Sloan, E.D., *Clathrate Hydrates of Natural Gases*. 2nd ed. 1998: New York: Marcel Dekker, Inc.

167. Kang, S.-P., H. Lee, and B.-J. Ryu, *Enthalpies of dissociation of clathrate hydrates of carbon dioxide, nitrogen,(carbon dioxide+ nitrogen), and (carbon dioxide+ nitrogen+ tetrahydrofuran)*. The Journal of Chemical Thermodynamics, 2001. **33**(5): p. 513-521.
168. Anderson, G.K., *Enthalpy of dissociation and hydration number of methane hydrate from the Clapeyron equation*. The Journal of Chemical Thermodynamics, 2004. **36**(12): p. 1119-1127.
169. Delahaye, A., et al., *Effect of THF on equilibrium pressure and dissociation enthalpy of CO₂ hydrates applied to secondary refrigeration*. Industrial & engineering chemistry research, 2006. **45**(1): p. 391-397.
170. Jean-Baptiste, P. and R. Ducroux, *Potentiel des méthodes de séparation et stockage du CO₂ dans la lutte contre l'effet de serre*. Comptes Rendus Geoscience, 2003. **335**(6-7): p. 611-625.
171. Tam, S., et al. *A high pressure carbon dioxide separation process for IGCC plants*. in *First National Conference on Carbon Sequestration, Washington DC, USA*. 2001.
172. Volmer, M. and A. Weber, *Keimbildung in übersättigten Gebilden*. Z. Phys. Chem. 1925. **119**.
173. Becker, D. and W. Döring, *The kinetic treatment of nuclear formation in supersaturated vapors*. . Annalen der Physik., 1935. **24**: p. 719-52.
174. Frenkel, J.A., *A general theory of heterophase fluctuations and pretransition phenomena*. The Journal of Chemical Physics, 1939. **7**(7): p. 538-547.
175. Zeldovich, J.B., *Acta Physicochimica USSR* 18, 1 1943.
176. Kvamme, B., *Fundamentals of Natural Gas Hydrates and Practical Implications, Unpublished Work: PTEK 232, Course Material, Spring Semester 2017, Department of Physics and Technology, University of Bergen, Norway*. 2017.
177. Bauman, J.M., *Kinetic Modelling of Hydrate Formation, Dissociation, and Reformation 2015*, University of Bergen, Norway.
178. Mullen, J.W., *Crystallization*. 3rd Edition ed. 1993, Oxford, U.K.: Butterworth-Heinmann.
179. Kashchiev, D. and A. Firoozabadi, *Nucleation of gas hydrates*. Journal of crystal growth, 2002. **243**(3): p. 476-489.
180. Kvamme, B., et al., *Can hydrate form in carbon dioxide from dissolved water?* Physical Chemistry Chemical Physics, 2013. **15**(6): p. 2063-2074.
181. Buanes, T., *Mean-field approaches applied to hydrate phase transition kinetics*. 2008, PhD thesis, University of Bergen, Norway.
182. Kvamme, B., et al., *Hydrate Formation During Transport of Natural Gas Containing Water And Impurities*. International Journal of Engineering Research and Development, 2017. **13**(5): p. .01-16.
183. Kvamme, B., *Kinetics of hydrate formation from nucleation theory*. International journal of offshore and Polar Engineering, 2002. **12**(04).
184. Long, J.P., *Gas hydrate formation mechanism and kinetic inhibition*. 1994, Colorado School of Mines.
185. Kvamme, B. *A New Theory for the Kinetics of Hydrate Formation*. in *Proc. 2nd Int Conf Natural Gas Hydrates*, 1996. Toulouse, France.
186. Kvamme, B. and H. Tanaka, *Thermodynamic stability of hydrates for ethane, ethylene, and carbon dioxide*. The Journal of Physical Chemistry, 1995. **99**(18): p. 7114-7119.
187. Kvamme, B., *Kinetics of Hydrate Formation on Unstirred Water Surfaces from Classical Nucleation Theory*, in *13th Int. Symp. Thermophy Properties*. 1997: Boulder, Colorado, USA.

188. Song, G. and R. Kobayashi, *NMR studies of hydrate formation*, in *Submitted for presentation on the sixth International Offshore and Polar Engineering Conference*. 1996: Honolulu, Hawaii.
189. Kobayashi, R., *Rice University, Houston, US, private communication with Prof. Bjørn Kvamme of University of Bergen*. 1997.
190. Makogon, Y.F., *Hydrates of Hydrocarbons*. 1997: PennWell Books.
191. Sloan, E. and F. Fleyfel, *A molecular mechanism for gas hydrate nucleation from ice*. *AIChE Journal*, 1991. **37**(9): p. 1281-1292.
192. Davies, S. *Nucleation Theory: A Literature Review and Applications to Nucleation Rates of Natural Gas Hydrates*.
193. Koh, C., et al., *Mechanisms of gas hydrate formation and inhibition*. *Fluid Phase Equilibria*, 2002. **194**: p. 143-151.
194. Radhakrishnan, R. and B.L. Trout, *A new approach for studying nucleation phenomena using molecular simulations: application to CO₂ hydrate clathrates*. *The Journal of chemical physics*, 2002. **117**(4): p. 1786-1796.
195. Christiansen, R.L. and E.D. Sloan, *Mechanisms and kinetics of hydrate formation*. *Annals of the New York Academy of Sciences*, 1994. **715**(1): p. 283-305.
196. Skovborg, P., *Gas Hydrate Kinetics*. 1993, Inst. for Chem Eng, Danmarks Tekniske Højskole, Lyngby, Denmark.
197. Youusif, M. *The kinetics of hydrate formation*. in *SPE Annual Technical Conference and Exhibition*. 1994. Society of Petroleum Engineers.
198. Natarajan, V., *Thermodynamics and nucleation of gas hydrates*,. 1993, University of Calgary, Alberta
199. Englezos, P., et al., *Kinetics of gas hydrate formation from mixtures of methane and ethane*. *Chemical Engineering Science*, 1987. **42**(11): p. 2659-2666.
200. Englezos, P. and P. Bishnoi, *Gibbs free energy analysis for the supersaturation limits of methane in liquid water and the hydrate-gas-liquid water phase behavior*. *Fluid Phase Equilibria*, 1988. **42**: p. 129-140.
201. Skovborg, P. and P. Rasmussen, *A mass transport limited model for the growth of methane and ethane gas hydrates*. *Chemical Engineering Science*, 1994. **49**(8): p. 1131-1143.
202. Kvamme, B. *Kinetics of Hydrate Formation*. in *Proc. 5th Asian Thermophys. Properties Conf*. 1998. Seoul.
203. Kvamme, B., *Initiation and Growth of Hydrate*, in *3rd Int. Conf. Natural Gas Hydrates*. 2000a, Ann. New York Acad. of Sci.: Park City, Utah, USA. p. 496-501.
204. Jorgensen, W.L., et al., *Comparison of simple potential functions for simulating liquid water*. *The Journal of chemical physics*, 1983. **79**(2): p. 926-935.
205. Tse, J., et al., *The lattice dynamics of clathrate hydrates. An incoherent inelastic neutron scattering study*. *Chemical physics letters*, 1993. **215**(4): p. 383-387.
206. Kvamme, B., et al., *Storage of CO₂ in natural gas hydrate reservoirs and the effect of hydrate as an extra sealing in cold aquifers*. *Int. J. Greenhouse Gas Control*, 2007. **1**: p. 236.
207. Svandal, A., *Modeling hydrate phase transitions using mean-field approaches*. 2006, University of Bergen.
208. Haymet, A. and T. Barlow, *Nucleation of Supercooled Liquids*. *Annals of the New York Academy of Sciences*, 2006. **715**(1): p. 549-551. Cross referenced from Almenningen, S. (2015). *An Experimental Study of Methane Hydrates in Sandstone Cores*, MSc Thesis, University of Bergen.

209. Bauman, J., *Kinetic modelling of hydrate formation, dissociation, and reformation*. 2015, Bergen: University of Bergen.
210. Gibbs, J.W., *On the Equilibrium of Heterogeneous Substances*. Scientific Papers, Dover, New York, 1961.
211. Gibbs, J., *The Collected Works of J. Willard Gibbs, Thermodynamics, vol. 1, 55–349*. 1928, Longmans, Green and Co., New York.
212. Kvamme, B., et al., *Consequences of CO₂ solubility for hydrate formation from carbon dioxide containing water and other impurities*. Physical Chemistry Chemical Physics, 2014. **16**(18): p. 8623-8638.
213. Ohgaki, K., Y. Makihara, and K. Takano, *Formation of CO₂ hydrate in pure and sea waters*. Journal of chemical engineering of Japan, 1993. **26**(5): p. 558-564.
214. Anderson, G.K., *Enthalpy of dissociation and hydration number of carbon dioxide hydrate from the Clapeyron equation*. The Journal of Chemical Thermodynamics, 2003. **35**(7): p. 1171-1183.
215. Nakamura, T., et al., *Stability boundaries of gas hydrates helped by methane—structure-H hydrates of methylcyclohexane and cis-1, 2-dimethylcyclohexane*. Chemical engineering science, 2003. **58**(2): p. 269-273.
216. Maekawa, T., *Equilibrium conditions for gas hydrates of methane and ethane mixtures in pure water and sodium chloride solution*. Geochemical Journal, 2001. **35**(1): p. 59-66.
217. Vysniauskas, A. and P. Bishnoi, *A kinetic study of methane hydrate formation*. Chemical Engineering Science, 1983. **38**(7): p. 1061-1072.
218. Natarajan, V., P. Bishnoi, and N. Kalogerakis, *Induction phenomena in gas hydrate nucleation*. Chemical Engineering Science, 1994. **49**(13): p. 2075-2087.
219. Christiansen, R.L. and E.D. Sloan Jr. *A compact model for hydrate formation*. 1995. San Antonio, TX (United States): 74. Annual Gas Processors Association (GPA) meeting.
220. Kashchiev, D. and A. Firoozabadi, *Driving force for crystallization of gas hydrates*. Journal of crystal growth, 2002. **241**(1): p. 220-230.
221. Anklam, M.R. and A. Firoozabadi, *Driving force and composition for multicomponent gas hydrate nucleation from supersaturated aqueous solutions*. J. Chem. Phys., 2004. **121**.
222. Arjmandi, M., et al., *Is subcooling the right driving force for testing low-dosage hydrate inhibitors?* Chemical engineering science, 2005a. **60**(5): p. 1313-1321.
223. Qorbani, K., B. Kvamme, and R. Olsen, *Non-equilibrium simulation of hydrate formation and dissociation from CO₂ in the aqueous phase*. Journal of Natural Gas Science and Engineering, 2016. **35**: p. 1555-1565.
224. Parrish, W.R. and J.M. Prausnitz, *Dissociation Pressures of Gas Hydrates Formed by Gas Mixtures*. Industrial & Engineering Chemistry Process Design and Development, 1972. **11**: p. 26-34.
225. Klauda, J.B. and S.I. Sandler, *A fugacity model for gas hydrate phase equilibria*. Industrial & engineering chemistry research, 2000. **39**(9): p. 3377-3386.
226. Koh, C.A., *Towards a fundamental understanding of natural gas hydrates*. Chemical Society Reviews, 2002. **31**(3): p. 157-167.
227. Westacott, R.E. and P. Rodger, *Full-coordinate free-energy minimisation for complex molecular crystals: type I hydrates*. Chemical physics letters, 1996. **262**(1-2): p. 47-51.
228. Zele, S., S.-Y. Lee, and G. Holder, *A theory of lattice distortion in gas hydrates*. The Journal of Physical Chemistry B, 1999. **103**(46): p. 10250-10257.
229. Soave, G., *Equilibrium constants from a modified Redlich-Kwong equation of state*. Chemical Engineering Science, 1972. **27**(6): p. 1197-1203.
230. Kvamme, B., *Kinetics of Hydrate Formation from Nucleation Theory*. Int. J. Offshore Polar Eng., 2002. **12**: p. 256.

231. Kvamme, B., *Droplets of Dry Ice and Cold Liquid CO₂ for Self-Transport of CO₂ to Large Depths*. Int. J. Offshore Polar Eng., 2003. **13**: p. 139.
232. Kvamme, B., et al., *Kinetics of solid hydrate formation by carbon dioxide: Phase field theory of hydrate nucleation and magnetic resonance imaging*. Phys. Chem. Chem. Phys., 2004. **6**: p. 2327-2334.
233. Kvamme, B., et al., *Hydrate phase transition kinetics from Phase Field Theory with implicit hydrodynamics and heat transport*. Int. J. Greenhouse Gas Control, 2014. **29**: p. 263.
234. Pilvi-Helinä Kiveläe, et al., *Phase field theory modeling of methane fluxes from exposed natural gas hydrate reservoirs*. AIP Conference Proceedings, 2012. **1504**(1): p. 351-363.
235. Tegze, G., et al., *Multiscale approach to CO₂ hydrate formation in aqueous solution: Phase field theory and molecular dynamics. Nucleation and growth*. The Journal of chemical physics, 2006. **124**(23): p. 234710.
236. Ebbrell, H.K., *The composition of Statoil (Norway) gas well*. 1984. p. 1-26.
237. Unruh, C.H. and D.L. Katz, *Gas hydrates of carbon dioxide-methane mixtures*. Journal of Petroleum Technology, 1949. **1**(04): p. 83-86.
238. Adisasmito, S., R.J. Frank III, and E.D. Sloan Jr, *Hydrates of carbon dioxide and methane mixtures*. Journal of Chemical and Engineering Data, 1991. **36**(1): p. 68-71.
239. Adisasmito, S. and E.D. Sloan Jr, *Hydrates of hydrocarbon gases containing carbon dioxide*. Journal of Chemical and Engineering Data, 1992. **37**(3): p. 343-349.
240. Berecz, E. and M. Balla-Achs, *Gas hydrates (as summarized In: Gas Hydrates; Studies In Inorganic Chemistry)*, in *Research Report No. 37 (185-XI-1-1974 OGIL)*. 1983: Elsevier: New York, U.S.A. p. 343.
241. Ma, Z., et al., *Review of fundamental properties of CO₂ hydrates and CO₂ capture and separation using hydration method*. Renewable and Sustainable Energy Reviews, 2016. **53**: p. 1273-1302.
242. Nazeri, M., B. Tohidi, and A. Chapoy, *An evaluation of risk of hydrate formation at the top of a pipeline*. Oil and Gas Facilities, 2014. **3**(02): p. 67-72.
243. Anderson, R., H. Mozaffar, and B. Tohidi. *Development of a crystal growth inhibition based method for the evaluation of kinetic hydrate inhibitors*. in *Proceedings of the 7th International Conference on Gas hydrates*. 2011. Domestic Organizing Committee ICGH-7, Edinburgh.
244. Glénat, P., et al. *Application of a new crystal growth inhibition based KHI evaluation method to commercial formulation assessment*. in *Proceedings of the 7th International Conference on Gas hydrates*. 2011. Domestic Organizing Committee ICGH-4, Edinburgh.
245. Fenter, D. and D. Hadiatno. *Reservoir simulation modeling of natuna gas field for reservoir evaluation and development planning*. in *SPE Asia Pacific Oil and Gas Conference*. 1996. Society of Petroleum Engineers.
246. Kaarstad, O. and C.-W. Hustad, *CO₂-Supply Report, Elsam A/S – Kinder Morgan CO₂ Company L.P. – New Energy/Statoil AsA*. 2003.
247. Schuchardt, B., G. Krause, and H.G. Kulp, *Environmental impact assessment. Europe II in Germany offshore and onshore section*. Bioconsult Schuchardt & Scholle. Bremen, Germany. 1998.
248. Kvamme, B., T. Kuznetsova, and P.-H. Kiveläe, *Adsorption of water and carbon dioxide on hematite and consequences for possible hydrate formation*. Physical Chemistry Chemical Physics, 2012. **14**(13): p. 4410-4424.
249. Kvamme, B.r., T. Kuznetsova, and M. Haynes. *Molecular dynamics studies of water deposition on hematite surfaces*. in *AIP Conference Proceedings*. 2012. AIP.

250. Kuznetsova, T., et al., *Water-wetting surfaces as hydrate promoters during transport of carbon dioxide with impurities*. Physical Chemistry Chemical Physics, 2015. **17**(19): p. 12683-12697.
251. Kvamme, B. and A. Sapate, *Hydrate risk evaluation during transport and processing of natural gas mixtures containing ethane and methane*. Research & Reviews: Journal of Chemistry, 2016. **5**: p. 64-74.
252. Gengliang, C., *Formation and prevention of hydrate during process of gas exploitation and transmission*. Natural Gas Industry, 2004. **24**: p. 89-91.
253. Huo, Z., et al., *Hydrate plug prevention by anti-agglomeration*. Chemical Engineering Science, 2001. **56**(17): p. 4979-4991.
254. Budd, D., et al. *Enhanced hydrate inhibition in Alberta gas field*. in *SPE Annual Technical Conference and Exhibition*. 2004. Society of Petroleum Engineers.
255. Circone, S., S.H. Kirby, and L.A. Stern, *Direct measurement of methane hydrate composition along the hydrate equilibrium boundary*. The Journal of Physical Chemistry B, 2005. **109**(19): p. 9468-9475.
256. Henry, P., et al., *Formation of natural gas hydrates in marine sediments: 2. Thermodynamic calculations of stability conditions in porous sediments*. Journal of Geophysical Research: Solid Earth, 1999. **104**(B10): p. 23005-23022.
257. Englezos, P., et al., *Kinetics of formation of methane and ethane gas hydrates*. Chemical Engineering Science, 1987. **42**(11): p. 2647-2658.
258. Ke, W., T.M. Svartaas, and D. Chen, *A review of gas hydrate nucleation theories and growth models*. Journal of Natural Gas Science and Engineering, 2019. **61**: p. 169-196.
259. Davies, S.R., et al., *Studies of hydrate nucleation with high pressure differential scanning calorimetry*. Chemical Engineering Science, 2009. **64**(2): p. 370-375.
260. Sarupria, S. and P.G. Debenedetti, *Homogeneous nucleation of methane hydrate in microsecond molecular dynamics simulations*. The journal of physical chemistry letters, 2012. **3**(20): p. 2942-2947.
261. Takeya, S., et al., *Freezing-memory effect of water on nucleation of CO₂ hydrate crystals*. The Journal of Physical Chemistry B, 2000. **104**(17): p. 4164-4168.
262. Collett, T.S., *Gas hydrates as a future energy resource*. Geotimes, 2004. **49**: p. 24-27.
263. Makogon, Y.F., S. Holditch, and T.Y. Makogon, *Natural gas-hydrates—A potential energy source for the 21st Century*. Journal of petroleum science and engineering, 2007. **56**(1-3): p. 14-31.
264. Chong, Z.R., et al., *Review of natural gas hydrates as an energy resource: Prospects and challenges*. Applied energy, 2016. **162**: p. 1633-1652.
265. Aregbe, A.G., *Gas hydrate—properties, formation and benefits*. Open Journal of Yangtze Oil and Gas, 2017. **2**(1): p. 27-44.
266. Fu, X., et al., *Gas hydrate formation and accumulation potential in the Qiangtang Basin, northern Tibet, China*. Energy Conversion and Management, 2013. **73**: p. 186-194.
267. Liu, C., et al., *The characteristics of gas hydrates recovered from Shenhu Area in the South China Sea*. Marine Geology, 2012. **307**: p. 22-27.
268. Zhu, Y., et al., *Gas hydrates in the Qilian mountain permafrost, Qinghai, Northwest China*. Acta Geologica Sinica-English Edition, 2010. **84**(1): p. 1-10.
269. Lu, Z., et al., *Gas hydrate occurrences in the Qilian Mountain permafrost, Qinghai province, China*. Cold regions science and technology, 2011. **66**(2-3): p. 93-104.
270. Dallimore, S., T. Uchida, and T. Collett, *Scientific results from JAPEX/JNOC/GSC Mallik 2L-38 gas hydrate research well, Mackenzie delta, Northwest Territories, Canada*. Vol. 544. 1999: Geological Survey of Canada Ottawa, Ontario, Canada.

271. Falenty, A., et al., *Kinetics of CO₂ hydrate formation from water frost at low temperatures: Experimental results and theoretical model*. The Journal of Physical Chemistry C, 2011. **115**(10): p. 4022-4032.
272. Lirio, C. and F. Pessoa, *Enthalpy of dissociation of simple and mixed carbon dioxide clathrate hydrate*. Chemical Engineering Transactions, 2013. **32**.
273. Gupta, A., et al., *Measurements of methane hydrate heat of dissociation using high pressure differential scanning calorimetry*. Chemical Engineering Science, 2008. **63**(24): p. 5848-5853.
274. Sloan, E. and F. Fleyfel, *Hydrate dissociation enthalpy and guest size*. Fluid Phase Equilibria, 1992. **76**: p. 123-140.
275. Kvamme, B., *Thermodynamic Limitations of the CO₂/N₂ Mixture Injected into CH₄ Hydrate in the Ignik Sikumi Field Trial*. J. Chem. Eng. Data, 2016, 61 (3), pp 1280–1295, 2016.
276. Kvamme, B., et al., *Hydrate Production Philosophy and Thermodynamic Calculations*. Energies, 2020. **13**(3): p. 672.

Special References [Papers]

1. Aromada, S. A.; Kvamme, B. New approach for evaluating the risk of hydrate formation during transport of hydrocarbon hydrate formers of sl and sll. *AIChE Journal*, 2019, 65(3):1097-1110.
2. Kvamme, B.; Aromada S. A. Risk of hydrate formation during the processing and transport of Troll gas from the North Sea. *Journal of Chemical & Engineering Data*, 2017, 62(7):2163-2177.
3. Kvamme, B.; Aromada, S. A. Alternative routes to hydrate formation during processing and transport of natural gas with a significant amount of CO₂: Sleipner gas as a case study. *Journal of Chemical & Engineering Data*, 2018, 63(3):832-844.
4. Kvamme, B.; Aromada, S. A.; Kuznetsova, T.; Gjerstad, P. B.; Canonge, P. C.; Zarifi, M. Maximum tolerance for water content at various stages of a Natuna production. *Heat and Mass Transfer*, 2019, 55(4):1059-1079.
5. Aromada, S. A.; Kvamme, B. Impacts of CO₂ and H₂S on the risk of hydrate formation during pipeline transport of natural gas. *Frontiers of Chemical Science and Engineering*, 2019, 13(3):616-627.
6. Aromada, S. A.; Kvamme, B. Simulation of Hydrate Plug Prevention in Natural Gas Pipeline from Bohai Bay to Onshore Facilities in China. *Simulation Notes Europe Journal*, SNE 31(3), 2021, 151-157, DOI: 10.11128/sne.31.tn.10576
7. Kvamme, B.; Aromada, S. A.; Saeidi, N. Heterogeneous and homogeneous hydrate nucleation in CO₂/water systems. *Journal of Crystal Growth*, 2019, 522: 160-174.
8. Kvamme, B.; Aromada, S.A.; Saeidi N.; Hustache-Marmou, T.; Gjerstad, P.B. Hydrate nucleation, growth and induction. *ACS Omega*, 2020, 5(6): 2603-2619.
9. Kvamme B.; Aromada S. A.; Gjerstad, P. B. Consistent enthalpies of the hydrate formation and dissociation using residual thermodynamics. *Journal of Chemical & Engineering Data*, 2019, 2019, 64(8):3493-3504.

10. Aromada, S. A.; Kvamme, B. Modelling of Methane Hydrate Formation and Dissociation using Residual Thermodynamics. *Simulation Notes Europe Journal*, SNE 31(3), 2021, 143-150. DOI: 10.11128/sne.31.tn.10575
11. Aromada, S. A.; Kvamme, B. Production of methane from hydrate and CO₂ zero-emission concept. Proceedings in: The 10th EUROSIM Conference, Logroño (La Rioja), Spain, July 1– 5, 2019.
12. Aromada, S. A.; Kvamme, B.; Wei, N.; Saeidi, N. Enthalpies of hydrate formation and dissociation from residual thermodynamics. *Energies*, 2019, 12, 24, 4726.

Part 2

Paper 1

New approach for evaluating the risk of hydrate formation during transport of hydrocarbon hydrate formers of sl and sll

By

Solomon Aforkoghene Aromada and Bjørn Kvamme

Published in

AIChE Journal, 2019, 65(3):1097-1110



New Approach for Evaluating the Risk of Hydrate Formation During Transport of Hydrocarbon Hydrate formers of sl and sll

Solomon Aforkoghene Aromada and Bjørn Kvamme

Dept. of Physics and Technology, University of Bergen, Allegaten 55, 5007, Bergen, Norway

DOI 10.1002/aic.16493

Published online December 25, 2018 in Wiley Online Library (wileyonlinelibrary.com)

Classical industrial hydrate risk evaluation schemes are commonly based on water dew-point calculation. This method ignores another (new) route to hydrate formation based on adsorption of water onto rusty surfaces. Maximum allowable water contents in pure and mixtures of hydrate formers of Structures I and II hydrocarbons to avoid the risk of hydrate nucleation during pipeline transport have been studied using both the dew-point method and the new approach of adsorption of water onto hematite (rust). The estimates from this study suggest that the new approach (adsorption of water onto the rusty internal walls of pipelines and equipment) dominates. Thus, this approach could have an impact on designing natural gas dehydration systems. Free energy analysis has also been performed to show which molecule forms hydrate first based on the combined first and second laws of thermodynamics in terms of Gibbs free energy. © 2018 American Institute of Chemical Engineers *AIChE J.* 65: 1097–1110, 2019

Keywords: natural gas hydrate, Structure II hydrate, Structure I hydrate, hematite, rust, adsorption

Introduction

Formation of natural gas hydrate during processing and transport of hydrocarbons is a crucial problem that could result in eventual plugging and destruction of pipelines and equipment, thereby halting operations and consequentially economic losses, and can even result in loss of lives.¹ These explain the significance of evaluating the risk of hydrate formation. Gas hydrate could form during the processing and transport of hydrocarbons if free water is available at high pressure and low temperature conditions, with favorable mass and heat transport. Methane, ethane, propane, and isobutane (C₁–C₄) are the hydrocarbon guest molecules that could be entrapped in water cavities to form Structures I and II hydrates. Structure H hydrates can host up to C₇. Structure H hydrate type is not commonly encountered in industrial operations; no record of it being found in industrial applications, thus they are not considered in this work. Nevertheless, naturally occurring Structure H hydrates have been reported in Gulf of Mexico.² In the presence of propane or/and isobutane, Structure II hydrate will form first after which the formation of Structure I will commence.

In laboratory studies of hydrates, it is possible to control the number of independent thermodynamic variables so as to study equilibrium systems. The balance between number of independent thermodynamic variables, conservation laws and equilibrium conditions leaves only one degree of freedom for a system of methane, liquid water, and hydrate. So fixing either temperature or pressure opens up for equilibrium measurements of hydrate. In a flowing system, both temperature

and pressure are given by hydrodynamics locally and the same system is not able to reach equilibrium unless one of the phases is totally consumed and out of the balance equation. In a nonequilibrium situation, the equilibrium conditions are replaced by minimum free energy condition according to the combined first and second laws of thermodynamics. This is also the reason that adding another hydrate former to the system does not change the picture toward equilibrium. Hydrate formation, like any other phase transition is coupled to mass and heat transports. Adding, for instance, carbon dioxide to the methane gas will result in a selective adsorption³ of carbon dioxide so that the concentration of carbon dioxide and methane will be different than the gas composition. And since the composition and density of a gas adsorbed on liquid water is different from that of the gas phase, it is a different phase by thermodynamic definition. And it is indeed the adsorbed molecules, and corresponding liquid side interface molecules that will be active in hydrate nucleation. And since the gas phase composition will change during consumption over to hydrate also, the hydrate phases formed will be different. In theory, it can result in an infinite number of hydrate phases with small differences in free energy between each hydrate. And the picture gets even more complex when dealing with realistic natural gas containing significant portions of hydrocarbons up to butanes. As mentioned above, hydrate is typically formed from very exotic mixtures and typically for same reason have slow formation kinetics due to this balance needed to stabilize the hydrate. It is therefore quite different from hydrocarbon in geological setting where things happen over millions of years.

This balance between independent thermodynamic variable in all coexisting phases minus conservation laws and equilibrium conditions is normally called Gibbs phase rule, although it is merely a balance between independent variable and governing equations. Hydrate formation from natural gas mixtures

Correspondence concerning this article should be addressed to B. Kvamme at bjorn.kvamme@uh.no

will also, for same reasons, form mixtures of Structures I and II since the heavier hydrocarbons (C₃ and C₄) will adsorb to a higher concentration than methane and ethane, and hydrates from these components result in more stable hydrates of lower free energy than methane hydrates. In summary, hydrate formation will only happen when the free energy of the hydrate phase is lower than the free energies of the separate guest molecules phase and the water phase, because thermodynamic processes strive toward minimum free energy. Nucleation stage and stable growth stage of hydrate formation involving hydrate formers of both Structures I and II hydrate types in natural gas during processing and pipeline transport is a complicated and intricate processes that involve competing phase transition mechanisms (of benefit and penalty) and routes, where both kinetics and thermodynamics play a vital role. In the North Sea of Norway and several offshore operations, pipelines for natural gas transport are laid on seafloor with temperature range of 272.15–279.15 K and the pressures are around 5000–25,000 kPa, these conditions are appropriate for hydrate to form if free water is present; hydrate formation conditions are low temperature and high pressure as already mentioned above. Natural gas processing involves unit operations like turbines, compressors, and separators. Expansion in turbines leads to cooling of gas and hydrate can form if the end point is inside hydrate stability region and water drops out to provide free water. Compression during processing and transport can also lead to situation inside hydrate stability region since it involves raising the pressure of the system. Risk of hydrate formation is also possible at the final separator in gas processing because it is always at low temperature and high pressure; where lean gas (high in methane concentration) is processed at about 251 K and 7000 kPa, and rich gas (with significant ethane and other higher hydrocarbons) processing is at around 203 K and 7000 kPa.

A common industrial practice in hydrate risk evaluation for processing or transport of hydrocarbon mixtures goes through a calculation of water dew point, followed by an analysis of the actual range of thermodynamics conditions and possible situations that fall into hydrate stability. That is, the core of the analysis is the assumption that liquid water will drop out of the bulk hydrocarbon gas stream during processing and transport to form a separate water phase that can possibly lead to hydrate formation.⁴ This method is implemented by calculating the dew-point pressure of water in the gas stream. Then, check if the estimated dew-point pressure at the local temperature is within the temperature and pressure projection of the hydrate stability region. If it is, then water will drop out as liquid droplets. Thus, the theoretical quantity of water that could condense out can be calculated and measures are taken to dehydrate the gas. Otherwise, the required amount of a particular hydrate inhibitor that can satisfactorily shift the hydrate stability curve's pressure and temperature projections beyond the risk region is estimated and implemented in the system to prevent hydrate formation. In this study, this approach is referred to as "Route 1."

The shortcoming of this traditional scheme is that it totally disregards an alternative route (a new approach referred to as "Route 2" in this study) to hydrate formation due to the presence of hematite (rust) on the internal walls of processing equipment and on transport pipelines. These rusty surfaces provide water adsorption sites that can also lead to hydrate formation. Nucleation and growth of hydrate could happen when water and hydrate formers are adsorbed together on these rusty surfaces in the internal walls of gas processing equipment and

gas transport pipelines or when only water is adsorbed on these hematite surfaces with molecules of hydrate formers being imported from the bulk natural gas stream. The chemical potentials of the hydrate guest molecules will be different across the phases due to the inability of industrial or real systems outside of laboratory to attain equilibrium. However, hydrate cannot attach to the rusty surfaces. This can be seen from the incompatibility of partial charges on the oxygens and hydrogens in hydrate waters vs. negative and positive charges on the surface of hematite. From a thermodynamic point of view, it can be seen from the average chemical potential of water in the adsorbed layer⁵ which may be in the order of 3.4 kJ/mol lower than liquid water chemical potential. As such, the rusty surfaces are a thermodynamic hydrate inhibitor, although mineral surfaces can play a role in heterogeneous hydrate nucleation from structured water and hydrate formers from gas, adsorbed state, or from trapped hydrate formers in structured water. The rusty surface works as a catalyst that helps to take out the water from the gas stream via the process of adsorption, and hydrate formation can follow slightly outside of the first two or three water layers of about 1 nm. Iron and oxygen form rust when exposed to water. Rust comprises a number of different oxides of iron like magnetite (Fe₃O₄), hematite (Fe₂O₃), and iron oxide (FeO). Magnetite forms very early, but it is hematite that is most dominant over time, and one of the most thermodynamically stable forms of ordinary rust.⁴

Another pathway which can be considered as a third route for the formation of hydrate also exists but only in theory. Here, the formation of hydrate happens directly from the water that is dissolved in the bulk natural gas. However, the limited amount of the water, and the heat transport limitations related to transporting the hydrate heat of formation away from the formed nuclei through a heat insulator makes it doubtful for hydrate to form through this pathway. Consequently, this route is not considered in this work. Nevertheless, if the water/hydrocarbon system is not affected at all by surface stress from flow, a rapid formation of hydrate film on the water/hydrocarbon interface would follow, which will result in rapid blockage of further transport of guest molecules and waters through the hydrate film (i.e., very low coefficient of diffusivity). In this scenario, hydrate formation can result from both the guest molecules dissolved in water and water dissolved in gas, gaining from nucleation on the hydrate surface. It is, however, not a realistic phenomenon when a flowing situation is considered. Another factor that distinguishes a flowing scenario from that of a stationary constant volume and constant mass experiment in laboratory is that new mass is continuously supplied. Thus, the restrictive situation where the water is completely consumed, which could result in hydrate formation termination does not exist.

Kvamme et al.⁴ have analyzed comprehensively alternative pathways to formation and dissociation of hydrate Structure I relevant for pipeline transport of natural gas using free energy changes. And Kvamme and Sapate⁶ have investigated the risk of hydrate formation of Structure I hydrate from methane and ethane hydrate formers. However, natural gas from gas fields offshore of Norway, like Troll gas field⁷ and Sleipner gas field contain some amount of Structure II hydrate guest molecules of propane and isobutane. Therefore, this work aims to evaluate the risk of hydrate formation when significant amount of Structure II hydrate formers are present in the natural gas stream; we have applied our new approach of adsorption of water onto hematite and compared results with the conventional dew-point water drop-out scheme.

Managing the Risk of Hydrate During Processing and Transport of Natural Gas

To manage the risk of hydrate formation, the temperature–pressure conditions in a given gas system beneficial for hydrate to form have to be calculated first. Then followed by the required evaluation of the upper limit of water that should be allowed in natural gas during processing and transport without the risk of hydrate formation. However, this later step is a very complex problem. This is due to the competing phase transition process and the different pathways to the hydrate formation where both kinetics and thermodynamics play a very key role as mentioned above. The dynamic situation comes to be more complex for the reason that thermodynamic equilibrium can never be attained by the hydrates formed in the hydrocarbons transport pipelines and inside the gas processing equipment because of the limitations of Gibbs phase rule. The Gibbs phase rule is given by:

$$\tau = n - \pi + 2 \quad (1)$$

where τ stands for defined independent thermodynamic variables known as “degrees of freedom” and n is the number of active components in terms of hydrate phase transitions, while π is the number of actively coexisting phases. With our system in consideration, prior to any nucleation in the system, the number of active components (n) is 5 (methane, ethane, propane, isobutane, and water). And if we ignore possible adsorbed phase, then the number of actively coexisting phases (π) will be 2 (water and hydrocarbon gas). Then, the independent thermodynamic variables required to be defined or specified for the system to achieve equilibrium will be 5 ($\tau = 5 - 2 + 2 = 5$). Similarly, it will be 4 when a hydrate phase exists and number of active components remains constant. This system is overdetermined and cannot reach equilibrium because the maximum independent variables we can specify in this situation are the local temperature and pressure. Furthermore, mass transport limitation could hinder the hydrate nucleus from attaining critical size where stable growth can commence. And since hydrate formation is exothermic, there could be a problem of getting the heat of formation (crystallization heat) out of the system and this could seriously hinder the rate at which hydrate is formed, because the hydrocarbon, especially methane (natural gas is mainly methane rich) is relatively worse in thermal conduction in comparison to hydrate and liquid water clusters before hydrate formation.⁴

Hydrate analysis thus follows these steps: evaluate which possible phases that are active and significant with respect to hydrate phase transitions; Gibbs phase rule analysis, can equilibrium be reach? If not, like our system in consideration, then minimize free energy under the constraints of mass and heat conservation. And we use this method of free energy analysis in this work considering the reality that hydrate formed from different phases will not have the same but different free energies consequent on the different chemical potentials of hydrate guest molecules. For equilibrium situation, the classical scheme applied for estimation of equilibrium is to simultaneously compute the conditions for equilibrium, conservation of mass, and conservation of energy. However, for a nonequilibrium situation, the combined first and second laws of thermodynamics are used instead of the equilibrium conditions by means of certain strategies for minimizing free energy locally under constraints of conservation of both mass and energy. To

model each phase change for formation and dissociation of hydrate, it is done as pseudoreactions in consistent with changes in free energies as driving force for phase transition and coupled dynamically to mass and heat transport.⁸ The free energy changes associated with all phase changes are evaluated using Eq. 2:

$$\Delta G_i = \delta \left[x_w^{H,i} (\mu_w^{H,i} - \mu_w^P) + x_{\text{gas}}^{H,i} (\mu_{\text{gas}}^{H,i} - \mu_{\text{gas}}^P) \right] \quad (2)$$

where x is the composition; H is the hydrate phase; i is the phase transition scenario; μ is the chemical potential; P is the liquid, gas, and adsorbed phases; and δ is +1 for hydrate formation and –1 for hydrate dissociation. For a nonequilibrium situation, we need to remember that the chemical potentials for guest molecules in different phases are not the same but are different as already mentioned above. This shows that the chemical potentials for the hydrate formers in the hydrate will also be different, as it is observed from a Taylor expansion from an equilibrium point.⁹ The hydrate phase change, for both formation and dissociation, is a nanoscale process directed kinetically by what occurs on a thin interface of about three to four layers of water, which is around 1 to 1.5 nm. Hence, the implicitly coupled mass transport is a molecular scale diffusion transport.⁹ This diffusion is coupled to hydrodynamics of the flow situation by the supply of mass from the larger surrounding. The enthalpy (heat) of formation necessarily has to be transported out of the system to ensure hydrate formation. However, in the case of hydrate dissociation, heat is required to be supplied from the larger surrounding. Equation 3 is the thermodynamic relationship that gives the absolute value of the heat required to be transported away:

$$\frac{\partial \left[\frac{\Delta G_i}{RT} \right]_{P, \bar{N}}}{\partial T} = - \frac{\Delta H_i}{RT^2} \quad (3)$$

where ΔH_i is the enthalpy change associated with a certain route i to hydrate formation, T is the temperature in Kelvin, \bar{N} is the vector of mole numbers in the system, and R is the gas constant (8.3143 J/molK). This can be solved numerically and analytically on the basis of incorporated chemical potentials models. The real heat transport dynamics, which is implicitly coupled to the phase change thermodynamics as expressed in Eq. 2 is not the same but distinct for each phase change and given by the possible directions to transport away the hydrate formation heat. For the case of hydrate formation slightly outside of the first water molecules on a pipeline wall, the heat is transported fast toward the adsorbed water layer and subsequently then through the pipeline walls. The formation of hydrate on the interface of water adsorbed on rusty surface will therefore have rapid heat transport. This is also true for hydrate formed from dissolved or adsorbed guest molecules in this layer. Heat transport possibly will be two to three orders of magnitudes more fast than mass transfer,¹⁰ hence, there is no rate limiting process for these two pathways for hydrate formation.

Thermodynamics

As clearly explained above, the system considered in this study will not reach equilibrium. Even if we consider the simplest system which has only one hydrate former (guest molecule), let us say methane in a separate (gas) phase and liquid water phase, after the appearance of a nucleus (hydrate

formation), the system has two components and three phases. Hence, for equilibrium to be possible, we can specify only one thermodynamic variable. And for a system of a flowing pipeline, hydrodynamics and hydrostatics together with phase transitions which involve heat exchange, the local pressure, and temperature are determined; therefore, equilibrium is not possible even for the simplest system with one guest molecule. This simple system case is even more complex consequent on the fact that a hydrate film will slow down the transfer of methane gas to the liquid water and the other way around. Hydrate formation can also occur from dissolved methane in water and even from water dissolved in methane. However, the latter case or possibility is not very probable in terms of mass and heat transport. And since the system is not in equilibrium, the chemical potential of the guest molecule in the gas phase and in the dissolved phase (dissolved in water) will be different. By means of the statistical mechanical relationship between chemical potential for guest molecules going into the hydrate clathrate and the chemical potential of water in the hydrate,⁸ it is uncomplicated to validate that each of these hydrate phases has a different composition, different density, and different free energy. From fundamental thermodynamics, the phases are then unique. And the number of degrees of freedom according to Gibbs phase rule (see Eq. 1) is thus reduced further and the system is even more overdetermined. The system gets even further complex when more hydrate formers are added (like our system in consideration, C₁–iC₄) because the first and second laws will dictate that the lowest free energy phases form first given that these paths do not involve penalties in mass as heat transport. Practically, this indicates that if ethane, propane, and isobutane are added to the system that will cause a variation of hydrate phases. And initial formation of hydrate which is dominated by the C₂₊ does not experience penalties in terms of mass transport, because it will by fundamental thermodynamic considerations,³ condense out first on the water/hydrocarbon surface.

Equilibrium Thermodynamics

To achieve thermodynamic equilibrium in a system, the temperatures, pressures, and chemical potentials of all components in all coexisting phases must be equal across all phase boundaries. The phase distributions and compositions in equilibrium systems can be evaluated by means of free energy minimization. Equations 4 and 5 express equilibrium situation:

$$T^{(i)} = T^{(ii)} = T^{(iii)} \dots = T \text{ (Thermal equilibrium)} \quad (4)$$

$$p^{(i)} = p^{(ii)} = p^{(iii)} \dots = P \text{ (Newton's law/mechanical equilibrium)} \quad (5)$$

$$\mu^{(i)} = \mu^{(ii)} = \mu^{(iii)} \dots = \mu \text{ (Chemical equilibrium)} \quad (6)$$

The superscripts (i), (ii), (iii) and further stand for phase index for each of the coexisting phases in the system. Despite the fact that we cannot attain equilibrium, we can apply a quasi-equilibrium technique to enable us evaluate the thermodynamic benefits of different paths of either hydrate formation or hydrate dissociation using Eqs. 4–6 as asymptotic limits of possible stability for each given phase transition. Residual thermodynamics by the use of Soave–Redlich–Kwong equation of state¹¹ is utilized for all components in all phases that are hydrate, liquid water, and ice inclusive. This has been implemented by the use of molecular dynamics (MD) results for water in different phases (empty hydrates, liquid water, and ice).¹²

Fluid Thermodynamics

The chemical potential of component *j* in gas is estimated from Eq. 7. In order to make sure that there is the same reference value for free energy of all of the chemical potential estimates, irrespective the phase, ideal gas should be used as the reference state:

$$\mu_j(T, P, \bar{y}) = \mu_j^{\text{ideal gas}}(T, P, \bar{y}) + RT \ln \phi_j(T, P, \bar{y}) \quad (7)$$

lim (ϕ_j) → 1.0...for ideal gas

where ϕ_j is the fugacity coefficient for component *j* in given phase and \bar{y} stands for mole fraction vector of the gas. The chemical potential of the ideal gas comprises the trivial mixing term because of ideal gas mixing of gases at constant pressure.

Aqueous Thermodynamics

The chemical potential of pure water is evaluated from results from MD simulations. For pure water, estimation is on the basis of absolute thermodynamics and Eq. 8, symmetric excess thermodynamic model is used. We need to state here that in this study data from Kvamme and Tanaka¹² are used.

Symmetric Excess

As stated above, Eq. 8 is used to model the chemical potential of component *j* in water phase. The ideal liquid chemical potential also comprises the trivial ideal mixing term in addition to the pure liquid value.

$$\mu_j(T, P, \bar{x}) = \mu_j^{\text{ideal liquid}}(T, P, \bar{x}) + RT \ln \gamma_j(T, P, \bar{x}) \quad (8)$$

lim (γ_j) → 1.0 when $\bar{y} \rightarrow 1.0$

where γ_j is the activity coefficient for component *j* in the liquid phase and \bar{x} stands for mole fraction vector of the liquid.

Asymmetric Excess

It is appropriate to apply a reference state of infinite dilution consequent on the fact that the solubility of methane, ethane, and higher hydrocarbons in water is limited, thus, Eq. 9 is appropriate.

$$\mu_j^{\text{H}_2\text{O}}(T, P, \bar{x}) = \mu_j^{\text{H}_2\text{O}, \infty}(T, P, \bar{x}) + RT \ln \left[x_j^{\text{H}_2\text{O}} \cdot \gamma_j^{\text{H}_2\text{O}, \infty}(T, P, \bar{x}) \right] \quad (9)$$

lim ($\gamma_j^{\text{H}_2\text{O}, \infty}$) when $x_j \rightarrow 0$

where $\mu_j^{\text{H}_2\text{O}, \infty}$ is the chemical potential of component *j* in water, ∞ signifies infinite dilution, $\gamma_j^{\text{H}_2\text{O}, \infty}$ is the activity coefficient of component *j* in aqueous phase based on the same reference state, and *R* is the universal gas constant. The solubility of methane, ethane, propane, and that of isobutane are each very low. Thus, Eq. 10 could be applied together with Eq. 9; this approximation should consequently prove satisfactorily accurate for most industrial applications where the risk of hydrate formation is a concern:

$$\mu_j^i(T, P, \bar{x}) \approx \mu_j^{i, \infty}(T, P, \bar{x}) + RT \ln \left[x_j^i \cdot \gamma_j^{i, \infty}(T, P, \bar{x}) \right] \quad (10)$$

Here, the subscript *i* refers to the different phases with low solubility and subscript *j* refers to different components.

Hydrate Thermodynamics

The chemical potential for water in hydrate is usually modeled by using the statistical mechanical model, a classic Langmuir type of adsorption model, but applied in the form derived by Kvamme and Tanaka¹² as given in Eq. 11. This model takes into account lattice movements and corresponding impacts of different guest molecules; it accounts for collisions between guest molecules and water which are strong enough to affect water motions. While that of van der Waals and Platteeuw¹³ assumed "rigid lattice"—it presumes that water movements in the lattice are not affected by guest j .

$$\mu_{\text{H}_2\text{O}}^{(H)} = \mu_{\text{H}_2\text{O}}^{(0,H)} - R.T \sum_{i=1}^2 v_i \ln \left(1 + \sum_{j=1}^{n_{\text{guest}}} h_{ij} \right) \quad (11)$$

where H refers to hydrate phase, $\mu_{\text{H}_2\text{O}}^{(H)}$ is the chemical potential of water in hydrate, $\mu_{\text{H}_2\text{O}}^{(0,H)}$ is the chemical potential of water in empty hydrate structure, and v_i is the fraction of cavity type i per water molecule. A unit cell of Structure I hydrate contains 46 water molecules and there are two small and six large cavities, thus, $v_{\text{small}} = 1/23$ and $v_{\text{large}} = 3/23$. The h_{ij} in Eq. 11 is the canonical cavity partition function of component j in cavity type i , and n_{guest} is the number of guest molecules in the system. The canonical partition function is evaluated from the relation given in Eq. 12:

$$h_{ij} = e^{-\beta(\mu_j^H - \Delta g_{ij}^{\text{inc}})} \quad (12)$$

where $\beta = \frac{1}{RT}$ is the inverse of gas constant times temperature, and $\Delta g_{ij}^{\text{inc}}$ is the impact on hydrate water from inclusion of the guest molecules j in the cavity i .

Equilibrium Thermodynamics of Hydrate

The chemical potential of component j in hydrate phase " H " must be equal to its chemical potential in the (parent) phase it is extracted from Ref.⁴ at equilibrium. In this study,

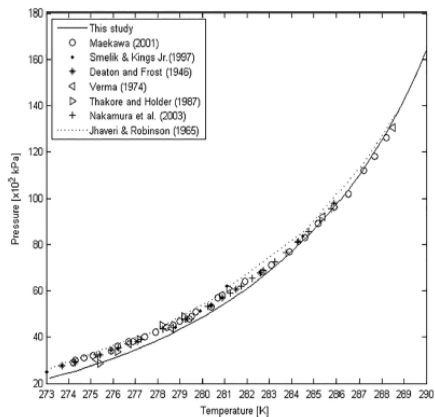


Figure 1. Top curve is estimated equilibrium pressures for hydrate from methane compared with experimental data.¹⁸⁻²⁴

water completely dominates the dew point. Equation 13 is applied for evaluation of hydrate formation for the route of liquid water dropped out. Nevertheless, the chemical potential of all gas components (guest molecules) of hydrate are evaluated utilizing Eq. 7 in the case of water dissolved in gaseous phase.

$$\mu_{\text{H}_2\text{O}}^{(0,H)} - R.T \sum_{i=1}^2 v_i \ln \left(1 + \sum_{j=1}^{n_{\text{guest}}} h_{ij} \right) = \mu_{\text{H}_2\text{O}}^{\text{Pure water}}(T, P) + RT \ln [x_{\text{H}_2\text{O}} \gamma_{\text{H}_2\text{O}}(T, P, \vec{x})] \quad (13)$$

The model of Kvamme and Tanaka¹² is used to estimate the chemical potential of water in the empty hydrate structure. This model has been validated to have predictive capabilities; hence, it causes any empirical formulations for these chemical potentials to be pointless and maybe unphysical consequent on the fact that chemical potential is a fundamental thermodynamic property. We approximated the right-hand side of Eq. 13 by pure water because no ions are present in the water, but merely limited amounts of dissolved gases. The effect would be just a slight shift in chemical potential of liquid water. To give an instance, at 15,000 kPa and 274 K, the correction is -0.07 kJ/mol, though a little bit greater for 20,000 and 25,000 kPa, even so it is still not dramatic for the purpose of this work. Nevertheless, Eq. 14 has been verified to be beneficial to estimate free energy change associated with a hydrate phase transition Δg^H .

$$\Delta g^H = \delta \sum_{j=1}^{n_H} x_j^H (\mu_j^H - \mu_j^P) \quad (14)$$

where H is the hydrate phase of molecule j , P is the parent phase of molecule j . And Eq. 15 gives the relation between the filling fraction, the mole fractions, and cavity partition function as follows:

$$\theta_{ij} = \frac{x_{ij}^H}{v_j(1-x_T)} = \frac{h_{ij}}{1 + \sum_j h_{ij}} \quad (15)$$

where x_T is the total mole fraction of all guests in the hydrate, θ_{ij} is the filling fraction of component j in cavity type i , and x_{ij}^H is the mole fraction of component j in cavity type i .

Verification of Theoretical Model

Comparison of equilibrium pressures estimates from our novel theoretical model with experimental data are presented here. Estimates for pure components of methane, ethane, propane, and isobutane together with mixture of hydrocarbons with composition varying in molar concentrations are provided in Figures 1–7. To compare estimates from theoretical model and experimental data, it is imperative to bear in mind that the free energy of inclusions has been evaluated by MD simulations without tuning of the model. It is also vital to remember that a number of gas mixtures form more than one hydrate with different densities, composition, and free energies. From the first and second laws of thermodynamics, we know that the most stable hydrates form first, after which a variety of hydrate compositions will form.¹⁴ In a natural gas mixture containing hydrate formers of both Structures I and II as in this work, Structure II hydrate guest molecules should form hydrates first before those of hydrate Structure I. Therefore, the hydrate that would finally form as given in Figures 5–7 could be a mixture of Structures I and II hydrates of varying

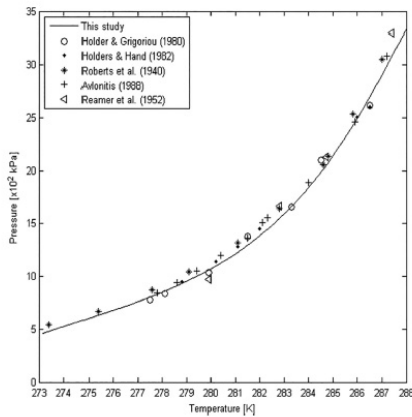


Figure 2. Estimated equilibrium pressures for hydrate from ethane compared with experimental data.²⁵⁻²⁹

compositions of the initial guest molecules. Thus, for several experimental gas mixtures, it is not specified that the final hydrate is uniform.¹⁴ Rather, it is more likely that it is a mixture of several hydrates with varying compositions of the initial hydrate formers from gas or liquid will result.¹⁴

We do not intend to tune empirical model parameters, thus for this work, a fair qualitative agreement is quite acceptable. We see the deviations as sufficiently acceptable for further illustration of the upper limit of water content that should be allowed without the risk of hydrate formation for pure methane, ethane, propane, and isobutane; and different mixtures of

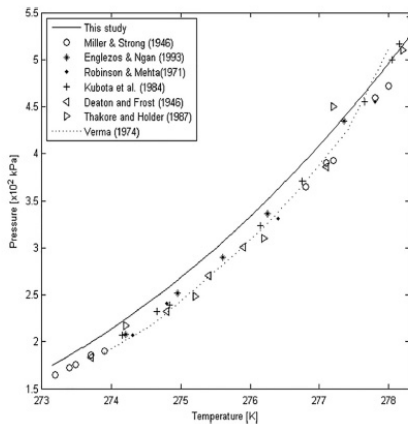


Figure 3. Top curve is estimated equilibrium pressures for hydrate from propane compared with experimental data.^{20-22,30-33}

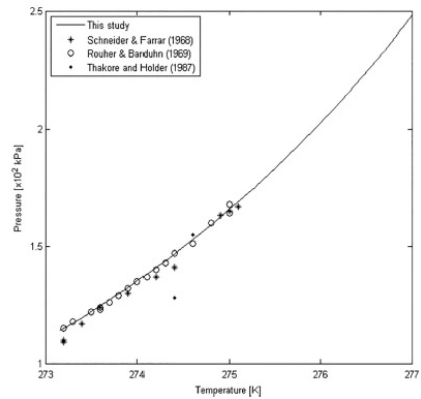


Figure 4. Top curve is estimated equilibrium pressures for hydrate from isobutane compared with experimental data.^{22,34,35}

hydrocarbons of methane to isobutane with varying compositions. Specifically, predicted estimates are very suitable for the range of applicable temperatures of 274 to 280 K.

Analysis of Different Approaches for Evaluating the Risk of Hydrate Formation

This work is principally aimed at qualitatively comparing a new approach (Route 2) of evaluating the risk of hydrate formation with the traditional technique (Route 1) currently

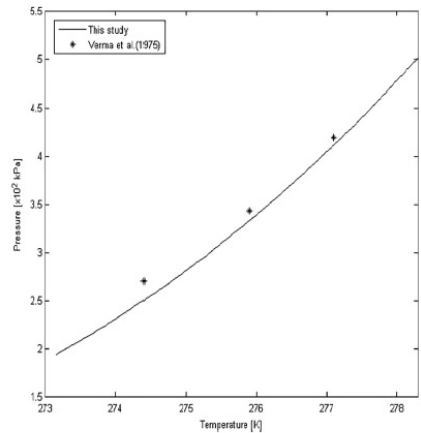


Figure 5. Estimated equilibrium pressures for hydrate from 0.371 and 0.629 mol of methane and propane respectively compared with experimental data.³⁶

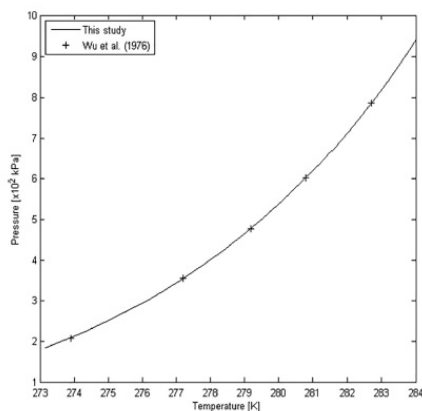


Figure 6. Top curve is estimated equilibrium pressures for hydrate from 0.714 and 0.286 mol of methane and isobutane, respectively, compared with experimental data.³⁷

utilized by the industry in respect of pipeline transport and processing of hydrocarbons. This analysis is performed for the pure components of methane, ethane, propane, and isobutane, which are the main Structures I and II hydrate forming hydrocarbons. The new approach here is based on the impact of solid surface in water dropping out from hydrocarbons to eventually lead to hydrate formation. And in this study, hematite, which has been described above is the solid surface considered. Moreover, free energy analysis is done to qualitatively give insight into the selectivity of the different

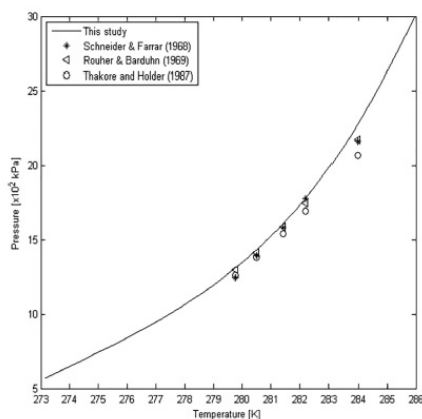


Figure 7. Top curve is estimated equilibrium pressures for hydrate from 0.174, 0.705, and 0.121 mol of methane, ethane and propane compared with experimental data.^{22,34,35}

hydrocarbons during hydrate formation, to show which molecule forms hydrate first as a consequence of the combined first and second laws of thermodynamics in terms of Gibbs free energy. This means that all systems will strive toward minimum free energy as function of temperature, pressure, and distribution of masses in the system over possible phases, under constraints of mass and heat transport. The impacts of varying compositions of Structure II hydrate formers of propane and isobutane in binary mixture with methane based on maximum tolerance of water is also qualitatively analyzed.

Analysis of Upper Limit of Water to Prevent Hydrate Formation Risk from Pure Hydrocarbons Based on Routes 1 and 2

The estimates of maximum water tolerance in systems of pure hydrocarbons (methane, ethane, propane, and isobutane) are presented in Figures 8–15 and Table 1. The temperature and pressure ranges considered in this work are representative of what is obtainable in the natural gas processing and pipeline transport operations in the North Sea of Norway. The seafloor temperatures are typically low; because of the seawater salinity, it could be as low as 272.15 K in the northern part, and seldom rise above 279.15 K in the south. Pressures are generally high too, between 5000 and 30,000 kPa. That is why we use the temperature range of 273–280 K and pressure range of 5000–25,000 kPa for all the analysis in this project.

The estimated water tolerance at 274 K (approximately 1°C) based on Route 1, that is the dew-point technique (Figures 8, 10, 12, and 14) is around 19.2 times higher than the upper limit of water content for the Route 2 which is based on the approach of water adsorbed onto hematite (Figures 9, 11, 13, and 15). The calculated values for Route 1 are about 17.8 times higher than the estimates of Route 2 at 280 K. These results clearly suggest that water would drop out as adsorbed on hematite before it drops out as liquid based on the difference in the limits of allowable water content. In other words, Route 2 (the new approach of adsorption of water onto solid surfaces, hematite in this work) completely dominates in evaluating the risk of liquid water condensing out from each of the pure hydrocarbon gases examined, to form a separate water phase and in due course lead to the formation of hydrate. This can be explained from the fact that the average chemical potential of the water adsorbed on rusty (hematite) surfaces could be about 3.4 kJ/mol less than the chemical potential of liquid water. This could be understood based on the fact that thermodynamic processes always strive toward the least free energy. However, because of the low chemical potential of the water adsorbed on hematite, the initial hydrate nuclei cannot attach directly to the hematite surface. The hydrate that will be formed will be bridged by three to four layers of structured water on the surface of the hematite; then, hydrate nucleation can occur on the liquid water above these first set of layers. Even though, hematite (Fe_2O_3) is the one of the most thermodynamically stable form of rust (oxides of iron), there could be a need to examine the impact of other oxides of iron such as magnetite (Fe_3O_4) and other solid surfaces relevant to processing and transport operations of hydrocarbons. A more rigorous dynamic analysis can be implemented through model systems by the application of phase field theory¹⁵ with solid surface models extracted from MD simulations.^{16,17}

The solubility of hydrocarbons in water is sensitive to density; for heavier hydrocarbon (C_{2+}) gases, here we refer to

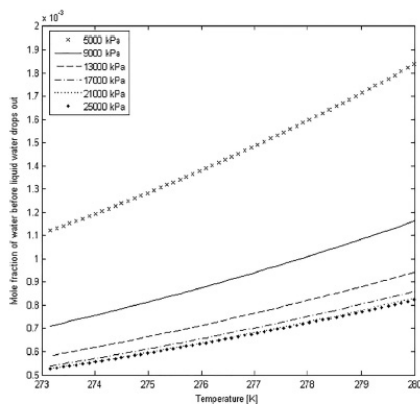


Figure 8. Maximum content of water in pure methane before liquid water drops out (Route 1).

ethane, propane, and isobutane, the solubility increases. And by implication, a corresponding increase of tolerance for water with increase in pressure is the characteristic trend exhibited by each pure C₂₊ system as can be observed by comparing Figures 10–15. This is in contrast with the light methane system where the permitted maximum water content decreases with increase in pressure due to the limited solubility in water. Moreover, the tolerance for water also increases with increase in the number of carbon in each pure hydrocarbon molecule; that is pure isobutane tolerates a little more water relative to pure propane, and propane a little more than ethane without the risk of liquid water dropping out at dew point or through

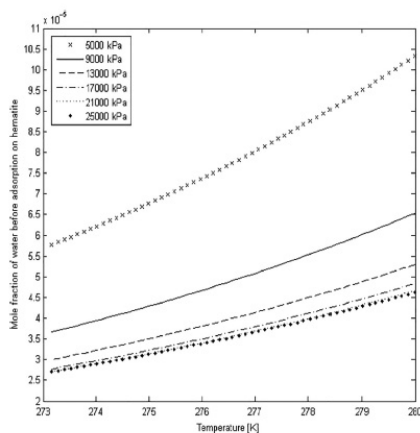


Figure 9. Maximum content of water in pure methane before adsorption of water on hematite happens (Route 2).

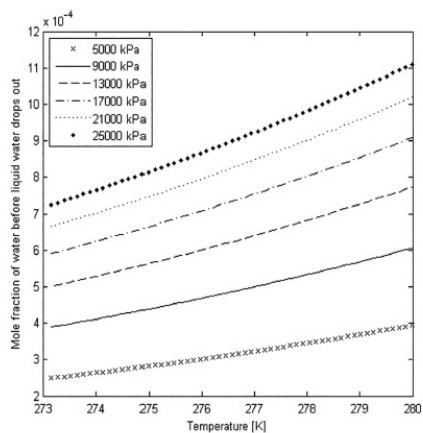


Figure 10. Maximum content of water in pure ethane before liquid water drops out (Route 1).

adsorption on hematite surface. Natural gas, though predominantly comprises methane, normally also consists of some amount of heavier hydrocarbons especially ethane and propane, and sometimes, the amount of isobutane may be significant enough to have some effect in respect of hydrate formation. Propane and isobutane are both Structure II hydrate forming molecules and their impact on maximum water tolerance in mixture with methane is investigated in the next section; the solubility of hydrocarbons in water is sensitive to composition and density.

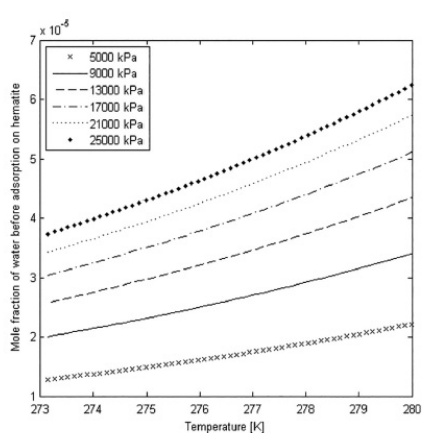


Figure 11. Maximum content of water in pure ethane before adsorption of water on hematite happens (Route 2).

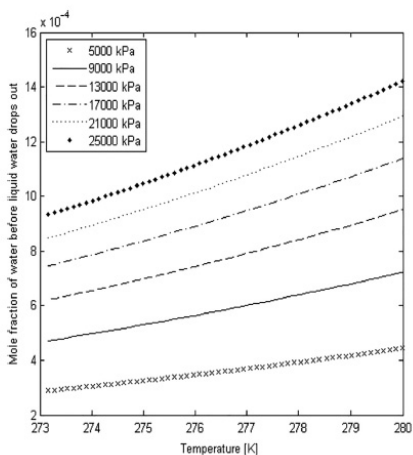


Figure 12. Maximum content of water in pure propane before liquid water drops out (Route 1).

Analysis of Upper Limit of Water to Prevent Hydrate Formation Risk from Mixture of Structures I and II Hydrocarbons Guest Molecules

Natural gas predominantly comprises methane, but it also contains other higher hydrocarbons (C_{2+}) in varying amount. And in this section, molar concentrations of 0.83 methane, 0.10 ethane, 0.045 propane, and 0.005 isobutane are used to represent a realistic natural gas composition to

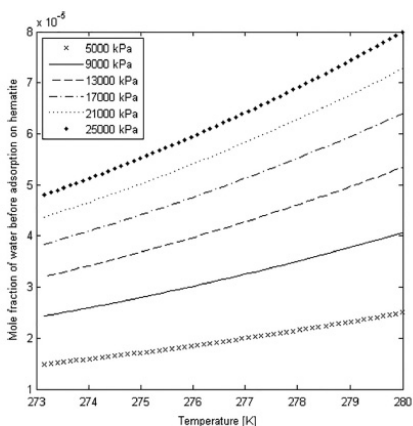


Figure 13. Maximum content of water in pure propane before adsorption of water on hematite happens (Route 2).

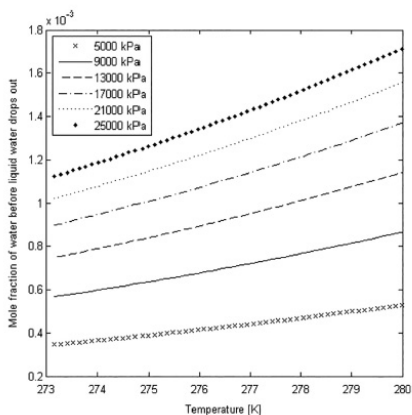


Figure 14. Maximum content of water in pure isobutane before liquid water drops out (Route 1).

investigate the risk of water dropping out of the multicomponent hydrocarbon mixture based on Routes 1 and 2. Figures 16 and 17 give the illustration of the maximum allowable mole fraction of water based on the conventional technique (Route 1) and the new approach (Route 2), respectively. Similar results as seen for pure hydrocarbon components are observed here, at 274 K, the estimates of the dew-point method is 19.2 times higher than the calculated values with the new approach of water dropping out of the gas mixture due to adsorption of water onto the internal

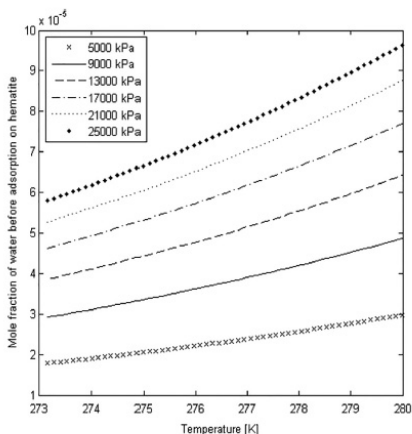


Figure 15. Maximum content of water in pure isobutane before adsorption of water on hematite happens (Route 2).

Table I. Maximum Allowable Water Content in Pure Methane, Propane, and Isobutane to Avoid the Risk of Hydrate Formation

Temperature (K)	Pressure (kPa)	Maximum Concentration of Water							
		Methane		Ethane		Propane		Isobutane	
		Dew Point	Hematite	Dew Point	Hematite	Dew Point	Hematite	Dew Point	Hematite
274	5000	0.001194	0.000062	0.000264	0.000014	0.000306	0.000016	0.000366	0.000019
	9000	0.000758	0.000039	0.000412	0.000021	0.000498	0.000026	0.000598	0.000031
	13,000	0.000619	0.000032	0.000529	0.000028	0.000656	0.000034	0.000789	0.000041
	17,000	0.000571	0.000030	0.000624	0.000033	0.000787	0.000041	0.000948	0.000049
	21,000	0.000558	0.000029	0.000702	0.000037	0.000895	0.000047	0.001078	0.000056
280	25,000	0.000556	0.000029	0.000765	0.000040	0.000984	0.000051	0.001186	0.000062
	5000	0.001838	0.000103	0.000394	0.000022	0.000445	0.000025	0.000053	0.000030
	9000	0.001162	0.000653	0.000605	0.000034	0.000722	0.000041	0.000087	0.000049
	13,000	0.000942	0.000053	0.000773	0.000043	0.000950	0.000053	0.001141	0.000064
	17,000	0.000860	0.000048	0.000908	0.000051	0.001138	0.000064	0.001369	0.000077
21,000	0.000831	0.000047	0.001019	0.000057	0.001293	0.000073	0.001557	0.000088	
25,000	0.000823	0.000046	0.001110	0.000062	0.001421	0.000080	0.001713	0.000096	

walls of pipeline and gas processing equipment covered by hematite (rust). And at 280 K, it is also 17.8 as in the case of pure components of hydrocarbons.

Since this system is methane dominated, the characteristic trend of methane is also exhibited where the maximum water tolerance decreases with increasing pressures from 5000 to 25,000 kPa for a temperature range of 273 to 280 K. However, there are some shifts in absolute values of maximum mole fraction of water permitted in the gas mixture without the risk of hydrate formation compared with that of methane (comparing Figures 8 and 16, and Figures 9 and 17). This is due to the presence of some amount of C₂₊ in the gas mixture. It can be observed that there is a reversal of the characteristic trend exhibited by methane to that of C₂₊ from 21,000 to 25,000 kPa. This is due to the presence of the high density nonpolar phase of the C₂₊ at the high pressures; the resistance of the higher density of the heavier hydrocarbons. The effects of varying mole fractions of Structure II guest

molecules of propane and isobutane in binary mixture with methane is investigated in the subsequent section.

Impact of Structure II Hydrocarbon Guest Molecules on Methane (Structure I) Guest Molecule: Maximum Water Concentration in Natural Gas Stream to Avoid the Risk of Hydrate Formation

The impact of propane and isobutane on water tolerance in a methane-propane and methane-isobutane binary mixtures, respectively, have been investigated. Only pressures of 5000–13,000 kPa are investigated since maximum water tolerance in hydrocarbons is virtually insensitive to pressure at higher pressures especially beyond 13,000 kPa, particularly with the presence of heavier hydrocarbons.⁷ The maximum water tolerance decreases with increasing concentrations of propane and isobutane with the heavier isobutane having more

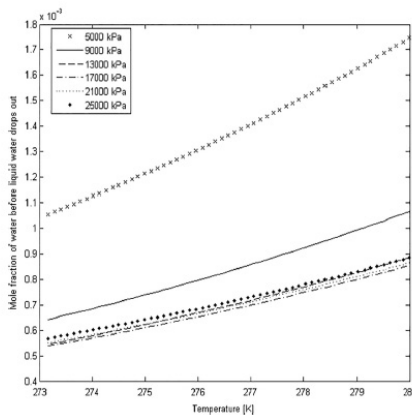


Figure 16. Maximum content of water before liquid water drops out (Route 1) from a mixture of methane, ethane, propane, and isobutane with mole fractions of 0.83, 0.12, 0.045, and 0.005, respectively.

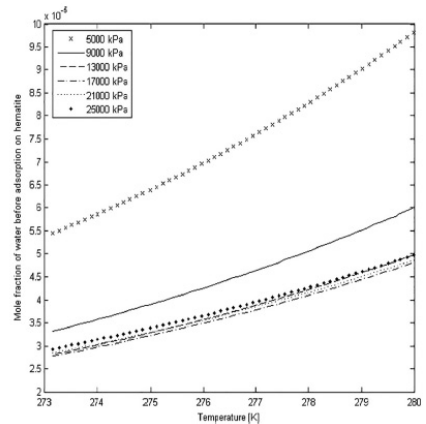


Figure 17. Maximum content of water before adsorption on hematite happens (Route 2) from a mixture of methane, ethane, propane, and isobutane with mole fractions of 0.83, 0.12, 0.045, and 0.005, respectively.

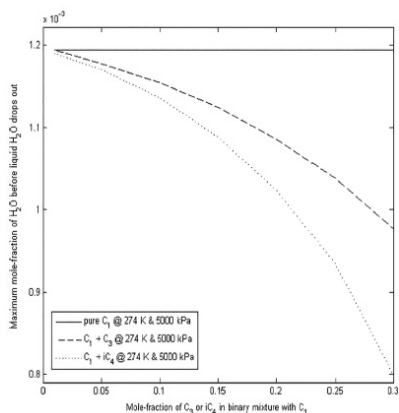


Figure 18. Impacts of varying compositions of propane/isobutane on binary mixtures with methane in respect of maximum content of water permitted before liquid water drops out (Route 1) at 274 K and 5000 kPa.

impact as illustrated in Figures 18–23. These may suggest that the presence of Structure II guest molecules in considerable amounts in natural gas could make water drop out before water can drop out from pure methane, and the safe limit of water reduces with increase in the concentration of the heavier hydrocarbons. Plots for only the dew-point analysis (Route 1)

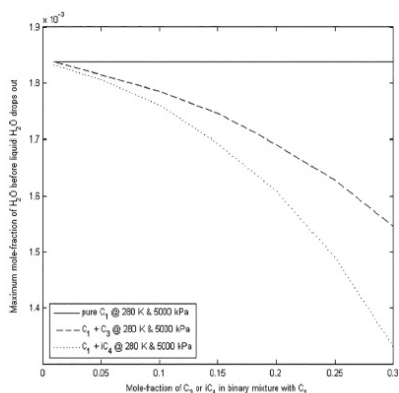


Figure 19. Impacts of varying compositions of propane/isobutane on binary mixtures with methane in respect of maximum content of water permitted before adsorption of water on hematite (Route 1) at 280 K and 5000 kPa.

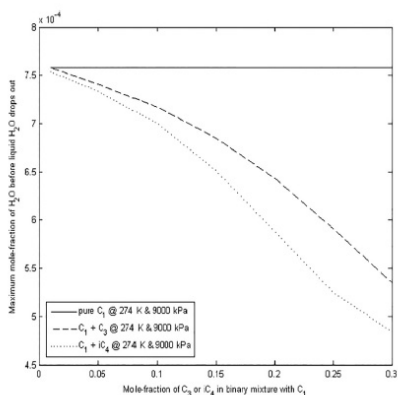


Figure 20. Impacts of varying compositions of propane/isobutane on binary mixtures with methane in respect of maximum content of water permitted before liquid water drops out (Route 1) at 274 K and 9000 kPa.

are presented because the trends for both approaches are similar with difference only in absolute values. With varying molar concentration of propane from 0.01 to 0.30, at 274 K, average of 20 times higher is estimated if the conventional dew-point technique (Route 1) is used instead of the new approach (Route 2) for analyzing the risk of water dropping out from

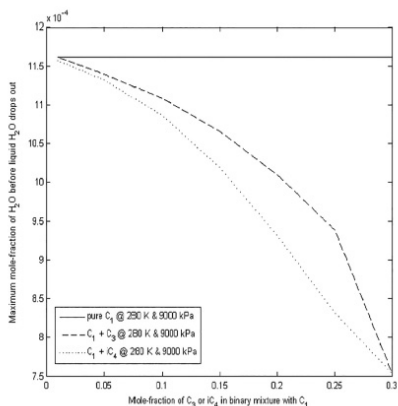


Figure 21. Impacts of varying compositions of propane/isobutane on binary mixtures with methane in respect of maximum content of water permitted before adsorption of water on hematite (Route 1) at 280 K and 9000 kPa.

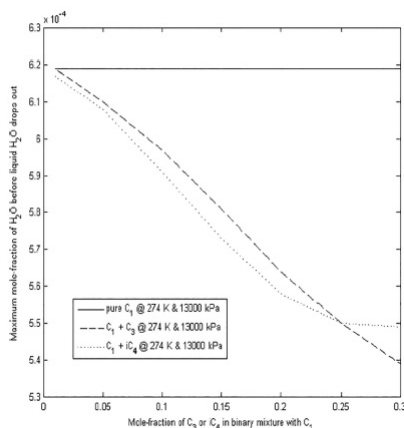


Figure 22. Impacts of varying compositions of propane/isobutane on binary mixtures with methane in respect of maximum content of water permitted before liquid water drops out (Route 1) at 274 K and 13,000 kPa.

hydrocarbon mixture and subsequently leading to hydrate formation. While the value is 18.2 times at 280 K. Same analysis for isobutane gives 20.1 times at 274 K and 18.5 times at 280 K. What can be observed in Figures 21–23 where curves for propane and isobutane intersect imply the change from

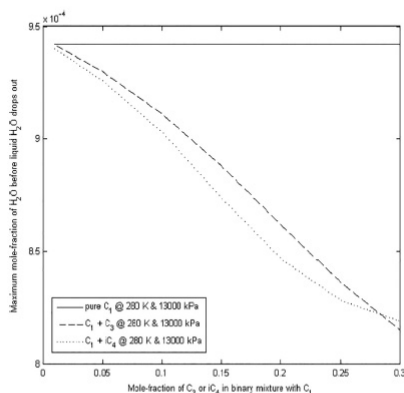


Figure 23. Impacts of varying compositions of propane/isobutane on binary mixtures with methane in respect of maximum content of water permitted before adsorption of water on hematite (Route 1) at 280 K and 5,000 kPa.

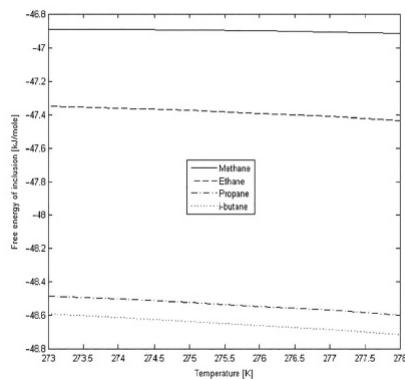


Figure 24. Free energy analysis of inclusion of methane, ethane, propane, and isobutane.

methane dominance characteristic trend to that of C₂. This has been discussed in the sensitivity analysis section in Ref.⁷

Selective Hydrate Formation Analysis of Structures I and II Hydrate Formers

Based on the first and second laws of thermodynamics, in a multicomponent mixture of hydrocarbons, the most stable hydrates will form first, under constraints of mass and heat transport, followed by the next most stable hydrates and so on. The combined first and second laws of thermodynamics in terms of Gibbs free energy help us to understand that all systems will strive toward minimum or least free energy as function of temperature, pressure, and distribution of masses in the system over possible phases, under constraints of mass transport and heat transport. In a quaternary mixture of methane, ethane, propane, and isobutane in this study as illustrated in Figure 24, the Structure II components hydrate formers have lower free energies of inclusion compared to those of Structure I. Therefore, hydrate nucleation will commence with isobutane then propane filling the large cavities of the Structure II hydrate type depending on distribution of masses. Then, ethane with lower free energy of inclusion compared to methane will occupy the large cavity of hydrate Structure I before hydrate of methane will form the small-sized molecules of methane will fill the small cavities of Structure I hydrate.

Conclusion

The conventional hydrate risk evaluation method based on water dew-point calculation currently used by the industry and a new approach based on adsorption of water onto hematite have been applied for investigation of the upper limit of water contents that can be permitted in pure and mixtures of hydrate Structures I and II hydrocarbon guest molecules (methane, ethane, propane, and isobutane) to prevent the risk of hydrate formation during processing and transport. Estimations of the safe limit of water mole fractions in pure hydrocarbons based on water dew point is around 19.2 times higher than calculations based on adsorption of water on hematite, that is the new

approach at the temperature of 274 K. The value is roughly 17.8 times higher at 280 K. The results clearly indicate that water will choose to drop out more quickly via the process of adsorption onto rusty surfaces (rust) than dropping out below dew-point conditions. Same results have been calculated for a multicomponent hydrocarbon mixture with molar concentrations of 0.83 methane, 0.10 ethane, 0.045 propane, and 0.005 isobutane.

Impacts of varying the concentration of the Structure II hydrocarbon guest molecules in binary mixtures with methane have also been examined. The safe limit of water content decreases with increasing concentrations of propane and isobutane with the heavier isobutane having more impact. These suggest that the presence of Structure II hydrate formers in substantial amounts in natural gas might cause water to drop out more quickly compared to the case of only pure methane. Using the dew-point analysis instead of the new approach gives an average values roughly 20 times higher at 274 K and 18.2 times at 280 K. For isobutane, it is around 20.1 times at 274 K and 18.5 times higher at 280 K.

We also performed free energy analysis to qualitatively give insight into the selectivity of the different hydrocarbons during hydrate formation, to show which molecule forms hydrate first based on the combined first and second laws of thermodynamics in terms of Gibbs free energy—all systems will strive toward minimum free energy as function of temperature, pressure, and distribution of masses in the system over possible phases, under constraints of mass and heat transport. The Structure II guest molecules form hydrate first and they form more stable hydrate compare to especially methane.

The estimates from this study suggest that the new approach of evaluating the risk of hydrate formation based on adsorption of water onto the internal walls of pipelines and equipment covered with rust absolutely dominates. This study therefore recommends that the industry should consider this new approach in examination of the risk of hydrate nucleation and growth during processing and transport of hydrocarbons.

Notation

C_1	methane
C_2	ethane
C_3	propane
iC_4 or $i-C_4$	isobutane
C_2+	higher hydrocarbons of ethane, propane, and isobutane
T	temperature, K
T_c	critical temperature, K
P	pressure, bar or kPa
μ	chemical potential, kJ/mol
H	hydrate phase
ΔG	free energy change
G	free energy change, kJ/mol
P	parent phase
R	universal gas constant, kJ/(K mol)
ϕ	fugacity coefficient
γ	activity coefficient
\bar{x}	mole fraction of liquid
\bar{y}	mole fraction of gas
h_{ij}	canonical cavity partition function of component j in cavity type i
Δg_{ij}^{inc}	free energy of inclusion of the guest molecules j in the cavity i
θ_{ij}	filling fraction of component j in cavity type i
β	inverse of gas constant times temperature
x_T	total mole fraction of all guests in the hydrate
r	defined independent thermodynamic variables a the system
n	number of active components in terms of hydrate phase transitions
π	number of actively coexisting phases

Literature Cited

- Sloan ED, Koh CA. *Clathrate Hydrates of Natural Gases*. Chemical industries. Vol 119. 3rd ed. Boca Raton, FL: CRC Press; 2008.
- Sassen R, MacDonald IR. Evidence of structure H hydrate, Gulf of Mexico continental slope. *Org Geochem*. 1994;22:1029-1032.
- Kvamme B. Thermodynamic limitations of the CO₂/N₂ mixture injected into CH₄ hydrate in the Ignik Sikumi field trial. *J Chem Eng Data*. 2016;61(3):1280-1295.
- Kvamme B, Kuznetsova T, Bauman JM, Sjöblom S, Kulkarni AA. Hydrate formation during transport of natural gas containing water and impurities. *J Chem Eng Data*. 2016;61:936-949.
- Kvamme B, Kuznetsova T, Kivelæ P-H. Adsorption of water and carbon dioxide on hematite and consequences for possible hydrate formation. *Phys Chem Chem Phys*. 2012a;14:4410-4424.
- Kvamme B, Sapate A. Hydrate risk evaluation during transport and processing of natural gas mixtures containing ethane and methane. *Res Rev: J Chem*. 2016;5:64-74.
- Kvamme B, Aromada SA. Risk of hydrate formation during the processing and transport of troll gas from the North Sea. *J Chem Eng Data*. 2017;62:2163-2177.
- Jemai K, Kvamme B, Vafaei MT. Theoretical studies of CO₂ hydrates formation and dissociation in cold aquifers using RetrasoCodeBright simulator. *WSEAS Transactions on Heat and Mass Transfer*, 2015;6: 150-168.
- Kvamme B, Kuznetsova T, Kivelæ P-H, Bauman J. Can hydrate form in carbon dioxide from dissolved water? *Phys Chem Chem Phys*. 2013;15:2063-2074.
- Svandal A. Modeling Hydrate Phase Transitions Using Mean-Field Approaches [PhD dissertation], Bergen, Norway: University of Bergen, 2006.
- Soave G. Equilibrium constants from a modified Redlich-Kwong equation of state. *Chem Eng Sci*. 1972;27:1197-1203.
- Kvamme B, Tanaka H. Thermodynamic stability of hydrates for ethane, ethylene, and carbon dioxide. *J Phys Chem*. 1995;99:7114-7119.
- Van der Waals JH, Platteuw JC. Clathrate solutions. *Adv Chem Phys*. 1959;2:1-57.
- Kvamme B, Iden E, Tveit J, Veland V, Zarifi M, Qorbani K. Effect of H₂S content on thermodynamic stability of hydrate formed from CO₂/N₂ mixtures. *J Chem Eng Data*. 2017;62:1645-1658.
- Kvamme B, Qasim M, Baig K, Kivelæ PH, Bauman J. Hydrate phase transition kinetics from phase field theory with implicit hydrodynamics and heat transport. *Int J Greenh Gas Con*. 2014;29:263-278.
- Kvamme BR, Kuznetsova T, Haynes M. Molecular dynamics studies of water deposition on hematite surfaces. AIP Conference Proceedings; December, 2012.
- Kuznetsova T, Jensen B, Kvamme B, Sjöblom S. Water-wetting surfaces as hydrate promoters during transport of carbon dioxide with impurities. *Phys Chem Chem Phys*. 2015;17:12683-12697.
- Maekawa T. Equilibrium conditions for gas hydrates of methane and ethane mixtures in pure water and sodium chloride solution. *Geochem J*. 2001;35:59-66.
- Smelik EA, King H Jr. Crystal-growth studies of natural gas clathrate hydrates using a pressurized optical cell. *Am Mineral*. 1997;82:88-98.
- Deaton W, Frost E Jr. Gas hydrate composition and equilibrium data. *Oil Gas J*. 1946;45:170-178.
- Verma VK. *Gas Hydrates from Liquid Hydrocarbon-Water Systems* [Doctoral dissertation], University of Michigan, 1974.
- Thakore JL, Holder GD. Solid vapor azeotropes in hydrate-forming systems. *Ind Eng Chem Res*. 1987;26:462-469.
- Nakamura T, Makino T, Sugahara T, Ohgaki K. Stability boundaries of gas hydrates helped by methane—structure-H hydrates of methylcyclohexane and cis-1, 2-dimethylcyclohexane. *Chem Eng Sci*. 2003;58: 269-273.
- Jhaveri J, Robinson DB. Hydrates in the methane-nitrogen system. *Can J Chem Eng*. 1965;75-78.
- Holder G, Grigoriou G. Hydrate dissociation pressures of (methane+ethane+ water) existence of a locus of minimum pressures. *J Chem Thermodyn*. 1980;12:1093-1104.
- Holder G, Hand J. Multiple-phase equilibria in hydrates from methane, ethane, propane and water mixtures. *AIChE J*. 1982;28:440-447.
- Roberts OL, Brownscombe ER, Howe LS, Ramsar H. Constitution diagrams and composition of methane and ethane hydrates. *Oil Gas J*. 1940;39:37-41.

28. Avlonitis D. Multiphase Equilibria in Oil–Water Hydrate Forming Systems [MSc thesis], Edinburgh, Scotland: Heriot-Watt University, 1988.
29. Reamer H, Selleck F, Sage B. Some properties of mixed paraffinic and olefinic hydrates. *J Pet Technol.* 1952;4:197-202.
30. Miller B, Strong E. Hydrate storage of natural gas. *Am Gas Assoc Monthly.* 1946;28:63-67.
31. Englezos P, Ngan YT. Incipient equilibrium data for propane hydrate formation in aqueous solutions of sodium chloride, potassium chloride and calcium chloride. *J Chem Eng Data.* 1993;38:250-253.
32. Robinson DB, Mehta BR. *J Can Pet Tech.* 1971;10:33-35. Cross ref. from Sloan ED, Koh CA. (*Clathrate Hydrates of Natural Gases*, Chemical industries. Vol. 119. 3rd ed. Boca Raton, FL: CRC Press; 2008).
33. Kubota H, Shimizu K, Tanaka Y, Makita T. Thermodynamic properties of R13 (CClF₃), R23 (CHF₃), R152a (C₂H₄F₂), and propane hydrates for desalination of sea water. *J Chem Eng Jpn.* 1984;17:423-429.
34. Schneider GR, Farrar J OSW R and D Progress Report No. 292, Rocketdyne, 1968.
35. Rouher OS, Barduhn AJ. Hydrates of iso- and normal butane and their mixtures. *Desalination.* 1969;6:57-73.
36. Verma V, Hand J, Katz D. Gas hydrates from liquid hydrocarbons (methane-propane-water system). Paper presented at: the GVC/AIChE Joint Meeting, 1975.
37. Wu BJ, Robinson DB, Ng HJ. Three and four-phase hydrate forming conditions in methane + isobutane + water. *J Chem Thermodyn.* 1976; 8:461-469.

Manuscript received Jan. 10, 2018, and revision received Sep. 3, 2018.

Paper 6

Simulation of hydrate plug prevention in natural gas pipeline from Bohai Bay to onshore facilities in China

By

Solomon Aforkoghene Aromada and Bjørn Kvamme

Published in:

Simulation Notes Europe Journal, SNE 31(3), 2021, 151-157.

Simulation of Hydrate Plug Prevention in Natural Gas Pipeline from Bohai Bay to Onshore Facilities in China

Solomon Aforkoghene Aromada^{1*}, Bjørn Kvamme¹

¹Department of Physics and Technology, University of Bergen, Allegaten 55, 5007 Bergen, Norway;

*Solomon.Aromada@student.uib.no, saromada@gmail.com

²Strategic Carbon LLC, Vestre Holbergsallmenningen 17, 5011 Bergen, Norway; kvamme@strategic-carbonllc.com

SNE 31(3), 2021, 151-157, DOI: 10.11128/sne.31.tn.10576
Received: March 10, 2021 (Selected EUROSIM 2019 Postconf. Publ.); Revised: Sept. 1, 2021; Accepted: September 3, 2021
SNE - Simulation Notes Europe, ARGESIM Publisher Vienna
ISSN Print 2305-9974, Online 2306-0271, www.sne-journal.org

Abstract. Natural gas hydrates occasionally plug the 58 km subsea pipeline that transports natural gas from Platform QK18-1 in southwest of Bohai Bay to the processing facility onshore in Northeast China. This is because it is a wet gas subsea pipeline that operates at high pressures and low temperatures, which are the conditions that are appropriate for hydrate formation to occur. In this study, we proposed that the best way to prevent the occasional plugging of the pipeline is to rightly evaluate the upper limit of water that can be permitted in the bulk gas and dehydrate the gas accordingly before transport. Current industrial techniques are mainly based on water dewpoint evaluations. In our recent work we have proposed another approach that considers the impact of the rust (Hematite) on the internal walls of pipelines. These two methods have been used for this study. The results of the method of adsorption of water onto rusty (Hematite) surfaces suggest that the current approach (dewpoint method) overestimates the safe-limit of water about 18 to 19 times higher. Thus, the risk of hydrate formation may still exist if the dewpoint method is used as basis for drying the gas. Sensitivity analysis shows the influence of pressure on the upper limit of water- the higher the pressure the lower the maximum concentration of water that is safe to accompany the gas. Our calculations were done using a FORTRAN code that utilize thermodynamic data from molecular dynamics simulation.

Introduction

Hydrate discovery is dated back to 1810 and credited to Sir Humphrey Davy [1-3]. But natural gas hydrate (NGH) formation in pipeline transporting natural gas became a major research focus in the 1930's through the work of Hammerschmidt [4]. NGH are non-stoichiometric crystalline inclusion compounds formed when hydrogen-bonded water molecules form three-dimensional solid cage-like structures with cavities which entrap suitably small sized molecules of certain gases and volatile liquids known as guest molecules. Methane, ethane, propane, isobutane, carbon dioxide (CO₂) and hydrogen sulphide (H₂S) [5, 6] are guest molecules that can form hydrate in their pure form. Hydrates are ice-like solid substances that form at high pressures and low temperatures conditions when free water (liquid) is available in a gas containing guest molecules. Hydrate formation is a crucial flow assurance challenge to the oil and gas industry since water is always produced together with hydrocarbons. This water can drop out of the bulk gas. With the appropriate thermodynamic conditions of high pressure and low temperature [6-8], and favourable mass and heat transport, this could lead to hydrate formation. Subsequently, accumulation and agglomeration of the formed hydrate can occur and eventually lead to plugging [4] of pipelines. This results in stopping of operations which means economic losses [9]. Sometimes there could be destruction [9, 10] of pipelines and equipment, and even loss of life [5].

There are many pipeline networks all over the world transporting hydrocarbons [11]. In this work we have focused on the 58 km subsea pipeline [12] from Platform QK18-1 in southwest of Bohai Bay (part of the Bohai Gulf), transporting natural gas to the processing facility

onshore in Northeast China. It is a wet gas subsea pipeline and it is exposed to elevated pressure and low temperature [12]. Plugging of the pipeline by hydrate occurs once in a while [12]. Li et al. [12] performed an experimental study on the pipeline and suggested the following solutions: pressure reduction or raising the temperature (heating the pipeline), dehydration of gas before subsea pipeline transport, and thirdly, addition of chemical additives such as kinetic hydrate inhibitors (KHI), to ensure safe operations.

In this work, our focus is on the second recommendation. This is also in accordance with what Li et al. [12] proposed as the best choice out of their three recommendations. However, their work did not go into details of how to estimate the upper limit of water content in the gas for prevention of hydrate formation in the subsea pipeline. In a recent work [13], we proposed an alternative approach for evaluating the upper limit of water in natural gas during pipeline transport to avoid the risk of hydrate formation. The study focused on hydrocarbon components of methane, ethane, propane and isobutane which are the primary hydrocarbon hydrate guest molecules. Therefore, there is a need to carry out this study with a real and specific gas field data. This also involves some content of inorganic gases like CO₂ which is a very strong hydrate former. Nitrogen cannot form hydrate in its pure form [14] but can still enter hydrate which is mainly stabilized by other components. In the other end of the guest molecule size scale is normal butane [15-17], which does not make hydrate as pure component, but gauche conformation can fit into large cavity of structure I when methane fills small cavities. Both trans and gauche conformations fit large cavities of structure II although the trans configuration gives low stabilization and will only form hydrate with methane or other good hydrate former in small cavities.

1 Thermodynamics of Hydrate: Description and Validation of Model

We used residual thermodynamics with Soave-Redlich-Kwong (SRK) equation of state [18] for all components in each phase (hydrate, ice and liquid water). We did that by making use of molecular dynamics (MD) simulations results for water in empty hydrates, liquid water, and ice phases [19]. We used equation (1) to estimate the chemical potential of component j in the gas phase.

To ensure the same reference value for free energy of all the estimates of chemical potentials, regardless of the phase, ideal gas is used as the reference state:

$$\mu_j(T, P, \bar{y}) = \mu_j^{ideal\ gas}(T, P, \bar{y}) + RT \ln \phi_j(T, P, \bar{y}) \quad (1)$$

$$\lim(\phi_j) \rightarrow 1.0 \dots \text{for ideal gas}$$

Where ϕ_j is the fugacity coefficient for component j in the given phase, R is universal gas constant, \bar{y} is the mole fraction vector of the gas, P and T are pressure and temperature respectively. The chemical potential of component j in water is estimated as:

$$\mu_j(T, P, \bar{x}) = \mu_j^{ideal\ liquid}(T, P, \bar{x}) + RT \ln \gamma_j(T, P, \bar{x}) \quad (2)$$

$$\lim(\gamma_j) \rightarrow 1.0 \text{ when } x_j \rightarrow 1.0$$

Where γ_j stands for the activity coefficient of component j in the liquid phase and \bar{x} is the mole fraction vector of the liquid. It is also proper to use a reference state of infinite dilution since the solubility of methane and higher hydrocarbons in water is low:

$$\mu_j^{H_2O}(T, P, \bar{x}) = \mu_j^{H_2O, \infty}(T, P, \bar{x}) + RT \ln [\chi_j^{H_2O} \cdot \gamma_j^{H_2O, \infty}(T, P, \bar{x})] \quad (3)$$

$$\lim(\gamma_j^{H_2O, \infty}) \text{ when } x_j \rightarrow 0$$

Where $\mu_j^{H_2O, \infty}$ represents the chemical potential of component j in water, ∞ denotes infinite dilution, $\gamma_j^{H_2O, \infty}$ stands for activity coefficient of component j in aqueous phase based on the same reference state. The solubility of methane and higher hydrocarbons are each very low. Thus, equation (4) could be applied together with equation (3):

$$\mu_j^i(T, P, \bar{x}) \approx \mu_j^{i, \infty}(T, P, \bar{x}) + RT \ln [\chi_j^i \cdot \gamma_j^{i, \infty}(T, P, \bar{x})] \quad (4)$$

Superscript i stands for different phases with low solubility, while subscript j represents different components. We evaluated the chemical potential of water in hydrate using the statistical mechanical model for water in hydrate (equation 5). This is a typical Langmuir type of adsorption model. The version we used is different from that of van der Waal and Platteuw [20] which assumes rigid lattice.



It is the one proposed by Kvamme and Tanaka [19]. This one takes into account the movements of the lattice and the corresponding impacts of different guest molecules. That is, the collisions between guest molecules and water which are adequately strong enough to affect the water motion.

$$\mu_{H_2O}^{(H)} = \mu_{H_2O}^{(0,H)} - \sum_{i=1}^2 R.T.v_i \cdot \ln \left(1 + \sum_{j=1}^{n_{guest}} h_{ij} \right) \quad (5)$$

Where H stands for hydrate phase, $\mu_{H_2O}^{(H)}$ refers to the chemical potential of water in hydrate, $\mu_{H_2O}^{(0,H)}$ signifies the chemical potential of water in empty hydrate structure, and v_i is the fraction of cavity type i per water molecule. The h_{ij} in equation (11) is the canonical cavity partition function of component j in cavity type i , and n_{guest} is the number of guest molecules in the system. We evaluated the canonical partition function using the relation:

$$h_{ij} = e^{-\beta(\mu_i^H - \Delta g_{ij}^{inc})} \quad (12)$$

Where β is inverse of gas constant times temperature ($\frac{1}{R.T}$), and Δg_{ij}^{inc} is the effects of inclusion of the guest molecules j in the cavity i on hydrate water. The free energy change related to hydrate phase transition (Δg^H) is evaluated using equation (14):

$$\Delta g^H = \delta \sum_{j=1}^H x_j^H (\mu_j^H - \mu_j^P) \quad (14)$$

Where H refers to hydrate phase of molecule j , P here is parent phase of molecule j . And equation (15) gives the relation between the filling fraction, the mole fractions and cavity partition function as shown below:

$$\theta_{ij} = \frac{x_{ij}^H}{v_j(1-x_T)} = \frac{h_{ij}}{1 + \sum_j h_{ij}} \quad (15)$$

Where x_T signifies total mole fractions of all hydrate formers in the hydrate, θ_{ij} refers to the filling fraction of component j in cavity type i , and x_{ij}^H stands for mole fraction of component j in cavity type i .

2 Composition of the Natural Gas from Bohai Bay

The composition of the wet natural gas from the southwestern Bohai Bay and the dry gas (City gas) used by Reference [12] are given in the Table 1. All other hydrocarbon components after iC_4 , that is nC_4 and C_{5+} and CO are not considered in this study as they are not relevant. Therefore, the molar compositions are normalised.

Components	Composition [Mole fractions]	
	Wet gas from subsea pipeline	Dry gas
C ₁	0.8868	0.9259
C ₂	0.0612	0.0319
C ₃	0.0332	0.0136
<i>i</i> C ₄	0.0066	0.0034
CO ₂	0.0072	0.0093
N ₂	0.0050	0.0159

Table 1. Composition of the Natural gas from Bohai Bay [12]

3 Model Validation

The estimates of hydrate equilibrium pressures from our theoretical model used for the simulations in FORTRAN are compared with experimental data relevant for the compositions of the gas in this study. Experimental data of Reference [21] (Figure 1) and Reference [22] (Figure 2) are the best we could find for this comparison based on closeness to the composition of the gas.

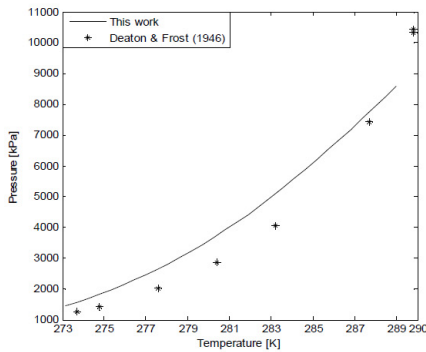


Figure 1. Estimated equilibrium pressures for hydrate formed from a gas mixture containing 96.50 mole % CH₄, 0.90 mole % C₂H₆, 1.80 mole % C₃H₈, 0.20 mole % CO₂, and 0.60 mole % N₂ [21].

It is important to state that the free energy of inclusions has been evaluated by MD simulations. And that we did not tune the model (no empirical data fitting was done) because our priority is to keep the statistical mechanical model [19] free of adjustable parameters in all terms.

These comprises the chemical potentials of empty hydrate, ice, and liquid water. Therefore, a fair qualitative

agreement is adequately acceptable for this study. So, the expectation is not perfect match with experimental data. The deviations are satisfactorily acceptable for further illustration of the maximum concentration of water content that should be allowed without the risk of hydrate formation.

It is also imperative to point out that more than one hydrate, that is having different densities, composition, and free energies do result from multicomponent gas mixtures [8, 13]. We know that the most stable hydrate will first form [13] based on the combined first and second laws of thermodynamics, then formation of a variety of hydrate compositions will occur. Therefore, the hydrate that would probably form in case of Figure 1 ought to be a mixture both structure I and II. But based on the very low concentration of propane, Reference [21] assumed only structure I hydrate is formed. In Figure 2, we took the presence of propane into consideration (the solid line) and disregarded it (dash-dot line) in a second run. That revealed that Wilcox et al. [22] also assumed only structure I hydrate is formed. The solid line in Figure 2 shows that there is a phase split by the propane (liquid and gas) at 278.5 K [7]. Most literature are wrong for straightening the curve as it is not the real situation. CO₂ also undergo a phase split [24] as pressure increases. Therefore, the final hydrate that would form as in these figures could likely be a mixture of several hydrates (sI and sII) with varying compositions of the initial hydrate formers from gas or liquid will result [13].

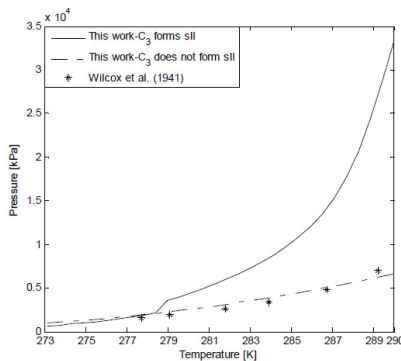


Fig.2. Estimated equilibrium pressures for hydrate formed from a gas mixture containing 93.20 mole % CH₄, 4.25 mole % C₂H₆, 1.61 mole % C₃H₈, 0.51 mole % CO₂, and 0.43 mole % N₂[22].

4 Safe-limits of Water in Natural Gas from Bohai Bay through Subsea Pipeline to Onshore Facilities in China and the City Gas

4.1 Alternative evaluation approaches: Impact of rust

The typical industrial practice for evaluating the risk of hydrate formation during pipeline transport of natural gas assumes that liquid water will condense out from the bulk gas stream to form a separate liquid water phase that can subsequently cause hydrate nucleation. This is done by estimating the dew-point pressure of water in the gas stream, then, check whether the computed dew-point pressure at the local temperature is within the temperature and pressure projection of the hydrate stability zone. If it is, it means water will drop out as liquid droplets. Afterwards, the theoretical amount of water that would condense out can be estimated and steps are taken to dry the gas. Or else, the necessary amount of a hydrate inhibitor that can adequately shift the hydrate stability curve's pressure and temperature projections beyond the risk zone is calculated and applied in the system to avoid hydrate formation. This we refer to as the dew point method.

In our recent work [13], we proposed an alternative approach for evaluation of the risk of hydrate formation in pipelines for gas mixtures containing methane, ethane, propane, and iso-butane which we call the Hematite approach. By Hematite we mean the most dominant and most thermodynamically stable form of rust. In this study, we have applied both methods (dew point method and hematite approach) to study a real gas mixture [12], a wet gas transported from offshore China to onshore processing facility using a 58 km subsea pipeline that is exposed to high pressures and low temperatures. However, in this situation, the gas mixture contains some inorganic gases, CO₂ that is a strong hydrate former compared to the hydrocarbons, and nitrogen that can also fill the small cages of sI hydrate in the presence of a helping molecule (methane). Nitrogen in its pure form cannot form hydrate [6], rather it has a dilution effect, that is why it has been proposed for use to reduce the reactivity of CO₂ during a simultaneous CO₂ storage in form of CO₂ hydrate and production of CH₄ [23].

The results of our investigation using the two approaches are presented in Figure 3 for the wet gas and Figure 4 in the case of the dry gas. Pressure range of 5000-25000 kPa and temperature range of 273 -280 K are used because these are the relevant ranges in such operations, for instance in the North Sea of Norway [6]. The maximum concentration of water that can be permitted in both the wet gas and dry gas are plotted in logarithm to base 10 (\log_{10}) to enable us plot results with both methods on the same figure. The only essence of including the dry gas in this analysis is merely for sensitivity analysis: to show how a slight change in composition of the same components in the gas mixture can cause slight change in water tolerance as can be observed in Figure 5 and Figure 6.

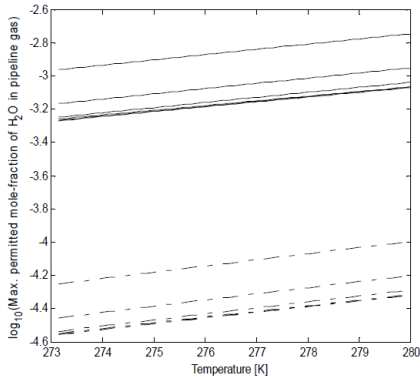


Figure 3. Estimated maximum concentration of water that should be permitted in the pipeline gas (wet gas) in logarithm to the base 10 (\log_{10}) vs temperature. Upper solid lines (-) represent estimates with the conventional dew point calculation, lines from top to bottom are for 5000 kPa, 9000 kPa, 13000 kPa, 17000 kPa, 21000 kPa, and 25000 kPa respectively. Lower dash-dot lines (-.) represent estimates with the approach of adsorption of water onto hematite, lines from top to bottom are also for 5000 kPa, 9000 kPa, 13000 kPa, 17000 kPa, 21000 kPa, and 25000 kPa respectively.

After processing the gas, the dry gas (city gas) is slightly richer in the lightest hydrocarbon component (methane) and that also caused the permitted water concentration to also move up slightly, which indicate that presence of the heavier hydrocarbon components like ethane, propane, and isobutane means a lower allowable water content [6,7,13] to avoid the risk of hydrate formation in a subsea pipeline operating at a high pressure and low temperature.

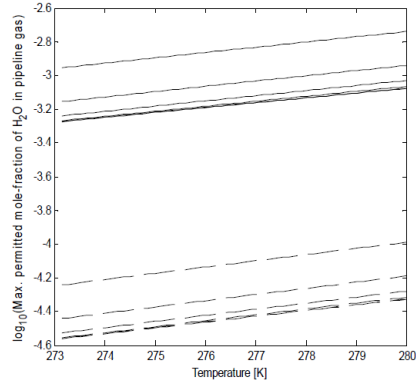


Figure 4. Estimated maximum concentration of water that should be permitted in the pipeline gas (dry gas) in logarithm to the base 10 (\log_{10}) vs temperature. Upper solid lines (-) represent estimates with the conventional dew point calculation, lines from top to bottom are for 5000 kPa, 9000 kPa, 13000 kPa, 17000 kPa, 21000 kPa, and 25000 kPa respectively. Lower dash lines (-) represent estimates with the approach of adsorption of water onto hematite, lines from top to bottom are also for 5000 kPa, 9000 kPa, 13000 kPa, 17000 kPa, 21000 kPa, and 25000 kPa respectively.

How much lower depends on the amount of the higher hydrocarbons present in mixture with methane.

In this analysis, estimation of maximum allowable water content using the dew point method instead of the new approach may not ensure safe operation in respect of hydrate formation, since rust (Hematite) which is usually present in surfaces of inner walls of pipelines would still make water available through the mechanism of adsorption even at much lower mole-fractions than what is estimated by the dew point method. Hematite acts as a catalyst that helps to pull out the water from the bulk gas stream through adsorption, then hydrate can subsequently form slightly outside of the first two or three water layers of about 1 nm. Using the dew point approach overestimates the safe-limit of water about 18 to 19 times more than what is calculated by the method of water adsorption on Hematite. Additionally, the chemical potential of adsorbed water is about -3.4 kJ/mol lower [6, 7] than that of ordinary liquid water.

This mean absorbed water on rusty surfaces will more readily lead to hydrate formation than ordinary liquid water based on the combined first and second laws of thermodynamics (thermodynamic systems strive towards the least free energy). Therefore, the approach of adsorption of water on rusty surfaces dominates, and possibly will have an impact on designing natural gas dehydration systems.

4.2 Impacts of temperature and pressure

The work of Reference [12] focused on the impacts of pressure on temperature, density, and flowrate. But in this work our focus is on the recommended best measure to prevent [12] hydrate formation, that is reducing the water concentration to allowable limits.

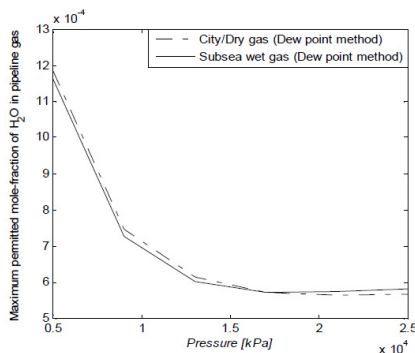


Figure 5. Impact of pressure on the maximum amount of water that should be permitted in the pipeline gases, conventional dew point estimates

The higher the temperature, the higher the upper limit of water in the gas stream to prevent hydrate formation during transport through the subsea pipeline as can be seen in Figure 3 and Figure 4. While Figure 5 and Figure 6 show that the higher the pressure, the lower the safe-limit of water in the gas. The results are the same with evaluations by both approaches. The only difference is the absolute values of mole-fractions of water. The last three lines for pressures of 17000 kPa, 21000 kPa and 25000 kPa as can be observed in Figure 3 and Figure 4, almost overlap. Figure 5 and Figure 6 make that clearer. This is a result of the high density of the non-polar hydrocarbons at these very high pressures.

The maximum water content becomes almost insensitive to increase in pressure due to the resistance of the tightly packed molecules of the non-polar hydrocarbon gases present in the system. It can also be seen on Figure 5 and Figure 6 that the slightly heavier wet gas curve crosses that of the slightly lighter city (dry) gas. This only shows that the heavier wet gas responds slightly faster in resistance to pressure than the slightly lighter city gas.

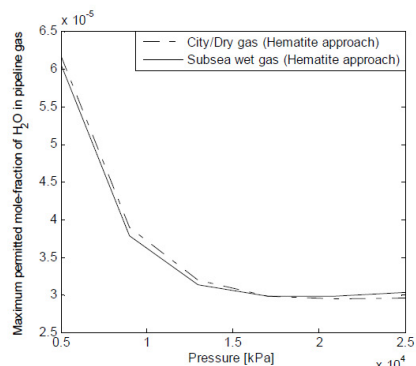


Figure 6. Impact of pressure on the maximum amount of water that should be permitted in the pipeline gases, hematite approach.

5 Conclusion

We conducted a study on how to prevent the occasional plugging of the wet gas subsea pipeline that transports natural gas from Platform QK18-1 in southwest of Bohai Bay to the processing facility onshore in Northeast China. This pipeline is operated at temperature and pressure conditions that are suitable for hydrate to form: high pressures and low temperatures. The thermodynamic scheme we used was simulated using a FORTRAN code based on the results of Kvamme and Tanaka molecular dynamics simulations. We used residual thermodynamics by means of Soave-Redlich-Kwong (SRK) equation of state for each component in every phase: hydrate, ice, and liquid water phases. The typical schemes currently employed by the petroleum industry for hydrate risk analysis are normally based on evaluation of water dewpoint, with the assumption that water will drop out of the bulk gas at the temperature and pressure conditions of dewpoint if the amount of water is up to or above the dewpoint concentration.

This water can subsequently lead to hydrate formation and eventually to plugging of the pipeline. In our recent work, we have proposed an alternative route for water to drop out of the bulk gas, that is through the process of adsorption of water onto rusty (Hematite) surfaces of the internal walls of pipelines. Pipelines are usually rusty before they are mounted in place for natural gas transport. The results of the method of adsorption of water onto rusty (Hematite) surfaces suggest that the current method based on water dewpoint calculation overestimates the allowable upper limit of water about 18 to 19 times higher. This means the risk of hydrate forming in the subsea pipeline may still exist if the dewpoint method is used. A pressure sensitivity analysis was also performed, and it shows that the higher the pressure the lower the maximum content of water that is safe to follow the gas.

References

- [1] Campbell J.M. Gas Conditioning and Processing, Vol. 1. Basic Principles. 157-200, (2003).
- [2] Schroeder W: In Ahren's Sammlung Chemischer und Chemisch-Technik Vortrage. 21- 71. (1926-28). Cross referenced from [4].
- [3] Vafaei M T. Reactive transport modelling of hydrate phase transition dynamics in porous media. PhD Dissertation, University of Bergen, Norway, 2015.
- [4] Hammerschmidt E G. Formation of gas hydrates in natural gas transmission lines. *Industrial & Engineering Chemistry* 26(8), 851-855 (1934).
- [5] Sloan Jr E D, Koh C. Clathrate hydrates of natural gases. 3rd edn. Boca Raton, Florida CRC press, (2007).
- [6] Kvamme B, Aromada S A. Risk of hydrate formation during the processing and transport of Troll gas from the North Sea. *Journal of Chemical & Engineering Data* 62(7), 2163-2177 (2017). DOI: 10.1021/acs.jced.7b00256
- [7] Kvamme B, Aromada S A. Alternative routes to hydrate formation during processing and transport of natural gas with a significant amount of CO₂: Sleipner Gas as a Case Study. *Journal of Chemical & Engineering Data* 63(3), 832-844 (2018). DOI: 10.1021/acs.jced.7b00983
- [8] Aromada, S A, Kvamme B. Impacts of CO₂ and H₂S on the risk of hydrate formation during pipeline transport of natural gas. *Frontiers of Chemical Science and Engineering*, 1-12 (2019). DOI: 10.1007/s11705-019-1795-2
- [9] Makogon, Y. F.: Natural gas hydrates—A promising source of energy. *Journal of Natural Gas Science & Engineering* 2, 49-59 (2010). DOI: 10.1016/j.jngse.2009.12.004
- [10] Woehler F. Krystallisiertes Schwefelwasserstoff-Hydrat. *Justus Liebigs Annalen der Chemie* 33, 125-126 (1840) Cross referenced from Hammerschmidt (1934)
- [11] Chartsbin Website, Total Length of Pipelines for Transportation by Country, <http://chartsbin.com/view/1322>, last accessed 2017/01/16.
- [12]] Li W, Gong J, Lü X, Zhao J, Feng Y, Yu D. A study of hydrate plug formation in a subsea natural gas pipeline using a novel high-pressure flow loop. *Petroleum Science* 10(1), 97-105 (2013). DOI: 10.1007/s12182-013-0255-8
- [13] Aromada S A, Kvamme B. New approach for evaluating the risk of hydrate formation during transport of hydrocarbon hydrate formers of sI and sII. *AIChE Journal* 65(3), 1097-1110. (2019). DOI: 10.1002/aic.16493
- [14] Kvamme B. Fundamentals of Natural Gas Hydrates and Practical Implications. Unpublished Work: PTEK 232. Course Material, Spring Semester 2017, Dept of Physics and Technology, University of Bergen, Norway, 2017.
- [15] Kumar S. Gas Production Engineering. Gulf Publishing Company, Book Division, (1987).
- [16] John V, Holder G. Hydrates of methane+ butane below the ice point. *Journal of Chemical and Engineering Data* 27, 18-21 (1982).
- [17] Ng H-J, Robinson D B. Equilibrium-phase properties of the toluene-carbon dioxide system. *Journal of Chemical and Engineering data* 23, 325-327 (1978).
- [18] Soave G. Equilibrium constants from a modified Redlich-Kwong equation of state. *Chemical Engineering Science* 27, 1197-1203. (1972).
- [19] Kvamme B, Tanaka H: Thermodynamic stability of hydrates for ethane, ethylene, and carbon dioxide. *The Journal of Physical Chemistry* 99(18), 7114-7119 (1995).
- [20] van der Waals J H, Platteeuw J C. Clathrate solutions. *Advance Chemical Physics* 2,1-57 (1959).
- [21] Deaton W M, Frost Jr E M. Gas hydrate composition and equilibrium data. *Oil & Gas Journal* 45, 170-178(1946).
- [22] Wilcox W I, Carson D B, Katz D L. Natural gas hydrates. *Industrial & Engineering Chemistry* 33(5), 662-665 (1941).
- [23] Kvamme B, Aromada S A, Kuznetsova T, Gjerstad P B, Canonge P C, Zarifi M. Maximum tolerance for water content at various stages of a natuma production. *Heat and Mass Transfer* 1-21 (2018). DOI: 10.1007/s00231-018-2490-4
- [24] Aromada S A, Kvamme B, Wei N, Saeidi N. Enthalpies of hydrate formation and dissociation from residual thermodynamics. *Energies*, 12(24), 4726 (2019).

Paper 7

Heterogeneous and homogeneous hydrate nucleation in CO₂/water systems

By

Bjørn Kvamme, Solomon Aforkoghene Aromada, and Navid Saeidi

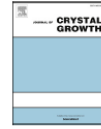
Published in

Journal of Crystal Growth, 2019, 522: 160-174



Contents lists available at ScienceDirect

Journal of Crystal Growth

journal homepage: www.elsevier.com/locate/jcrysgroHeterogeneous and homogeneous hydrate nucleation in CO₂/water systemsBjørn Kvamme^a, Solomon Aforkoghene Aromada^{b,*}, Navid Saeidi^c^a Strategic Carbon LLC, Vestre Høibergsallmenningen 17, 5011 Bergen, Norway^b Department of Physics and Technology, University of Bergen, Allegaten 55, 5007 Bergen, Norway^c Department of Environmental Engineering, University of California Irvine, Henry Samueli School of Engineering, 4200 Engineering Gateway Building, Irvine, CA 92697-3975, United States

ARTICLE INFO

Communicated by M. Uwaha

Keywords:

- A1. Nucleation
- A1. Mass transfer
- A1. Hydrate
- B1. Carbon dioxide
- A1. Induction time
- A1. heterogeneous

ABSTRACT

The strong international focus on reduction of CO₂ emissions to the atmosphere involves many situations in which hydrate may form from water and CO₂. Transport of CO₂ in pipelines typically involves high pressures and low temperatures favourable for hydrate formation. Aquifer storage of CO₂ also frequently involves regions of the storage sediments which are inside CO₂ hydrate formation. CO₂ hydrate can even be an active phase in CO₂ separation technology. Hydrate formation, like any other phase transition, has two physically well-defined stages. The initial nucleation is an unstable phase in which the thermodynamic benefit of the phase transition competes with the thermodynamic penalty of pushing away the existing phases. The latter term depends on size as well as shape of the growing hydrate nuclei. The transition from nucleation over to stable growth is therefore generally dependent on the geometrical dimension of the crystal, which can range from one for a spherical core and upwards to complex crystal morphologies. A third stage which is not uniquely defined physically is the so-called induction time. This is the stage at which the hydrate growth is massive and visible by various detection methods like pressure change, laser detection of crystals or other imaging techniques. Frequently, the induction time is misinterpreted as nucleation time. Nucleation is a nano-scale process, but several situations of hydrate formation leads to changes in access to hydrate building blocks. Formation of a hydrate film on the interface between water and a hydrate former phase will substantially delay mass transport for further growth. The slow, mass transport limited, growth towards detectable hydrate is therefore frequently misinterpreted as absence of hydrate. Yet another set of misunderstandings arise from the fact that hydrates in industry and nature can never approach equilibrium. Some of these are well known for simple systems, but there are also some relevant phases that are rarely accounted for, for a deeper understanding of the hydrate. Finally, there are frequently misconceptions that only one type of hydrate is formed always. In this work we utilize classical thermodynamics with residual thermodynamics description for all phases, including hydrate, to analyse various routes to hydrate formation between CO₂ and water. We utilize classical nucleation theory for simplified hydrate geometries in order to illustrate the range of likely hydrate nucleation times as well as ranges of different hydrate that can form. Hydrate forming homogeneously from dissolved CO₂ in water can form a range of different hydrates since the composition will change depending on the concentration of CO₂ in water. Hydrate nucleation times are very fast and in the nanoseconds range. Times for onset of massive growth in systems without stirring or other hydrodynamic forces that can break hydrate films can be very long due to slow transport through initial hydrate films.

1. Introduction

International agreements on reduction of CO₂ emissions to the atmosphere have increased international investments in development of renewable energy sources. It is still hard to foresee that the increasing worldwide demands for energy can be replaced with renewables within the next 3–5 decades. The international efforts to capture, transport and

store or utilize CO₂ are therefore important steps to at least minimize the footprints of fossil fuel use. Transporting CO₂ in pipelines requires high pressures and, in many cases, low temperatures, like on the sea-floor in the North Sea offshore Norway. Storing CO₂ in aquifers may involve hydrate forming conditions in sections of the storage reservoir. This will affect sealing integrity but may also reduce horizontal spreading of CO₂ in those regions [1–5]. These are just two examples

* Corresponding author.

E-mail address: Solomon.Aromada@student.uib.no (S.A. Aromada).<https://doi.org/10.1016/j.jcrysgro.2019.06.015>

Received 16 September 2018; Received in revised form 10 June 2019; Accepted 12 June 2019

Available online 13 June 2019

0022-0248/ © 2019 Elsevier B.V. All rights reserved.

that illustrate different situations which may lead to the formation of hydrate between CO₂ and water.

Hydrate formation has two physically well-defined stages. The first stage is the nucleation stage, which is an unstable phase whereby there is a competition between the thermodynamic benefit of the phase transition and the thermodynamic penalty of pushing away the existing phases. The latter term hinges on size as well as shape of the growing hydrate nuclei. The transition from nucleation over to the second stage known as stable growth is consequently mostly governed by the geometrical dimension of the crystal, and this can range from one for a spherical core and upwards to complex crystal morphologies. A third stage, which is known as induction time is not distinctively defined physically. At this stage the hydrate growth is massive and visible, it is detectable by various detection means such as pressure change, laser detection of crystals or other imaging techniques.

The induction time is often misinterpreted as nucleation time. Nucleation is a nano-scale process, nonetheless, numerous situations of hydrate formation cause changes in access to hydrate building blocks. The formation of a hydrate film on the interface between water and a hydrate former phase will significantly impede mass transport for further hydrate growth. The slow, that is the mass transport limited growth towards detectable hydrate is thus normally misinterpreted as absence of hydrate. Besides, additional set of misunderstandings emerge because hydrates in industry and nature can never attain equilibrium. The last misconception worthy of mention here is that it is only one type of hydrate that does form. This work aims at clarifying these misconceptions, especially nucleation time and induction time. We applied classical thermodynamics with residual thermodynamics description for all phases, including the hydrate phase, to analyse various routes to hydrate formation between CO₂ and water. We used classical nucleation theory (CNT) for simplified hydrate geometries to illustrate the range of probable hydrate nucleation times as well as ranges of different hydrate that can form.

The paper is organized as follows; theoretical analysis, then, different routes to hydrate formation are discussed in the next section. The latter is followed by calculations of upper-limit of water in a CO₂ transport pipeline. The following section presents our work on hydrate nucleation and hydrate growth limitations, then heterogeneous hydrate nucleation on water/gas interface, and homogeneous hydrate nucleation from dissolved carbon dioxide. Then a section for induction time follows, and a general discussion as the last section.

2. Theoretical analysis

We mentioned above two examples that illustrate different situations which may lead to the formation of hydrate between CO₂ and water. In the first case, water will be dissolved in the CO₂ and this water can drop out in various forms as discussed later in more detail. It can condense out in the form of liquid droplets or it can adsorb on rusty pipeline walls. In either case, the free water can form hydrate with CO₂. In the case of a CO₂ plume that migrates upwards in a reservoir due to buoyancy and enters a region of hydrate forming conditions, then hydrate can form on the interface between CO₂ and water. The free energy change for the hydrate formation needs to be negative and more negative than the work needed to push away original phases (discussed in more detail later in the paper). We denote this interface hydrate as H₁, and the free energy change of the phase transition can be expressed as:

$$\Delta G^{(H_1)} = \left[x_{H_2O}^H (\mu_{H_2O}^H(T, P, \vec{x}^H) - \mu_{H_2O}^{water}(T, P, \vec{x})) + \sum_j x_j^H (\mu_j^H(T, P, \vec{x}^H) - \mu_j^{gas}(T, P, \vec{y}^{gas})) \right] \tag{1}$$

where *G* is free energy. The symbol Δ represents change, thus, Δ*G* is the

change in free energy, and superscript *H_i* indicates this hydrate formation route (route 1 in this case). *x* is mole-fraction in liquid or hydrate (superscript *H*) and *y* is mole-fraction in hydrate former phase. The vector signs on mole-fractions denote vectors of mole-fractions in the actual phase. *μ* denotes chemical potential. Subscripts *H₂O* and *j* denote water and hydrate formers respectively. Superscripts *H*, *water* and *gas* denote hydrate, liquid water and gas phases respectively. *T* and *P* are temperature and pressure respectively.

Liquid water chemical potential is calculated from the symmetric excess conventions as:

$$\mu_{H_2O}(T, P, \vec{x}) = \mu_{H_2O}^{pure, H_2O}(T, P) + RT \ln(x_{H_2O} \gamma_{H_2O}(T, P, \vec{x})) \approx \mu_{H_2O}^{pure, H_2O}(T, P) + RT \ln(x_{H_2O}) \tag{2}$$

lim(*γ_{H₂O}*) = 1.0 when *x_{H₂O}* approaches unity.

The notations are the same as for Eq. (1) with the change that there is no need for superscript on mole-fraction in liquid water since this is a liquid water description. Pure means pure liquid water. Gamma is activity coefficient.

The approximation on the right-hand side is strictly not necessary. We could utilize a theoretical model for the activity coefficient or we could also use Gibbs-Duhem [6] to relate this to the activity of CO₂ in water as we have done in our Phase Field Theory modelling of CO₂ hydrate phase transition dynamics studies [7,8]. Since the focus here is to illustrate the complexity of multiple hydrate formation in systems of water and CO₂ we use a simpler kinetic model which is more visible in terms of the various contributions to the hydrate phase transition dynamics. As such the approximation on the right-hand side of (2) is accurate enough for the purpose.

Chemical potential for water in the hydrate structure is given by [9]:

$$\mu_{H_2O}^H = \mu_{H_2O}^{0,H} - \sum_{k=1,2} RT \nu_k \ln \left(1 + \sum_i h_{ij} \right) \tag{3}$$

in which *H* denotes hydrate and 0 in the superscript on first term on right hand side means empty clathrate. These chemical potentials are readily available from model water (TIP4P) simulations [10]. The number of cavities per water *v_k* is 1/23 for small cavities of structure I and 3/23 for large cavities. With CO₂ as only guest, *i* is 1 in the sum over canonical partition functions for small and large cavities.

$$h_{ij} = e^{-\beta(\nu_j \epsilon + \Delta g_j)} \tag{4}$$

where β is the inverse of the universal gas constant times temperature. At equilibrium chemical potential of guest molecules *j* in hydrate cavity *i* is equal to the chemical potential of molecule *j* in the co-existing phase it comes from. I.e., for Fig. 1, it is gas chemical potential while in Fig. 7, it is chemical potential of aqueous solution. For non-equilibrium, the chemical potential is adjusted for distance from equilibrium through a Taylor expansion as discussed later. The free energies of inclusion (latter term in the exponent) are reported by [11–14].

The corresponding filling fractions and mole-fractions of methane in the hydrate is given by:

$$\theta_{ij} = \frac{h_{ij}}{1 + \sum_j h_{ij}} \tag{5}$$

θ_{*ij*} is the filling fraction of component *j* in cavity type *i*

$$x_j^H = \frac{\theta_{arg, e, j} \nu_{arg, e} + \theta_{small, j} \nu_{small}}{1 + \theta_{arg, e, j} \nu_{arg, e} + \theta_{small, j} \nu_{small}} \tag{6}$$

where *ν* is the fraction of cavity per water for the actual cavity type as indicated by subscripts. Corresponding mole-fraction of water is then given by:

$$x_{H_2O}^H = 1 - \sum_j x_j^H \tag{7}$$

and the associated hydrate free energy is then:

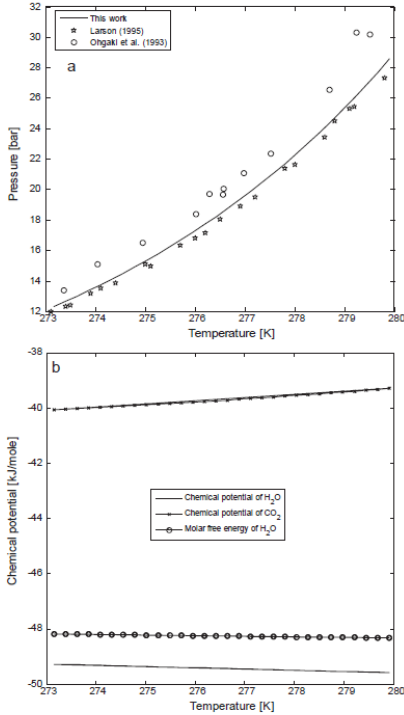


Fig. 1. (a) Estimated equilibrium pressures for CO₂ hydrate as function of temperature and pressure compared with experimental data from Larson [16] and Ohgaki et al. [17] (b) Chemical potential for methane along the equilibrium curve in (a) (dash dot), chemical potential of water (solid) and molar free energy (dashed).

$$G^{(H)} = x_{H_2O}^H \mu_{H_2O}^H + \sum_j x_j^H \mu_j^H \quad (8)$$

where x is mole-fraction. Subscripts denote component type, while superscripts denote the phase. H is hydrate phase. Component index j is hydrate former index. μ is chemical potential, and the meaning of subscripts and superscripts are the same as for mole-fractions. G is molar free energy.

The chemical potential for guest molecule j (in this case CO₂) which enters Eqs. (1) and (4) at equilibrium is, according to residual thermodynamics:

$$\mu_j(P, T, \vec{y}) = \mu_j^{pure,ideal}^{gas}(P, T, \vec{y}) + RT \ln(y_j \phi_j(P, T, \vec{y})) \quad (9)$$

where y_j is mole-fraction of component j in the gas mixture. ϕ_j is the fugacity coefficient for j . Ideal gas chemical potential for pure j can be trivially calculated for any model molecule via statistical mechanics using molecular mass and intramolecular structure (bond lengths and bond angles). Together with density and temperature, the ideal gas chemical potential is available from the momentum space canonical partition function. We have utilized the SRK [15] equation of state for

calculating the fugacity coefficient and the density needed for the ideal gas free energy calculations.

A typical example for hydrate H₁ formation conditions of temperature and pressure is plotted in Fig. 1 along with chemical potentials of water and CO₂. These chemical potentials are convenient in discussing other routes to hydrate formation and associated hydrate former chemical potentials since any variation in chemical potential of hydrate formers will lead to changes in hydrate compositions and hydrate free energies. This is fundamentally important since any assembly of molecules with unique density and composition is a unique phase.

For a given pure component (or mixture), a small amount of water is added to the gas. Because the mole-fraction of water in gas is proportional to vapour pressure divided by total pressure (Raoult's law) but corrected for non-ideal gas through fugacity coefficient of water in the gas. Since the water mole-fraction is in the order of 10⁻³ in mole-fraction of gas, this small water content does not affect CO₂ properties in the gas significantly. And due to the small water mole-fractions in gas, the water-water contributions to the water fugacity coefficient is negligible and as such water fugacity coefficients are only a function of CO₂ properties and a small impact of cross contributions between water and CO₂ through the mixing rules for the attractive parameter a in the SRK [15] equation. For defined temperature and pressure, the solution of chemical equilibrium between hydrate and the two separate fluid phases implies that the chemical potential of gas is equal to the chemical potential of a guest molecules in small or large cavity in Eq. (4). And at chemical equilibrium then the chemical potential of water in hydrate according to Eq. (3) has to be equal to chemical potential of water in liquid. Solubility of CO₂ is significant but small enough to be neglected as an approximation in calculations of water dew-point. At water dew-point, the chemical potential of pure liquid water is equal to the chemical potential of water in gas phase as calculated from Eq. (9). Direct formation of hydrate from gas is theoretically possible but highly unlikely due to limitations in mass supply of water and thermal insulation by gas which makes it hard to get rid of formation heat. In this case the chemical potential of water in gas is equal to the chemical potential of water in hydrate according to Eq. (3). Chemical potential of water in gas is solved iteratively for the only unknown which is mole-fraction of water in gas.

A third scenario is that water adsorbs on Hematite. This calculation is similar to the dew-point calculation but instead of liquid water chemical potential, the water chemical potential is now the chemical potential of water adsorbed on Hematite [2,13,14,44].

When the hydrate film on the surface of water closes in, then the transport of hydrate building block according to 1 becomes very slow due to transport limitations of CO₂ across the hydrate membrane. This opens up for hydrate formation from dissolved hydrate former in water.

This route to hydrate formation is important for several reasons. One reason is that this hydrate can form even if the direct contact between a separate hydrate former phase and water is almost closed (read: slow transport through hydrate). This hydrate formation is specially facilitated towards the existing hydrate film. Released heat from this hydrate formation will therefore also have impact on the dynamics of the initial hydrate film since parts of the released heat will be transported to the hydrate film. Yet another motivation is the need to define the hydrate stability window, which is more limited than the typical pressure-temperature projection used in hydrate risk evaluation. For CO₂ hydrate, it is specifically defined by Fig. 1 and the concentration limits for hydrate stability presented in Fig. 8 below.

We denote this hydrate as H₂ although this will be a range of different hydrates since chemical potential of hydrate former (dissolved CO₂ in water) will vary proportional to change in liquid water concentration of CO₂ according to Eq. (10) below.

$$\Delta G^{(H_2)} = \left[x_{H_2O}^H (\mu_{H_2O}^H(T, P, \vec{x}^H) - \mu_{H_2O}^{water}(T, P, \vec{x})) + \sum_j x_j^H (\mu_j^H(T, P, \vec{x}^H) - \mu_j^{water}(T, P, \vec{x})) \right] \quad (10)$$

We also use residual thermodynamics for dissolved CO₂ in water but utilize experimental data for the partial molar volume of CO₂ in water as published by [18], where we have used their Eq. (4) with corresponding parameters as given in their paper.

The infinite dilution ideal gas chemical potential is not very sensitive to pressure so the following approximation to only temperature dependency is considered as adequate:

$$\mu_{CO_2}^{\infty,ideal,ig} = -130.006 + \frac{163.818}{T_{0,R}} - \frac{64.898}{T_{0,R}^2} \quad (11)$$

where $T_{0,R}$ is 273.15 K divided by the actual temperature. Eq. (11) does not apply to temperatures above 303, due to the limited range of temperatures for which infinite partial molar volumes are used, and for temperatures above 273.15 K.

The fugacity coefficient for CO₂ in water is fitted to the following function:

$$\ln \phi_{CO_2}^{water}(T, P, \vec{x}) = \sum_{i=1,2}^{39} \left[a_0(i) + \frac{a_1(i+1)}{T_R} \right] (x_{CO_2})^{[0.05 + \frac{i-1}{40}]} \quad (12)$$

where T_R is reduced temperature and defined as actual T in Kelvin divided by critical temperature for CO₂ (304.35 K). The lower summation (1), 2 indicates starting from 1 and counting in steps of 2. Parameters are given in Table 1 below. The vector sign on mole-fraction x denote the vector of mole-fractions.

The chemical potential for CO₂ which applies to Eqs. (10) and (4) for an equilibrium case is the given by

$$\mu_{CO_2}(P, T, \vec{y}) = \mu_{CO_2}^{\infty,ideal}{}^{gas}(P, T, \vec{y}) + RT \ln(x_{CO_2} \mathcal{Z}_{CO_2}(P, T, \vec{y})) \quad (13)$$

Since the chemical potential of CO₂ is not necessarily, the same for dissolved CO₂ in water, and CO₂ in gas (or liquid) in a non-equilibrium situation, then hydrate formed according to Eq. (2) will be different from the first hydrate and accordingly denoted H_2 . The composition of this hydrate will be different as seen from the corresponding compositions, which follows from Eqs. (4) to (8).

Yet a third theoretical possible route to hydrate formation is from water dissolved in gas as given by equation (14) below.

$$\Delta G^{(H_3)} = \left[\begin{aligned} &x_{H_2O}^H \mu_{H_2O}^H(T, P, \vec{x}^H) - \mu_{H_2O}^{gas}(T, P, \vec{y}^{gas}) \\ &+ \sum_j x_j^H (\mu_j^H(T, P, \vec{x}^H) - \mu_j^{gas}(T, P, \vec{y}^{gas})) \end{aligned} \right] \quad (14)$$

x is mole-fraction. Subscripts denote component type while superscripts

Table 1
Parameters for Eq. (12).

i	a_0	a_1
1	-139.137483	-138.899061
3	-76.549658	-72.397006
5	-20.868725	-14.715982
7	18.030987	24.548835
9	44.210433	52.904238
11	63.353037	71.596515
13	74.713278	82.605791
15	80.411175	88.536302
17	82.710575	90.262518
19	82.017332	89.094887
21	79.373137	85.956670
23	75.429910	81.519167
25	70.680932	76.270320
27	65.490785	70.551406
29	60.125698	64.683147
31	54.782421	58.865478
33	49.592998	53.235844
35	44.500001	47.728622
37	39.869990	42.730831
39	35.597488	38.125674

denote the phase. H is hydrate, $water$ is liquid water and gas is hydrate former phase. Component index j is hydrate former index. The vector sign on mole-fractions denote vectors of mole-fractions in the actual phase. y is mole-fraction in hydrate former phase. μ is chemical potential and the meaning of subscripts and superscripts are the same as for mole-fractions. G is molar free energy and the delta symbol indicate hydrate minus original phases.

This is highly unlikely in terms of mass transport and heat transport. It might happen for gas close (nano scale) to a solid surface that might assist in transporting heat away. Close to liquid water surface the gas will be dynamically super-saturated with water due to capillary waves. These situations still remains as speculations and it is unlikely that they will even happen in significant amounts.

In this case chemical potentials for dissolved water in CO₂ and for CO₂ are calculated using residual thermodynamics from Eq. (9). The only reason that SRK can be utilized even for water in this case is due to the extremely low mole-fractions of water which makes the water-water contributions to the attractive mixture parameter approximately disappear. That makes the fugacity coefficient for water in the gas to only depend on short range attractive contributions. This is more visible when the virial equation of state is utilized [9].

Strictly speaking, a more favourable phase transition from gas would be that water condenses to a hydrate surface and then creates hydrate with gas phase CO₂. Similar for the phase transition in (10) in which it is more favourable, the dissolved CO₂ enriches and adsorbs in structured water below the existing hydrate film. And we have not so far discussed impact of solid surfaces. Mineral surfaces have distributed partial charges that structure adsorbed water. The resulting density profiles, and associated chemical potentials, results in additional ways to nucleate hydrate. As such it makes a substantial difference if a hydrate experiment is conducted in a glass cell or a stainless steel cell. In the latter case the atoms are neutral, except for some differences related to content of other atoms than iron.

2.1. Hydrate formation kinetics

There is a huge amount of published papers related to the concept of storing CO₂ in the oceans, and several papers have discussed the kinetics of hydrate formation. Several of these papers misinterpret induction times (onset of massive hydrate growth) for being nucleation times. Some of these are discussed below. We have used Phase Field Theory (PFT) to calculate nucleation times for CO₂ hydrate earlier (see references under discussion), which clearly indicates nano scale (time and volume) nucleation times in accordance with what is expected. The problem is that rapid nucleation results in hydrate films with very slow diffusivity for hydrate formers and water. Utilization of Classical Nucleation Theory to illustrate these aspects now serves several purposes. First, the theory is easier to illustrate for people that are not well versed in statistical mechanics. But even more important is that the equations are simple enough to find their way into risk evaluation packages as well as in reservoir simulators (we have implemented it into our simulator).

The kinetics of phase transitions consists of two physically well-defined stages. Nucleation is the stage at which the thermodynamic benefits of the phase transition competes with the penalty of the push work involved in given space for the new phase. There is normal randomness in this stage as related to molecular movements and heat diffusion. The resulting transition over to stable growth when the benefits are larger than the penalties will, in the classical theory, involve stable hydrate growth. For a spherical crystal this transition point will be critical size. Induction time is a qualitative term which can be more loosely interpreted as “time for onset of massive hydrate growth”. This is of course dependent on level of monitoring, which can range from laser detection of crystals to effects on pressure, or detection of visible crystals through a window in an experimental set-up. In more general terms, even the physically well-defined stages are more

complex since constraints of mass- and/or heat-transport can lead to rearrangements controlled by thermodynamic laws. These issues are clearly seen in more advanced theories like Density Functional Theories or Phase Field Theories [7,8,19,20].

In the open literature, frequently, induction times are discussed as nucleation times, even though critical sizes of crystals are on nano-scale for most substances and including hydrate [21]. The reason for confusion is therefore likely that hydrate films in the range from nano scale to micro-scale are not visible, even when using ordinary microscopes for evaluation.

Yet another misunderstanding is that published experimental data, as well as theoretical calculations, normally only discuss one type of hydrate. As discussed in the previous section, any change in chemical potential of hydrate former will lead to changes in hydrate compositions. And by thermodynamic fundamentals, any phase with unique density and unique composition is a separate phase. For the simple system of two components, water and CO₂, without any active solid surfaces, the fastest hydrate to form is H₁ because masses are available and heat transport is easy through liquid water. Then a range of hydrate H₂ can form homogeneously from dissolved CO₂ and water. Every change in concentration of remaining CO₂ in water gives rise to a new hydrate composition, and then a new phase.

Kinetic models for hydrate are implicit in terms of mass transport, heat transport and thermodynamic control of the phase transition. This is true even for the simplest theory of all – the classical nucleation theory. The mass transport fluxes need various kinetic theories like for instance MDIT theory [22–24] which reduce to the classical nucleation theory for a multi-component system when interface thickness in MDIT theory goes to zero. For illustration of the coupled transport and thermodynamic control of the phase transition kinetics, the classical nucleation theory serves as an easy method here because of the separation of contributions.

$$J = J_0 e^{-\beta \Delta G^{Total}} \tag{15}$$

where J_0 is the mass transport flux supplying the building blocks for the hydrate growth. For the phase transition in Eq. (1) it will be supply of CO₂ to the interface growth. In (10) it will be the diffusion rate for dissolved CO₂ to crystal growth from aqueous solution. And in (14) the rate limiting mass transport is the supply of water by diffusion through gas. For (1) and (10), transport through structured water interface between hydrate and surrounding liquid water will normally be rate limiting mass transport. The units of J_0 will be moles/m³ for homogeneous hydrate formation in (10) and (14), and moles/m²s for heterogeneous hydrate formation in (1). As discussed earlier, it is more likely that growth of hydrate from dissolved CO₂ below the initial film will happen on the initial interface hydrate from (1). As such these two hydrate growth scenarios, that is (10) and (14) will also be heterogeneous hydrate growth. β is the inverse of the gas constant times temperature and ΔG^{Total} is the molar free energy change of the phase transition. This molar free energy consists of two contributions. The phase transition free energy as described by (1), (10) and (14), as examples, and the penalty work of pushing aside old phases. Since the molar densities of liquid water and hydrate are reasonably close, it is a fair approximation to multiply the molar free energy of the phase transition with molar density of hydrate times the volume of hydrate core. The push work penalty term is simply the interface free energy times the surface area of the hydrate crystal. The lines below the symbols are used to indicate extensive properties (unit Joule):

$$\underline{\Delta G}^{Total} = \underline{\Delta G}^{PhaseTransition} + \underline{\Delta G}^{Pushwork} \tag{16}$$

For the simplest possible geometry of a crystal, which is a sphere, with radius R , we then get:

$$\underline{\Delta G}^{Total} = \frac{4}{3} \pi R^3 \rho_N^H \Delta G^{PhaseTransition} + 4 \pi R^2 \gamma \tag{17}$$

where ρ_N^H is the molar density of the hydrate and γ is the interface free

energy between hydrate and surrounding phase. Even if a hydrate core which grows on the surface of water is floating, it is expected that small crystals are likely to be covered by water also towards the gas side due to capillary forces that will facilitate transport and adsorption of water molecules from the liquid water side to cover the hydrate particle also on the gas side.

Differentiation of (17) with respect to R and solving for the maximum free energy radius (the critical core size) we get the usual result:

$$R^* = - \frac{2\gamma}{\rho_N^H \Delta G^{PhaseTransition}} \tag{18}$$

in which the superscript * denote critical nuclei radius.

The associated heat transport kinetics is implicitly coupled to (15) and (16) through the thermodynamic relationship between enthalpy and free energy:

$$\frac{\partial \left[\frac{\underline{\Delta G}^{Total}}{RT} \right]_{p,N}}{\partial T} = - \left[\frac{\underline{\Delta H}^{Total}}{RT^2} \right] \tag{19}$$

where $\underline{\Delta H}^{Total}$ is the enthalpy change due to the phase transition and the associated push work penalty. For the situation of a quasi-equilibrium (slow transport through hydrate film), we can calculate the enthalpy of phase transition without the penalty term along the equilibrium curve plotted in Fig. 2. It is of course not a substantial challenge to calculate the same quantities outside of equilibrium. The best way will be to keep the temperature as an equilibrium temperature and calculate the equilibrium pressure. In this way we only need to correct for pressure dependency. And since pressure dependency is very small for liquids and solids (hydrate) as well as for low pressure gas (for ideal gas it is by definition zero) this is a feasible calculation route. But for now, we limit ourselves to plotting the calculated enthalpy differences of hydrate formation along the same temperature range of the equilibrium curve as used in Fig. 2. For the gas phase portion of supply to the hydrate formation, the ideal gas part is trivially given by the number of degrees of freedom, which for a rigid linear CO₂ molecule is five and then adding 2RT for the translation from ideal gas energy to ideal gas enthalpy. The residual contribution to the enthalpy of CO₂ on the gas side follows trivially from the SRK and this term can be found in any handbook that lists properties which can be derived from the SRK equation of state. For the liquid water part and as well as water in hydrate, we utilize a numerical derivation. The correction of CO₂ chemical potential in hydrate is calculated using the average partial molar volume of CO₂ in the cavities as evaluated from Monte Carlo sampling using the algorithm (and code) discussed by Kvamme, Lund & Hertzberg [25]. Methane is not a general focus in this paper and is only interesting in this context because it is highly supercritical in the range of temperatures of Fig. 2, in contrast to CO₂ which is sub-critical, and this will reflect in the temperature and pressure dependencies of the heat of hydrate formation along the two equilibrium curves (the methane equilibrium curve is not plotted here but the end point on the equilibrium curve for methane is calculated to 26.1 bars at 273.16 K and to 52.0 bars at 280 bars. But then, the difference for methane is not very substantial and small compared to that of CO₂ along the equilibrium temperature over the same temperature range. For methane the difference is 0.4 kJ/moles from the lowest point of the equilibrium curve to the highest temperature.

$$\dot{Q} \propto \underline{\Delta H}^{Total} \tag{20}$$

The various ways that heat is transported (conduction, convection, radiation etc.) by the heat transport rate on left hand side of the proportionality is not essential for the phase transitions considered in this work, since they are characterized by either very good heat transport or almost heat insulated like through the CO₂ phase for the phase transition according to (1).

If the initial phases of water and CO₂ are large and not close to being

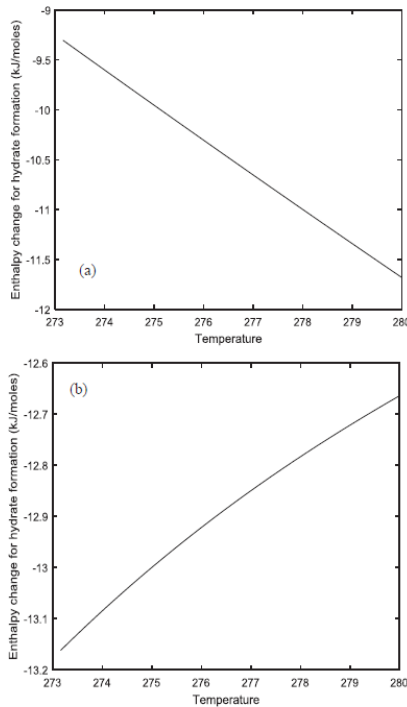


Fig. 2. (a) Heats of hydrate formation for CO₂ along the equilibrium curve. (b) Heats of formation for CH₄ hydrate along the equilibrium curve for CH₄ hydrate.

consumed, then a typical simplified heat transport scenario in (20) would involve heat conduction through water below the growing film according to (10). The simplest approach would be spherically symmetric heat conduction for a half sphere below hydrate from a point of hydrate growth plus heat conduction through the hydrate film towards CO₂ side. Heat conduction for CO₂ could be set to zero as an approximation. When the temperature at the hydrate surface reaches hydrate dissociation temperature and additional term of hydrate dissociation dynamics enters the mass and energy balances. Even with simple models it would be possible to model the associated heat transport according to (20). But since heat transport through liquid water is typically 2–3 orders of magnitudes faster [26–28] than the mass transport (diffusion) of bringing CO₂ to hydrate growth position, we disregard heat transport in this work on hydrate nucleation and leave the heat transport for subsequent work on hydrate growth along these lines.

When the liquid water phase has been depleted with CO₂ down to a level of quasi-equilibrium with CO₂ hydrate, then a new hydrate can only form if CO₂ is transported into the water phase or water is transported out to the CO₂ phase. This can happen in several ways. Diffusion through hydrate is very slow and likely governed by the existence of empty cavities. In absence of “fresh” building blocks, the first and second laws of thermodynamics will lead to a dynamic process in which

the hydrates of lowest stability (highest free energy) is going through a dissociation in favour of supporting growth of hydrate regions of lower free energy. These processes by itself can generate mass fluxes across the hydrate membrane. These free energy governed processes can also even lead to holes in the hydrate membrane and supply of new building blocks. Efficient handling of all these non-equilibrium processes requires theoretical concepts far beyond classical nucleation theory, like for instance Phase Field Theory [7,8,19,20]. But the use of classical nucleation theory in this work makes it easier to shed light on the variation of hydrates that can be formed in a real system as well as getting a better picture of critical nuclei sizes and nucleation times.

2.2. Routes to hydrate formation if water drops out during pipeline transport of CO₂ stream

Thermodynamically, three routes to hydrate formation based on how water is made available have been identified [13,29,30]. The first route is the dew-point route, which is the classical route currently considered and used for examining the risk of hydrate formation in industrial systems such as pipeline transport of CO₂ stream. The analysis of the risk of water dropping out from the CO₂ stream to form separate (liquid) water phase that can subsequently lead to hydrate formation is based on estimation of water dew-point (temperature-pressure) in the CO₂ stream. This is followed by checking if the calculated water dew-point pressure at the local temperature is inside the T-P projection of the hydrate stability zone. If it is, liquid droplets of water will condense out. The amount of water that can drop out is estimated and necessary steps are taken to dehydrate the CO₂ stream. If not, the right amount of a specific hydrate inhibitor that can adequately shift the hydrate stability curve’s T-P projections beyond the hydrate risk region is evaluated and used in the system to prevent hydrate formation.

The second route to hydrate formation involves the impact of solid surfaces. The relevant solid surface in transport of CO₂ is rust. The internal walls of pipelines are already normally covered by rust even before they are mounted together for operations. Rust which is formed from iron and oxygen under exposure to water is a mixture of different oxides of iron like magnetite (Fe₃O₄), hematite (Fe₂O₃), and iron oxide (FeO) [29]. Even though magnetite normally forms very early, but ultimately Hematite is the most dominant and one of the most thermodynamically stable forms of the ordinary rust. By ordinary rust we mean different oxides of iron formed by exposure of iron to water and oxygen. Therefore, in this work, rust is referred to as Hematite. These rusty (hematite) surfaces provide water adsorption sites that can also make water available for hydrate to form. Hydrate nucleation and growth can occur when water and CO₂ are adsorbed together on these hematite surfaces in the internal walls of gas transport pipelines or when merely water is adsorbed on these rusty surfaces with molecules of CO₂ being imported from the bulk gas. The chemical potentials of the CO₂ will be different across the phases consequent on the inability of industrial or real systems outside of laboratory to reach equilibrium. The hematite acts as a catalyst [14] for pulling out the water from the gas through mechanism of adsorption, thereby making liquid water available for hydrate to form slightly outside of the first two or three layers of water of approximately one nanometre. For water to be adsorbed on hematite, the chemical potential of water in the adsorbed phase must be lower than that of water in the gas phase.

Theoretically, a third route [13,29] to nucleation of hydrate exists and it is termed the “direct route”. This involves hydrate forming directly from water dissolved in CO₂. This route is thermodynamically feasible, but in real situation, it is highly doubtful due to the low concentration of the water in the gas, and limitations in heat and mass transport also make it questionable. The heat of formation must unavoidably be transported away to ensure dissociation does not occur. Nevertheless, if surface stress from flow does not have any influence on water/CO₂ system, then hydrate formation would occur rapidly on the

water/CO₂ interface and will very quickly hinder further transport of hydrate formers and waters through the hydrate film due to effect of very low coefficient of diffusivity. In this situation, hydrate formation can occur from CO₂ dissolved in water, and it can also form from water dissolved in CO₂, then this will benefit from nucleation on the surface of the hydrate. But considering a flowing case with turbulent shear forces, this is not a realistic.

2.3. Limits of water content in a CO₂ stream during pipeline transport to offshore storage site

The Norwegian continental shelf has a great potential [31] to store large amount of CO₂ from industrial processes. This large quantity of CO₂ can be transported from source to offshore storage sites using either pipelines for reasonable distances or ships for very long distances. Based on this potentiality, several pipelines for transport of CO₂ offshore for storage underground have been proposed in Europe and some already developed and in use. One of these is the proposed [32] approximately 1.1 m diameter (oversized) high pressure 900 km long pipeline along the route of Europe I for transport of CO₂ from Germany to the Norwegian North Sea (Sleipner area) for storage. Another offshore pipeline in the same region is that from Esbjerg in Denmark to Gullfaks-A (GFA) platform offshore of Norway [33,34]. These pipelines would play a significant role in mitigating global warming. But if the CO₂ is to be transported contains more water vapour than a specific limit at a given pressure and temperature, liquid water could condense out of the stream to make free water available through dew-point condensation or through the mechanism of adsorption onto rusty surfaces for hydrate nucleation to occur, or hydrate could form directly from the water in gas phase (not realistic, only theoretical as discussed above). CO₂ is a better hydrate former compare to the hydrate forming alkanes. Hydrate nucleation and growth is a crucial flow assurance challenge which could lead to total blocking of the pipeline cross-section thereby frustrating the purpose of this all-important project. The vital question therefore is, “what is the limit of water content that can be permitted in the CO₂ stream through the pipeline at the elevated pressures and lower temperature range expected during operation?” Another important question will be “what is the impact of the purity of the CO₂ stream on this maximum amount of water that can be allowed to avoid the risk of hydrate nucleation?” In this section, we have done a qualitative study of the risk of liquid water dropping out of the CO₂ stream transported via the pipeline from Esbjerg to Gullfaks applying the three different routes discussed in the previous section.

This proposed Esbjerg - Gullfaks pipeline is 683 km long with a diameter of 0.457 m and expected to transport five metric tonnes of CO₂ annually [33]. The CO₂ stream contains 0.9950 mol of CO₂, 0.0048 mol of N₂ and 0.0002 mol of CH₄, where all other impurities other than N₂ (C₂H₆, SO₂, NO_x, O₂ and CO) [33] are approximated to methane (the amount is very small and negligible and only hydrocarbon can take part in hydrate nucleation among them). The CO₂ stream will be sent from Esbjerg at 240 bar and the receiving pressure at Gullfaks is 100 bar. The temperature is expected to be 5 °C, the temperature range of the sea-floor of the North Sea is usually between -1 °C and 6 °C [13]. We applied these specifications in our study to qualitatively investigate the limit of water that can be permitted to follow the CO₂ stream in the pipeline from Esbjerg to Gullfaks without the risk of hydrate formation. The study is done for the three routes to hydrate nucleation discussed above. The typical measures for preventing hydrate nucleation in the pipeline are to ensure that liquid water does not drop out from the CO₂ stream. Theoretical studies [26] have shown that chemical potential of water adsorbed on rust could be lower than that of liquid water with 3.4 kJ/mole. A more novel water tolerance limit in a CO₂ stream will thus be the maximum mole-fraction of water before adsorption of water on rust can be triggered. In the case of water dropping out as liquid droplets this can result in nucleation of hydrate particles distributed in the CO₂ stream, but droplets can as well be adsorbed on the internal

walls of the pipeline. In any of these cases the first hydrate that forms would be heterogeneous hydrate nucleation on the interface between CO₂ and water. Water droplets following the CO₂ stream will be subjected to considerable surface stress that would possibly break up hydrate films and lead to more or less continuous heterogeneous hydrate nucleation. A nano-scale film of water on the rusty surface may be less exposed to surface stress because of flow since the roughness of the pipeline creates pockets of shielded regions which may generally be in size range of micrometre up to millimetre. In this case dissolved CO₂ gas in the water films on the solid (rusty) surface can cause homogeneous hydrate nucleation, an also two types of heterogeneous hydrate nucleation. First the initial hydrate film on the interface between CO₂ and water and followed by heterogeneous hydrate nucleation from dissolved CO₂ and water from below. Though both water and CO₂ come from the same liquid water phase the actual hydrate nucleation towards the initial hydrate film uses water which is structured by hydrate. This structured water is, strictly speaking, a different phase since structure and density are unique. From a purely thermodynamic point of view there is also the possibility of dissolved water and CO₂ to form hydrate directly. It is reasonably clear that this possibility is highly doubtful if mass-transport of building blocks (low concentration of water) and heat-transport limitations are added to the evaluation of hydrate risk.

The results are presented in Figs. 3a–3c and Table 2. The trends for upper limit of water permitted in the CO₂ stream to avoid the risk of liquid water condensing out and leading to hydrate nucleation (or direct hydrate formation for the direct route) for the three different routes to hydrate formation are the same. The only difference among the routes is the absolute values. The upper limit of water that can be allowed in the CO₂ stream to avoid liquid water dropping out or to prevent direct formation of hydrate from water that is dissolved in CO₂ stream (in the gas phase) declines with increasing pressures as can be observed in Figs. 3a–3c. From these results, estimates from the dew-point method are about 19 times higher than the estimates using the method of adsorption of water on hematite (rust) at temperature of 274 K, and 18 times higher at temperature of 278 K. These show that the risk of water dropping out of the CO₂ stream and subsequently leading to hydrate nucleation is about 18–19 times higher or more likely when rust is present in the internal walls of the pipeline. Comparing the estimates from the dew-point method with estimates from the theoretical route (direct hydrate nucleation route), the dew-point estimates are also higher; at temperature of 274 K, it is 29 per cent

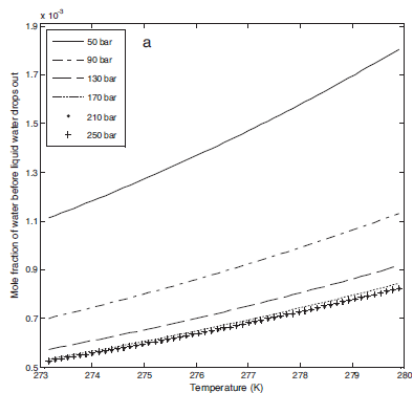


Fig. 3a. Maximum water content before liquid water drops out from the CO₂ stream.

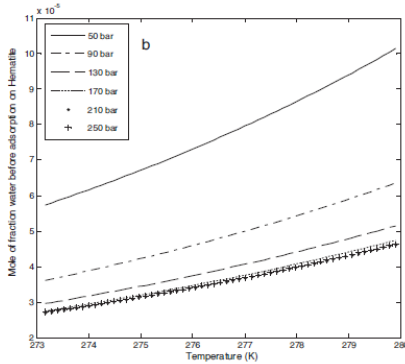


Fig. 3b. Maximum water content before adsorption of water onto Hematite from the CO₂ stream.

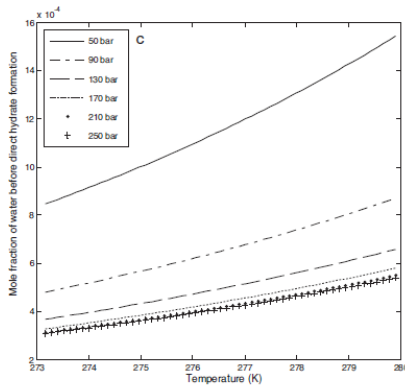


Fig. 3c. Maximum water content before hydrate formation directly from water in gas phase in the CO₂ stream.

higher at 50 bar and the difference increases with increasing pressure (the dew-point estimates are 69 per cent higher at 250 bar). And at 278 K, it is 21 per cent higher at 50 bar and 58 per cent higher at 250 bar. Higher differences occur at the higher pressures and lower temperatures, while less difference occurs at the lower pressures and higher temperatures (see Table 2). As has been discussed earlier, hydrate formation via this direct route is highly improbable. Sensitivity analysis has also been performed by reducing the purity of the CO₂ in the gas stream to 0.95 and 0.90 mol in binary mixtures of CO₂ and N₂. It shows the more the purity of the CO₂ the less the maximum amount of water that can be allowed to follow the gas stream. But it is very marginal; it is only 0.6 and 1.2 per cents increase in maximum limit of water content at 0.95 and 0.90 per cents of CO₂ respectively, and the differences decline with increasing pressure.

2.4. Hydrate nucleation and hydrate growth limitations

The fairly fixed positions of oxygens and hydrogens in hydrate waters is long range but the highly structured portion that can be assigned to the interface in which the phase transition (formation or dissociation) occur is roughly 1 nm. In earlier studies we have used 0.85 nm for a 90% confidence interval. This thickness is not entirely unique since it depends on which atom or charge that is being sampled and analysed. More details on this are given by [8,26,35]. Within the simplified models below, we therefore use a fixed interface thickness value of 1 nm (10 Å). The original pre-factor in classical nucleation theory (CNT) does not apply to the systems discussed in this work because diffusional transport of two different types of molecules are involved and they may even come from different phases in the case of hydrate formation from liquid water and gas as in Eq. (1). Strictly speaking, CNT does not even contain an interface thickness. Nevertheless - we can still use a model picture to estimate diffusional transport and concentration gradients. It will still end up with a diffusional transport flux for every different size of a growing hydrate nucleus and we can make use of sampled data from molecular dynamics simulations for concentration profiles across the interface from liquid to hydrate interface. Results from a sampling are plotted in Fig. 4 along with a smoothed fit for a 1.2 nm interface thickness.

The solid curve in Fig. 4(a) is constructed from the following fit to the Molecular Dynamics simulation data [26]:

$$C(R) = \sum_{i=1}^7 a_i \left[\arctan \left(0.6 \left(\frac{z}{12} \right) \left(\frac{\pi}{2} \right) \right)^{i-1} \right], \quad z \in (0, 12) \quad (21)$$

where z is the distance variable from liquid side towards hydrate side of the interface and as such only takes values between zero and twelve. Coefficients for equation (21) are given in Table 3 below.

Fick's law for the mass transport part related to J_0 in equation (16) can be expressed as:

$$\frac{\partial C(z)}{\partial t} = -D_{CO_2} \frac{\partial^2 C(z)}{\partial z^2} \quad (22)$$

where C is concentration of CO₂, t is time and D_{CO_2} is the diffusivity of CO₂ through the interface. R is the direction of the mass transport. The solution to Eq. (22) depends on the geometry and in the simplest case it is transport through a planar interface. And strictly speaking, it presumes that the diffusivity coefficient is constant. This often appropriate in liquid solutions or in a gas mixture but hardly across an interface where structure change substantially, and the local diffusivity coefficient change accordingly by orders of magnitude. In a numerical evaluation across the interface, the diffusivity coefficient should follow the local concentration for any given position z across the interface, i.e.:

$$\frac{\partial C(z)}{\partial t} = -\frac{\partial^2 [D_{CO_2} C(z)]}{\partial z^2} \quad (23)$$

The diffusion of CO₂ through the interface between liquid water and the hydrate surface is not known experimentally. Typical values for transport of CO₂ through the hydrate from various open sources vary, depending on approach used in theoretical estimations. Most values are based on Monte Carlo studies for models systems of hydrate and guest molecules jumping between cavities, which means "hole-in-the-cage-wall" mechanism [36–38] recommends that the solid-state diffusion occurs when the hydrate guest jumps from an occupied cage to the neighboring empty cage through a hexagonal or pentagonal faces of water ring of structure I or II hydrate [37,38]. These hops are only possible when the water vacancies presented in the ring, also with self-diffusion constant mostly proportional to the fraction of unoccupied cages in the 0.02 to 0.1 range. Most of published results concur on its order of magnitude and solid-state diffusion will be various orders of magnitude slower than diffusion through grain boundaries [38]. For example, in situ studies of mass transfer across a CO₂ hydrate film [22]

Table 2

Maximum water content permitted to prevent hydrate formation during transport of CO₂ stream from Esbjerg in Denmark to Gullfaks in Norway.

Composition of CO ₂ stream	Temperature [K]	Route to hydrate formation	Maximum allowable mole-fraction at different temperatures and pressures					
			50 bar	90 bar	130 bar	170 bar	210 bar	250 bar
y _{CO2} = 0.9950; y _{N2} = 0.0048; y _{CH4} = 0.0002 (the CO ₂ stream from Esbjerg)	274	Dew-point	0.001184	0.000746	0.000610	0.000567	0.000557	0.000559
		Hema'tic	0.000062	0.000039	0.000032	0.000030	0.000029	0.000029
	278	Direct	0.000914	0.000518	0.000396	0.000353	0.000337	0.000332
		Hema'tic	0.001590	0.000998	0.000811	0.000749	0.000733	0.000734
	274	Dew-point	0.000087	0.000055	0.000044	0.000041	0.000040	0.000040
		Direct	0.001319	0.000745	0.000565	0.000499	0.000475	0.000466
y _{CO2} = 0.95; y _{N2} = 0.05	274	Dew-point	0.001191	0.000753	0.000615	0.000568	0.000556	0.000555
		Hema'tic	0.000062	0.000039	0.000032	0.000030	0.000029	0.000029
	278	Direct	0.000724	0.000406	0.000306	0.000268	0.000253	0.000247
		Hema'tic	0.001599	0.001008	0.000819	0.000752	0.000732	0.000729
	274	Dew-point	0.000088	0.000055	0.000045	0.000041	0.000040	0.000040
		Direct	0.001044	0.000583	0.000438	0.000381	0.000358	0.000347
y _{CO2} = 0.90; y _{N2} = 0.10	274	Dew-point	0.001198	0.000761	0.000620	0.000570	0.000554	0.000551
		Hema'tic	0.000062	0.000040	0.000032	0.000030	0.000029	0.000029
	278	Direct	0.000657	0.000370	0.000279	0.000243	0.000228	0.000220
		Hema'tic	0.001608	0.001018	0.000826	0.000755	0.000730	0.000723
	274	Dew-point	0.000088	0.000056	0.000045	0.000041	0.000040	0.000040
		Direct	0.000948	0.000532	0.000399	0.000345	0.000322	0.000311

have found that CHD₃ tracer failed to replace methane even after 84 h in case of annealed hydrate film. So far, we will denote the diffusion of CO₂ at the surface as D_H and assign a value higher than the value for transport through the hydrate itself. On the outer limit of the interface, facing liquid water, the value is also uncertain since it is still lower than "bulk" liquid water due to the very long-range structuring effect of water hydrogen bonds. Based on Molecular Dynamics simulation of model systems we approximate the interface thickness to 10 Å and model the change in diffusion of CO₂ across the interface by a linear logarithmic approximation.

$$\ln D_{CO_2}(z) = \frac{\ln D_H - \ln D_L}{12} z + \ln D_L \quad (24)$$

which now is formulated in the direction of hydrate growth from liquid side of interface in positive z towards hydrate side.

In which the transport in this case is one-dimensional and not dependent on the curvature of a spherical crystal, or any other crystal morphology. z is the zero at the left-hand side (liquid) of the solid curve in Fig. 4(a), and 12 at the hydrate side of the solid curve of Fig. 4(a). Numerical differentiations of the concentration profile in Fig. 4(a) using Eqs. (23) and (24) results in the second derivatives plotted in Fig. 5 below for two different set of diffusivities for two different sets of D_H and D_L in Eq. (24). Fig. 5(a) corresponds to $D_H = 10^{-14} \text{ m}^2/\text{s}$ and $D_L = 10^{-8} \text{ m}^2/\text{s}$ and Fig. 5(b) corresponds to $D_H = 10^{-15} \text{ m}^2/\text{s}$ and $D_L = 10^{-11} \text{ m}^2/\text{s}$. The corresponding times for CO₂ to cross the interface and enter hydrate is calculated according to Eq. (25) to be $7.0 \cdot 10^{-5} \text{ s}$ for the first case (5 a) and $5.2 \cdot 10^{-3} \text{ s}$ for (5b). These are the relevant numbers that should enter J_0 in Eq. (15). But both of these sets of parameters are fairly unrealistic and slow for D_H . In the first example case this would correspond to a flux through interface which is trivially available from the hydrate density and the average velocity based on interface thickness and time to be $3.7 \cdot 10^{-5}$ molecules CO₂ per second and per Å². The corresponding number for the second set of examples for D_H and D_L gives $4.9 \cdot 10^{-7}$ molecules CO₂ per second and per Å². Corresponding numbers based on Eqs. (22) and (25) are also substantially faster; $4.1 \cdot 10^{-3}$ molecules CO₂ per second and per Å² and $2.0 \cdot 10^{-4}$ molecules CO₂ per second and per Å² respectively.

The integrated form of (22) reads:

$$t(C_H) - t(C_L) = \int_{C_L}^{C_H} \frac{dC(z)}{\left(-D_{CO_2}(z) \frac{\partial^2 [C_{CO_2}(z)]}{\partial z^2}\right)} \quad (25)$$

And the integrated form of equation (23) reads:

$$t(C_H) - t(C_L) = \int_{C_L}^{C_H} \frac{dC(z)}{\left(-\frac{\partial^2 [D_{CO_2}(z) C_{CO_2}(z)]}{\partial z^2}\right)} \quad (26)$$

2.5. Heterogeneous hydrate nucleation on water/gas interface

For heterogeneous hydrate formation in a system of 2 components and 3 phases there is only one free variable. A first order Taylor expansion from equilibrium is then written as:

$$G_{\text{non-equilibrium}}^H(T, P, \bar{x}) = G^{H, \text{Eq}}(T^{\text{Eq}}, P^{\text{Eq}}, \bar{x}^{\text{Eq}}) + \sum_r \frac{\partial G^H}{\partial x_r} \Big|_{P, T, x_{r'}} (x_r - x_r^{\text{Eq}}) + \frac{\partial G^H}{\partial P} \Big|_{T, \bar{x}} (P - P^{\text{Eq}}) + \frac{\partial G^H}{\partial T} \Big|_{P, \bar{x}} (T - T^{\text{Eq}}) \quad (27)$$

in which the reference state is the pressure, temperature equilibrium curve for the actual gas composition. Choosing freely any temperature on the equilibrium curve then the last term vanishes, and the non-equilibrium free energy needed for Eqs. (5) and (6) for phase transition according to Eq. (1) is evaluated according to equation (21).

In Fig. 6 we compare the results from Eqs. (25) and (26) for heterogeneous nucleation on CO₂/water interface for 3 temperatures (274 K, 275 K and 276 K) and a range of pressures from 20 to 70 bars. For these three temperatures, the equilibrium pressures are 13.6 bars for 274 K, 15.3 bars for 275 K and 17.5 bars for 276 K. Note that they are on a single line with the same linear gradient within the scale of the figure. The difference is mainly for the low driving force close to the lowest pressure of 20 bars which gives the shortest nucleation time for the highest driving force. For the 20 bar limit, the nucleation times are 3.0 ns (274 K, solid line), 3.7 ns (275 K, dashed line) and 5.4 ns (276 K, dash dot line). Corresponding calculations based on Eq. (26) is plotted in Fig. 6(b). Nucleation times for 20 bars pressure are 93.0 ns (274 K, solid line), 97.2 ns (275 K, dashed line) and 109.3 ns (276 K, dash dot line). For transport from the changing interface structure and up to critical radius, the final growth gradient derived from the final point of 3(a) as applied in (25) and (26) respectively, and in terms of Angstroms transported per time, were used as a constant value. This value might be at least an order of magnitude faster than reported values for Diffusivities of CO₂ through hydrate [35–37].

2.6. Homogeneous hydrate nucleation from dissolved carbon dioxide

Dissolved carbon dioxide will be able to form hydrate in a

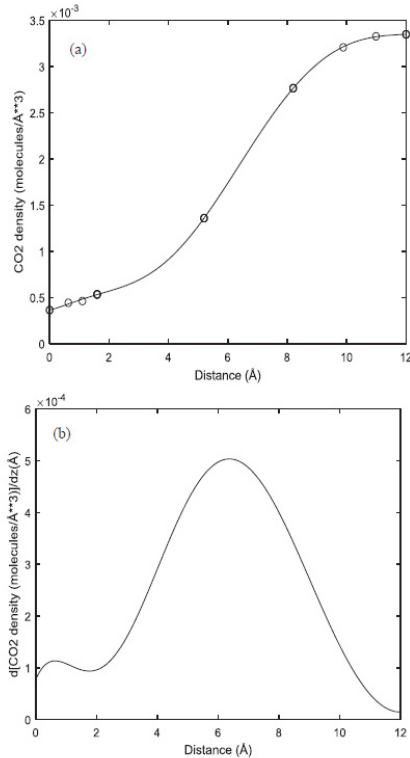


Fig. 4. (a) Average CO₂ density [26,35] as function of distance from solid hydrate, as sampled from Molecular Dynamics simulations. Right side of the solid curve is close to hydrate and right hand side is close to liquid water for the particular simulation set-up [26]. Only the solid curve, which represents a 1.2 nm thick interface, is considered to belong to the mass transport related to hydrate formation dynamics. Circles are points from the MD samplings and the curve is a smoothed fit (Eq. (21) and parameters in Table 3) needed to calculate the first and second order derivatives. (b) First derivative of concentration with respect to distance from liquid towards hydrate across the interface.

Table 3
Coefficients for the fitted model of interface concentrations of CO₂, Eq. (21).

Coefficients	
a_1	$3.649712 \cdot 10^{-4}$
a_2	$9.895427 \cdot 10^{-4}$
a_3	$1.091582 \cdot 10^{-2}$
a_4	$-1.112258 \cdot 10^{-1}$
a_5	$4.381832 \cdot 10^{-1}$
a_6	$-6.201765 \cdot 10^{-1}$
a_7	$2.896391 \cdot 10^{-1}$

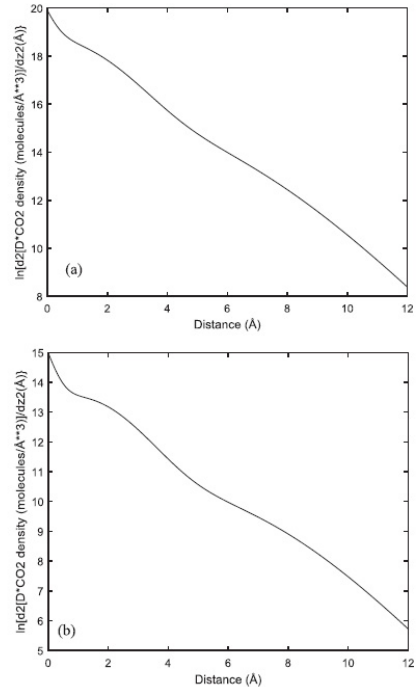


Fig. 5. Second derivative of the change in concentration times diffusivity coefficient through the interface between hydrate and aqueous solution as function of distance from the hydrate surface for two different sets of values for Diffusivity coefficients. (a) corresponds to $D_H = 10^{-14} \text{ m}^2/\text{s}$ and $D_L = 10^{-9} \text{ m}^2/\text{s}$ and the resulting time to cross the interface is $1.5 \cdot 10^{-8} \text{ s}$. (b) corresponds to $D_H = 10^{-15} \text{ m}^2/\text{s}$ and $D_L = 10^{-10} \text{ m}^2/\text{s}$ and the resulting time to cross the interface is $3.7 \cdot 10^{-7} \text{ s}$.

concentration region between the solubility of carbon dioxide in liquid water and the carbon dioxide concentration in water which is minimum to keep the hydrate stable. When the hydrate exists outside of equilibrium it is the lowest free energy in the system that will dictate the outside concentration on carbon dioxide in the liquid water. Strictly speaking, hydrate growth from carbon dioxide dissolved in water is also dominated by heterogeneous hydrate formation since the most beneficial situation is that dissolved carbon dioxide forms hydrate towards the original hydrate film formed from gas and water. Calculation of this nucleation process requires thermodynamic properties of CO₂ adsorbed on existing hydrate film and/or secondary adsorbed as trapped in water structures cause by hydrate crystal. Work is in progress on establishing these thermodynamic properties and associated transport properties (diffusion). This will be subject to a follow up work. It is also possible for water to nucleate homogeneously inside the water phase and this is the type of hydrate formation discussed here.

Comparison of the guest chemical potentials in Fig. 1(b) for carbon dioxide in gas with chemical potentials of carbon dioxide in solution in Fig. 7(b) illustrates the variations in resulting hydrate compositions.

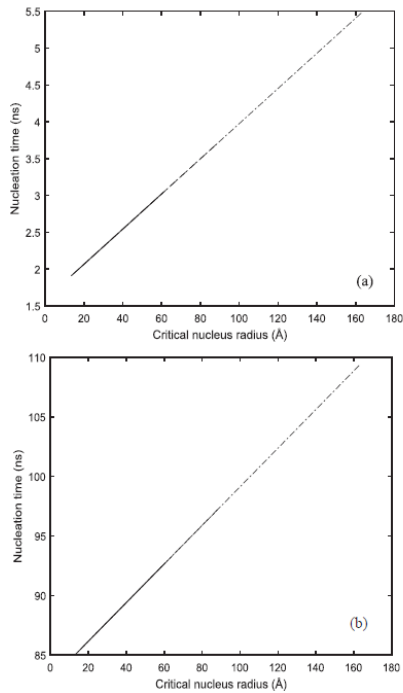


Fig. 6. (a). Calculated nucleation times for a pressure range of 20–70 bar for heterogeneous nucleation on CO₂/water interface for three different temperatures, 274 K (solid), 276 K (dash) and 285 K (dash dot) using Eq. (25). (b) Same results and notations as (a) but now with Eq. (26). These examples are based on Diffusivity coefficients (Eq. (24)) on hydrate side of 10⁻¹⁴ m²/s and on liquid side 10⁻⁷ m²/s.

Different chemical potentials for guest molecules in the phases they come from in building the hydrate results in different hydrate filling fractions and different hydrate free energies. This can be seen from the statistical-mechanical adsorption theory for hydrate used in most codes for hydrate equilibrium calculations. The statistical mechanical equilibrium theory in Kvamme & Tanaka [9] contains the same solution for rigid water lattice as is typically used in other hydrate equilibrium codes. But that version [9] also contain solutions for large guest molecules that affects the water vibrational movements. The canonical partition h_{ij} for a guest molecule j in cavity type i is given by:

$$h_{ij} = e^{-\beta[\mu_j + \Delta\mu_j]} \quad (28)$$

where β is the inverse of the universal gas constant times temperature. Chemical potential of guest molecules j in hydrate cavity i is equal to the chemical potential of molecules j in the co-existing phase it comes from. I.e. in Fig. 1, it is gas chemical potential while in Fig. 7, it is chemical potential is aqueous solution.

The corresponding filling fractions and mole-fractions of carbon dioxide in the hydrate is given by:

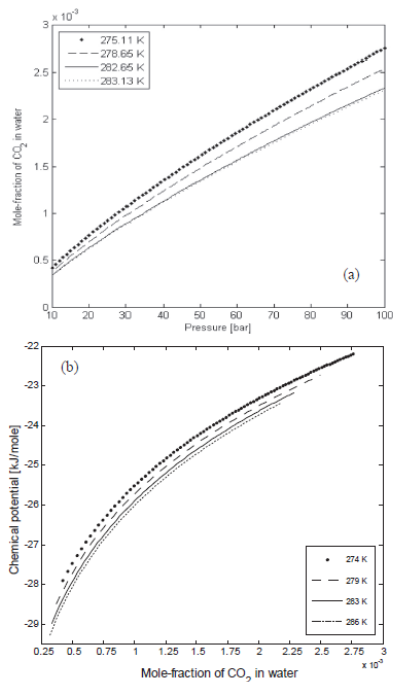


Fig. 7. (a) Calculated solubility of CO₂ in water for 4 different temperatures. Top curve (•) is for temperature of 275.11 K, next curve (–) for 278.65 K, then solid curve (–) for 282.65 K and lowest dot curve (·) is for 283.13 K. (b) CO₂ chemical potential is aqueous solutions as function of mole-fraction along the solubility curves in figure: top solid curve is for temperature of 275.11 K, next is for 278.65 K, then for 282.65 K and lowest solid curve is for 283.13 K.

$$\theta_{ij} = \frac{h_{ij}}{1 + \sum_j h_{ij}} \quad (29)$$

θ_{ij} is the filling fraction of component j in cavity type i

$$x_j^H = \frac{\theta_{large,j} \nu_{large} + \theta_{small,j} \nu_{small}}{1 + \theta_{large,j} \nu_{large} + \theta_{small,j} \nu_{small}} \quad (30)$$

where ν is the fraction of cavity per water for the actual cavity type as indicated by subscripts. Corresponding mole-fraction water is then given by:

$$x_{H_2O}^H = 1 - \sum_j x_j^H \quad (31)$$

and the associated hydrate free energy is then:

$$G^{(H)} = x_{H_2O}^H \mu_{H_2O}^H + \sum_j x_j^H \mu_j^H \quad (32)$$

where superscript H refers to hydrate phase. In view of CO₂ chemical potential variations between the heterogeneous case of carbon dioxide in Fig. 1, and the variations of CO₂ chemical potentials in Fig. 7(b). In

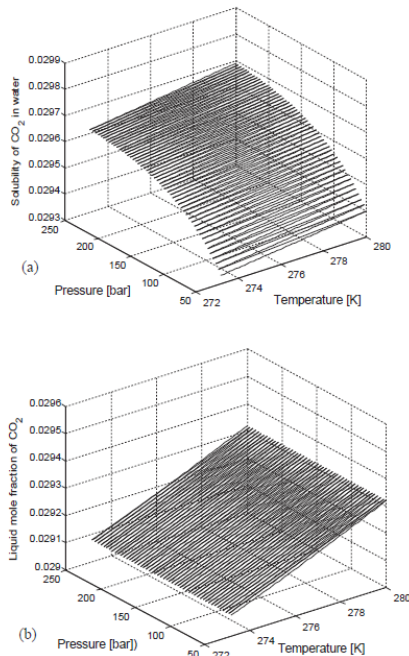


Fig. 8. (a) Solubility of carbon dioxide in water as function of temperature and pressure. (b) Minimum carbon dioxide in water for hydrate stability as function of temperature and pressure.

view of Eqs. (26) and (22) to (25) each of these hydrates will, by definition, be a unique phase because composition, density and free energy is different.

The experimental data in 8(b) is from different system in the sense that there is free gas in the experimental cell. That means that the hydrate formed will be heterogeneous hydrate at gas/water interface, heterogeneous hydrate formed towards initial hydrate film from liquid water side as well as homogeneous hydrate formation from carbon dioxide in water solution. Despite the differences between experimental conditions and the theoretical predictions from homogeneous hydrate formation, the agreement is strikingly good.

Fig. 9 shows when mole fraction of CO₂ in water increases, the nucleation time decreases as expected. And getting closer to the minimum mole-fraction of carbon dioxide in surrounding water for hydrate stability, nucleation size approaches infinity and practically implies that hydrate cannot form when the free energy benefit just balances the penalty. As such this is of course as expected. Also, when we compare different diffusion coefficients, it shows that nucleation time is substantially faster for the example with diffusivity of 10^{-11} m²/s than the example with diffusivity 10^{-12} m²/s. For hydrate formed on gas/water interface, this is the range of limiting transport diffusivities we expect based on comparison between experiments and results derived from Phase Field Theory (PFT) modelling [39]. In the worst case of low thermodynamic driving forces, nucleation times vary from less than seconds to few minutes.

2.7. Induction times

As discussed in the previous sections, critical nucleation size is on nano scale for the systems discussed in this work. This is as expected and also in accordance with nano to meso scale modelling published earlier from our research group [8] using Phase Field Theory (PFT). Onset of massive growth is frequently delayed by several factors – most often mass transport limitations. One example is illustrated in Fig. 10. For details of the experiment the reader is directed to references [38,39], but briefly, the experimental cell is constructed by cutting a plastic cylinder of diameter 4 cm and length 10 cm into two half cylinders. These two half cylinders are then squeezed together against a 4 mm thick plastic spacer which then gives an empty space for fluids surrounded by a medium that will not be affected by magnetic radiation, and as such the hydrate phase transition dynamics can be traced by Magnetic Resonance Imaging (MRI). In the current set-up and frequencies applied, the hydrogen proton spin in hydrate water will be invisible while liquid water will be visible. The resolution of the experiment is, however, limited to 300 μ m and will as such not be able to detect the nucleation stage and first stages of growth. As can be seen from Fig. 10, the time for onset of massive hydrate growth (induction time) is 100 h in this case. Temperature of the experiment is 3 °C and pressure is 1200 psia (83 bars). An induction time of 3.6–105 s seems far beyond any reasonable value for nucleation times. This is supported by Phase Field Theory modelling [26,39,40] which reproduce experimental observations. Interpretations of these results indicate a dominating (rate controlling) diffusivity in the order of 10^{-12} m²/s or faster if also flow is taken into account (interface stress and increased interface dynamics). Two plausible reasons for the onset of massive growth are capillary transport of methane (and corresponding methane accumulation) along the non-polar walls of the cell and rearrangements of the methane/hydrate/water surface as controlled by first and second laws of thermodynamics. This latter effect is something that happens on all scales – from nano [8,26,39,40] to visible scales as observed in experiments [41]. In absence of new building materials for hydrate growth the most stable hydrate regions will consume neighbouring less stable hydrate regions and as such result in regions of thinner hydrate films.

There is no similar experiment like that of Fig. 10 for CO₂ but there are a series of papers from AIST in Japan which have conducted experiments on water droplets surrounded by CO₂ liquid phase and attached at the end of the stainless steel pipeline and they indicate nucleation times in the order of 11 h at pressure of 3.9 MPa and temperature of 277 K. Uchida et al. [42] and another paper from Uchida also which used same experimental procedure [43] (Uchida et al.) but different in condition of pressure and temperature (due to higher pressure and lower temperature), indicate nucleation time around 20 h which is, as discussed above, really induction times. In their case it is onset of massive growth as they can observe through a microscope. Also, it shows that induction time delay is really caused from blocking due to hydrate film (net result of mass transport limitation) and it takes longer at higher pressure, because hydrate film forms very fast and repair by itself fast and easy due to dissociation of hydrate film from release of heat of new hydrate formation (hydrate formed in liquid water side). They did not consider that the primary mechanism is shear stress which associates with interfacial tension due to buoyancy force in upward direction from seawater into the CO₂ bubble, so maybe it can have effect on induction times too.

We can do some very rough and simple calculations for the case in which hydrate has created a film of certain thickness z on the CO₂/water interface. After hydrate has grown to a limit from the dissolved CO₂ in water, then several processes of rearrangements will happen due to the 1st and 2nd laws of thermodynamics. As consequence of the combined laws, hydrate sections of highest free energy may dissociate in favour of growth of the neighbouring hydrates of lower free energy. These types of processes have been examined in a number of papers

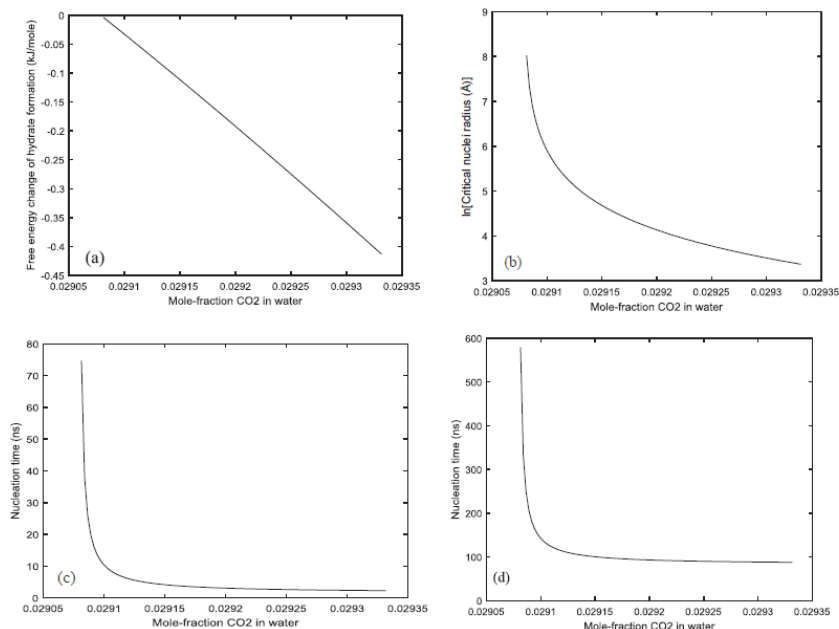


Fig. 9. (a) Free energy change of hydrate formation from dissolved CO₂ in water at 273.16 K and 50 bars as function of mole-fraction CO₂ in water. Minimum CO₂ in water for hydrate stability at this condition of temperature and pressure is a mole-fraction of 0.02079. (b) Corresponding critical radius as function of concentration in logarithmic scale. Maximum critical radius for lowest driving force in the plotted concentration range is 3062 Å and lowest critical radius is 29 Å. (c) Nucleation times based on Eq. (25). (d) Nucleation times based on Eq. (26). These examples are based on Diffusivity coefficients (Eq. (24)) on hydrate side of 10⁻¹⁴ m²/s and on liquid side 10⁻⁹ m²/s.

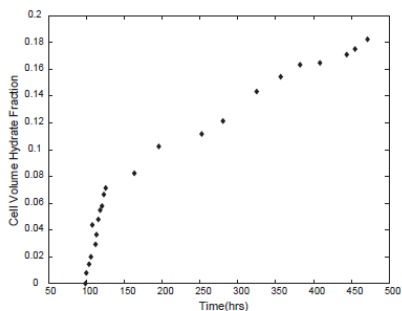


Fig. 10. Experimental data for methane hydrate formation from water and methane at 1200 psia (83 bars) and 3 °C [39].

which are compiled in the PhD thesis of Trygve Buanes [27]. But let's now consider a very simple model picture using Fick's law. The concentration of CO₂ on the CO₂ side is given by the thermodynamic state of the CO₂ phase. But CO₂ cannot be transported unless it has entered

the hydrate structure. If we, just as an approximation, assume almost full filling of large cavities and zero CO₂ in small cavities, the mole-fraction of CO₂ in water at that end is 0.12 and on the other end there will be a concentration of adsorbed CO₂ towards hydrate facing liquid water and outside of that a hydrate governed by minimum CO₂ concentration in water. Most studies on transport of guest molecules through hydrate are based on some cavity jumping model as discussed above. This is feasible since there will be empty cavities which will enable enough flexibility for cavity water molecules to open up and close again. Nevertheless – if it is the same mechanism that transports CO₂ all the way we may formulate within Fick's law:

$$\frac{\partial C}{\partial z} \approx \frac{\Delta C}{z} \tag{33}$$

where z is the thickness of the hydrate film and ΔC is the difference in concentration of the CO₂ in the hydrate at the CO₂ side of the hydrate and the liquid water concentration of CO₂. The hydrate is governed by limit of CO₂ as given by Fig. 8(b). Since this concentration difference is independent of the thickness z then the second derivative of (33) trivially becomes:

$$\frac{\partial^2 C}{\partial z^2} = -\frac{\Delta C}{z^2} \tag{34}$$

Substituting z for C on left hand side of Eq. (25) using (33), inserting (34) for the second derivative we end up with a very simple

approximate equation:

$$t(z) - t(z=0) = -\frac{z^2}{2D_{CO_2}} \quad (35)$$

With the lowest value for D_{CO_2} of $10^{-17} \text{ m}^2/\text{s}$, the solution of Eq. (40) gives 500 s to reach 100 nm thickness. Similar number for the highest value for D_{CO_2} of $10^{-15} \text{ m}^2/\text{s}$ indicated that it could take 5 s to reach the same thickness. To reach a micro-meter the corresponding numbers would be $5 \cdot 10^8$ s and $5 \cdot 10^2$ s. To reach 1 mm the numbers will be 1388 h and 13.88 h respectively. The real processes involved will of course be very much more complicated for these slow mass transport rates, and clearly, the coupling with heat transport dynamics related to formation of new hydrate on the liquid water side of the hydrate film. The heat released from new hydrate formation can partly dissociate some hydrate, although heat transport through liquid water is significantly faster than heat transport through hydrate. And since the existing hydrate layers first needs to be heated up to dissociation temperature for the actual pressure, the actual numbers involve solution of coupled mass and heat transport equations. Rather than trying to do this within the CNT framework it is better to go to more rigorous tools like for instance PFT [6–8,15,17].

Nevertheless – these simple calculations indicate that mass transport limitations through solid hydrate is frequently a kinetic limiting factor in the process leading to observable hydrates and associated induction times. These induction times are of course not rigorously defined. It depends on when hydrate is detectable by the applied monitoring technology – whether it is laser light, microscope, pressure change or any other monitoring technology with a specified resolution. But the key message is that nucleation is a nano scale process and that observable hydrates in an experiment depends on monitoring technology but are typically on long time scales as related to what is induction or onset of massive growth.

3. Discussion

Unless for very low thermodynamic driving forces or severe limitations in access to mass and/or heat transport, nucleation of hydrate is a nano scale phenomena in both time and size of critical nuclei sizes. In contrast to well defined physical definitions of nucleation, onset of massive growth (induction) depends on detection method (laser, pressure changes etc.). Mass transport limitation is a very typical reason for delays in onset of massive growth. In the absence of hydrodynamic shear forces, the formation of a hydrate film between hydrate former phase and water will rapidly turn into a substantial mass transport barrier which can delay induction times for several hours. Another frequent misunderstanding is that hydrate only forms one structure, despite the fact that the adsorption theory utilized in most hydrate estimation codes clearly shows that any variation in chemical potential of hydrate formers, or equivalently fugacity, will lead to differences in the cell partition functions for the various cavities in the hydrate structure. And since hydrate equilibrium cannot be achieved in any real flowing system, then, there is no rule that chemical potentials across phase boundaries are equal. In non-equilibrium systems, chemical potentials for each component in each phase is determined by local minimum free energy under constraints of mass and heat. As illustrated in previous sections, hydrate can form from various phases and homogeneous hydrate formation from hydrate formers in solution will result in an infinite number of hydrate phases in the concentration window between liquid solubility and concentrations determined by hydrate stability. Yet another aspect which is often not considered is the impact of solid surfaces. All minerals with distributed positive and negative charges on the various atoms will lead to extreme structuring of water with maximum densities that can reach in the order of 3 times liquid densities in the first adsorption layer [44]. This results in an average chemical potential of water substantially lower than liquid

water [44,45]. Practically, this means that the first few layers of adsorbed liquid water, roughly 1 nm distance from surface of mineral, is unable to make hydrate. But structured water can capture hydrate formers and lead to increased concentration of hydrate formers close to the mineral surfaces and lead to heterogeneous hydrate nucleation close to the mineral surfaces [46–48]. And what is very important for pipeline transport of CO₂ containing water is that water will prefer to adsorb on rust rather than drop out as liquid droplets. The kinetic analysis in this work has been based on classical nucleation theory for two reasons. One reason is the separation of the thermodynamic impact and the mass transport. This gives room for construction of mass transport models that are based on theoretical work and molecular simulations and still end up as numerically simple models which easily can be implemented as extensions of already existing hydrate risk evaluation software. As such the various calculations presented in this work can extend current hydrate risk evaluation codes to more routes for hydrate formation as well as associated hydrate nucleation times. This can result in cost savings because it is possible to exclude possible hydrate formations routes which are thermodynamically possible but appears to be kinetically unfavourable. It is also important to keep in mind that there are no non-physical empirical parameters in these calculations. There are approximate models for how we assume that diffusivity of carbon dioxide changes across the interface, and also concentration profiles across the interface which are fitted to a simple second order polynomial. It is possible to refine these models through more extensive use of data from MD simulations which are already available, and as referred to. And the extension over to MDT theory is also fairly trivial and expected to increase the accuracy of predictions. Nevertheless – even as it stands now, the models presented in this work is a step forward as compared to totally empirical correlations with limited or no capability for extrapolations.

4. Conclusion

In the open literature there are frequently misconceptions about hydrate nucleation times and induction times. In this work we have utilized a simple nucleation theory and classical thermodynamics to illustrate the nano-scale nature of nucleation. Typical nucleation sizes for the range of thermodynamic conditions that we have evaluated, which covers typical industrial hydrate problem temperatures and pressures varies around 2 nm in radius. Exceptions are situations of very low thermodynamic driving forces. And the small size of this initially stable hydrate may be the reason nucleation is often misinterpreted with induction times. A thin hydrate film formed on the interface between hydrate former phase and liquid water will represent a massive transport barrier for getting water and hydrate former in contact. Depending on the type of situation and possible influence of solid surfaces, this can lead to several hours of delay before onset of massive growth. Solid surfaces often play a role in these transitions over to induction (onset of massive growth) but also rearrangements of hydrate structures according to first and second laws of thermodynamics can lead to regions of thinner hydrate film locally. Solid surfaces like for instance, rusty surfaces on pipelines, play an active role in kicking out water which is transported as dissolved in gas. Conventional hydrate risk evaluation typically goes through a water dew-point calculation and the evaluate risk of hydrate formation between dropped out liquid water and hydrate formers. The tolerance limit for mole-fraction water in gas according this classical scheme may be in the order of 20 times higher than a criterion based on water adsorption on rust. It is also frequently assumed that only one hydrate structure and only one hydrate composition exist. As we have discussed in this work, a variety of hydrates will form because industrial and natural systems of hydrates can never reach equilibrium. Local chemical potential of water and hydrate formers is therefore subject to local free energy minimum as function of mass and heat transport constraints. This implies that the cavity partition functions in the statistical mechanical theory for

hydrate will vary with local chemical potentials for guest molecules. Hydrate forming from solution in water can form numerous hydrates as the concentration of hydrate former in the surrounding water changes. Estimated nucleation times for heterogeneous hydrate formation on water/CO₂ interface is on nanoseconds scale. Similar for homogeneous hydrate formation from dissolved CO₂ in water. Time for onset of massive hydrate growth, induction time, is delayed due to slow mass transport through hydrate films. Simple estimates indicate that these induction times may be several hours in the absence of hydrodynamic shear forces than can break these hydrate films.

Declaration of Competing Interest

The authors declared that there is no conflict of interest.

References

- [1] K. Qorbani, B. Kvamme, R. Olsen, Non-equilibrium simulation of hydrate formation and dissociation from CO₂ in the aqueous phase, *J. Nat. Gas Sci. Eng.* 35 (2016) 1555–1565.
- [2] B. Kvamme, et al., Effect of H₂S content on thermodynamic stability of hydrate formed from CO₂/N₂ mixtures, *J. Chem. Eng. Data* 62 (5) (2017) 1645–1658.
- [3] K. Qorbani, B. Kvamme, T. Kuznetsova, Simulation of CO₂ storage into methane hydrate reservoirs, non-equilibrium thermodynamic approach, *Energy Procedia* 114 (2017) 5451–5459.
- [4] B. Kvamme, et al., Thermodynamic implications of adding N₂ to CO₂ for production of CH₄ from hydrates, *J. Nat. Gas Sci. Eng.* 35 (2016) 1594–1608.
- [5] K. Qorbani, Non-equilibrium modelling of hydrate phase transition kinetics in sediments, Department of Physics and Technology, University of Bergen, Norway, 2017.
- [6] J.W. Gibbs, The Collected Works of J. Willard Gibbs, Thermodynamics vol. 1, (1928) 55–353.
- [7] B. Kvamme, et al., Kinetics of solid hydrate formation by carbon dioxide: Phase field theory of hydrate nucleation and magnetic resonance imaging, *Phys. Chem. Chem. Phys.* 6 (2004) 2327–2334.
- [8] G. Tegeze, et al., Multiscale approach to CO₂ hydrate formation in aqueous solution: phase field theory and molecular dynamics. Nucleation and growth, *J. Chem. Phys.* 124 (23) (2006) 234710.
- [9] B. Kvamme, H. Tanaka, Thermodynamic stability of hydrates for ethane, ethylene, and carbon dioxide, *J. Phys. Chem.* 99 (18) (1995) 7114–7119.
- [10] T. Kuznetsova, B. Kvamme, Grand canonical molecular dynamics for TIP4P water systems, *Mol. Phys.* 97 (3) (1999) 423–431.
- [11] B. Kvamme, Feasibility of simultaneous CO₂ storage and CH₄ production from natural gas hydrate using mixtures of CO₂ and N₂, *Can. J. Chem.* 93 (8) (2015) 897–905.
- [12] B. Kvamme, Thermodynamic limitations of the CO₂/N₂ mixture injected into CH₄ hydrate in the Iginik Sikumi field trial, *J. Chem. Eng. Data* 61 (3) (2016, 2016,) 1280–1295.
- [13] B. Kvamme, et al., Hydrate formation during transport of natural gas containing water and impurities, *J. Chem. Eng. Data* 61 (2) (2016) 936–949.
- [14] S.A. Aromada, New Concept for Evaluating the Risk of Hydrate Formation during Processing and Transport of Hydrocarbons, Master's Thesis The University of Bergen, Norway, 2017.
- [15] G. Soave, Equilibrium constants from a modified Redlich-Kwong equation of state, *Chem. Eng. Sci.* 27 (6) (1972) 1197–1203.
- [16] S.D. Larson, Phase studies of the two-component carbon dioxide-water system, involving the carbon dioxide hydrate, Ph. D. Thesis Univ. of Michigan, 1955.
- [17] K. Ohgaki, Y. Makihara, K. Takano, Formation of CO₂ hydrate in pure and sea waters, *J. Chem. Eng. Jpn.* 26 (5) (1993) 558–564.
- [18] J.P. O'Connell, A.V. Sharygin, R.H. Wood, Infinite dilution partial molar volumes of aqueous solutes over wide ranges of conditions, *Ind. Eng. Chem. Res.* 35 (8) (1996) 2808–2812.
- [19] B. Kvamme, et al., Hydrate phase transition kinetics from Phase Field Theory with implicit hydrodynamics and heat transport, *Int. J. Greenhouse Gas Control* 29 (2014) 263.
- [20] Pihvi-Helina Kivela, et al., Phase field theory modeling of methane fluxes from exposed natural gas hydrate reservoirs, *AIChE J.* 58 (1) (2012) 351–363.
- [21] K. Balg, Nano to Micro Scale Modeling of Hydrate Phase Transition Kinetics, University of Bergen, 2017.
- [22] B. Kvamme, Droplets of dry ice and cold liquid CO₂ for self-transport of CO₂ to large depths, *Int. J. Offshore Polar Eng.* 13 (2003) 139.
- [23] B. Kvamme, Kinetics of hydrate formation from nucleation theory, *Int. J. Offshore Polar Eng.* 12 (2002) 256.
- [24] B. Kvamme, Initiation and growth of hydrate, *Ann. New York Acad. Sci.* (2000) 496–501.
- [25] B. Kvamme, A. Lund, T. Hertzberg, The influence of gas-gas interactions on the Langmuir constants for some natural gas hydrates, *Fluid Phase Equilib.* 90 (1) (1993) 15–44.
- [26] A. Svdandal, Modeling Hydrate Phase Transitions using Mean-Field Approaches, University of Bergen, 2006.
- [27] T. Buanes, B. Kvamme, A. Svdandal, Two approaches for modelling hydrate growth, *J. Math. Chem.* 46 (3) (2009) 811–819.
- [28] T. Buanes, B. Kvamme, A. Svdandal, Computer simulation of CO₂ hydrate growth, *J. Cryst. Growth* 287 (2) (2006) 491–494.
- [29] B. Kvamme, S.A. Aromada, Risk of hydrate formation during the processing and transport of troll gas from the north sea, *J. Chem. Eng. Data* 62 (7) (2017) 2163–2177.
- [30] B. Kvamme, S.A. Aromada, Alternative routes to hydrate formation during processing and transport of natural gas with a significant amount of CO₂: sleeper gas as a case study, *J. Chem. Eng. Data* (2018).
- [31] Norwegian Petroleum. Carbon Capture and Storage. 10 June 2018; Available from: < <http://www.norskepctroleum.no/en/environment-and-technology/carbon-capture-and-storage> > .
- [32] C. Eickhoff, et al., GATEWAY: Developing a Pilot Case aimed at establishing a European infrastructure project for CO₂ transport. D4.1 Pilot Case Definition, Projected funded by European Union, 2017.
- [33] O. Kaarstad, C-W. Hustad, CO₂-Supply Report, Elsam A/S – Kinder Morgan CO₂ Company L.P. – New Energy/Statoll Asa, 2003.
- [34] Orkla Engineering, CO₂ Rock Caverns Storage Top Side Equipment Orkla Engineering on behalf of Statoil F&T KST, 2003.
- [35] A. Svdandal, T. Kuznetsova, B. Kvamme, Thermodynamic properties and phase transitions in the H₂O/CO₂/CH₄ system, *Fluid Phase Equilib.* 246 (1–2) (2006) 177–184.
- [36] A. Falenty, A. Salamatin, W. Kuhs, Kinetics of CO₂-hydrate formation from ice powders: data summary and modeling extended to low temperatures, *J. Phys. Chem. C* 117 (16) (2013) 8443–8457.
- [37] A. Salamatin, et al., Guest migration revealed in CO₂ clathrate hydrates, *Energy Fuels* 29 (9) (2015) 5681–5691.
- [38] B. Peters, et al., Path sampling calculation of methane diffusivity in natural gas hydrates from a water-vacancy assisted mechanism, *J. Am. Chem. Soc.* 130 (51) (2008) 17342–17350.
- [39] B. Kvamme, et al., Storage of CO₂ in natural gas hydrate reservoirs and the effect of hydrate as an extra sealing in cold aquifers, *Int. J. Greenhouse Gas Control* 1 (2007) 236.
- [40] T. Buanes, Mean-Field Approaches Applied to Hydrate Phase Transition, PhD thesis University of Bergen, 2006.
- [41] Y.F. Makogan, Hydrates of Hydrocarbons, PennWell Books, 1997.
- [42] T. Uchida, et al., Microscopic observations of formation processes of clathrate-hydrate films at an interface between water and carbon dioxide, *J. Cryst. Growth* 204 (3) (1999) 348–356.
- [43] T. Uchida, et al., CO₂ hydrate film formation at the boundary between CO₂ and water: effects of temperature, pressure and additives on the formation rate, *J. Cryst. Growth* 237 (2002) 383–387.
- [44] B. Kvamme, T. Kuznetsova, P.-H. Kivela, Adsorption of water and carbon dioxide on hematite and consequences for possible hydrate formation, *Phys. Chem. Chem. Phys.* 14 (13) (2012) 4410–4424.
- [45] B. Kvamme, et al., Can hydrate form in carbon dioxide from dissolved water? *Phys. Chem. Chem. Phys.* 15 (2013) 2063.
- [46] M.H. Austrheim, Evaluation of Methane and Water Structure at a Hematite Surface - A Hydrate Prevention Perspective, 2017.
- [47] A.B. Nesse Knarvik, Examination of water and methane structuring at a hematite surface: in the presence of MEG, 2017.
- [48] N. Mohammad, Heterogeneous Hydrate Nucleation on Calcite [1014] and Kaolinite [001] Surfaces: A Molecular Dynamics Simulation Study, 2016.

Paper 8

Hydrate nucleation, growth and induction

By

Bjørn Kvamme, S. Aromada, Navid Saeidi, T. Hustache, and Petter Gjerstad

Published in

ACS Omega, 2020, 5(6): 2603-2619



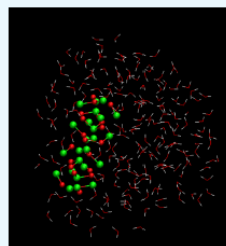
Cite This: ACS Omega 2020, 5, 2603–2619

Article

Hydrate Nucleation, Growth, and Induction

Bjørn Kvamme,^{*,†,‡} Solomon Aforkoghene Aromada,^{‡,§} Navid Saeidi,[§] Thomas Hustache-Marmou,^{||} and Petter Gjerstad[‡][†]State Key Laboratory of Oil and Gas Reservoir Geology and Exploitation, Southwest Petroleum University, Xindu Road No.8, Chengdu, Sichuan 610500, China[‡]Department of Physics and Technology, University of Bergen, Allegaten 55, 5007 Bergen, Norway[§]Department of Environmental Engineering, University of California Irvine, Henry Samueli School of Engineering, 4200 Engineering Gateway Building, Irvine, California 92697-3975, United States^{||}Department of Fluid Mechanics, E.N.S.E.E.I.H.T Engineering School, 2 rue Charles Camichel, 31500 Toulouse, France

ABSTRACT: The first stage of any phase transition is a dynamic coupling of transport processes and thermodynamic changes. The free energy change of the phase transition must be negative and large enough to also overcome the penalty work needed for giving space to the new phase. The transition from an unstable situation over to a stable growth is called nucleation. Hydrate formation nucleation can occur along a variety of different routes. Heterogeneous formation on the interface between gas (or liquid) and water is the most commonly studied. A hydrate can also form homogeneously from dissolved hydrate formers in water, and the hydrate can nucleate toward mineral surfaces in natural sediments or a pipeline (rust). A hydrate particle's critical size is the particle size needed to enter a region of stable growth. These critical sizes and the associated nucleation times are nanoscale processes. The dynamics of the subsequent stable growth can be very slow due to transport limitations of hydrate-forming molecules and water across hydrate films. Induction times can be defined as the time needed to reach a visible hydrate. In the open literature, these induction times are frequently misinterpreted as nucleation times. Additional misunderstandings relate to the first and second laws of thermodynamics and the number of independent thermodynamic variables. It is not possible to reach thermodynamic equilibrium in systems where hydrates form in a pipeline or in sediments. Finally, there are common misconceptions that only one type of hydrate will form. In a non-equilibrium situation, several hydrates will form, depending on which phases the hydrate formers and water come from. In this paper, we utilize a simple nucleation theory to illustrate nucleation and growth of some simple hydrates in order to illustrate the non-equilibrium nature of hydrates and the fast nucleation times. To illustrate this, we apply thermodynamic conditions for a real pipeline transporting natural gas from Norway to Germany. This specific example also serves as a case for illustration of the possible impact of rusty pipeline surfaces in kicking out water from the gas. Specifically, we argue that the tolerance limit for water concentration according to current industrial hydrate risk practice might overestimate the tolerance by a factor of 20 as compared to tolerance concentration based on adsorption on rust.



1. INTRODUCTION

The possible formation of hydrates is always a concern in natural gas processing and transport. During processing of natural gas, the conditions may be down to $-22\text{ }^{\circ}\text{C}$ at around 70 bar, like in the processing of gas from the Troll offshore, Norway. However, temperatures may be as low as $-70\text{ }^{\circ}\text{C}$ in plants with significant amounts of components from ethane and higher hydrocarbons. Transport of natural gas in the North Sea is normally at temperatures higher than $0\text{ }^{\circ}\text{C}$ but typically below $6\text{ }^{\circ}\text{C}$. Pressures during transport can be very high but are normally below 300 bar. Common to all these situations is that the conditions are well within hydrate-forming conditions in terms of temperature and pressure. Also, since both temperature and pressure are always given locally by process control and/or hydrodynamic flow, the system can never reach thermodynamic equilibrium. Even for the simplest system of pure methane in contact with water, this is easy to verify by summing up all

independent thermodynamic variables and subtracting conservation laws and conditions of equilibrium. This ends up with a maximum of one thermodynamic variable that can be specified for equilibrium to be achieved. This is of course well known to all since the methane equilibrium curve is always measured by keeping either P or T fixed and then monitoring the hydrate phase transition through slow variation of the other variable. A typical result comes out as plotted in Figure 1 below.

There is nothing unique about this figure, and there are numerous hydrate equilibrium codes worldwide that can calculate that curve. The reason for plotting it in the context of this paper is actually Figure 1b, which illustrates the chemical potential of water and the hydrate former as well as the free

Received: September 4, 2019

Accepted: December 6, 2019

Published: February 4, 2020

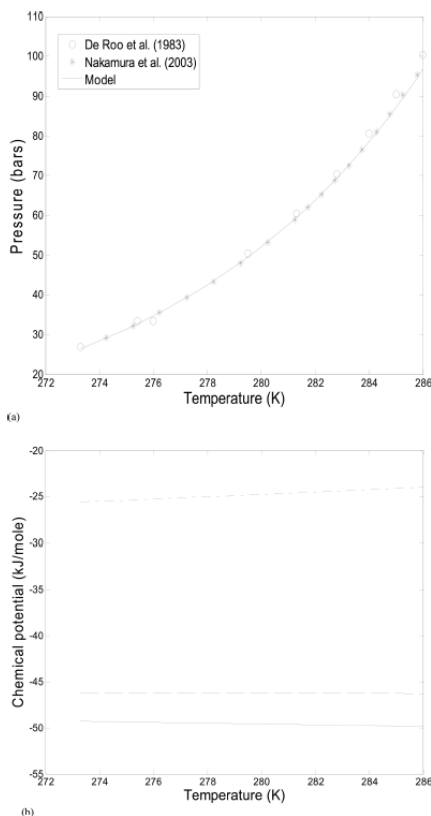


Figure 1. (a) Methane hydrate stability limits as a function of temperature and pressure. Solid curve is calculated; asterisks (*) are experimental data from Nakamura et al.,¹ and circles are experimental data from De Roo et al.² (b) Chemical potential for methane along the stability limit curve in panel (a) (dashed dotted line), chemical potential of water (solid line), and molar free energy (dashed line).

energy along the hydrate equilibrium curve. In general, in a non-equilibrium system, there is no rule that controls the chemical potential of each component to be equal across phase boundaries. On the contrary, it is minimum free energy under constraints of mass and energy conservation that controls the distribution of phases and phase compositions. Then, since chemical potentials of hydrate formers in various phases can be different, various routes to hydrates can result in different forms. In the simple system of a hydrate forming from water and methane, in the absence of solid surface effects, hydrate formation will then be on the interface as formulated in eq 1 below in terms of free energy change.

$$\Delta G^{(H_1)} = \left[x_{\text{H}_2\text{O}}^{\text{H}_1} (\mu_{\text{H}_2\text{O}}^{\text{H}_1}(T, P, \bar{x}^{\text{H}_1}) - \mu_{\text{H}_2\text{O}}^{\text{water}}(T, P, \bar{x})) + \sum_j x_j^{\text{H}_1} (\mu_j^{\text{H}_1}(T, P, \bar{x}^{\text{H}_1}) - \mu_j^{\text{gas}}(T, P, \bar{y}^{\text{gas}})) \right] \quad (1)$$

where μ denotes the chemical potential. Subscripts H₂O and j denote water and hydrate formers, respectively. The superscript H_{*j*} is the hydrate phase, the superscript water is the liquid water phase, and the superscript gas is a separate hydrate former phase (gas, liquid, or supercritical). Mole fractions in the liquid are denoted as x , and mole fractions in the hydrate are denoted as x with a superscript H. y is the mole fraction in the separate hydrate former phase. For all of these mole fractions, the arrow on top means a vector of mole fractions. T and P are the temperature and pressure, respectively, and G is the molar free energy. The Δ symbol denotes a change in free energy. The hydrate formed through this particular route is denoted as H₁. This interface hydrate will rapidly grow to a solid membrane with low diffusivity for transporting gas molecules toward contact with water on the lower side of the hydrate film. Parallel to this mass transport-limited continuation of the H₁ hydrate, another hydrate can grow from the dissolved hydrate former in water.

$$\Delta G^{(H_2)} = \left[x_{\text{H}_2\text{O}}^{\text{H}_2} (\mu_{\text{H}_2\text{O}}^{\text{H}_2}(T, P, \bar{x}^{\text{H}_2}) - \mu_{\text{H}_2\text{O}}^{\text{water}}(T, P, \bar{x})) + \sum_j x_j^{\text{H}_2} (\mu_j^{\text{H}_2}(T, P, \bar{x}^{\text{H}_2}) - \mu_j^{\text{water}}(T, P, \bar{y})) \right] \quad (2)$$

The chemical potential of methane in various phases (gas, dissolved in water) is not necessarily the same in a non-equilibrium situation. In a non-equilibrium situation, the equilibrium conditions are replaced by local minimum free energy under constraints of mass conservation. The composition of this hydrate, H₂, will be different. This will be discussed in more detail later, but it is trivially given by the difference in cavity partition functions. For hydrate modeling tools using the fugacity of the hydrate-forming molecule times the Langmuir constant, this will appear through the difference in the fugacity of the hydrate former. In the formulations of Kvamme & Tanaka,³ it appears through the chemical potential of the hydrate former in the cavity partition function.

Another possibility is that dissolved methane up-concentrates as it adsorbs toward the initial hydrate film H₁ and forms a hydrate heterogeneously there.

Theoretically, another possible route is from water dissolved in gas as given by eq 3 below.

$$\Delta G^{(H_3)} = \left[x_{\text{H}_2\text{O}}^{\text{H}_3} (\mu_{\text{H}_2\text{O}}^{\text{H}_3}(T, P, \bar{x}^{\text{H}_3}) - \mu_{\text{H}_2\text{O}}^{\text{gas}}(T, P, \bar{x}^{\text{gas}})) + \sum_j x_j^{\text{H}_3} (\mu_j^{\text{H}_3}(T, P, \bar{x}^{\text{H}_3}) - \mu_j^{\text{gas}}(T, P, \bar{y}^{\text{gas}})) \right] \quad (3)$$

Mass transport will be a substantial limitation for this particular route, and transporting hydrate formation heat through non-polar gas is also a substantial rate limitation. A limited amount of hydrate can, however, be formed from water

dissolved in gas if water condenses out on the already existing hydrate film. It is possible to estimate the theoretical amount of water that can condense out in this way by assuming a quasi-equilibrium situation. This calculation involves an estimation of how much water in the gas can be in quasi-equilibrium with hydrate water in H_1 . A mass balance between the actual water content in gas and the quasi-equilibrium content of water in gas (with reference to water in H_1) will give a theoretical maximum hydrate film for water in gas.

Some solid surfaces, for instance, stainless steel, consist of neutral atoms and will not have any significant thermodynamic effect on the water structure. Pipelines for transport of hydrocarbons are typically rusty even before they are installed. Ordinary rust is a mixture of iron oxide, FeO , hematite, Fe_2O_3 , and magnetite, Fe_3O_4 . These three minerals will have different charges on the oxygens and irons and, correspondingly, different structuring effects on adsorbed water. The density of the first layer of adsorbed water on hematite may be three times higher than that of liquid water. The chemical potential of adsorbed water on hematite is substantially lower than that of liquid water. A typical industrial example is the impact of rusty pipeline walls on hydrate formation, as discussed in the next section for a relevant pipeline transporting natural gas from Norway to Germany.

However, even for the simple system of one hydrate former and water, we now end up with three different hydrates, so the number of degrees of freedom is -1 and the conditions of both temperature and pressure are highly over-determined in terms of the possibility for equilibrium.

Kinetic models for phase transitions are implicit dynamic couplings between mass transport of building blocks, associated heat transport, and thermodynamic control. This is also the case for the various routes to hydrate formation. In the classical nucleation theory, these couplings are very transparent. Multicomponent diffuse interface theory (MDIT)^{4,5} reduces to the classical nucleation theory when the interface thickness approaches zero. Classical nucleation theory (CNT) can be expressed as

$$J = J_0 e^{-\beta \Delta G^{\text{Total}}} \quad (4)$$

where J_0 is the mass transport flux supplying building blocks for the hydrate growth. For the phase transition in eq 1, it will be the supply of methane to the interface growth. In eq 2, it will be the diffusion rate for dissolved methane to crystal growth from aqueous solution. Lastly, in eq 3, the rate-limiting mass transport is the supply of water by diffusion through gas. For eqs 1 and 2, transport through the structured water interface between the hydrate and surrounding liquid water will normally be the rate-limiting mass transport. The original classical nucleation theory is limited by a classical prefactor J_0 for single pure-component transport. As such, it is mainly limited to gas/liquid systems with very small or theoretically not significant interfaces.

The meaning of J_0 is still the same as in other systems, but it will be the limiting mass transport flux through the interface between the old phase and the new phases. In the case of hydrate nucleation and growth, a hydrate core will always be covered with water. For heterogeneous nucleation on the liquid water/gas interface, the capillary waves as well as capillary forces between hydrate water and liquid water will ensure that the hydrate core during nucleation is covered by liquid water. The actual rate-limiting transport in J_0 is therefore the transport of hydrate-forming molecules across an interface of gradually more

structured water from the liquid side toward the hydrate side. The units of J_0 are $\text{mol}/\text{m}^3 \text{ s}$ for homogeneous hydrate formation in eqs 2 and 3 and $\text{mol}/\text{m}^2 \text{ s}$ for heterogeneous hydrate formation in eq 1. J has the same units as J_0 . β is the inverse of the gas constant times the temperature, and ΔG^{Total} is the molar free energy change of the phase transition. This molar free energy consists of two contributions. The phase transition free energy as described by eqs 2 to 3, as examples, and the penalty work of pushing aside old phases. Since the molar densities of liquid water and hydrate are reasonably close, it is a fair approximation to multiply the molar free energy of the phase transition with the molar density of the hydrate times the volume of the hydrate core. The push work penalty term is simply the interface free energy times the surface area of the hydrate crystal. Lines below the symbols were used to indicate extensive properties (unit, Joules)

$$\underline{\Delta G}^{\text{Total}} = \underline{\Delta G}^{\text{Phase transition}} + \underline{\Delta G}^{\text{Pushwork}} \quad (5)$$

For the simplest possible geometry of a crystal, which is a sphere, with radius R , we then get

$$\underline{\Delta G}^{\text{Total}} = \frac{4}{3} \pi R^3 \rho_N^H \Delta G^{\text{Phase transition}} + 4 \pi R^2 \gamma \quad (6)$$

where ρ_N^H is the molar density of the hydrate and γ is the interface free energy between the hydrate and surrounding phase. A small methane hydrate core growing on the surface of water is floating since the density of methane hydrate is lower than that of liquid water. Crystals below the critical size (and likely larger) will also be covered with water toward the gas side due to capillary forces and water adsorption.

The solution for maximum free energy and transition over to stable growth is found by differentiation of eq 6 with respect to R . The critical core size is indicated by the superscript * on R

$$R^* = - \frac{2\gamma}{\rho_N^H \Delta G^{\text{Phase transition}}} \quad (7)$$

For formation of the methane hydrate at various pressures inside the hydrate-forming regions, the critical hydrate core radius is typically between 18 and 22 Å for temperatures in the range of 274 and 278 K and pressures above 150 bar (see Figures 4 and 7 for examples of interface hydrate nucleation according to phase transition (eq 1)).

The implicit coupling to heat transport goes through the relationship between enthalpy changes and free energy changes. Equations 4 and 5 give a direct connection to the enthalpy change through the standard thermodynamic relationship

$$\frac{\partial \left[\frac{\underline{\Delta G}^{\text{Total}}}{RT} \right]_{p, \bar{N}}}{\partial T} = - \left[\frac{\underline{\Delta H}^{\text{Total}}}{RT^2} \right] \quad (8)$$

where $\underline{\Delta H}^{\text{Total}}$ is the enthalpy change due to the phase transition and the associated push work penalty.

$$\dot{Q} \propto \underline{\Delta H}^{\text{Total}} \quad (9)$$

Figure 2 illustrates the enthalpy of hydrate formation as calculated from the thermodynamic models for free energy based on residual thermodynamics and the use of eq 8. For details, see the studies of Kvamme³³ and Kvamme et al.³⁴

Heat is mainly transported by conduction, convection, and radiation. Heat transport through liquid water and hydrate is 2 to 3 orders of magnitude faster than mass transport.¹⁵ The

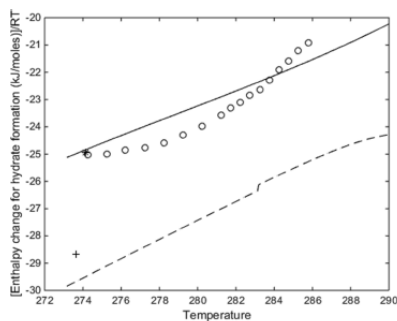


Figure 2. Calculated enthalpies of hydrate formation, in dimensionless units, along the pressure–temperature hydrate stability limit curve for CH₄. Solid line was obtained using eq 8. Circles are data from Nakamura et al.¹⁴ for the CH₄ hydrate as calculated using a Clapeyron approach. The point (*) is a measured point from calorimetry experiments from Kang et al.³⁵ Dashed curve is the calculated enthalpy of hydrate formation from eq 8 for the CO₂ hydrate in dimensionless units. The plus symbol (+) is measured by calorimetry by Kang et al.³⁵

details of eq 9 are not important in this work since the heat transport is not kinetically rate-limiting for the systems discussed here. The heat transport is of course proportional to the heat release (associated with the phase transitions), as expressed through eq 9 and coupled to eq 8 for the various hydrate formation routes in eqs 1–3. For phase transitions according to eqs 1 and 2, the heat transport is very fast and there is no rate-limiting factor in the phase transition kinetics. For eq 3, as mentioned above, there are limitations in mass transport due to low concentrations of water in the gas. However, the heat transport limitations of getting rid of the heat of hydrate formation given by eq 8 and various transport mechanisms through a non-polar gas in eq 8 are also critical.

This brings the discussion over to the title of the paper. There appears to be a lot of confusion in terms of the physical meaning of nucleation, growth, and induction. Equation 7 above defines the transition over to steady growth in classical nucleation theory. Onset of massive growth, as observed by induction times, is a function of many factors, but normally simple mass transport limitations. The purpose of this paper is to shed more light on this, and that is also why a simple theory is chosen. We use mostly more advanced concepts^{5–8} in which the three components are much more implicitly integrated. However, classical nucleation theory provides a more visible distinction between the various contributions and serves better to illustrate that hydrate nucleation is really a nanoscale phenomenon and that the observed long induction times are a result of mainly mass transport limitations through hydrate films and/or a non-equilibrium situation that leads to dissociation of hydrates through contact with under-saturated phases.

The paper is organized as follows. Various routes to hydrate nucleation are discussed in the next section. This is followed by a section where a specific pipeline for transport of natural gas from Norway to Germany, Europipe II, is discussed in terms of hydrate risk evaluation based on the different routes to hydrate nucleation. The following section contains numerical calculations of the most relevant hydrate nucleation and growth paths. The final sections are a discussion of the results and the

various stages of hydrate formation kinetics followed by our conclusions.

2. ROUTES TO HYDRATE FORMATION IF WATER DROPS OUT

Thermodynamically, three routes to hydrate formation based on the modes by which water is made available have been identified.^{9–11} The first route is the dew-point route, which is the classical route currently considered and used for examining the risk of hydrate formation in industrial systems like during natural gas processing and pipeline transport. In this approach, the first step is calculation of the water dew-point concentration for the actual gas mixture at local conditions of pressure and temperature. If the actual water content in the gas is higher than the calculated dew-point concentration of water and the temperature and pressure are inside hydrate formation conditions, then there is a risk of hydrate formation. In this case, the gas is normally dried to below dew-point concentration.

Adding methanol, glycols, or other thermodynamic inhibitors at critical points for possible hydrate formation is frequently used. These thermodynamic inhibitors will change the hydrate stability region in the temperature–pressure projection of independent thermodynamic variables. Methanol will to a larger degree dissolve in gas as compared to glycols. This will shift the dew point, which is now a water/methanol dew point. Condensation of water/methanol droplets will therefore have a unique hydrate stability limit for the specific mole fraction of methanol in water that is shifted to higher pressures for hydrate formation. Injection of glycols are frequently preferred because glycols also have a corrosion-inhibiting effect and they are efficient in preventing hydrates from forming toward pipeline walls, as discussed below.

Water wetting solid surfaces gives rise to a second route toward hydrate formation. Stainless steel is neutral since it consists of uncharged atoms. However, normally, stainless steel is far too expensive for long transport lines. Plastic-covered pipelines are also neutral in terms of water adsorption. Any form for rust will be water-wetted due to the atomic charge distributions in the rust surface. Steel pipelines are normally stored outside before they are eventually transported and mounted together. The first rust that forms will normally be dominated by magnetite (Fe₃O₄) because of ready access to oxygen from air. Then, hematite (Fe₂O₃) and iron oxide (FeO)⁹ will also form. Hematite is the thermodynamically most stable of these, and the other rust forms will gradually reorganize over to a dominating fraction of hematite. In this work, we therefore use hematite as a model for rust. The distribution of charged oxygens and irons in the hematite surface helps in making the surface very efficient for water adsorption. The average chemical potential for water adsorbed on hematite is very low^{8,13,28} and far lower than the liquid water chemical potential. A hydrate can therefore not form from the first adsorbed water layers. The density of this first water layer is in the order of three times the liquid water density.²⁸ This is very typical for water adsorption on minerals, and experimental data are available for a variety of minerals like calcite and kaolinite, but we could not find experimental data for water adsorbed on hematite. Beyond the first layer, the density oscillates and the density minima outside of roughly five water molecules serve as traps for adsorbing hydrate formers in structured water.

Some minerals, like calcite and kaolinite, can adsorb CO₂ directly, but there is no evidence that CO₂ adsorbs directly on hematite, in competition with water. However, CO₂, CH₄, and

other small molecules that form gas can up-concentrate in structured water and/or condense on water films that have been generated by adsorption on hematite. From a mathematical point of view, an adsorbed water film represents an infinite number of phases because the density and structure of water change continuously. However, even if we only consider the adsorbed water as one phase, it is obvious that the number of independent thermodynamic variables is significantly higher than those obtained from conservation laws and conditions of equilibrium. Water drops out as a liquid or is adsorbed, and subsequent hydrate formation leads to systems that can never lead to equilibrium since the number of phases will never change in a continuous flow situation with a new supply of mass to all phases. In summary, the alternative route to hydrate formation involves water adsorbing on hematite, and the water layers beyond roughly five water molecules forming on the hematite surface can trap hydrate formers, or liquids like water further from the hematite surface make hydrate with hydrate formers from gas in the usual way like any liquid water phase. It should be kept in mind that the visible rust on pipelines that are being shipped out for mounting onto an offshore (or onshore) pipeline has rugged surfaces with visible peaks of rust heights. The relative adsorption surface per geometric pipeline surface is therefore huge on a molecular adsorption scale.

It is thermodynamically possible to form hydrates directly^{8,12} from water dissolved in gas. The mass and heat transport limitation of this "direct route" is, however, substantial. Collecting in the order of 150 water molecules from a very dilute non-polar solution is a mass transport challenge. Restructuring water molecules around non-polar solvent molecules releases heat. A second challenge is to get rid of the released heat. Heat transport through non-polar gas is extremely slow. It is much faster to redistribute the released heat through the structured water, and a re-dissociation of the hydrate cluster is a likely result.

If surface stresses from flow do not have any influence on the water/hydrocarbon system, then the hydrate formation occurs rapidly on the water/gas interface. Further transport of hydrate formers and water through the hydrate film will therefore be very slow, as discussed in more detail related to hydrate H₁ above. Formation of H₂ (see discussion above) will proceed until a quasi-equilibrium between water and methane in solution and the same components in hydrate occurs. In a flowing system with turbulent shear forces blocking the hydrate, films (membranes) will likely be broken and reformed continuously. The exceptions to this might be the shielded regions close to the pipeline walls. The rust in a pipeline wall, as mentioned above, appear as a rugged surface in which peak heights are normally visible and, as such, which is several orders of magnitudes larger than the nanoscale size from a hydrate phase transition. In valleys between the high rust peaks, the effects of hydrodynamic stresses from outside flow decrease proportional to the distance from the rust peaks, toward the depth of the valleys. Also, unlike hydrate nucleation on a water/hydrate former interface, the hydrates formed toward hematite surfaces can only be bridged by structured water to the hematite surface. This opens up the potential of hematite surfaces to act as dynamic sites for nucleation of hydrates that will eventually detach from the surface and give room for new nucleation processes.

3. LIMITS OF WATER CONTENT IN HYDROCARBON FOR PIPELINE TRANSPORT

In this subsection, we have investigated the safety limit of water in gas pipeline systems based on the three routes of making water available as discussed in the previous section. Europipe II (EP II) is selected for this study because the temperature–pressure conditions are favorable for hydrate nucleation and growth. The EP II pipeline is around 660 km^{13,14} long, out of which 627 km of the pipeline is offshore and goes through the Norwegian, Danish, and German parts of the North Sea. It is an export gas pipeline for transporting 65.9 mega standard cubic meters of gas per day^{13,14} from the Kårstø processing plant in Norway to the Europipe receiving facilities (ERF) reception center at Dornum in Germany. This pipeline is laid on the seafloor of the North Sea where temperatures are generally low; they can be as low as $-1\text{ }^{\circ}\text{C}$ and seldom exceed $+6\text{ }^{\circ}\text{C}$.^{9,11,12} At the landfall in Germany, the temperature of the gas is expected to be as low as $-5\text{ }^{\circ}\text{C}$.¹³ The transport operation involves high pressures. The gas is sent from Norway at 190 bar, and it is received in Germany at 90 bar. These conditions of temperature and pressure are favorable for hydrate nucleation if water condenses out from the gas.

This practical industrial system is appropriate for our study of the limit of water content in natural gas to prevent water from dropping out to lead to hydrate nucleation. Therefore, our study covers a temperature range of -5 to $+6\text{ }^{\circ}\text{C}$ and a pressure range of 90 to 210 bar. The export natural gas is predominantly methane, so pure methane is assumed in this subsection. The usual criterion for avoiding hydrate formation in the pipeline is to make sure that water will not condense out from the gas. Molecular dynamics studies²⁸ indicate that the average chemical potential of adsorbed water on rust may be 3.4 kJ/mol lower than the chemical potential of liquid water. A more novel tolerance limit for water in natural gas will therefore be the maximum mole fraction of water in the hydrate former phase before water can drop out and adsorb on rust.

In classical hydrate risk evaluation, the formation of a separate liquid water phase through condensation will then be followed by hydrate formation if the local pressure and temperature are inside the hydrate stability curve. In the case of water adsorption on the pipeline walls, the hydrate will essentially form heterogeneously between water molecules slightly outside (roughly five water layers) of the rust surface where the water chemical potential is close to that of liquid water. In this region, there are still some density minima in the water structure that can dynamically trap hydrate formers and lower the energy barrier for the hydrate phase transition. Water droplets that follow the gas flow will be subjected to substantial surface stresses. The interface stress between the hydrate film covered by water droplets and surrounding flow can lead to hydrate film breakup. This might end up in a continuous chain of hydrate film breaking and heterogeneous formation of new hydrate films. As discussed above, hydrate films generated toward rust may be more shielded by roughness while at the same time having different dynamics in the formation and detachments of new hydrate nuclei toward rust. This roughness may be as large as that in visible hydrates (millimeter range) and creates pockets of shielded regions. In this case, dissolved natural gas in the water films on the solid surface can give rise to homogeneous hydrate formation as well as to two types of heterogeneous hydrate formations. The former is the initial hydrate film on the interface between natural gas and water, and the latter are the

subsequently heterogeneous hydrate formation from dissolved methane and water from below. Even though both water and methane come from the same liquid water phase, the real hydrate formation toward the initial hydrate film utilizes water, which is structured by the hydrate.

The results of our study of the Europipe II range of conditions are presented in Figures 3–5 and Table 1. The trends for the maximum amount of water allowable in the gas system without the risk of liquid water dropping out and/or hydrate formation for the three different routes to hydrate nucleation are the same. The difference is in absolute values. The maximum mole fraction of water that can be permitted without condensation of water or a hydrate forming directly from dissolved water in gas decreases with increasing pressures as can be observed in Figures 3 and 4. However, comparing values computed based on the different routes, the dew-point method estimates are in the order of 18 to 20 times higher than that of adsorption of water on hematite (rusty surfaces). This indicates that the presence of rust in pipelines makes it ~20 times riskier for water to drop out through an adsorption process. The dew-point estimates are also 9 to 40% higher than those of the route of direct nucleation of hydrates where the highest difference occurs at the highest pressure and lowest temperature, while the least difference occurs at the lowest pressure and highest temperature (see Table 1). However, practically, hydrate nucleation through this direct route is highly unlikely as discussed above.

For defined pressure, temperature, and hydrocarbon composition, the water dew point is calculated by iteration of the mole fraction of water in the gas that will result in a water chemical potential in the gas equal to the liquid water chemical potential. Water adsorbed on hematite has a lower chemical potential than liquid water. Our estimates indicate that the chemical potential for water adsorbed on hematite may be 3.6 kJ/mol lower than the chemical potential for liquid water at 278 K. The mole fraction of water in the hydrocarbon phase before adsorption is solved in the same way as the dew point but now using the water chemical potential on hematite. For direct hydrate formation, the solution is using the water content in gas that results in zero for eq 3 above.

The pipeline gas may also contain more variety of hydrate formers. Some amount of higher hydrocarbons like ethane and propane might be present in Europipe II as given in Table 2, a report of composition data of export gas from Norway¹⁶ published in 2012. This indicates that some amount of structure II hydrate are expected to form due to propane but this would be a very small amount as a consequence of the limited amount of propane in the reported gas mixture.¹⁶ Therefore, different hydrates having different compositions of hydrate formers and different densities are expected in this situation. Hydrate risk analysis for this gas mixture was performed as done for the pure methane above. Figure 4a–c represents the results of the dew-point method, the method of adsorption of water onto rust, and the route of direct formation of hydrates from dissolved water in the gas mixtures, respectively. We can observe the impact of the heavier hydrocarbons on the upper limit of water allowable in the pipeline system by comparing Figure 3a–c with Figure 4a–c and Table 1 with Table 3. The maximum content of water permitted in the gas mixture reduces a bit by the presence of the higher hydrocarbons.

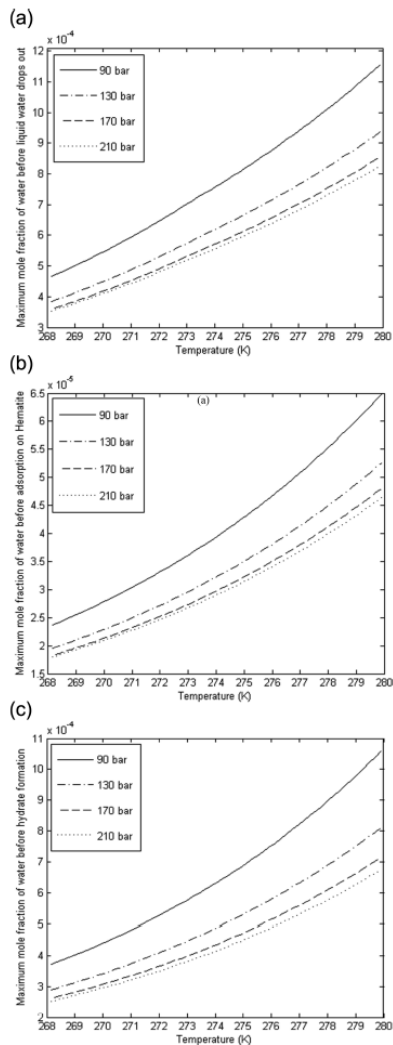


Figure 3. (a) Maximum water content before liquid water drops out of the transport gas. (b) Maximum water content before adsorption of water onto hematite. (c) Maximum water content before hydrate formation directly from water in the gas phase.

4. HYDRATE NUCLEATION AND HYDRATE GROWTH LIMITATIONS

Oxygens and hydrogens in hydrate water molecules are almost fixed, except from limited vibrations from energy minimum.³

Table 1. Maximum Water Content To Prevent Hydrate Formation during Transport of Export Gas [Pure Methane] from Kårstø in Norway to Dornum in Germany

temperature	route to hydrate formation	maximum allowable mole fraction at different temperatures and pressures			
		90 bar	130 bar	170 bar	210 bar
268 K	dew point	0.000466	0.000384	0.000359	0.000354
	hematite	0.000024	0.000020	0.000018	0.000018
	direct	0.000371	0.000289	0.000261	0.000252
274 K	dew point	0.000758	0.000620	0.000572	0.000558
	hematite	0.000040	0.000032	0.000030	0.000029
	direct	0.000632	0.000488	0.000435	0.000415
280 K	dew point	0.001155	0.000936	0.000855	0.000826
	hematite	0.000065	0.000053	0.000048	0.000046
	direct	0.001058	0.000811	0.000714	0.000674

Coulomb interactions between partial charges on oxygen and hydrogen are long-range. The phase transition occurs over a very thin interface of gradually changing water structure.^{15,17,18} In earlier studies,^{15,17,18} we used a 90% confidence interval for the distance from liquid water structure toward the hydrate water structure. This corresponds to a 1 nm interface thickness.

In classical nucleation theory (CNT), the prefactor is based on a single-molecule constant diffusional transport. Diffusional mass transport of two different types of molecules across the interface is involved in the hydrate formation dynamics. While the hydrate former is transported toward the hydrate core, the water closer to the hydrate core will expand and reform to cavity structures. Dynamically, this will be like a domino effect that leads to continuous renewal of the interface structure between the hydrate core and the liquid water outside. For mixtures, there will be diffusional transport of different hydrate formers, and in a dynamic situation, this can contribute in determining the hydrate composition. A hydrate core floating on liquid water can even be supplied with different hydrate formers from the gas side and the liquid water side (dissolved hydrate formers). Thermodynamically, CNT does not contain an interface thickness. However, the prefactor accounts for the transport across the interface to supply growth. In this work, we estimate diffusional transport and concentration gradients. These values are used in a Fick's type of approach for estimation of a realistic average value for J_0 in eq 4. It will still end up with a diffusional transport flux for every different size of a growing hydrate nucleus, and we can make use of sampled data from molecular dynamics simulations for concentration profiles across the interface from the liquid to hydrate interface.

The maximum hydrate filling will be below 100%, which would correspond to a methane hydrate mole fraction in the hydrate of 0.148. On the liquid side of the interface, it would be expected to be close to a value corresponding to the mole fraction of methane in water in equilibrium with the hydrate and lower than liquid water solubility. A second order fit of 0.14 for z equals to zero at the hydrate side and a liquid-side mole fraction 10 Å outside of that can be formulated as

$$\langle x_{\text{CH}_4}(z) \rangle = a_0 + a_1 z + a_2 z^2 \quad (10)$$

where the brackets denote average.

For a given stage of the growth, at size R , the average mole fraction of methane in the surrounding interface toward liquid water is estimated by

$$\langle x_{\text{CH}_4}(R) \rangle = \frac{2\pi \int_R^{R+10} [x_{\text{CH}_4}(z)] z^2 dz}{2\pi \int_R^{R+10} z^2 dz} \quad (11)$$

$$\begin{aligned} \langle x_{\text{CH}_4}(R) \rangle &= \frac{2\pi \int_R^{R+10} [x_{\text{CH}_4}(z)] z^2 dz}{2\pi \int_R^{R+10} z^2 dz} \\ &= \frac{c_4 R^4 + c_3 R^3 + c_2 R^2 + c_1 R + c_0}{c_2^* R^2 + c_1^* R + c_0^*} \end{aligned} \quad (12)$$

where

$$c_4 = 10a_2$$

$$c_3 = 200a_2 + 10a_1$$

$$c_2 = 2000a_2 + 150a_1 + 10a_0$$

$$c_1 = 10^4 a_2 + 1000a_1 + 100a_0$$

$$c_0 = 2000a_2 + 2500a_1 + \frac{1000}{3} a_0$$

$$c_2^* = 10$$

$$c_1^* = 100$$

$$c_0^* = \frac{1000}{3}$$

$$\begin{aligned} \frac{\partial x_{\text{CH}_4}(R)}{\partial R} &= -\frac{(2c_2^* R + c_1^*)(c_4 R^4 + c_3 R^3 + c_2 R^2 + c_1 R + c_0)}{(c_2^* R^2 + c_1^* R + c_0^*)^2} \\ &\quad + \frac{4c_4 R^3 + 3c_3 R^2 + 2c_2 R + c_1}{(c_2^* R^2 + c_1^* R + c_0^*)} \end{aligned} \quad (13)$$

$$\begin{aligned} \frac{\partial^2 x_{\text{CH}_4}}{\partial R^2} &= \frac{12c_4 R^2 + 6c_3 R + 2c_2}{c_2^* R^2 + c_1^* R + c_0^*} \\ &\quad - \frac{2c_2^*(c_4 R^4 + c_3 R^3 + c_2 R^2 + c_1 R + c_0)}{(c_2^* R^2 + c_1^* R + c_0^*)^2} \\ &\quad + \frac{2(2c_2^* R + c_1^*)(c_4 R^4 + c_3 R^3 + c_2 R^2 + c_1 R + c_0)}{(c_2^* R^2 + c_1^* R + c_0^*)^3} \\ &\quad - \frac{2(2c_2^* R + c_1^*)(4c_4 R^3 + 3c_3 R^2 + 2c_2 R + c_1)}{(c_2^* R^2 + c_1^* R + c_0^*)^2} \end{aligned} \quad (14)$$

Diffusivity coefficient gradients for CH₄ across the interface between liquid water and the hydrate surface cannot be measured experimentally. Theoretical estimates for transport

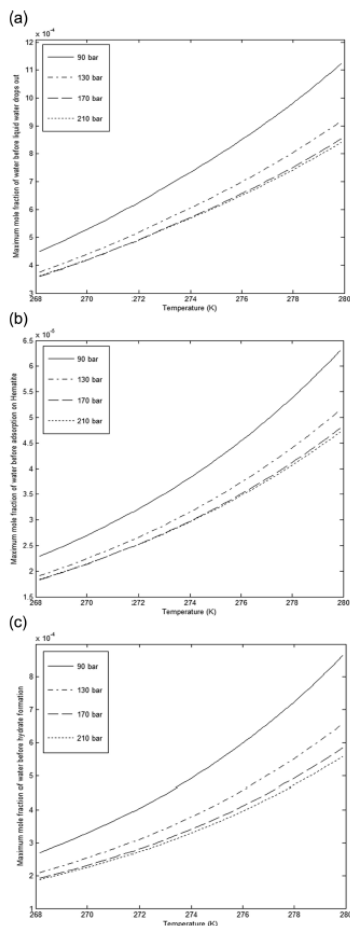


Figure 4. (a) Maximum water content before liquid water drops out of the export gas with a variety of hydrate formers. (b) Maximum water content before adsorption of water onto hematite (system with a variety of hydrate formers). (c) Maximum water content before hydrate formation directly from water in the gas phase (system with a variety of hydrate formers).

Table 2. Composition of Export Gas from Norway¹⁶

[mole fractions]				
methane	ethane	propane	<i>n</i> -butane	nitrogen
0.9203	0.0575	0.0131	0.0045	0.0046

of CH₄ through the solid hydrate are available from various open sources, but the relevance is questionable. Most estimated

diffusivity coefficients are based on Monte Carlo studies for model systems of hydrate and guest molecules jumping between cavities.^{19–21} The assumption is that a solid-state diffusion occurs when the hydrate guest jumps from an occupied cage to the neighboring empty cage through hexagonal or pentagonal faces of the water ring of structure I or II hydrate.^{20–22} There is no verified mechanism involved in this cavity jumping mechanism. Molecular dynamics simulations³ indicate that water molecules between filled and empty cavities have larger vibration amplitudes from minimum energy positions. These less stable boundary water molecules may be easier to be pushed temporarily out of position to let molecules pass from the filled cavity to the empty cavity.

The diffusivity coefficient of CH₄ at the surface of a hydrate is now denoted as D_H . The diffusivity coefficient of the liquid side of the interface is denoted as D_L . Since this is the 90% confidence interval of the interface structure, D_L should be somewhat lower than the diffusivity of CH₄ through “bulk” liquid water. D_H should be higher than the diffusivities through hydrates. Molecular dynamics studies³ give substantially higher values for the diffusivity of CH₄ through hydrates than the Monte Carlo studies referenced above. As discussed above, we approximate the interface thickness to 10 Å and model the change in diffusion of CH₄ across the interface by a linear logarithmic approximation.

$$\ln D_{\text{CH}_4}(R, z) = \frac{\ln D_H - \ln D_L}{10} [(R+z) - R] + \ln D_L \quad (15)$$

For every radius R of a growing spherical hydrate particle, a volumetric average diffusivity in the interface layer surrounding the core is then estimated as

$$\begin{aligned} \langle D(R) \rangle &= \frac{4\pi \int_R^{R+10} e^{\ln D_H - \ln D_L / 10 [(R+z) - R] + \ln D_L} z^2 dz}{4\pi \int_R^{R+10} z^2 dz} \\ &= \frac{\int_R^{R+10} e^{b_0 + b_1 z} z^2 dz}{10R^2 + 100R + \frac{1000}{3}} = \frac{R^2 d_0 + d_1}{b_1 (d_2^* R^2 + d_1^* R + d_0^*)} \\ &\quad - \frac{R d_2 + d_3}{b_1^2 (d_2^* R^2 + d_1^* R + d_0^*)} + \frac{d_4}{b_1^3 (d_2^* R^2 + d_1^* R + d_0^*)} \end{aligned} \quad (16)$$

where $b_0 = \ln D_L$ and $b_1 = \frac{\ln D_H - \ln D_L}{10}$ and coefficients in eq 14 are given as follows

$$\begin{aligned} d_4 &= 2e^{b_0 + b_1 R} (e^{10b_1} - 1) \\ d_3 &= 20e^{b_0 + b_1(R+10)} \\ d_2 &= 2e^{b_0 + b_1 R} (e^{10b_1} - 1) \\ d_1 &= (20R + 100)e^{b_0 + b_1(R+10)} \\ d_0 &= e^{b_0 + b_1 R} (e^{10b_1} - 1) \\ d_2^* &= 10 \\ d_1^* &= 100 \\ d_0^* &= 333.33 \end{aligned}$$

Then, we substitute X and D in Fick's second law equation

$$\rho \frac{\partial X_{\text{CH}_4}}{\partial t} = -D_{\text{CH}_4}(R) \rho \frac{\partial^2 X_{\text{CH}_4}}{\partial R^2} \quad (17)$$

Table 3. Maximum Water Content To Prevent Hydrate Formation during Transport of Export Gas with a Variety of Hydrate Formers

temperature	route to hydrate formation	maximum allowable mole fraction at different temperatures and pressures			
		90 bar	130 bar	170 bar	210 bar
268 K	dew point	0.000450	0.000376	0.000360	0.000362
	hematite	0.000023	0.000019	0.000018	0.000018
	direct	0.000270	0.000209	0.000192	0.000188
274 K	dew point	0.000736	0.000607	0.000573	0.000570
	hematite	0.000038	0.000032	0.000030	0.000030
	direct	0.000495	0.000379	0.000341	0.000330
280 K	dew point	0.001125	0.000919	0.000855	0.000841
	hematite	0.000063	0.000052	0.000048	0.000047
	direct	0.000866	0.000659	0.000586	0.000560

Since X is now only a function of R and t , we can substitute the integration variable X in eq 17 using

$$\frac{\partial X_{\text{CH}_4}}{\partial t} = \left(\frac{\partial X_{\text{CH}_4}}{\partial R} \right) \left(\frac{\partial R}{\partial t} \right) \quad (18)$$

which when inserted into eq 15 results in

$$\frac{\partial R}{\partial t} = - \frac{D_{\text{CH}_4}(R) \frac{\partial^2 X_{\text{CH}_4}}{\partial R^2}}{\frac{\partial X_{\text{CH}_4}}{\partial R}} \quad (19)$$

or

$$t(R) - t(R_0) = \int_{R_0}^R \left(\frac{D_{\text{CH}_4}(R) \frac{\partial^2 X_{\text{CH}_4}}{\partial R^2}}{\frac{\partial X_{\text{CH}_4}}{\partial R}} \right) dR \quad (20)$$

where R_0 is the starting size for the evaluation and the corresponding time appears on the left-hand side. Equation 19 is most conveniently integrated numerically.

The liquid-side concentration of methane in eq 10 is highly temperature- and pressure-dependent. It is beyond the scope of this work to do an extensive study of various liquid-side concentrations as a sensitivity analysis of surface concentration of methane. For this reason, we fix these parameters for a specific example. Parameters of $a_0 = 0.14$, $a_1 = -0.015$, and $a_2 = 2 \times 10^{-4}$ result in a mole fraction of methane equal to 0.14 at the hydrate surface. On the other side of the interface, 10 Å outside of the hydrate surface, the concentration of CH_4 is expected to be supersaturated relative to the solubility of CH_4 at specific temperature and pressure. For pipeline transport with pressure ranges in the order of 50 to 250 bar, a mole fraction of CH_4 equal to 0.01 10 Å outside the hydrate surface can be one example (see for instance Figures 6 and 7 below for bulk solubility as a function of temperatures and pressures).

4.1. Heterogeneous Hydrate Nucleation on Water/Gas Interface. There is only one degree of freedom in heterogeneous hydrate formation from liquid water and a single-component hydrate former phase. Equilibrium can therefore not be achieved when two independent thermodynamic variables are given. In any industrial situation of hydrate formation or any situation of hydrates in nature, both temperature and pressure are given locally. A first-order Taylor expansion from the stability limit can be written as

$$G_{\text{Non-equilibrium}}^{\text{H}}(T, P, \bar{x}) = G^{\text{H,Eq}}(T^{\text{Eq}}, P^{\text{Eq}}, \bar{x}^{\text{Eq}}) + \sum_r \left. \frac{\partial G^{\text{H}}}{\partial x_r} \right|_{P, T, x_{r \neq r}} (x_r - x_r^{\text{Eq}}) + \left. \frac{\partial G^{\text{H}}}{\partial P} \right|_{T, \bar{x}} (P - P^{\text{Eq}}) + \left. \frac{\partial G^{\text{H}}}{\partial T} \right|_{P, \bar{x}} (T - T^{\text{Eq}}) \quad (21)$$

The reference state is the pressure–temperature stability limit curve for the actual gas composition. Any temperature on the equilibrium curve can be chosen freely. The last term in eq 21 therefore vanishes. The non-equilibrium free energy needed for eqs 5 and 6 can therefore be evaluated for eq 1 based on eq 21.

In Figure 5, we calculated the critical radius for hydrate formation from methane gas and liquid water on the interface according to eq 1. As in all other nucleation calculations, we have used a constant interface thickness between the hydrate and liquid water of 10 Å. We expect the nucleation to happen in the liquid water interface (10 Å). The applied value for interface free energy is 30×10^{-6} kJ/m^{2,23} and this value comes from experimental results for liquid water/ice. Except for very low driving forces, the critical nuclei radius is small.

4.2. Homogeneous Hydrate Nucleation from Dissolved Methane. The lowest limit of hydrate stability in terms of the surrounding water can be calculated from a quasi-equilibrium consideration. For the actual temperature and pressure, the chemical potentials of water and methane in the hydrate and in the solutions of water in contact are then the same. This will give a contour map of concentrations of methane in the surrounding water needed to keep the hydrate stable. The solubility of methane in water gives another contour map, which is calculated by the methane chemical potential in gas (or liquid or supercritical) being equal to the chemical potential of dissolved methane in water. Methane dissolved in water will be able to form a hydrate between the solubility of methane in liquid water and the minimum concentration for hydrate stability. Hydrate growth from methane dissolved in water is also dominated by heterogeneous hydrate formation. The reason is that methane dissolved in water will benefit from a heterogeneous growth toward the existing hydrate film. In order to calculate the kinetics of this nucleation process, we need the thermodynamic properties of methane adsorbed on the existing hydrate film and/or secondary adsorbed as trapped in water structures caused by the hydrate crystal. Separate studies are in progress using molecular dynamics simulations. The goal of these studies is to be able to quantify thermodynamic properties (chemical potentials and energies) as well as

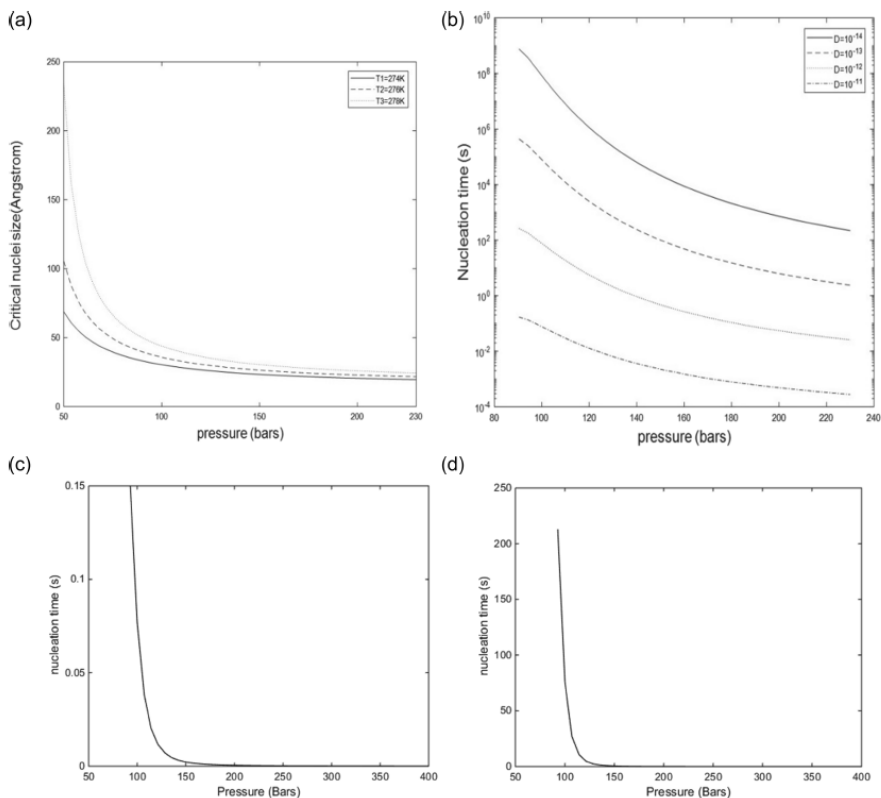


Figure 5. (a) Critical nuclei size for methane hydrate at three different temperatures for various supersaturations in pressure. Solid curve is for 274 K (equilibrium pressure of 28.4 bar). Dashed curve is for 276 K (equilibrium pressure of 34.7 bar). Dashed dotted curve is for 278 K (equilibrium pressure of 42.5 bar). All calculations were conducted using $30 \times 10^{-6} \text{ kJ/m}^2$ for interface free energy between liquid water and the hydrate in eq 6. (b) Natural logarithm of nucleation time as a function of various pressures with different diffusion coefficients at a constant temperature of 274 K. (c) Nucleation time as a function of pressure for the CH₄ hydrate formed on the gas/water interface. Temperature is 274 K. The methane diffusivity on the hydrate side of the 10 Å-thick interface is $10^{-11} \text{ m}^2/\text{s}$. (d) Nucleation time as a function of pressure for the CH₄ hydrate formed on the gas/water interface. The methane diffusivity on the hydrate side of the 10 Å-thick interface is $10^{-12} \text{ m}^2/\text{s}$. Equilibrium pressure for 274 K is 28.4 bar.

diffusivities related to the structurally trapped methane. Homogeneous nucleation of the hydrate inside the water phase is also possible. This is the type of hydrate formation discussed in this work. As for the thermodynamic aspects related to the heterogeneous formations toward the hydrate film versus the homogeneous hydrate formation from solution, we may assume that the methane chemical potential toward the hydrate film is in quasi-equilibrium with the outside methane dissolved in water.

Guest chemical potentials in Figure 1b for methane in the gas phase as compared to chemical potentials of methane in solution in Figure 6b illustrate the variations in the resulting hydrate compositions through eqs 22–24 below. The associated differences in free energies for the various hydrates formed

through different routes and “parent” phases (the phase where the molecule comes from) for the guest molecules are given by eq 25. The statistical mechanical equilibrium theory derived by Kvamme and Tanaka³ differs from the classical methods in the sense that it gives the possibility of either a rigid lattice, like those used in other codes, or the use of a harmonic oscillator guest movement model in a molecular dynamics simulation for evaluation of the cavity partition functions. The canonical partition h_j for a guest molecule j in cavity-type i evaluated by the latter option can be expressed as

$$h_{ij} = e^{-\beta(\mu_j + \Delta\epsilon_{ij})} \quad (22)$$

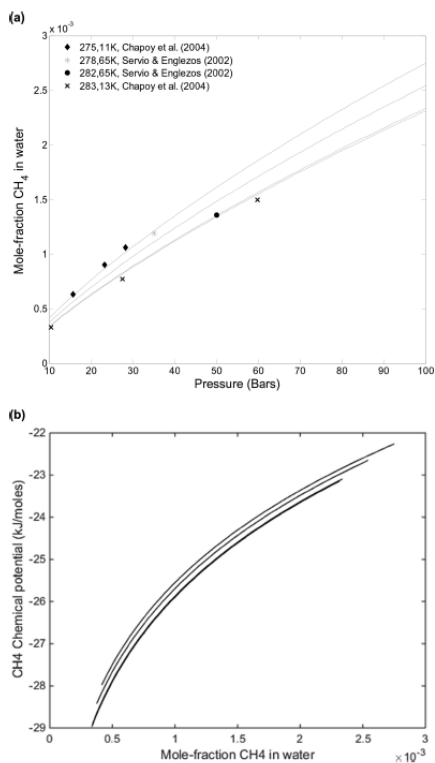


Figure 6. (a) Calculated solubility of CH_4 in water for four different temperatures. Top solid curve is for a temperature of 275.11 K, the next is for 278.65 K, then for 282.65 K, and the lowest solid curve is for 283.13 K. Experimental data from Chapoy et al.²⁴ are marked with solid diamonds and x marks, and experimental data from Servio and Englezos²⁵ are marked with asterisks and solid circles. (b) Chemical potential for CH_4 in aqueous solutions as a function of mole fraction along the solubility curves in panel (a). Top solid curve is for a temperature of 275.11 K, the next is for 278.65 K, then for 282.65 K, and the lowest solid curve is for 283.13 K.

In molar units, β is the inverse of the universal gas constant times the temperature. In molecular units, β is the inverse of Boltzmann's constant times the temperature. At equilibrium or at the stability limit for a non-equilibrium situation, the chemical potential of guest molecules j in hydrate cavity i is equal to the chemical potential of molecules j in the co-existing phase it comes from. For Figure 1, the hydrate former comes from a gas phase, while in Figure 6, it is the chemical potential for CH_4 in aqueous solution.

The corresponding filling fractions and mole fractions of methane in the hydrate are given by

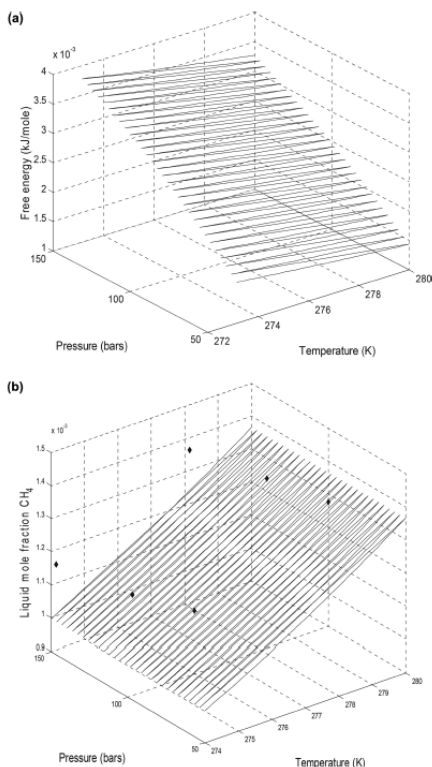


Figure 7. (a) Solubility of methane in water as a function of temperature and pressure. (b) Minimum methane in water for hydrate stability as a function of temperature and pressure. Solid line is estimated, and solid black dots are experimental data from Yang et al.²⁶

$$\theta_{ij} = \frac{h_{ij}}{1 + \sum_j h_{ij}} \quad (23)$$

where θ_{ij} is the filling fraction of component j in cavity type i

$$x_j^H = \frac{\theta_{\text{large},j} \nu_{\text{large}} + \theta_{\text{small},j} \nu_{\text{small}}}{1 + \theta_{\text{large},j} \nu_{\text{large}} + \theta_{\text{small},j} \nu_{\text{small}}} \quad (24)$$

where ν is the fraction of the cavity per water for the actual cavity type (indicated by subscripts). The corresponding mole fraction of water is then given by

$$x_{\text{H}_2\text{O}}^H = 1 - \sum_j x_j^H \quad (25)$$

The associated hydrate free energy is then

$$G^{(H)} = x_{\text{H}_2\text{O}}^H \mu_{\text{H}_2\text{O}}^H + \sum_j x_j^H \mu_j^H \quad (26)$$

Superscript H refers to the hydrate. CH₄ chemical potentials for the heterogeneous formation from methane and liquid water in Figure 1 are different from CH₄ chemical potentials for homogeneous hydrate formation from water solutions in Figures 6b. From eq 26 and eqs 22–25, each of these hydrates will, by thermodynamic definition, be a unique phase because the composition, density, and free energy are different. Furthermore, as seen from Figure 6b, every different concentration of CH₄ between the solubility limit and hydrate stability limit will result in a unique hydrate. Mathematically, this means that an infinite number of hydrate phases can be formed from CH₄ in solution. The impact of the combined first and second laws of thermodynamics will, however, lead to reorganization of hydrates when the supply of new CH₄ is limited.

The experimental data referred to in the caption to Figure 6b are not directly comparable. Since there is free gas in the cell, there will be combinations of H₁ and H₂. Also, when CH₄ from solution is converted over to a hydrate, then new CH₄ will be dissolved from the free gas phase. It is therefore expected that the experimental values should be higher than what we calculated based on homogeneous hydrate formation from solution only. In view of this, the agreement is strikingly good.

Nucleation time decreases when the mole fraction of CH₄ in water increases, as illustrated in Figure 8. This is of course expected since the maximum thermodynamic driving force is when the concentration is at the solubility limit. For the concentration at the hydrate stability limit, the driving force is zero, and the closer we get to this limit, the higher the nucleation times become. Comparing different diffusivity coefficients shows that nucleation time is substantially faster for the example with a diffusivity of 10⁻¹¹ m²/s than the example with a diffusivity coefficient of 10⁻¹² m²/s. The expected range of limiting transport diffusivities based on comparison between experiments and results derived from phase field theory (PFT) modeling⁷ is in agreement with this diffusivity coefficient.

4.3. Induction Times. As discussed in the previous sections, critical nucleation size is on the nanoscale order for the systems discussed in this work. As mentioned above, this is in accordance with the nano- to-mesoscale modeling published earlier from our research group¹⁷ using phase field theory (PFT). Induction times, or times for “onset of massive growth”, are frequently delayed by several factors. Mass transport limitations are frequently the most important.

As an example we may consider the reported result from an experiment in a stationary cell without stirring or other induced hydrodynamic effects.⁹ The result is plotted in Figure 9 below. The reader is directed to ref 7 for more complete details on the experiment. The experimental cell is constructed by cutting a plastic cylinder of a diameter of 4 cm and length of 10 cm into two half cylinders. These two half cylinders are then squeezed together against a 4 mm-thick plastic spacer. The resulting empty space for fluids is then surrounded by a cooling medium. For monitoring, a magnetic resonance imaging system is utilized. For the applied frequencies, the hydrogen proton spin in hydrate water and methane hydrogen spin will be invisible. Liquid water spin is visible. Massive hydrate growth is then detected by the time when liquid water regions turn invisible due to hydrate conversion. Resolution of the experiment is limited to 300 μm. This number is different than the 100 μm resolution indicated by Kvamme et al.⁷ and based on a more critical review of the experimental setup for this special experiment with a plastic container. The only thing that can be detected with this monitoring system is the transition over to rapid massive hydrate

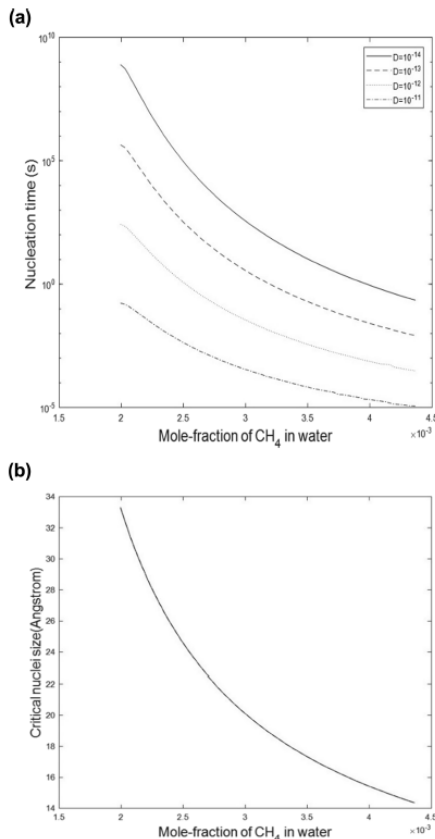


Figure 8. (a) Mole fraction of CH₄ dissolved in liquid water with respect to nucleation time at a temperature of 274 K and pressure of 200 bar with different diffusion coefficients. (b) Critical size as a function of mole fraction of CH₄ in water at constant temperature (274 K) and pressure (200 bar).

growth, as seen from Figure 9. The induction time (“time for onset of massive hydrate growth”) was recorded to 100 h at conditions of 4 °C and a pressure of 1200 psig (84 bar). This level of induction time of 3.6 × 10⁵ s is far beyond any possible value for nucleation times. Water and methane are both readily available on both sides of the interface between methane and water. Phase field theory modeling^{7,15,27} reproduces the experimental observations with a diffusivity coefficient in the order of 10⁻¹² m²/s. For this particular setup, the plastic walls are methane-wetted. Capillary migration of methane along the plastic wall is one reason for accumulation of methane that is in contact with water along the wall. Another reason for the onset of massive growth is the rearrangements of the initial hydrate film between the gas and liquid water. The combined first and

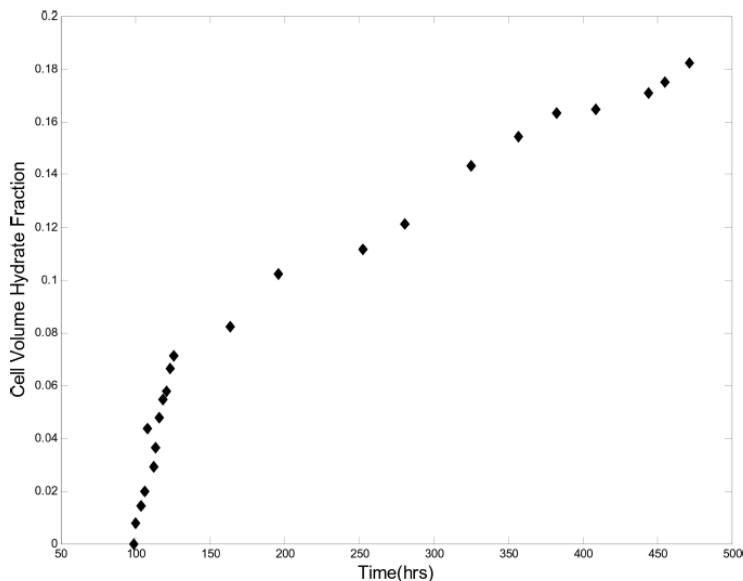


Figure 9. Experimental data for methane hydrate formation from water and methane at 1200 psia (83 bar) and 3 °C.⁷

second laws of thermodynamics will lead to rearrangements of the hydrate film. When there is a lack of new hydrate building blocks, then the most stable regions of the hydrate film will consume building blocks from less stable neighboring regions of the film. Eventually, this will lead to holes in the hydrate film. This latter effect is something that happens on all scales—from nano^{7,15,17,27} to the visible scale as observed in experiments.³²

5. DISCUSSION

Nucleation of hydrates can happen along a variety of routes. For natural gas hydrates in sediments or formation of hydrates in a rusty pipeline, the two most important routes are formation on the water/hydrate former phase and toward mineral surfaces. The relative importance of hydrate nucleation and growth from dissolved hydrate formers is related to the solubility of the hydrate former. In all cases, nucleation is a nanoscale phenomenon in time and space. Mass transport through a hydrate is very slow, and the time needed for a hydrate to grow to a visible size can be substantial, unless shear forces die to flow or other factors break the kinetically rate-limiting hydrate films. The time needed for a hydrate to reach a massive size to a visible hydrate is called the induction time. This time is frequently misinterpreted as nucleation time because the resolution of the monitoring device (magnetic resonance imaging, microscope, etc.) is not able to detect the presence of any hydrate.

Hydrates can never reach equilibrium in nature or industry. Even without the impact of solid surfaces, it is straightforward to verify that equilibrium of a single hydrate former and water distributed over three phases (water, hydrate, and hydrate former phases) is mathematically over-determined by one independent thermodynamic variable when temperature and

pressure are both defined/given. Also, the situation does not improve if more hydrate formers are added since the first and second laws of thermodynamics will drive the phase transitions to a variety of different hydrate phases (different compositions). In a non-equilibrium system, the chemical potentials for a hydrate former in different phases are different because the first and second laws determine distribution of masses over the various possible phases. The result is that there are many different hydrates (different compositions and free energies). This variety is further enhanced for mixtures since the relative ability to adsorb on water is one part of the mass transport that brings water and hydrate formers in contact.

The most important routes to hydrate formation in sediments or industrial pipelines are via the water/hydrate former phase interface and toward mineral surfaces. The reason that the latter route is important is that the atomic charges on the mineral surface will dominate the structuring of water. The density of water in the first layer on a mineral surface can be three times the density of liquid water.²⁸ The associated chemical potential is substantially lower than the liquid water chemical potential.^{1,8,28} The subsequent variations in water density as a function of distance from the mineral surface also involve regions of low water density that will be able to trap hydrate formers.^{29–31}

Natural gas being transported in pipelines always contains water. It can be because of the equilibrium water saturation amount from the time the hydrocarbon system entered separation and processing units and finally ended up in a pipeline for transport. Normally, hydrodynamics will also distribute water into the hydrocarbon phases.

The low chemical potential of adsorbed water on rust implies that the rusty surface acts like a magnet for extracting water out

from the gas. Hydrate formation toward rusty pipeline walls can therefore be substantially more important than water condensing as droplets and the formed hydrate with gas. As discussed above, the hydrate is unable to stick to the rust surface. The hydrate formed toward rusty pipeline walls will also nucleate on hydrate films generated by dropped out water, roughly 6 water molecules distance (2 nm) from the surface of hematite.

For mixtures of various hydrate formers, the accessibility to hydrate formers on the water surface depends on the thermodynamic state for the various guest molecules and the attraction to the water surface. If we think about mixtures of CH₄ and CO₂ as one example, then CH₄ is supercritical in the liquid water hydrate range and does not have a tendency to condense. CO₂ is subcritical and has a favorable attraction to liquid water compared to CH₄. These aspects are illustrated by Kvamme³⁶ using a 2D adsorption theory. The average availability for hydrate formation on the liquid water surface and the associated average adsorption mole fraction on the liquid water surface are therefore very different from the gas mole fraction.

Another aspect that will also lead to a variety of different hydrates forming from CH₄ and CO₂ mixtures is the effect of the combined first and second laws of thermodynamics. The most stable hydrates will form first, under constraints of mass and heat transport. There are a number of common misunderstandings about hydrate stability. The stability limit in a temperature pressure projection is not the proper way to discuss stability. Since residual energy is used for all phases and all components, the molar free energy of each phase is the actual measure of the relative stability. In Figure 10a, we show a logarithmic plot of the temperature and pressure regions in which hydrates of CH₄ and CO₂ can form. For CO₂, the range of temperatures includes a phase transition to a lower density. In some published work, this transition is smoothed out. Still in other publications, it is discussed as a discontinuity.

However, the most important misunderstanding is in the discussion of stability in which it is frequently argued that the CH₄ hydrate is more stable above a certain temperature. This is not the case. If we plot the free energies of the two hydrates along the hydrate formation curves in Figure 10a, we can compare directly the stability of the two hydrates in Figure 10b,c. The stability limits of the CH₄ hydrate are compared to experimental data in Figure 1a, while those of the CO₂ hydrate are compared to experimental data elsewhere.^{36,37} The free energy of the two hydrates in the three-dimensional plot in Figure 10b is hard to read in terms of specific numbers and only serves the purpose of showing the very different pressure dependencies for the two components after the temperature of the phase transition to higher density for CO₂. Figure 10c is easier to read and shows that the CO₂ hydrate is more stable than the CH₄ hydrate over the entire range of temperatures and pressures of the two *P*–*T* stability curves in Figure 10a. These features are not directly visible in the old-fashioned hydrate *P*–*T* stability limit curves because they are based on semi-empirical fitting of the liquid water chemical potential minus the empty hydrate chemical potential.

In this work, we have utilized a numerically very simple theory, but it is still a theory with roots in physics as opposed to empirical fitting equations. The relative importance of the mass transport, the heat transport, and the thermodynamic control for each different system in consideration is easy to visualize. It is easy to implement as extensions of existing hydrate risk evaluation tools. This approach can save industries money in terms of chemical additives because there may be situations that

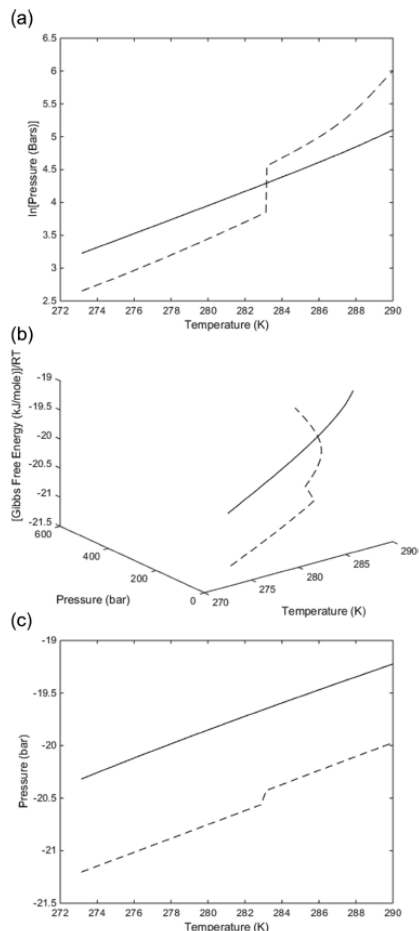


Figure 10. (a) Temperature–pressure stability limits for the CH₄ hydrate (solid) and CO₂ hydrate (dashed). (b) Dimensionless free energies of the CH₄ hydrate (solid line) and CO₂ hydrate (dashed line) along their corresponding hydrate stability limits in a pressure–temperature projection. (c) Dimensionless free energies of the CH₄ hydrate (solid line) and CO₂ hydrate (dashed line) along their corresponding hydrate stability limits in the temperature projection of the pressure–temperature space.

are in favor of hydrate formation from a pure thermodynamic analysis, while a more complete dynamic analysis may reveal that there are substantial kinetic limitations in mass transport or heat transport associated with the hydrate formation.

6. CONCLUSIONS

Misconceptions about hydrate nucleation times and hydrate induction times are frequently found in the open literature. In order to illustrate this, we have utilized a simple nucleation theory, CNT. Thermodynamic properties related to the phase transitions in this model are calculated using classical thermodynamics. Hydrate properties are derived from available results from molecular modeling in order to obtain a consistent and transparent reference level for all components in all phases. Except for situations of extremely low thermodynamic driving forces in terms of temperature and pressure, then the typical smallest hydrate cores (critical size) that enter growth regions are around 2 nm in radius. In the liquid water region, there is no experimental method that can detect such small hydrate cores and this is likely the reason that many researchers wrongly assume that there is no hydrate. The slow transport of hydrate formers through a hydrate film can cause substantial delays before hydrates of a visible size can be detected.

The influence of solid surfaces will often play a role in the transition to massive hydrate growth (induction time), but there are also several other factors related to thermodynamics. When there is no new material available for hydrate growth, the combined first and second laws will lead to a situation in which more stable regions of the hydrate film (regions of lower free energy) will consume neighboring regions of the hydrate film with higher free energy. Eventually, this can lead to holes in the hydrate film at a stage where massive hydrate growth is feasible due to the existing hydrate.

Minerals contain charged atoms that structure water to extreme densities compared to liquid water. Rust is a mix of various combinations of iron and oxygen, but the most stable is hematite. Pipelines for transporting hydrocarbons are rusty even from the point when they were welded together into a pipeline. The low chemical potential of water as adsorbed on hematite makes water substantially more favorable to adsorb on hematite rather than condensing out as liquid droplets during transport of hydrocarbon systems containing water. The first step in a hydrate risk evaluation analysis is a calculation of the water dew-point concentration for a local temperature and pressure in the pipeline. If this concentration is considered as the maximum amount of water to be permitted, then our calculations show that 18 to 20 times higher concentrations of water might be permitted as compared to a criterion based on the maximum concentration before adsorption on rust.

Another assumption that frequently occurs in the open literature is that only one hydrate structure forms. A variety of hydrates will form because industrial and natural systems of hydrates can never reach equilibrium. The chemical potentials of water and hydrate formers are therefore subjected to local free energy minimum as a function of mass and heat transport constraints. Cavity partition functions in the statistical mechanical theory for hydrates will therefore vary with local chemical potentials for guest molecules.

Hydrates forming from dissolved hydrate formers in water can come in many forms, depending on the concentration of the hydrate former versus solubility concentration and concentration at the limit of hydrate stability. Even though most of the focus in this paper has been on the CH₄ hydrate, we have also pointed out that comparison of hydrate formers need to be based on two levels of analysis. In a dynamic situation, subcritical components will have a stronger driving force to adsorb on liquid water than super critical components. Various compo-

nents have their individual average attractions to liquid water prior to nucleation. In addition to these aspects, there will also be a selectivity based on gradients in free energy that directs the system toward the formation of most stable hydrates first. In real situations of mixtures of hydrate formers, many hydrates can form initially.

AUTHOR INFORMATION

Corresponding Author

*E-mail: kvamme_uib@outlook.com.

ORCID

Bjorn Kvamme: 0000-0003-3538-5409

Solomon Aforkoghene Aromada: 0000-0002-9054-4604

Notes

The authors declare no competing financial interest.

ACKNOWLEDGMENTS

Support from the University of California, Irvine and from Hyzen Energy is highly appreciated.

NOMENCLATURE

\AA	Angstrom
δ	partial charge
P	pressure
P	number of phases (Gibbs phase rule)
T	temperature
T_R	actual temperature divided by the critical temperature
$T_{0,R}$	273 K divided by the actual temperature
R	universal gas constant
R	radius of hydrate core
R^*	critical radius for the hydrate core
ρ_N^H	molar density of hydrate
γ	interface free energy
γ_i	activity coefficient of a component
γ_i^∞	activity of a component at infinite dilution
μ	chemical potential
μ_i^H	chemical potential of component i in the hydrate cavity
μ_i^{gas}	chemical potential of component i in the hydrate former phase
μ_i^{water}	chemical potential of component i in liquid/gas or solid water
$\mu_{\text{H}_2\text{O}}^{\text{Water}}$	chemical potential of water in liquid/gas or solid water
$\mu_{\text{H}_2\text{O}}^{0,H}$	chemical potential of water in an empty hydrate cavity
μ_i^{sol}	chemical potential of a component at infinite dilution
G_i^ψ	Gibbs free energy of a component at phase ψ
ΔG	change in Gibbs free energy
$\Delta G_i^{\text{Total}}$	total change in Gibbs free energy
$\Delta G_{ik}^{\text{inc}}$	Impact on hydrate water from the inclusion of guest i in cavity k
H	hydrate
H	enthalpy
H_{ik}^R	residual enthalpy of a component inside the cavity
ΔH	change in enthalpy
ΔS	change in entropy
x_i^H	mole fraction of component i in the hydrate
x_i^H	mole fraction of component i in cavity k
$x_{\text{H}_2\text{O}}^H$	mole fraction of water in the hydrate
$x_{\text{H}_2\text{O}}^H$	mole fraction of component i in the hydrate former phase
y_i^{gas}	mass transport rate
J	

J_0	mass transport flux
β	inverse of Boltzmann's constant multiplied with temperature
m	mass
c and c^e	supersaturated and equilibrium concentration
C	number of components (Gibbs phase rule)
F	degree of freedom
A	surface area of a crystal
K	overall transfer coefficient
K_d	diffusion coefficient
K_r	reaction coefficient
K_B	Boltzmann's constant
U	internal energy
U_{ik}^{residual}	residual contribution of energy for the guest in the cavity
S	entropy
N_j^i	number of particles of component j in phase i
n	hydration/occupation number
$\Delta U_{ord}U$	change in energy

REFERENCES

- (1) Nakamura, T.; Makino, T.; Sugahara, T.; Ohgaki, K. Stability boundaries of gas hydrates helped by methane—structure-H hydrates of methylcyclohexane and cis-1, 2-dimethylcyclohexane. *Chem. Eng. Sci.* **2003**, *58*, 269–273.
- (2) De Roo, J. L.; Peters, C. J.; Lichtenhaler, R. N.; Diepen, G. A. M. Occurrence of methane hydrate in saturated and unsaturated solutions of sodium chloride and water in dependence of temperature and pressure. *AIChE J.* **1983**, *29*, 651–657.
- (3) Kvamme, B.; Tanaka, H. Thermodynamic stability of hydrates for ethane, ethylene, and carbon dioxide. *J. Phys. Chem.* **1995**, *99*, 7114–7119.
- (4) Kvamme, B. Kinetics of Hydrate Formation from Nucleation Theory. *Int. J. Offshore Polar Eng.* **2002**, *12*.
- (5) Kvamme, B. Droplets of Dry Ice and Cold Liquid CO₂ for Self-Transport of CO₂ to Large Depths. *Int. J. Offshore Polar Eng.* **2003**, *13*.
- (6) Kvamme, B.; Qasim, M.; Baig, K.; Kivela, P.-H.; Bauman, J. Hydrate phase transition kinetics from Phase Field Theory with implicit hydrodynamics and heat transport. *Int. J. Greenhouse Gas Control* **2014**, *29*, 263.
- (7) Kvamme, B.; Graue, A.; Buanes, T.; Kuznetsova, T.; Ernsland, G. Storage of CO₂ in natural gas hydrate reservoirs and the effect of hydrate as an extra sealing in cold aquifers. *Int. J. Greenhouse Gas Control* **2007**, *1*, 236–246.
- (8) Kvamme, B.; Kuznetsova, T.; Kivela, P.-H.; Bauman, J. Can hydrate form in carbon dioxide from dissolved water? *Phys. Chem. Chem. Phys.* **2013**, *15*, 2063–2074.
- (9) Kvamme, B.; Aromada, S. A. Risk of Hydrate Formation during the Processing and Transport of Troll Gas from the North Sea. *J. Chem. Eng. Data* **2017**, *62*, 2163–2177.
- (10) Kvamme, B.; Aromada, S. A. Alternative Routes to Hydrate Formation during Processing and Transport of Natural Gas with a Significant Amount of CO₂: Sleipner Gas as a Case Study. *J. Chem. Eng. Data* **2018**, *63*, 832–844.
- (11) Kvamme, B.; Kuznetsova, T.; Bauman, J. M.; Sjöblom, S.; Avinash Kulkarni, A. Hydrate Formation during Transport of Natural Gas Containing Water and Impurities. *J. Chem. Eng. Data* **2016**, *61*, 936–949.
- (12) Aromada, S. A. New Concept for Evaluating the Risk of Hydrate Formation during Processing and Transport of Hydrocarbons. Master's Thesis, Department of Physics and Technology, University of Bergen: Norway, 2017.
- (13) Schuchardt, D.; Krause, D.-G. G.; Kulp, D. *Environmental Impact Assessment Europe II in Germany: Offshore and Onshore Section*; Bioconsult Schuchardt & Scholle: Bremen, Germany, 1998.
- (14) Gassco. *Europe II*. Available: <http://www.gassco.no/hva-gjor-vi/orr-plattform/eurpipe-II/> (Accessed on April 5, 2018).
- (15) Svandal, A. Modeling hydrate phase transitions using mean-field approaches. Dissertation for the Degree Philosophiae Doctor (PhD), University of Bergen: 2006.
- (16) Denys, F.; de Vries, W. *Gas Composition Transition Agency Report 2013*; Gas Composition Transition Agency: Assen, The Netherlands, 2013.
- (17) Tegze, G.; Pusztai, T.; Tóth, G.; Gránágy, L.; Svandal, A.; Buanes, T.; Kuznetsova, T.; Kvamme, B. Multiscale approach to CO₂ hydrate formation in aqueous solution: Phase field theory and molecular dynamics. Nucleation and growth. *J. Chem. Phys.* **2006**, *124*, 234710.
- (18) Svandal, A.; Kuznetsova, T.; Kvamme, B. Thermodynamic properties and phase transitions in the H₂O/CO₂/CH₄ system. *Fluid Phase Equilib.* **2006**, *246*, 177–184.
- (19) Falenty, A.; Salamatin, A. N.; Kuhs, W. F. Kinetics of CO₂-hydrate formation from ice powders: Data summary and modeling extended to low temperatures. *J. Phys. Chem. C* **2013**, *117*, 8443–8457.
- (20) Salamatin, A. N.; Falenty, A.; Hansen, T. C.; Kuhs, W. F. Guest migration revealed in CO₂ clathrate hydrates. *Energy Fuels* **2015**, *29*, 5681–5691.
- (21) Peters, B.; Zimmermann, N. E. R.; Beckham, G. T.; Tester, J. W.; Trout, B. L. Path sampling calculation of methane diffusivity in natural gas hydrates from a water-vacancy assisted mechanism. *J. Am. Chem. Soc.* **2008**, *130*, 17342–17350.
- (22) Davies, S. R.; Sloan, E. D.; Sum, A. K.; Koh, C. A. In situ studies of the mass transfer mechanism across a methane hydrate film using high-resolution confocal raman spectroscopy. *J. Phys. Chem. C* **2009**, *114*, 1173–1180.
- (23) Tuckerman, M. E. *Statistical Mechanics: Theory and Molecular Simulation*; Oxford University Press: 2010.
- (24) Chapoy, A.; Mohammadi, A. H.; Richon, D.; Tohidi, B. Gas solubility measurement and modeling for methane–water and methane–ethane–n-butane–water systems at low temperature conditions. *Fluid Phase Equilib.* **2004**, *220*, 111–119.
- (25) Servio, P.; Englezos, P. Measurement of dissolved methane in water in equilibrium with its hydrate. *J. Chem. Eng. Data* **2002**, *47*, 87–90.
- (26) Yang, S. O.; Cho, S. H.; Lee, H.; Lee, C. S. Measurement and prediction of phase equilibria for water+ methane in hydrate forming conditions. *Fluid Phase Equilib.* **2001**, *185*, 53–63.
- (27) Buanes, T. Mean-field approaches applied to hydrate phase transition. Ph.D. Thesis, University of Bergen: 2006.
- (28) Kvamme, B.; Kuznetsova, T.; Kivela, P.-H. Adsorption of water and carbon dioxide on hematite and consequences for possible hydrate formation. *Phys. Chem. Chem. Phys.* **2012**, *14*, 4410–4424.
- (29) Austrheim, M. H. Evaluation of Methane and Water Structure at a Hematite Surface - A Hydrate Prevention Perspective. MSc Thesis, Department of Physics and Technology, University of Bergen: Norway, September 2017.
- (30) Nesse Knarvik, A. B. Examination of water and methane structuring at a hematite surface in the presence of MEG. MSc Thesis, Department of Physics and Technology University of Bergen, Norway, September 2017.
- (31) Mohammad, N. Heterogeneous Hydrate Nucleation on Calcite [1014] and Kaolinite [001] Surfaces: A Molecular Dynamics Simulation Study. Master's Thesis, Department of Physics and Technology University of Bergen: Norway, June 2016.
- (32) Makogon, I. F.; Makogon, Y. F. *Hydrates of Hydrocarbons*; 1st Ed.; Penn Well: Tulsa, ISBN-0-87814-618-7, 1997, 189–197.
- (33) Kvamme, B. Enthalpies of hydrate formation from hydrate formers dissolved in water. *Energies* **2019**, *12*, 1039.
- (34) Kvamme, B.; Aromada, S. A.; Gjerstad, P. B. Consistent Enthalpies of the Hydrate Formation and Dissociation Using Residual Thermodynamics. *J. Chem. Eng. Data* **2019**, *64*, 3493–3504.
- (35) Kang, S.-P.; Lee, H.; Ryu, B.-J. Enthalpies of Dissociation of Clathrate Hydrates of Carbon Dioxide, Nitrogen, (Carbon Dioxide + Nitrogen), and (Carbon Dioxide + Nitrogen + Tetrahydrofuran). *J. Chem. Thermodyn.* **2001**, *33*, 513–521.

(36) Kvamme, B. Thermodynamic limitations of the CO₂/N₂ mixture injected into CH₄ hydrate in the Ignik Sikumi field trial. *J. Chem. Eng. Data* **2016**, *61*, 1280–1295.

(37) Kvamme, B.; Aromada, S. A.; Saeidi, N. Heterogeneous and homogeneous hydrate nucleation in CO₂/water systems. *J. Cryst. Growth* **2019**, *522*, 160–174.

Paper 10

Modelling of methane hydrate formation and dissociation using residual thermodynamics

By

Solomon Aforkoghene Aromada and Bjørn Kvamme

To be published in the Proceedings in:

Simulation Notes Europe Journal, SNE 31(3), 2021, 143-150.

Modelling of Methane Hydrate Formation and Dissociation using Residual Thermodynamics

Solomon Aforkoghene Aromada^{1*}, Bjørn Kvamme²

¹Department of Physics and Technology, University of Bergen, Allegaten 55, 5007 Bergen, Norway;

**Solomon.Aromada@student.uib.no, saromada@gmail.com*

²Strategic Carbon LLC, Vestre Holbergsallmenningen 17, 5011 Bergen, Norway; *kvamme@strategic-carbonllc.com*

SNE 31(3), 2021, 143-150, DOI: 10.111128/sne.31.tn.10575
Received: March 10, 2021 (Selected EUROSIM 2019 Postconf. Publ.); Revised: August 30, 2021; Accepted: September 2, 2021
SNE - Simulation Notes Europe, ARGESIM Publisher Vienna
ISSN Print 2305-9974, Online 2306-0271, www.sne-journal.org

Abstract. The available experimental data in literature for enthalpies of hydrate formation and dissociation are limited and often lacks relevant information required for interpretation. Commonly missing information include hydrate composition, hydration number, temperature and/or pressure data, and degree of super heating during dissociation of hydrate.

Clausius-Clapeyron equations used with measured or calculated hydrate formation pressure-temperature equilibrium data is the simplest indirect methods used for evaluating enthalpy change involved in phase transition during hydrate formation or dissociation. This approach involves over-simplifications. These oversimplifications make all the data based on Clausius-Clapeyron to be unreliable. And old data using Clapeyron do not have appropriate volume corrections. We therefore propose a thermodynamic scheme (residual thermodynamics approach) which does not have these limitations. This method is based on residual thermodynamics for all properties like equilibrium (pressure-temperature) curves, free energy change as thermodynamic driving force in kinetic theories and enthalpies of hydrate formation and dissociation. The pressure-temperature equilibrium curve obtained in this work agrees well with literature.

Introduction

Natural gas hydrates are non-stoichiometric crystalline inclusion compounds (ice-like substances) formed when hydrogen-bonded water molecules form three-dimensional solid cage-like structures with cavities which entrap suitably small sized molecules of certain gases and

volatile liquids known as guest molecules, under the condition of high pressure and low temperature. Unlike ice, they exist above 273.15 K (0 °C). Lighter hydrocarbon components [1,2] and some inorganic gases [3,4] are guest molecules that can form hydrate in their pure form.

A vast amount of natural occurring methane hydrates is distributed all over the world in the permafrost and in the oceans [5]. This huge amount of methane gas trapped in the naturally existing hydrate could be a potential source of unconventional energy. In a time when decarbonization and the use of low-carbon energy resources have become exigent, successfully exploiting this huge amount of natural gas stored in form of hydrate will be important.

To produce this methane, any method that could be used will require supply of heat [6] to dissociate the methane hydrate. Therefore, a study of the heat of dissociation and formation of methane hydrate is important. Thus, it is essential to examine how best these heat (exothermic for formation and endothermic for dissociation) can be better evaluated. The amount of heat required for dissociation of the hydrate is the same amount that is released when the hydrate is form. The difference in representation is in the sign, negative for formation and positive for dissociation.

Hydrate formation is a complex exothermic process that involves competing phase transition mechanisms and routes where kinetics and thermodynamics play important role. The exothermic heat released (enthalpy of formation) during the phase transition is one of the most significant thermodynamic properties that we need for proper understanding of the phase transition process. This heat is either measured directly [7] by experiment or indirectly using Clausius-Clapeyron [8] or Clapeyron [9] modelling approaches. These approaches have some limitations and the results obtainable in literature often lack important information.



For example, the available experimental data in literature for enthalpies of hydrate phase transition are limited and often lacks relevant information required for interpretation. Frequently missing information are composition of the hydrates, hydration number, temperature and/or pressure data, and degree of super heating required during dissociation of hydrate. Clausius-Clapeyron equations used with measured or calculated hydrate formation pressure-temperature equilibrium data is the simplest indirect methods used for evaluating enthalpy change during hydrate phase transition. This approach involves over-simplifications. These oversimplifications make all the data based on Clausius-Clapeyron to be unreliable. And old data from Clapeyron do not have appropriate volume corrections.

Therefore, a consistent thermodynamic scheme, residual thermodynamics approach is proposed in this work and implemented based on the the trivial thermodynamic relationship between enthalpy change and free energy change. This method is based on using residual thermodynamics for all properties like equilibrium (pressure-temperature) curves, free energy change as thermodynamic driving force in kinetic theories and enthalpies of hydrate formation and dissociation. The approach eliminates the limitations.

The relevant modelling equations are presented, and simulations were performed. The results are discussed and compared with literature.

1 Modelling of Hydrate Dissociation with Residual Thermodynamics

Our modelling approach is summarized in this section. The free energy change for a specific hydrate phase transition can expressed as:

$$\Delta G^{(H_1)} = x_{H_2O}^H \left(\mu_{H_2O}^H(T, P, \bar{x}^H) - \mu_{H_2O}^{water}(T, P, \bar{x}) \right) + \sum_j x_j^H \left(\mu_j^H(T, P, \bar{x}^H) - \mu_j^{gas}(T, P, \bar{y}^{gas}) \right) \tag{1}$$

The superscript H_j distinguishes the specific heterogeneous phase transition from other hydrate formation phase transitions. T is temperature, P is pressure. x is mole-fraction in either liquid or hydrate (denoted with a subscript H) while y is mole-fraction in gas (or liquid) hydrate former phase. j is an index for hydrate formers.

Superscript *water* denotes water phase that is converted into hydrate. Generally, this is ice or liquid but, in this work, we only consider liquid water. μ is chemical potential. These chemical potentials are convenient in discussing other routes to hydrate formation and associated hydrate former chemical potentials since any variation in chemical potential of hydrate formers will lead to changes in hydrate compositions and hydrate free energies. This is fundamentally important since any assembly of molecules with unique density and composition is a unique phase. Liquid water chemical potential is calculated from the symmetric excess conventions as:

$$\begin{aligned} \mu_{H_2O}(T, P, \bar{x}) &= \mu_{H_2O}^{pure, H_2O}(T, P) + \\ R \cdot T \ln \left(x_{H_2O} \cdot \gamma_{H_2O}(T, P, \bar{x}) \right) &\approx \mu_{H_2O}^{pure, H_2O}(T, P) + \\ R \cdot T \ln(x_{H_2O}) &\tag{2} \end{aligned}$$

$$\lim(\gamma_{H_2O}) = 1.0 \text{ when } x_{H_2O} \text{ tends to unity}$$

The focus here is to illustrate the complexity of multiple hydrate formation in systems of water and CH_4 . We used a simpler kinetic model which is more visible in terms of the various contributions to the hydrate phase transition dynamics. As such the approximation on the right-hand side of equation (2) is accurate enough for the purpose. The solubility of CH_4 in water is small and the right-hand side will be close to pure water chemical potential. Chemical potential for water in the hydrate structure is given by [10]:

$$\mu_{H_2O}^H = \mu_{H_2O}^{O,H} - \sum_{k=1,2} RT v_k \ln \left(1 + \sum_i h_{ij} \right) \tag{3}$$

in which H denote hydrate and O in the superscript on first term on right hand side means empty clathrate. These chemical potentials are readily available from model water (TIP4P) simulations [11]. The number of cavities per water, v_k is 1/23 for small cavities of structure I and 3/23 for large cavities. With CH_4 as only the guest, i is 1 in the sum over the canonical partition functions for small and large cavities.

$$h_{ki} = e^{\beta[\mu_{ki} - \Delta g_{ki}]} \tag{4}$$

The enthalpy change is trivially related to the corresponding free energy change by the thermodynamic relationship:

$$\frac{\partial \left[\frac{\Delta G^{Total}}{RT} \right]_{P,\bar{N}}}{\partial T} = - \left[\frac{\Delta H^{Total}}{RT^2} \right] \quad (5)$$

The superscript total is introduced to also include the penalty of pushing aside the old phases.

Practically the total free energy change will be equation (2) plus the interface free energy times contact area between water and hydrate forming phase during the nucleation stage divided by number of molecules in the specific core size. Since critical nuclei sizes are small the whole particle can be considered as covered with water due to capillary forces. Above critical core size the penalty diminishes rapidly relative to the free energy benefits from (2).

$$\frac{\partial \left[\frac{\mu_{H_2O}^H}{RT} \right]_{P,\bar{N}}}{\partial T} = \frac{\partial \left[\frac{\mu_{H_2O}^{0,H}}{RT} \right]_{P,\bar{N}}}{\partial T} - \left[\frac{\partial}{\partial T} \right]_{P,\bar{N}} \left[\sum_{k=1,2} v_k \ln \left(1 + \sum_i h_{ki} \right) \right] \quad (6)$$

For the liquid water phase in (2), as well as for the empty hydrate chemical potential on right hand side of equation (6) results are trivially obtained from [12] while the second term on right hand side is reorganized as:

$$\left[\frac{\partial}{\partial T} \right]_{P,\bar{N}} \left[\sum_{k=1,2} v_k \ln \left(1 + \sum_i h_{ki} \right) \right] = \left[\sum_{k=1,2} v_k \frac{\sum_i \left[\frac{\partial h_{ki}}{\partial T} \right]_{P,\bar{N}}}{\left(1 + \sum_i h_{ki} \right)} \right] \quad (7)$$

And the derivatives of the cavity partition functions can be written as:

$$\left[\frac{\partial h_{ki}}{\partial T} \right]_{P,\bar{N}} = h_{ki} \left[-\frac{1}{RT^2} (\mu_{ki} - \Delta g_{ki}) + \frac{1}{RT} \left(\frac{\partial \mu_{ki}}{\partial T} - \frac{\partial \Delta g_{ki}}{\partial T} \right) \right] \quad (8)$$

The partial derivatives in the last term on right hand side is numerically differentiated from the polynomial fits of [11].

$$\frac{\partial \left[\frac{\mu_{H_2O}^H}{RT} \right]_{P,\bar{N}}}{\partial T} = \frac{\partial \left[\frac{\mu_{H_2O}^{0,H}}{RT} \right]_{P,\bar{N}}}{\partial T} + \left[\sum_{k=1,2} v_k \frac{\sum_i h_{ki} \left[\frac{1}{RT^2} (\mu_{ki} - \Delta g_{ki}) - \frac{1}{RT} \left(\frac{\partial \mu_{ki}}{\partial T} - \frac{\partial \Delta g_{ki}}{\partial T} \right) \right]}{[1 + \sum_i h_{ki}]} \right] \quad (9)$$

$$H_{H_2O}^{0,H} = -RT^2 \frac{\partial \left[\frac{\mu_{H_2O}^{0,H}}{RT} \right]_{P,\bar{N}}}{\partial T} + \left[\sum_{k=1,2} v_k \frac{\sum_i h_{ki} \left[\frac{1}{RT^2} (\mu_{ki} - \Delta g_{ki}) - \frac{1}{RT} \left(\frac{\partial \mu_{ki}}{\partial T} - \frac{\partial \Delta g_{ki}}{\partial T} \right) \right]}{[1 + \sum_i h_{ki}]} \right] \quad (10)$$

For liquid water, the enthalpy is even more trivially obtained by numerical differentiation of the polynomial fit of chemical potential as function of T given by [10].

In an equilibrium situation, chemical potential of the same guest in the two cavity types must be the same and these have to be equal to the chemical potential of the same molecule in the phase that it came from. For the heterogeneous case this means chemical potential of the molecule in gas (or liquid) hydrate former phase. But outside of equilibrium the gradients in chemical potentials as function of T, P and mole-fractions have to reflect how the molecule behaves in the cavity.

Enthalpies for various guest molecules in the two types of cavities can be evaluated by Monte Carlo simulations along the lines described by [10-12] by sampling guest water interaction energies and efficient volumes from the movements of the guest molecules. That is:

$$H_{ki}^R = U_{ki}^R + (z_{ki} - 1)RT \quad (11)$$

where U is energy and superscript R denote residual (interaction) contribution. z_{ki} is compressibility factor for the guest molecule i in cavity k. Consistent ideal gas values for the same interaction models that were applied in calculation of the residual values is trivial.

$$z_{ki} = \frac{PV_{ki}}{k_B T} \quad (12)$$



In which k_B is Boltzmann's constant and is the excluded volume of a molecule of type i in cavity of type k . This latter volume is calculated from the sampled volume of centre of mass movements plus the excluded volume due to water/guest occupation. Slightly more complex sampling and calculation for molecules which are not monoatomic (or approximated as monoatomic as methane) but still fairly standard (6, 7) and explicit discussion on this is not needed here. The derivative of the chemical potential of a guest molecule i in cavity type k with respect to temperature as needed in equation (9) is the negative of partial molar entropy for the same guest molecule and can be calculated according to:

$$\left[\frac{\partial \mu_{ki}}{\partial T} \right]_{P,\bar{N}} = \frac{\mu_{ki} - H_{ki}}{T} \quad (13)$$

Equation (10) can then be rearranged into:

$$H_{H_2O}^{0,H} = -RT^2 \frac{\partial \left[\frac{\mu_{H_2O}^{H,0}}{RT} \right]_{P,\bar{N}}}{\partial T} + \left[\sum_{k=1,2} V_k \frac{\sum_i h_{ki} [H_{ki} - \Delta g_{ki} + T \frac{\partial \Delta g_{ki}}{\partial T}]}{[1 + \sum_i h_{ki}]} \right] \quad (14)$$

Residual enthalpies for hydrate former in a separate hydrate former phase are trivially given by:

$$H_{ki}^R = -RT^2 \sum_i y_i \left[\frac{\partial \ln \phi_i^{gas}}{\partial T} \right]_{P,y_{j \neq i}} \quad (15)$$

In which the same equation of state (SRK) is utilized as the one used for calculating fugacity coefficients for the chemical potentials.

2 Methane Hydrate Equilibrium Pressure - Temperature

Hydrate equilibrium pressures for methane hydrate formation were estimated for a temperature range of 273K to 290 K as can be seen in Fig. 1. The estimates are compared with literature [9, 13] and there is a very good agreement even though we did not fit interaction parameters, which is not the priority here.

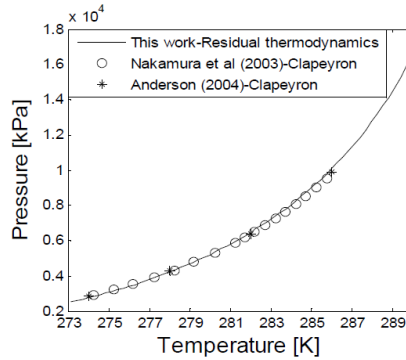


Figure 1: Estimated methane hydrate equilibrium pressures using residual thermodynamics (this work) compared with literature [9,15].

The priority is to keep the statistical mechanical model free of adjustable parameters in all terms, together also with empty hydrate chemical potentials and chemical potentials for ice and liquid water.

3 Enthalpies of Methane Hydrate Formation along Equilibrium Curve

The experimental data available in literature for enthalpies of hydrate formation and dissociation are limited and often lacks significant information required for interpretation. Commonly missing information include hydrate composition, hydration number, temperature and/or pressure data, and degree of super heating in the course of dissociation of hydrate. Hydrate dissociation enthalpy are measured directly or evaluated indirectly. Calorimetry, NMR, Raman, pressure drop X-ray diffraction are some of the methods used for direct measurement. And for the indirect method,

Clapeyron and Clausius-Clapeyron equations are the approaches that are usually employed. The simplest indirect method is the Clausius-Clapeyron equation [8] and it is used with measured or calculated hydrate formation pressure-temperature equilibrium data. The simplifications in this approach limit the accuracy of results for higher pressures. Therefore, more recent studies use the original Clapeyron equation with various models for the volume changes associated with the phase transitions [9].



These oversimplifications make data based on Clausius-Clapeyron to be unreliable. In addition, the old data using Clapeyron do not have appropriate volume corrections. The data from Anderson involves very high filling fractions of the hydrate. Some of the calculated filling fractions reported by Anderson [9] seem very high, even up to 282 K. And most calorimetry data do not have any measured filling fraction and often use a con

Therefore, there is a need for consistent and reliable enthalpies of hydrate formation or dissociation data, and that is why we propose the use of residual thermodynamics. This method is based on residual thermodynamics for all properties like equilibrium (pressure-temperature) curves, free energy change as thermodynamic driving force in kinetic theories, and enthalpies of hydrate formation and dissociation. This scheme is also not limited to heterogeneous hydrate formation from water, and a separate hydrate former phase. It can be used to evaluate associated enthalpy change in homogeneous hydrate formation from dissolved hydrate forming guest molecules in water. Even though we have applied the theory to one component (methane) because of the acceptable limit of work to be presented, there is no limitation in its application to other guest molecules and mixtures of hydrate formers (as we shall demonstrate in subsequent work), the formalism is written for mixtures. Another important advantage of this approach, unlike the Clapeyron method is that it can easily be extended to conditions outside of equilibrium as well as to other hydrate phase transitions. Applicable examples are enthalpy changes associated with hydrate forming from dissolved hydrate guest molecules in water, and the reverse process of hydrate dissociation to water under-saturated with guest molecules. Additional applicable hydrate phase transitions are nucleation of hydrate towards mineral surfaces. Our filling fractions seem realistic and reproduce equilibrium pressures as shown in Figure 1. Anderson [9] used a specific code. This code is based on fitting of also the difference between chemical potential of empty hydrate and water as well as associated fitting of several related differences needed to calculate chemical potential differences up to actual temperatures and pressures. Fitting fundamental properties like chemical potentials is by itself questionable.

Our estimates of enthalpy change for methane hydrate formation from pure methane and liquid water along the hydrate equilibrium (P, T) curve, that is three-phase co-existence conditions (liquid water, hydrate and gas simply represented as L-H-V) are presented in Figure 2 and have been calculated using residual thermodynamics.

In this figure, our intention is not to validate our scheme using these literature values. Based on all the limitations we have pointed out above, we do not expect our result to agree perfectly with literature. However, Nakamura et al. [12] results are closer to the results of our work compared to the other literature. The results estimated from Clapeyron approaches by Nakamura et al. [13] and Anderson [9] disagree significantly both in values and trend. There is a very wide difference or deviation in their results. The work of Nakamura et al. [13] even though it shows a very weak dependence on temperature till around 280 K, follows similar trend with our work, therefore, we have Table 1 for easy comparison. Table 2 gives the results from using our scheme and some literature [9, 14, 15]. Kang et al. [15] estimated enthalpy change of phase transition at 274.15 K from isothermal micro-calorimeter experiment is only also close to result of this scheme at 274.10 K, it is only 0.4 % higher than the estimated values from the residual thermodynamic approach. The pressure at this temperature is missing in the paper of Kang et al. [15]. It is also important to keep in mind that also experiments have various limitations. Some of these are discussed by Kvamme et al. [16]. Anderson's [9] results are the lowest and the trend is opposite to those of Nakamura et al. [13] and this work. Application of this scheme for CO₂ guest molecule and the implication of enthalpy changes of hydrate phase transitions for simultaneous methane production from in-situ methane hydrates and storage of CO₂ (zero-emission concept) as CO₂ hydrate can be found in [17, 18].

Clausius approach, or simplified Clausius-Clapeyron approach, is generally not applicable for mixtures. At least not in the simple form used by Anderson [9] and others. For a pure component there is no composition dependency on either side of the co-existence curve. This changes the formal derivation of Clausius when changing to mixtures and might make it difficult to use. Hydrate is a mixed component and even the use of Clapeyron for hydrate is not straightforward. There are publications that formaluate a fugacity for hydrate, which at best is empirical. Fugacity is uniquely related to chemical potential on individual component basis.

To the best of our knowledge, there are no other models for enthalpy that can be utilized for gas mixtures [19, 20], and for different hydrate phase transitions like for instance hydrate formation from dissolved hydrate formers in water [21]. In principle there is no limit in the various hydrate formation possibilities.



As long as chemical potential for water and hydrate formers can be calculated then the model can be utilized. See for instance Kvamme et. al [22] for example of work in progress on hydrate formation from adsorbed methane in structured water towards mineral surfaces. And since the model is derived from Gibbs free energy model it is also consistent [19] and incorporates impact of component in water that affects chemical potentials for water, also on enthalpies.

In this work, hydration number was also estimated as given in Table 2 where the results from this work are compared with literature. The enthalpies are negative because hydrate formation is exothermic. The hydrate formation enthalpy is the heat of hydrate crystallization that must be transported out of the system, the system must lose this heat if the hydrate must form when every other condition favourable for hydrate to form is met. The heat transport is about 2-3 times [23] the magnitude of mass transport, that is more rapid. Heat transport limitation could lead to hydrate dissociation. These enthalpy values are the same for methane hydrate dissociation. But for hydrate dissociation, the values will be positive since heat is added to the system, or heat is required by the system for hydrate dissociation to proceed.

4 Conclusion

We used a consistent thermodynamic approach to evaluate the enthalpies of hydrate formation and dissociation and hydration number of methane hydrate. The methane hydrate equilibrium pressure-temperature curve estimated with this scheme agrees well with literature.

The results estimated from Clapeyron approaches by Nakamura et al. [12] and Anderson [8] disagree significantly both in values and trend. Nakamura et al. [12] are closer to the results of this work compared to the other literature. The residual thermodynamic method does not have the limitations of Clausius-Clapeyron and Clapeyron approaches. The scheme has more capabilities like the ability for easy calculation of enthalpies of hydrate phase transitions for other phase transitions like for instance, in case of hydrate forming from aqueous solution, and it can straightforwardly be extended to conditions outside of equilibrium as well as to other hydrate phase transitions

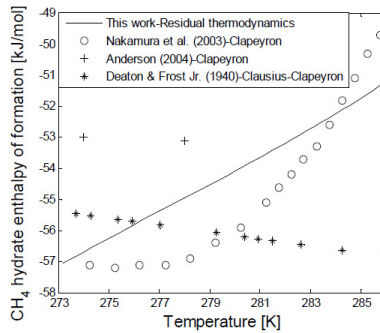


Figure 2: Estimated enthalpies of methane hydrate formation using residual thermodynamics (this work), Clapeyron equation [9, 15], and Clausius-Clapeyron equation [8].

Clapeyron equation (Nakamura et al. (2003))			Residual thermodynamics (This work)		
Temperature [K]	Pressure [bar]	Enthalpies of dissociation [kJ/mol]	Temperature [K]	Pressure [bar]	Enthalpies of formation [kJ/mol]
274.25	29.2	57.1	274.24	28.2	56.6
275.25	32.2	57.2	275.24	31.4	56.1
276.22	35.5	57.1	276.19	34.7	55.7
277.24	39.2	57.1	277.26	38.9	55.3
278.24	43.3	56.9	278.24	43.1	54.9
279.23	47.9	56.4	279.21	47.8	54.4

Table 1: Enthalpies of methane hydrate formation or dissociation [7].

	Method	Temperature [K]	Pressure [bar]	Enthalpy of formation/dissociation [kJ/mol]	Hydration number (n)
		273.15	25.19	-57.07	6.46
This work	Residual Thermodynamics	274.10	27.82	-56.64	6.43
		278.02	42.15	-54.94	6.35
		274.00	28.50	53.00	5.89
Anderson, G. K. (2004)	Clapeyron equation	278.00	42.80	53.10	5.79
		273.15	n/a	55.12	n/a
Deaton & Frost (1946)	Clausius-Clapeyron equation	273.15	n/a	55.12	n/a
Kang et al. (2001)	Experiment-Isothermal microcalorimeter	274.15	n/a	56.84	n/a

Table 2: Enthalpies of hydrate formation and dissociation and hydration number [8, 13, 14].

References

- [1] Aromada S A, Kvamme B. New approach for evaluating the risk of hydrate formation during transport of hydrocarbon hydrate formers of SI and sII. *AIChE Journal* 65(3), 1097-1110, (2019). DOI: 10.1002/aic.16493
- [2] Kvamme B, Aromada S A. Risk of hydrate formation during the processing and transport of Troll gas from the North Sea. *Journal of Chemical & Engineering Data* 62(7), 2163-2177 (2017). DOI: 10.1021/acs.jced.7b00256
- [3] Aromad S A, Kvamme B. Impacts of CO₂ and H₂S on the risk of hydrate formation during pipeline transport of natural gas. *Frontiers of Chemical Science and Engineering*, 1-12 (2019). DOI: 10.1007/s11705-019-1795-2
- [4] Kvamme B, Aromada S A, Saeidi N. Heterogeneous and homogeneous hydrate nucleation in CO₂/water systems. *Journal of Crystal Growth*, 522, 160-174 (2019).
- [5] Anderson R, Llamado M, Tohidi B, Burgass R W. Experimental measurement of methane and carbon dioxide clathrate hydrate equilibria in mesoporous silica. *The Journal of Physical Chemistry B*, 107(15), 3507-3514 (2003). DOI: 10.1021/jp0263370
- [6] Kvamme B. Environmentally Friendly Production of Methane from Natural Gas Hydrate Using Carbon Dioxide. *Sustainability* 11(7), 1-23 (2019). DOI: 10.3390/su11071964
- [7] Gupta A, Lachance J, Sloan E D, Koh C A. Measurements of methane hydrate heat of dissociation using high pressure differential scanning calorimetry. *Chemical Engineering Science*, 63, 5848-5853 (2008). DOI: 10.1016/j.ces.2008.09.002
- [8] Deaton W M, Frost Jr E M. In: Proceeding of American Gas Association, 1940, 122, Houston, Texas, May 6 (1940). Cross referenced from [6]
- [9] Anderson G K. Enthalpy of dissociation and hydration number of methane hydrate from the Clapeyron equation. *The Journal of Chemical Thermodynamics*, 36(12), 1119-1127, (2004). DOI: 10.1016/j.jct.2004.07.005
- [10] Kvamme B, Tanaka H. Thermodynamic stability of hydrates for ethane, ethylene, and carbon dioxide. *The Journal of Physical Chemistry*, 99(18), 7114-7119, (1995).
- [11] Kvamme B, Kuznetsova T, Stensholt S, Sjöblom S. Investigations of the Chemical Potentials of Dissolved Water and H₂S in CO₂ Streams Using Molecular Dynamics Simulations and the Gibbs-Duhem Relation. *Journal of Chemical & Engineering Data*, 60(10), 2906-2914 (2015). DOI: 10.1021/acs.jced.5b00267
- [12] Kvamme B, Forrisdahl O K. Polar guest-molecules in natural gas hydrates. *Fluid Phase Equilibria*, 83, 427-435, (1993). DOI: 10.1016/0378-3812(93)87047-5.
- [13] Nakamura T, Makino T, Sugahara T, Ohgaki K. Stability boundaries of gas hydrates helped by methane-structure-H hydrates or methylcyclohexane and cis-1,2-dimethylcyclohexane. *Chemical Engineering Science*, 58(2), 269-273, (2003). DOI: 10.1016/S0009-2509(02)00518-3
- [14] Deaton W M, Frost Jr E M. Gas hydrate composition and equilibrium data. *Oil Gas Journal*, 45, 170-178 (1946). Cross referenced from [6]



- [15] Kang S P, Lee H, Ryu B J. Enthalpies of dissociation of clathrate hydrates of carbon dioxide, nitrogen, (carbon dioxide + nitrogen), and (carbon dioxide + nitrogen + tetrahydrofuran). *The Journal of Chemical Thermodynamics*, 33(5), 513-521 (2001). DOI: 10.1006/jcht.2000.0765.
- [16] Kvamme B, Aromada S A, Gjerstad P B. Consistent enthalpies of the hydrate formation and dissociation using residual thermodynamics. *Journal of Chemical & Engineering Data*, 64(8), 3493-3504 (2019).
- [17] Aromada S A, Kvamme B, Wei N, Saeidi N. Enthalpies of hydrate formation and dissociation from residual thermodynamics. *Energies*, 12(24), 4726 (2019).
- [18] Aromada S A, Kvamme B. Production of Methane from Hydrate and CO₂ Zero-Emission Concept. Presented at the 10th EUROSIM2019 Congress, Logroño (La Rioja), Spain. Preprint: 1-5 (2019, July).
- [19] Kvamme B. Kinetics of hydrate formation, dissociation and reformation. *Chemical Thermodynamics and Thermal Analysis*, 1-2, 100004, March (2021).
- [20] Kvamme B, Clarke M. Hydrate Phase Transition Kinetic Modeling for Nature and Industry—Where Are We and Where Do We Go? *Energies*, 14(14), 4149 (2021).
- [21] Kvamme B. Enthalpies of hydrate formation from hydrate formers dissolved in water. *Energies*, 12(6), 1039 (2019).
- [22] Kvamme B, Zhao J, Wei N, Sun W, Saeid N, Pei J, Kuznetsova T. Hydrate production philosophy and thermodynamic calculations. *Energies*, 13(3), 672 (2020).
- [23] Svandal A. Modeling Hydrate Phase Transitions Using Mean-Field Approaches [PhD dissertation], Bergen, Norway: University of Bergen, (2006).

Paper 12

Enthalpies of hydrate formation and dissociation from residual thermodynamics

By


Solomon Aforkoghene Aromada, Bjørn Kvamme, Na Wei, and Navid Saeid

Published in

Energies, 2019, 12 (24): 4726

Article

Enthalpies of Hydrate Formation and Dissociation from Residual Thermodynamics

Solomon Aforkoghene Aromada ^{1,*} , Bjørn Kvamme ², Na Wei ² and Navid Saeidi ³¹ Department of Physics and Technology, University of Bergen, Allegaten 55, 5007 Bergen, Norway² State Key Laboratory of Oil and Gas Reservoir Geology and Exploitation, Southwest Petroleum University, Xindu Road No. 8, Chengdu 610500, China; Kvamme_uib@outlook.com (B.K.); weina8081@163.com (N.W.)³ Environmental Engineering Department, University of California, Irvine, CA 92697, USA; saeidin@uci.edu

* Correspondence: Solomon.Aromada@student.uib.no or saromada@gmail.com

Received: 18 November 2019; Accepted: 7 December 2019; Published: 11 December 2019



Abstract: We have proposed a consistent thermodynamic scheme for evaluation of enthalpy changes of hydrate phase transitions based on residual thermodynamics. This entails obtaining every hydrate property such as gas hydrate pressure-temperature equilibrium curves, change in free energy which is the thermodynamic driving force in kinetic theories, and of course, enthalpy changes of hydrate dissociation and formation. Enthalpy change of a hydrate phase transition is a vital property of gas hydrate. However, experimental data in literature lacks vital information required for proper understanding and interpretation, and indirect methods of obtaining this important hydrate property based on the Clapeyron and Clausius-Clapeyron equations also have some limitations. The Clausius-Clapeyron approach for example involves oversimplifications that make results obtained from it to be inconsistent and unreliable. We have used our proposed approach to evaluate consistent enthalpy changes of hydrate phase transitions as a function of temperature and pressure, and hydration number for CH₄ and CO₂. Several results in the literature of enthalpy changes of hydrate dissociation and formation from experiment, and Clapeyron and Clausius-Clapeyron approaches have been studied which show a considerable disagreement. We also present the implication of these enthalpy changes of hydrate phase transitions to environmentally friendly production of energy from naturally existing CH₄ hydrate and simultaneously storing CO₂ on a long-term basis as CO₂ hydrate. We estimated enthalpy changes of hydrate phase transition for CO₂ to be 10–11 kJ/mol of guest molecule greater than that of CH₄ within a temperature range of 273–280 K. Therefore, the exothermic heat liberated when a CO₂ hydrate is formed is greater or more than the endothermic heat needed for dissociation of the in-situ methane hydrate.

Keywords: hydrate; enthalpy; hydrate formation; residual thermodynamics; CO₂; methane; hydration number; hydrate dissociation

1. Introduction

The international interest in natural gas hydrates as a potential source of energy is increasing rapidly [1–7]. Important global economies [2,5,8] in the world, like for instance Japan and China, are highly dependent on import of energy. These countries have substantial resources of natural gas hydrates [2]. For China, the beneficial situation is that these hydrate energy sources are located offshore as well as onshore in permafrost regions [3,9]. These natural resources have been estimated to be huge in amount by Makogon et al. [2] and Collett [10]. However, the exact or accurate amount is still being debated, thus, uncertain [8]. Klauda and Sandler [11] predicted it is more than 74,200 metric gigatons (Gt) from thermodynamic modelling. While Milkov [12], based on the available information

on natural gas hydrate distribution puts this amount at 2500 Gt. Nevertheless, as stated above, natural gas hydrates are considered as a potential source of unconventional energy for the future [1–8].

A large variety of techniques for mining or production of the energy resources have been recommended in the last three decades till date. Most efforts have been devoted to investigation of thermal stimulation and pressure reduction. A more novel approach of using CO₂ is attractive due to the combination of energy production and long-term safe storage of CO₂ as hydrate. And as we show in this work the enthalpy changes of hydrate phase transitions of both (methane and carbon dioxide) components will play a vital function in this process. Thus, it is imperative to obtain accurate values of these heat of hydrate formation and dissociation.

However, the data that can be found in literature for enthalpy of hydrate phase transition obtained by experiment most times lack vital information needed for proper understanding and interpretation. Available experimental data for hydrate dissociation enthalpies are filled with various sources of bias that we have discussed in separate papers. Several data available in literature are limited and relevant information needed for proper understanding and interpretation are frequently missing. Sometimes information about pressure, temperature or of both properties is missing [13]. Hydration number and hydrate composition are also not available sometimes. The equation of state applied is also not reported in some literature.

The Clausius-Clapeyron approach is the simplest method that is generally applied to estimate enthalpy change of hydrate phase transition. The calculations are based on hydrate equilibrium data of pressure and temperature from experiments or calculated data. The Clausius-Clapeyron equation is over-simplified, which is the reason for the limitation of the accuracy of estimates especially at higher pressures. Therefore, the ordinary Clapeyron equation is favoured by most recent works applying different models for the change in volume associated with the hydrate phase transitions [14]. The estimates obtained by the use of the Clausius-Clapeyron approach are thus not reliable and not consistent because of its over-simplification. In addition, older data based on Clapeyron equation lack appropriate volume corrections. For example, the work of Anderson [14], hydrate filling fractions even up to 282 K seem very high. Several experimental data (calorimetry) also lack any measured filling fractions and regularly use a constant value that suggest that they might just be guessed values. Information about superheating above the hydrate equilibrium conditions to completely dissociate the gas hydrate to liquid water and gas is normally not lacking.

However, thermodynamically, enthalpy change is uniquely but trivially related to change in free energy. Therefore, thermodynamic models used for description of change in free energy associated with hydrate phase transition (formation or dissociation) will have a consistent change in enthalpy on the basis of the specific models. This kind of consistent method applies to kinetic theories like classical nucleation theory (CNT) [15], phase-field theory [16–20], and multicomponent diffuse interface theory (MDIT) [21], and other kinetic theory that is complete. Being complete implies there is implicit coupling of heat and mass transports, together with the thermodynamics of phase transition. This is why we propose the use of residual thermodynamics which able to evaluate real and not mere ideal thermodynamic properties and the approach does not have the limitations of the other aforementioned methods. With residual thermodynamics, we can calculate enthalpy changes of hydrate phase transition which are consistent. We can calculate values outside of equilibrium, while the Clausius-Clapeyron and Clapeyron approached are based on equilibrium. Real hydrate phase transitions, in industry and nature—except in the laboratory—cannot reach equilibrium. This has been extensively discussed in our previous studies [22–24]. We can obtain the degree of superheating needed for dissociation of hydrates to liquid water and guest molecule back to its original phase (this is not included in this study but in a subsequent work to this).

There are substantial deviations between various experimental data. Likewise, calculations based on both the Clapeyron and Clausius-Clapeyron also vary considerably. The proposed residual thermodynamic scheme is even very much numerically simpler than Anderson's Clapeyron scheme [14,25,26] that goes through ice, and it is directly adaptable to gas mixtures. This study is a

continuation of our previous work [26] in the Project, “Simultaneous production of energy from in-situ methane hydrate and long-termed offshore storage of CO₂”. However, this work focuses on application or implication of the enthalpies. This work also involves use of more extensive literature, and we also make available data of enthalpies of hydrate phase transitions from our residual thermodynamic approach that other researchers can make comparison with. This approach will be applied to hydrate systems involving mixture of hydrate formers in our subsequent work.

2. Theoretical Analysis

Pure methane forms a structure denoted as structure I. In this structure, water molecules form two types of cavities. The smallest cavity consists of 20 water molecules and is suitable for surrounding molecules like for instance methane. A larger cavity consisting of 24 water molecules is large enough to larger molecules like for instance ethane.

The cavities are stabilized by the molecular volume of the “guest” that enters the cavity and weakens attractive forces which typically decay proportionally to the distance between water and methane to the inverse of power 6. This is similar to the attractive part of the Lennard-Jones (12-6) potential, and also the Kihara potential, which contains an additional parameter which is intended to imitate effects of molecular elongation.

Van der Waal and Platteeuw [27] used a semi grand canonical ensemble to derive a Langmuir type adsorption theory in which water molecules are fixed and rigid while molecules that enter cavities (guest molecules) are open to exchange with surrounding phases. The final result of the derivation is expressed in terms of chemical potential of water in hydrate:

$$\mu_{H_2O}^H = \mu_{H_2O}^{0,H} - \sum_{k=1,2} RTv_k \ln \left(1 + \sum_i h_{ij} \right) \quad (1)$$

$\mu_{H_2O}^H$ is the chemical potential of water in hydrate, while $\mu_{H_2O}^{0,H}$ is the chemical potential of water in an empty clathrate for the given structure in consideration. Historically, this value has not been calculated by theoretical methods but rather fitted to experimental data in the form of chemical potential of pure liquid water minus empty clathrate water chemical potential. See Sloan and Koh [28] for some examples of values. T stands for temperature, and P is pressure. k is an index for cavity types and j is an index for guest molecules in the various cavities. Number of cavities is v , with subscripts k for large and small cavities respectively. For structure I, which is the main focus here, $v_{\text{large}} = 3/24$ and $v_{\text{small}} = 1/24$. For structure II the corresponding numbers are $v_{\text{large}} = 1/17$ and $v_{\text{small}} = 2/17$.

The canonical partition functions for the cavities, h_{ij} that will be a result of the grand canonical derivation will generally be an exponential function of the chemical potential time Boltzmann integrals over interactions between guests and water (generally also with surrounding guest molecules [29]). In the classical formulation of van der Waal and Platteeuw [27] the result for a rigid lattice is:

$$h_{ki} = f_i^{\text{gas}}(T, P, \vec{x}) C_{ki}(T) = x_i \varphi_i(T, P, \vec{x}) P C_{ki}(T) \quad (2)$$

The Langmuir constant $C_{ki}(T)$ for a molecule i in cavity k and given below as Equation (3). In the simplest case of a monoatomic spherical guest molecules, the Langmuir constant is a simple integral over the Boltzmann factors of interaction energies between the guest molecule and surrounding waters.

$$C_{ki}(T) = \frac{1}{K_B T} \iiint e^{\beta[\varphi_{iw}(x,y,z)]} dx dy dz \quad (3)$$

For non-linear multi-atomic representations of guest molecules, the integration will involve rotational degrees of freedom.

The most common guest/water interaction model in present versions hydrate equilibrium codes based of the reference method is based on a spherically smeared out version of the Kihara potential for interactions between a water and a guest. The Kihara potential can be expressed as:

$$\varphi_{ij}(r_{ij}) = 4\varepsilon_{ij} \left[\left(\frac{\sigma_{ij}}{r_{ij} - a_{ij}} \right)^{12} - \left(\frac{\sigma_{ij}}{r_{ij} - a_{ij}} \right)^6 \right] \quad (4)$$

where i and j are molecular indices, while $r_{ij} - a_{ij}$ is the closest distance between the two molecules. σ_{ij} is a molecular diameter, and ε_{ij} is a well-depth. For a_{ij} equal to zero, Equation (4) reduces to the Lennard-Jones (12-6) potential. A summation of approximate pairwise interactions in Equation (3) is possible and integration can be conducted efficiently using a Monte Carlo approach [29,30]. It is, however, more common to use an integrated smeared interaction version in which the average water/guest interaction are smeared out over the surface of a spherically smoothed cavity radius R . Z is used as the number of waters represented in this spherical shell in Equation (4) below. Z is therefore 20 for small cavity and 24 for large cavity. The details of this integration to reach at the spherically smoothed potential is far too extensive to include here. See reference [28] for more details and further references as well as examples of values for Equation (4). The final results for each specific cavity k is:

$$\varphi_{iw}(r) = 2Z_k \varepsilon_{iw} \left[\frac{\sigma_{iw}^{12}}{R_k^{11} r} \left(\Delta^{10} + \frac{a_{iw}}{R_k} \Delta^{11} \right) - \frac{\sigma_{iw}^6}{R_k^5 r} \left(\Delta^4 + \frac{a_{iw}}{R_k} \Delta^5 \right) \right] \quad (5)$$

$$\Delta^N = \frac{1}{N} \left[\left(1 - \frac{r}{R_k} - \frac{a_{iw}}{R_k} \right)^{-N} - \left(1 - \frac{r}{R_k} - \frac{a_{iw}}{R_k} \right)^N \right] \quad (6)$$

The spherically symmetric integration version of Equation (3) can then be expressed as:

$$C_{ki}(T) = \frac{4\pi}{k_B T} \int_0^\infty e^{\beta[\varphi_{iw}(x,y,z)]} r^2 dr \quad (7)$$

Kvamme and Tanaka [31] also utilized a semi grand canonical ensemble and used molecular dynamics simulations to derive the same equation as Equation (1), but the meaning of chemical potential is now the physically average sampled chemical potential of water in empty clathrate based on a harmonic oscillator approach. These chemical potentials are therefore denoted as reference chemical potentials. Values for chemical potential of water in empty clathrates of structures I and II are plotted in Figure 1 below [30,31].

Parameters for linear fits of the various chemical potential in the plot is listed in Table 1 below.

$$\frac{\mu_{H_2O}^m}{RT} = a_0^m + a_1^m \left(\frac{273.15}{T} \right) \quad (8)$$

Table 1. Parameters for dimensionless chemical potential functions in Equation (8).

Water Phase, m	a_0	a_1
Empty structure I	-3.087	-18.246
Empty structure II	-3.188	-18.186
Ice ($T < 273.15$ K)	-2.639	-19.051
Liquid water ($T > 273.15$ K)	-5.610	-16.080

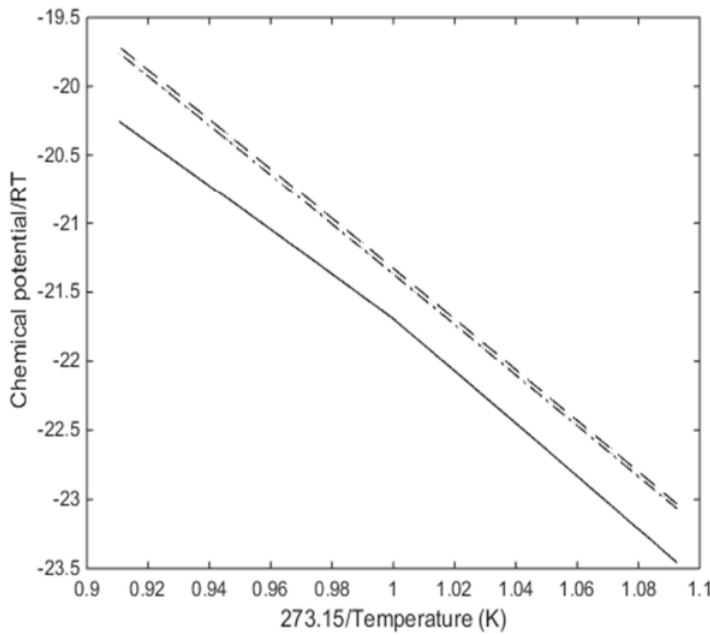


Figure 1. Dimensionless chemical potentials of water in empty clathrate of structure I (dashed-line), structure II (dash-dot line) and water as ice or liquid water (solid-line).

Similar for the evaluation of the canonical partition functions in Equation (1). These can also be evaluated for a rigid lattice in a similar fashion as Equation (2) but they can also be evaluated using a harmonic oscillator approach and be expressed as:

$$h_{ki} = e^{\beta[\mu_{ki} - \Delta g_{ki}]} \tag{9}$$

where β is equal to the inverse of the universal gas constant multiplied by temperature. Δg_{ki} stands for the effect on hydrate water for inclusion of a hydrate former (guest molecules) i in the hydrate cavity k . In an equilibrium situation, the chemical potential of the hydrate forming molecules i in the cavity (cage) k is uniform with its (guest molecules i) chemical potential in the co-existing (original) phase it emanates from. Considering a non-equilibrium situation, adjustment of the chemical potential is done for distance from equilibrium through a Taylor expansion as will be discussed later. The free energies of inclusion, that is Δg_{ki} have been reported in other works [22,32–34]. At thermodynamic equilibrium, μ_{ki} is the chemical potential of the hydrate forming guest molecule in its original phase (gas, liquid, or fluid) at the equilibrium pressure and temperature of the hydrate.

The composition of the hydrate is also trivially given by the derivation from the semi grand canonical ensemble and given by:

$$\theta_{ki} = \frac{h_{ki}}{\sum_j h_{kj}} \tag{10}$$

θ_{ki} is the filling fraction of component i in cavity (cage) type k . Then:

$$x_i^H = \frac{\theta_{large,i}v_{large} + \theta_{small,i}v_{small}}{1 + \theta_{large,i}v_{large} + \theta_{small,i}v_{small}} \tag{11}$$

where ν stands for the fraction of cavity in each water (i.e., per water) for the actual cavity (cage) type, as shown by the subscripts. The corresponding mole-fraction (concentration) of water is therefore:

$$x_{H_2O}^H = 1 - \sum_i x_i^H \quad (12)$$

And the associated hydrate free energy is then:

$$G^{(H)} = x_{H_2O}^H \mu_{H_2O}^H + \sum_i x_i^H \mu_i^H \quad (13)$$

Outside of equilibrium the corresponding result for a Taylor expansion is given by:

$$\begin{aligned} G_{Non-equilibrium}^H(T, P, \vec{x}) &= H^{H, Eq.}(T^{Eq.}, P^{Eq.}, \vec{x}^{Eq.}) + \sum_r \frac{\partial G^H}{\partial x_r} \bigg|_{P, T, i \neq r} (x_r - x_r^{Eq.}) \\ &+ \frac{\partial G^H}{\partial P} \bigg|_{T, x} (P - P^{Eq.}) + \frac{\partial G^H}{\partial T} \bigg|_{P, x} (T - T^{Eq.}) \end{aligned} \quad (14)$$

Residual Thermodynamic Modelling of Hydrate Phase Transition

With residual thermodynamics we are able to calculate real gas behaviour taking into account thermodynamic deviations from ideal gas behaviour [35]. A phase transition of hydrate (formation or dissociation) can be reversed along the pressure-temperature equilibrium curve of hydrate, just as it is used in the Clapeyron method for hydrate formation from a separate hydrate former phase (gas or liquid) and a free water phase. The change in the free energy for this hydrate phase change can be expressed as:

$$\Delta G^H = \left[x_{H_2O}^H (\mu_{H_2O}^H(T, P, \vec{x}^H) - \mu_{H_2O}^{water}(T, P, \vec{x})) + \sum_j x_j^H (\mu_j^H(T, P, \vec{x}^H) - \mu_j^{gas}(T, P, \vec{y}^{gas})) \right] \quad (15)$$

where superscript H signifies hydrate phase in Equation (15). T signifies temperature, and P is pressure. x signifies mole-fraction (hydrate or liquid phase), and y denotes mole-fraction in hydrate former phase (gas or liquid). j is an index for guest molecules or hydrate formers. Superscript *water* refers to water phase which is turned into hydrate. The water phase is usually liquid or ice, but in this study, we have considered liquid water only. And μ is chemical potential. The chemical potential of liquid water is estimated from the symmetric excess:

$$\begin{aligned} \mu_{H_2O}(T, P, \vec{x}) &= \mu_{H_2O}^{pure, H_2O}(T, P) + RT \ln [x_{H_2O} \gamma_{H_2O}(T, P, \vec{x})] \approx \mu_{H_2O}^{pure, H_2O}(T, P) + RT \ln [x_{H_2O}] \\ \lim(\gamma_{H_2O}) &= 1.0 \text{ when } x_{H_2O} \text{ approaches } 1 \end{aligned} \quad (16)$$

where γ represents activity coefficient, superscript H_2O signifies water phase and subscript H_2O is liquid water. In Equation (16) the approximation on the right-hand side (R.H.S) is not necessary. A theoretical model can be used for the activity coefficient or Gibbs-Duhem equation [36]. CH₄ solubility in water is very low, thus, the R.H.S of Equation (16) will then be close to pure water chemical potential. From to residual thermodynamics, the hydrate former j chemical potential is given as:

$$\mu_i(T, P, \vec{y}) = \mu_i^{pure, ideal\ gas}(T, P, \vec{y}) + RT \ln [y_i \varphi_i(T, P, \vec{y})] \quad (17)$$

where y_i denotes mole-fraction of component i in the gas mixture. φ_i represents the fugacity coefficient for component i . Ideal gas chemical potential for pure component i can be trivially computed for any model molecule by means of statistical mechanics from mass and intramolecular structure (bond

lengths and bond angles). The ideal gas chemical potential as well as density and temperature are obtainable from the momentum space canonical partition function. The Soave-Redlich-Kwong equation of state (SRK EOS) [37] have been used to calculate the fugacity coefficient and the density required for the ideal gas free energy evaluations.

Enthalpy change is trivially connected to the associated change in free energy thermodynamically as:

$$\frac{\partial \left[\frac{\Delta G^{Total}}{RT} \right]_{p,N}}{\partial T} = - \left[\frac{\Delta H^{Total}}{RT^2} \right] \tag{18}$$

superscript *Total* is brought in to also include the penalty of pushing away the old phases to make way for the new hydrate phase during hydrate formation. The total free energy change is in essence Equation (16) in addition to the interface free energy, multiplied by the area of contact between water and the hydrate forming phase in the nucleation stage of hydrate formation, divided by the number of molecules in the given core size. Since the critical nuclei sizes are small [15], the entire particle can be seen or considered as covered with water because of capillary forces. When the hydrate core grows beyond the critical core size, the penalty reduces rapidly in comparison to the free energy benefits of going into hydrate, given by Equation (16).

$$\frac{\partial \left[\frac{\mu_{H_2O}^H}{RT} \right]_{p,\vec{N}}}{\partial T} = \frac{\partial \left[\frac{\mu_{H_2O}^{0H}}{RT} \right]_{p,\vec{N}}}{\partial T} - \left[\frac{\partial}{\partial T} \right]_{p,\vec{N}} \left[\sum_{k=1,2} v_k \ln \left(1 + \sum_i h_{ki} \right) \right] \tag{19}$$

The water (liquid) phase in Equation (16), and the chemical potential of the empty hydrate, which is the first term on R.H.S. of Equation (19), is trivially evaluated from [31]. Then, the second term is rearranged as given in Equation (20):

$$\left[\frac{\partial}{\partial T} \right]_{p,\vec{N}} \left[\sum_{k=1,2} v_k \ln \left(1 + \sum_i h_{ki} \right) \right] = \left[\sum_{k=1,2} v_k \frac{\sum_i \left[\frac{\partial h_{ki}}{\partial T} \right]_{p,\vec{N}}}{\left(1 + \sum_i h_{ki} \right)} \right] \tag{20}$$

Differentiation of cavity partition functions can be written as:

$$\left[\frac{\partial h_{ki}}{\partial T} \right]_{p,\vec{N}} = h_{ki} \left[-\frac{1}{RT^2} (\mu_{ki} - \Delta g_{ki}) + \frac{1}{RT} \left(\frac{\partial \mu_{ki}}{\partial T} - \frac{\partial \Delta g_{ki}}{\partial T} \right) \right] \tag{21}$$

The partial differentiation in the last term on R.H.S. is numerically computed from the polynomial fits of [31]:

$$\frac{\partial \left[\frac{\mu_{H_2O}^H}{RT} \right]_{p,\vec{N}}}{\partial T} = \frac{\partial \left[\frac{\mu_{H_2O}^{0H}}{RT} \right]_{p,\vec{N}}}{\partial T} + \left[\sum_{k=1,2} v_k \frac{\sum_i h_{ki} \left[\frac{1}{RT^2} (\mu_{ki} - \Delta g_{ki}) + \frac{1}{RT} \left(\frac{\partial \mu_{ki}}{\partial T} - \frac{\partial \Delta g_{ki}}{\partial T} \right) \right]}{\left(1 + \sum_i h_{ki} \right)} \right] \tag{22}$$

$$\mu_{H_2O}^{0,H} = -RT^2 \frac{\partial \left[\frac{\mu_{H_2O}^{0H}}{RT} \right]_{p,\vec{N}}}{\partial T} + \left[\sum_{k=1,2} v_k \frac{\sum_i h_{ki} \left[(\mu_{ki} - \Delta g_{ki}) + T \left(\frac{\partial \mu_{ki}}{\partial T} - \frac{\partial \Delta g_{ki}}{\partial T} \right) \right]}{\left(1 + \sum_i h_{ki} \right)} \right] \tag{23}$$

the enthalpy of water (liquid) is yet more trivially estimated with the use of numerical differentiation of the polynomial fit of chemical potential as a function of temperature *T* as Kvamme and Tanaka [31] specified.

If we consider equilibrium scenario, the chemical potential of a specific hydrate former (guest molecule) in the two types of cages have to be uniform and they have to also be uniform with the

chemical potential of the same hydrate former in the original phase that it is taken or extracted from. Considering a heterogeneous hydrate formation, it means the chemical potential of the hydrate former phase, either gas or liquid. Nevertheless, outside of equilibrium which represent industrial situation and nature, the gradients in chemical potentials as function of pressure, temperature and concentrations (mole-fractions) need to reflect how the hydrate former behaves in the cage.

Enthalpies of different hydrate formers in the two cavity types can be computed utilizing Monte Carlo simulations along the lines described by Kvamme et al. (1993) [29] and Kvamme and Førrisdahl (1993) [30] by sampling interactions energies between water and guest molecule, and efficient volumes from the movements of the guest molecules:

$$H_{ki}^R = U_{ki}^R + (z_{ki} - 1)RT \quad (24)$$

U here stands for energy and superscript R signifies residual (interaction) contribution. z_{ki} is compressibility factor for the hydrate forming guest i in cavity k . The consistent ideal gas values for the same interaction models which have been used in computation of the residual values is trivial.

$$z_{ki} = \frac{PV_{ki}}{k_B T} \quad (25)$$

k_B is Boltzmann's constant and V_{ki} is the excluded volume of a hydrate forming molecule of type i in cavity of type k . This latter volume can be calculated from the sampled volume of centre of mass movements together with the excluded volume because of water/guest occupation.

The differentiation of chemical potential of a hydrate former molecule i in cavity (cage) type k with respect to temperature, T as required in Equation (22) is the negative of partial molar entropy for the same hydrate former molecule and can be computed as follows:

$$\left[\frac{\partial \mu_{ki}}{\partial T} \right]_{N, \vec{N}} = \frac{\mu_{ki} - H_{ki}}{T} \quad (26)$$

And Equation (23) can then be reorganised into:

$$\mu_{H_2O}^{0,H} = -RT^2 \left[\frac{\partial \left[\frac{\mu_{H_2O}^{0,H}}{RT} \right]}{\partial T} \right]_{P, \vec{N}} + \left[\sum_{k=1,2} v_k \frac{\sum_i h_{ki} [H_{ki} - \Delta g_{ki} + T \frac{\partial \Delta g_{ki}}{\partial T}]}{(1 + \sum_i h_{ki})} \right] \quad (27)$$

The residual enthalpies for guest molecule in a separate hydrate former (guest molecule) phase are trivially evaluated from:

$$H_{ki}^R = -RT^2 \sum_i y_i \left[\frac{\partial \ln \phi_i^{gas}}{\partial T} \right]_{P, y_{j \neq i}} \quad (28)$$

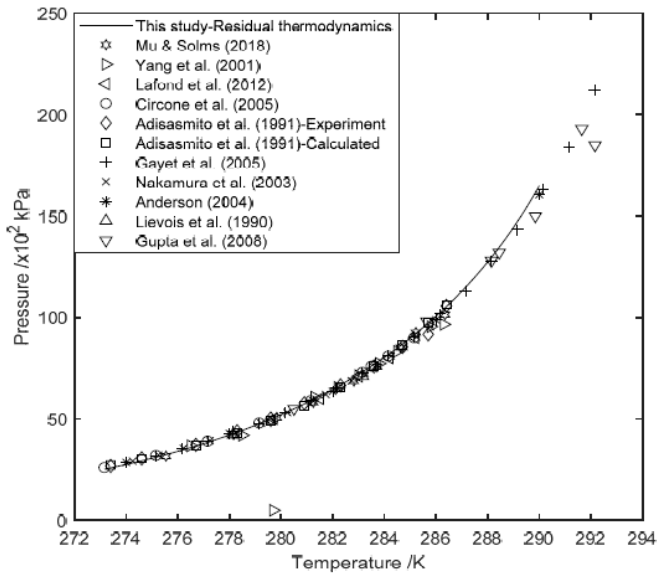
The same Soave-Redlich-Kwong [37] equation of state (SRK EOS) is applied for estimating fugacity coefficients for the chemical potentials.

3. Results and Discussion

3.1. Hydrate Equilibrium Curves Using Residual Thermodynamics

Hydrate equilibrium (P-T) curves calculated for methane and carbon dioxide hydrates using our scheme based on residual thermodynamic scheme approach are plotted with experimental (and some calculated) data in Figure 2a,b. For CH₄ hydrate, we compared our estimates with different 11 data sets from literature [14,38–46], and our CO₂ hydrate estimates are also compared with 11 different data sets [13,25,38,42,47–52]. The agreement is sufficiently good even though we did not do any empirical data fitting because it is not a priority. Our priority is to have the statistical mechanical

model used [31] without adjustable parameters in all aspect, including the chemical potential of empty hydrate and that of water (ice and liquid). For CO₂ (Figure 2b) at 283 K, a jump can be observed. This has been explained in some of our previous studies [53,54]. The jump represents a point where the hydrate former undergoes a phase split (from gas phase to both liquid + gas), if we increase the P-T conditions along the equilibrium curve. It is caused by a change to a higher density because of part of the CO₂ becoming liquid at this higher pressure. This point is called a “quadruple point”; hydrate + liquid water + liquid CO₂ + CO₂ gas co-exist at this point. Several literature do not show this jump. Some smoothen the curve and some stop their evaluations at this point. However, Ohgaki et al. [52] show this jump and show that these high pressures are due to liquid phase of CO₂. Our calculations took account of the presence of both liquid CO₂ and CO₂ gas as from this quadruple point, which is realistic. Ohgaki et al. [52] performed their evaluations for each of the separate phases (liquid and gas) of CO₂. However, this is not the focus of this paper. The focus is on reviewing and revealing the wide differences in values calculated for enthalpy changes of hydrate phase transition (formation or dissociation) and the importance of enthalpies in CH₄-CO₂ swap.



(a)

Figure 2. Cont.

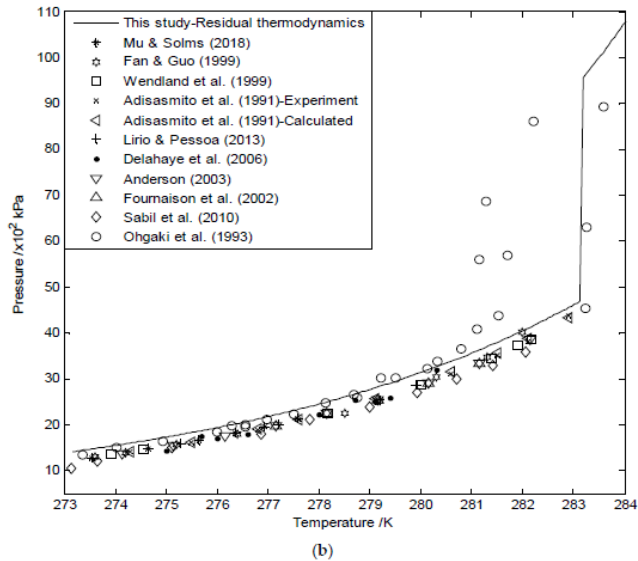


Figure 2. (a) Equilibrium (P, T) curve of methane (solid line) from residual thermodynamics compared with literature-experimental and calculated enthalpy data [14,38–46]; (b) Equilibrium (P, T) curve of carbon dioxide calculated from residual thermodynamics compared with literature-experimental and calculated enthalpy data [13,25,38,42,47–52].

3.2. Enthalpy Changes of Hydrate Formation or Dissociation: Residual Thermodynamics versus Other Approaches

Enthalpy change of a hydrate phase transition, hydrate formation or dissociation is a very vital property of gas hydrate [13] as we have mentioned earlier. For example, to produce natural gas from the vast amount of in-situ methane hydrates dispersed in the world, information about the dissociation heat of these hydrates is very vital. In gas transport in form of hydrate, we also require this information about heat of formation and dissociation of the hydrate for effective and efficient gas recovery. Enthalpy change of hydrate formation or dissociation is normally obtained by direct measurement by means of experiment [45,55,56], or indirectly by calculations based on thermodynamic models. The Clausius–Clapeyron [46,50,57] and Clapeyron [14,25,46] equations are generally used by many researchers. Some researchers use these equations with different modifications [50,58]. We have focused on only CH₄ and CO₂ hydrate guest molecules in this study because they are the relevant components in our project: simultaneous CH₄ production from in-situ CH₄ hydrate and long-term storage of CO₂ as hydrate. We have also reported our calculations in hydrate dissociation (positive values). However, both formation and dissociation have the same values, negative values for hydrate formation since it is exothermic process and positive values for dissociation being an endothermic process.

In this section and the subsequent Sections 3.3 and 3.4, we are not using literature data to verify or validate our thermodynamic scheme. That has been done in Section 3.1. This is to show the picture of how the values obtained from the literature (even values from the same method) vary substantially. A look at several literature shows remarkable disagreement in reported values obtained for enthalpy changes of hydrate phase transition. Lirio and Pessoa [13] acknowledged this variation in literature values and their results. Thus, they [13] and some other literature have more confidence in their average values.

Estimates using residual thermodynamics which we have proposed are plotted with several data sets (experimental and calculated data from the Clapeyron and Clausius-Clapeyron equations) from literature as can be seen in Figure 3a,b and Figure 4a,b. We have plotted enthalpy changes of hydrate dissociation in kJ/mol of guest molecule as a function of temperature for CH₄ and CO₂ in Figures 3a and 4a respectively. While Figures 3b and 4b present enthalpy changes of hydrate dissociation in kJ/mol of guest molecule as a function of pressure for CH₄ and CO₂ respectively. Figure 3a,b also include our calculations using Clapeyron and Clausius-Clapeyron approaches. These figures represent what we have in literature now. They present the picture of varying values of enthalpy changes of hydrate formation and dissociation as mentioned above. For example, Gupta et al. [46] obtained different values for the enthalpy changes from experiment, Clapeyron and Clausius-Clapeyron approaches as presented in both Figure 3a,b. Our estimates using residual thermodynamics and the other two indirect methods also show great difference in values as can be seen in Figure 3a–Figure 4b. It is observed that Clausius-Clapeyron calculations give very high values, except when used with some modifications. The deviations are more in the case of CO₂ as can be observed in Figure 4a,b. Nevertheless, for methane hydrate, the results of Nakamura et al. [44] are closed to our results, and also the experimental results of Gupta et al. [46] but only between 280 and 286 K. A lot of literature reports a single value and sometimes it is the average of all the values calculated within a temperature range [13]. That is why we have only one value plotted for some studies in the figures. The single point value of Kang et al. [54] and Sloan and Fleyfel [58] are close to our results. We do not expect much agreement with our results based on the limitations of the other methods, especially, the simplicity of both the Clapeyron and Clausius-Clapeyron equations. Our calculations of enthalpy changes of hydrate dissociation and hydration (occupation) number for a temperature range of 273–290 K are presented in Table 2 with their pressures.

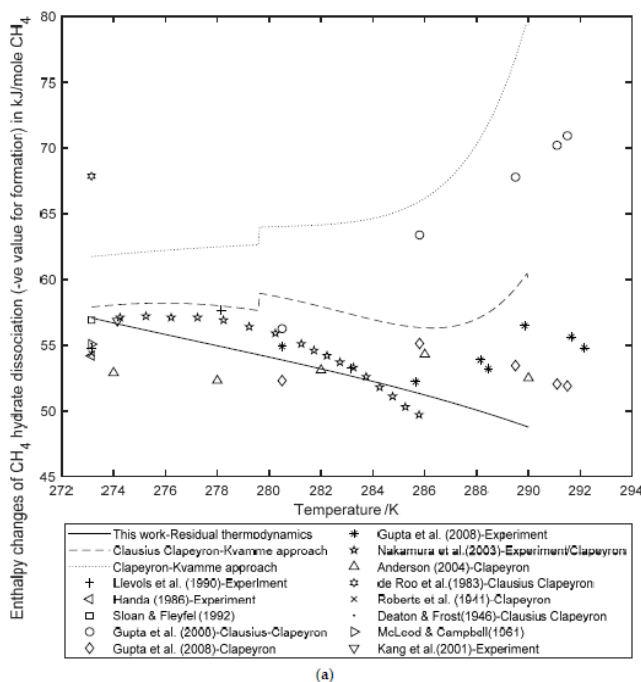


Figure 3. Cont.

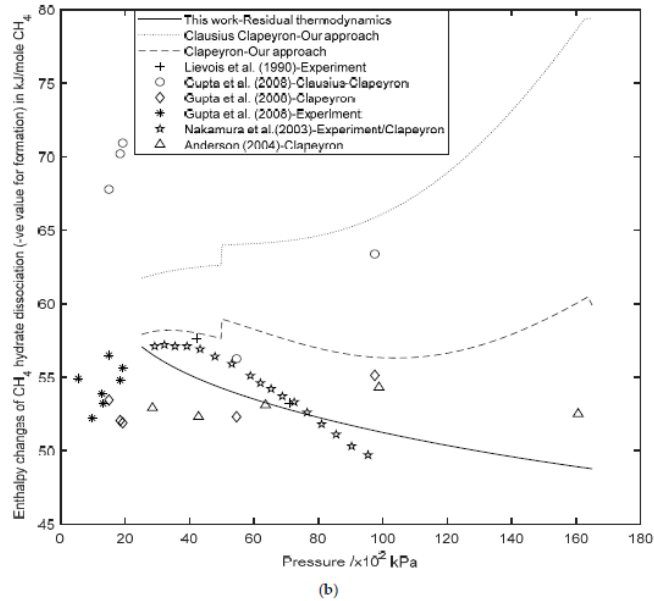
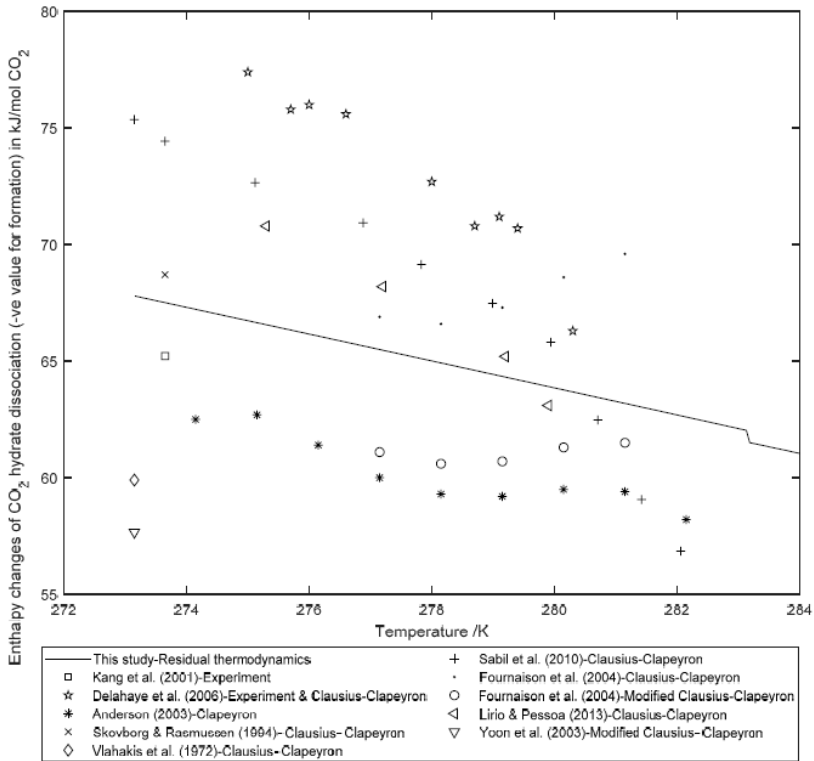
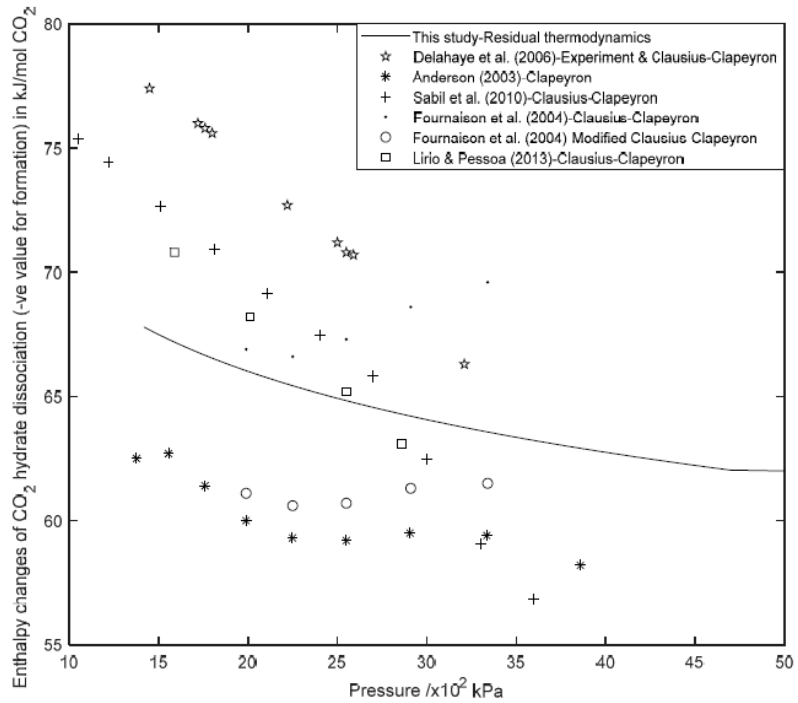


Figure 3. (a) Enthalpy changes of CH₄ hydrate dissociation (negative values for formation) in kJ/mol of CH₄ as a function of temperature from residual thermodynamics compared with the literature [14,44–46,55–57,59–62]; (b) Enthalpy changes of CH₄ hydrate dissociation (negative values for formation) in kJ/mol of CH₄ as a function of pressure from residual thermodynamics compared with the literature [14,44–46].



(a)

Figure 4. Cont.



(b)

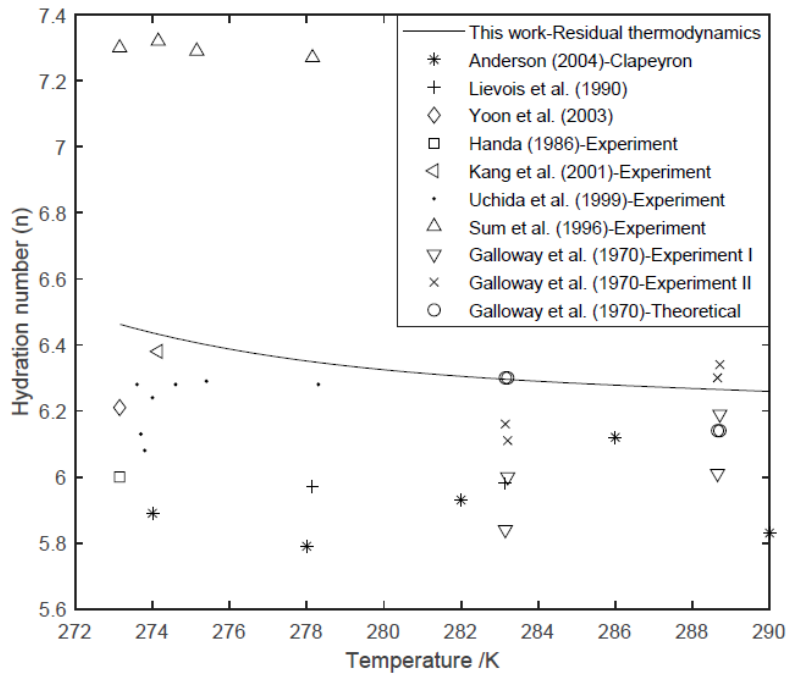
Figure 4. (a) Enthalpy changes of CO₂ hydrate dissociation (negative values for formation) in kJ/mol of CO₂ as a function of temperature from residual thermodynamics compared with the literature [13,25,49–51,55,58,63,64]; (b) Enthalpy changes of CO₂ hydrate dissociation (negative values for formation) in kJ/mol of CO₂ as a function of temperature from residual thermodynamics compared with the literature [13,25,49–51].

Table 2. Enthalpy changes of hydrate phase transition and hydration number of CH₄ and CO₂

Temperature (K)	Methane (CH ₄)			Carbon Dioxide (CO ₂)		
	Pressure	Hydration Number (n)	$\Delta H_{dissociation}$ (kJ/mol Guest)	Pressure	Hydration Number (n)	$\Delta H_{dissociation}$ (kJ/mol Guest)
	(kPa)			(kPa)		
273.16	25.19	6.46	57.07	14.19	7.26	67.79
274.17	27.87	6.43	56.63	15.73	7.24	67.24
275.13	31.01	6.41	56.19	17.59	7.22	66.67
276.15	34.53	6.38	55.75	19.73	7.20	66.08
277.16	38.45	6.37	55.31	22.21	7.18	65.50
278.17	42.83	6.35	54.88	25.06	7.16	64.91
279.13	47.43	6.34	54.47	28.17	7.14	64.36
280.14	52.87	6.32	54.03	31.96	7.11	63.77
281.16	58.97	6.31	53.57	36.34	7.09	63.18
282.17	65.80	6.30	53.11	41.42	7.07	62.59
283.13	73.03	6.30	52.66	46.95	7.05	62.03
284.14	81.64	6.29	52.17	109.88	6.69	60.96
285.15	91.41	6.28	51.65	128.38	6.67	60.40
286.17	102.55	6.28	51.11	152.24	6.64	59.86
287.13	114.65	6.27	50.57	183.38	6.62	59.39
288.14	129.55	6.27	49.97	233.44	6.59	58.96
289.16	147.28	6.26	49.33	313.22	6.57	58.68
290.00	164.94	6.26	48.76	404.15	6.55	58.55

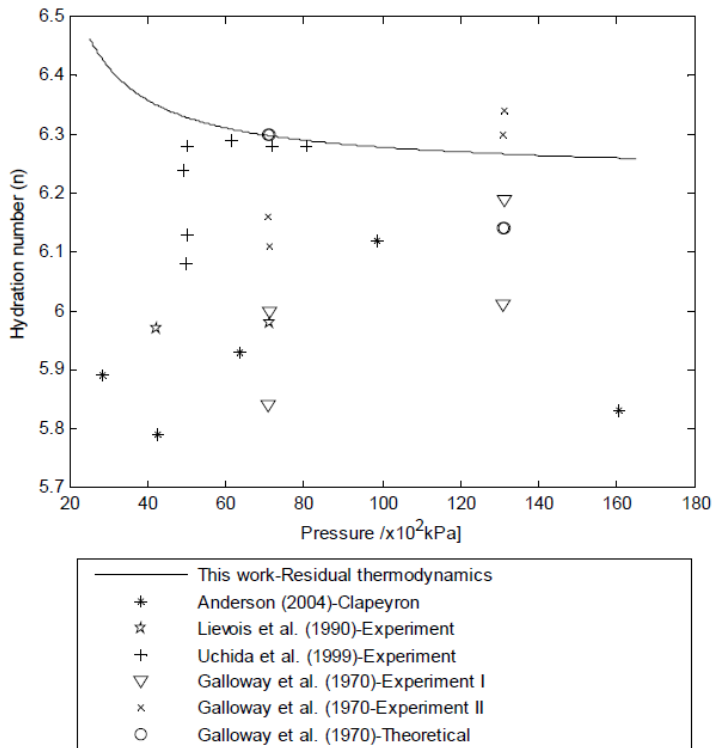
3.3. Hydration Number (n) Using Residual Thermodynamics versus Experimental Data

Figure 5a,b and Figure 6a,b present the overview of the values of our estimates of the hydration number (n), which is the number of water per guest molecule, and recalculated back from the calculated mole-fractions of guests in hydrate. Literature values are also plotted. We have plotted values of CH₄ and CO₂ as a function of temperature (Figures 5a and 6a) and as a function of pressure (Figures 5b and 6b). These figures also present the overview values calculated by various literature and our consistent approach. Essentially, our aim here is not to validate our studies with literature values, having seen the limitations in the other methods. However, in the case of CH₄ hydrate, the results of Galloway et al. [65] from their solid–solution theory at 283.15 K and 283.21 K agree with our results (Figure 5a,b). Kang et al. [55] value experimentally obtained at 273.65 K is also close (Figure 5a). In Figure 5b, that is from pressure perspective, the same theoretical results of Galloway [65] agree with our results. Uchida et al. [66] experimental results between 6000–8000 kPa also have good agreement.



(a)

Figure 5. Cont.

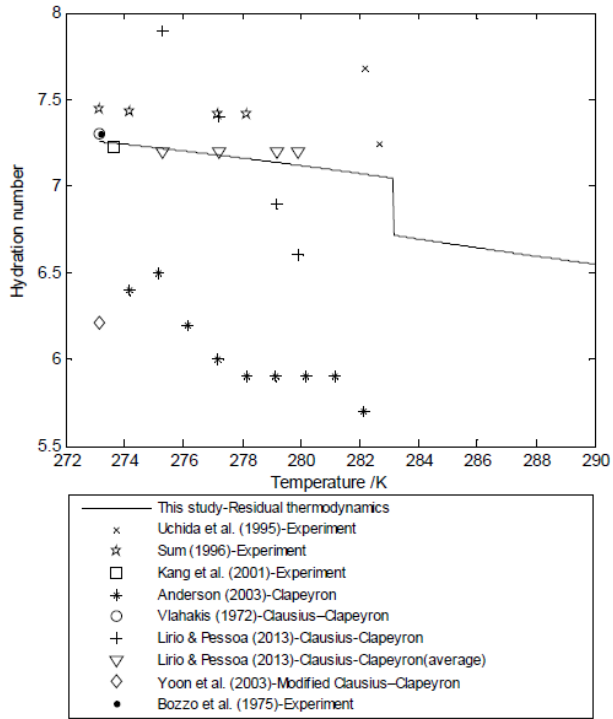


(b)

Figure 5. (a) Hydration number of CH_4 hydrate as a function of temperature from residual thermodynamics compared with the literature [14,45,55,56,58,65–67]; (b) Hydration number of CH_4 hydrate as a function of pressure from residual thermodynamics compared with the literature [14,45,65,66].

Both CH_4 and CO_2 are structure I hydrates. This structure has 46 molecules of water and two small and six large cavities. Since CH_4 can occupy both the small and large cavities, if we assume full occupation which is not realistic, then we will have $2 + 6 = 8$ cavities that CH_4 can occupy. This will give us a hydration number (n) of 46 water molecules divided by 8 cavities, which is 5.75. Therefore, the realistic hydration number of methane hydrate should be greater than this value.

The hydration number of CO_2 hydrate values obtained experimentally by Kang et al. [55], Bozzo et al. [68] and the value calculated by Vlahakis [64] from their Clausius-Clapeyron approach have good agreement with our results (Figure 6a). The results of Lirio and Pessoa. [13] along the hydrate equilibrium are not in agreement with our results. However, as mention earlier, they have more confidence in their average value and that is the value they compared with other literature. That is the value that is also in agreement with our results as can be seen in both Figure 6a,b.



(a)

Figure 6. Cont.

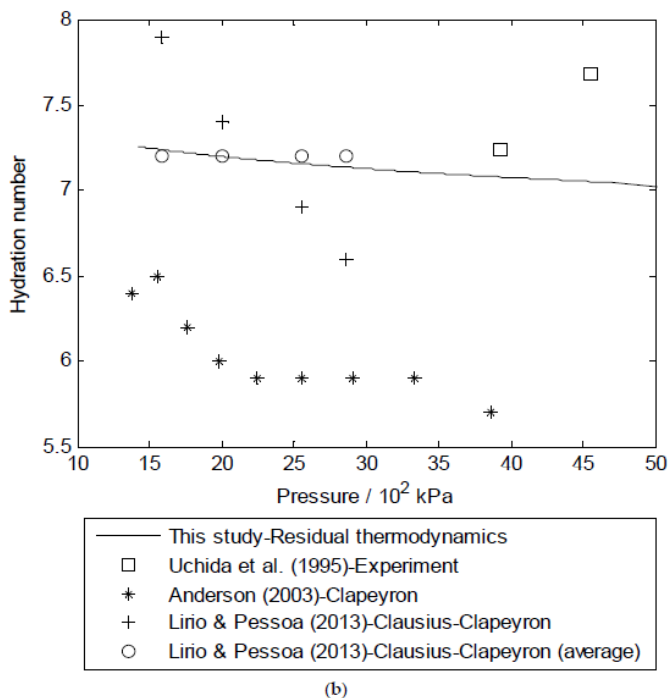


Figure 6. (a) Hydration number of CO₂ hydrate as a function of temperature from residual thermodynamics compared with the literature [13,25,55,58,64,67–69]; (b) Hydration number of CO₂ hydrate as a function of pressure from residual thermodynamics compared with the literature [13,25,69].

3.4. The Significance of Enthalpy Changes of Hydrate Formation or Dissociation in CH₄-CO₂ Swap

Beside the problem gas hydrates can pose in industrial applications involving pipeline transport of gas [23,24,53,70–73], the vast naturally occurring hydrates also offer potential possibility to provide a huge source of cleaner energy (compared to other fossil fuels) to the world, and a possibility of CO₂ sink (long-term storage) [54]. Much attention has been given to the production of natural gas from the abundant in-situ methane hydrate spread across the world. Highly populated nations like China, Japan, and Indian who depend on huge import of fuel for energy have been investing a lot of money in research and tests towards realizing self-sufficiency in energy through exploration of these vast source of cleaner energy. Pressure reduction [74] below hydrate stability pressure is one major method that is being explored. This can only take care of the thermodynamic driving force. However, whatever technology that will be used to produce these vast energy resources will require supply of heat to ensure successful operation. The lessons learnt from the two tests already carried out offshore of Japan [75] few years ago agree with this. Among other challenges, they encountered a freezing down problem because of insufficient heat supply from the surroundings. One solution to this is thermal stimulation [76], that is, by supplying heat using either hot water or steam. While it is possible technologically, economically, it has been assessed to be too expensive. Therefore, a novel solution which is an environmentally friendly solution is injection of carbon dioxide (CO₂) into the reservoir of in-situ CH₄ hydrate deposits. This is the focus in this section. Lee et al. [77] and also Falenty et al. [78] had confirmed a solid-state CO₂-CH₄ swap process but in the ice region. The main aim in this section is to draw our attention to the significance of the role enthalpies of CO₂ hydrate

formation and enthalpies of CH₄ hydrate formation can play in the swap process. Figure 7a and Figure 8b present our estimates of enthalpy changes of hydrate formation and dissociation.

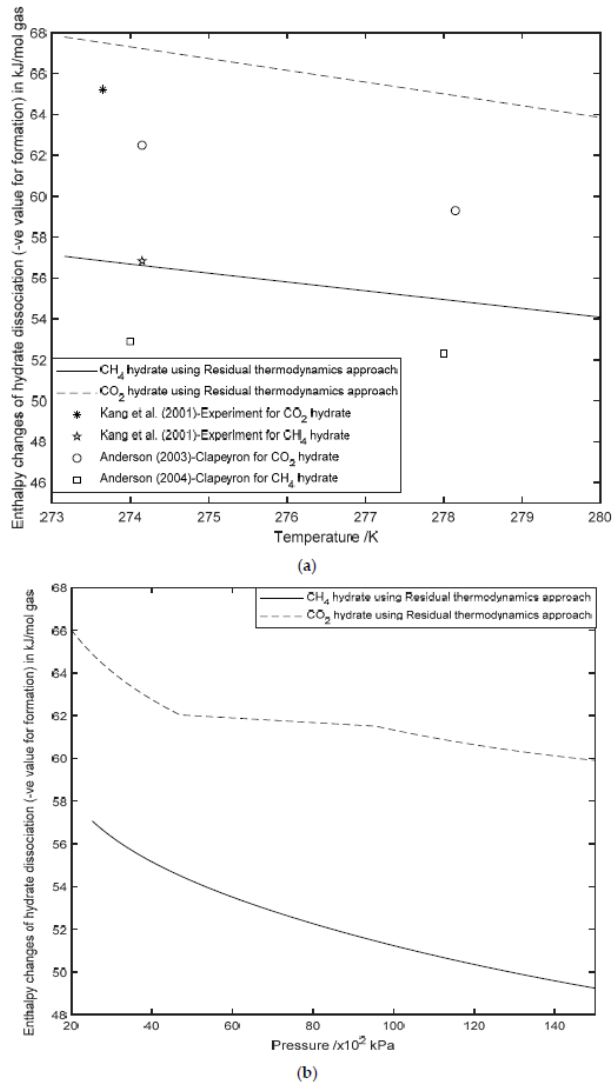
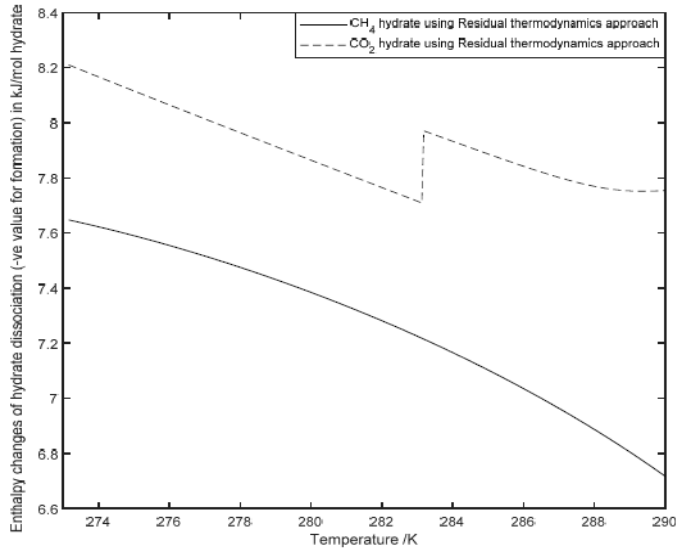
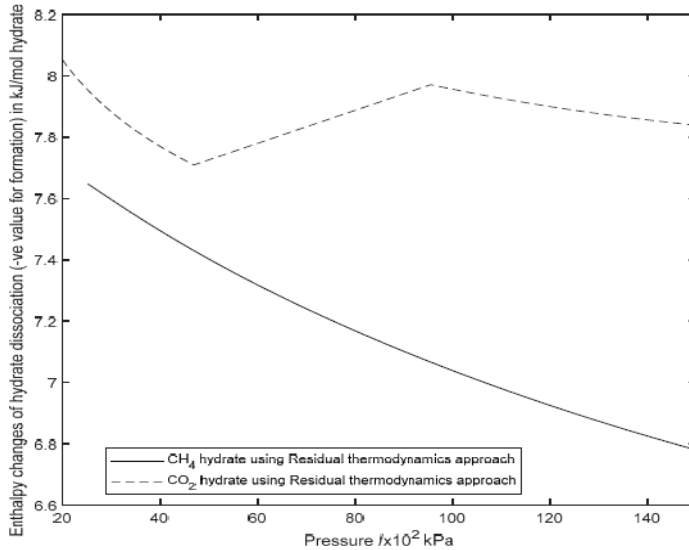


Figure 7. (a) Comparison of enthalpy changes of CH₄ and CO₂ hydrate dissociation (negative values for formation) as a function of temperature in kJ/mol of guest molecule from residual thermodynamics compared with the literature [14,25,55]; (b) Comparison of enthalpy changes of CH₄ and CO₂ hydrate dissociation (negative values for formation) as a function of pressure in kJ/mol of guest molecule from residual.



(a)



(b)

Figure 8. (a) Comparison of enthalpy changes of CH₄ and CO₂ hydrate dissociation (negative values for formation) as a function of temperature in kJ/mol of hydrate from residual thermodynamics; (b) Comparison of enthalpy changes of CH₄ and CO₂ hydrate dissociation (negative values for formation) as a function of pressure in kJ/mol of hydrate from residual thermodynamics.

Hydrate formation is an exothermic process, and hydrate dissociation process is endothermic. It can be seen clearly in Figure 7a,b and Figure 8a,b that the enthalpy changes for CO₂ hydrate phase transition are well over those for CH₄ hydrate formation or dissociation. Considering a temperature range of 273–280 K, the enthalpy changes we calculated from residual thermodynamics scheme for CO₂ hydrate formation are approximately 10–11 kJ/mol of guest molecule greater than the enthalpy changes of CH₄ dissociation (see Figure 7a,b). Kang et al. [55] calculated this difference to be 8.4 kJ/mol of guest molecule at 273.65 K. Anderson [14,25] calculated approximately 10 kJ/mol of guest molecule at 274 K and 7 kJ/mol of guest molecule at 278 K. These are significant differences (values). Basing the calculation on per mole of hydrate, we got about 0.5–0.6 kJ/mol hydrate within a temperature range of 273–280 K as can be observed in Figure 8a,b. The implication is, when CO₂ is injected into the in-situ methane hydrate reservoir, CO₂ hydrate will be formed either directly through a solid-state process or from the available free water (including pore water). Since CO₂ hydrate formation is an exothermic process, heat that is 10–11 kJ/mol of guest molecule greater than the heat requirement for CH₄ hydrate dissociation will be released. This heat is then available for further dissociation of CH₄ hydrate to liquid water and CH₄ gas. The CH₄ will be released through buoyancy forces and the liquid water will be available for further CO₂ hydrate formation and the process will go on. It is important to state here that this process is still under study and under development, and there are constraints which are also under investigation. CO₂ hydrate formation from CO₂ and pore water at the interface occurs very rapidly, which quickly forms a thin film of CO₂ hydrate at the interface [15] thereby blocking the pore space to limit further supply of CO₂. There have been suggestions of using nitrogen (N₂) in mixture with CO₂ to reduce the driving force. This reduces the driving force so much and leads to a very slow [33,71], ineffective and inefficient conversion of the in-situ CH₄ hydrate to CO₂ hydrate. Nevertheless, we recommend using surfactants instead of nitrogen, to reduce the hydrate nucleation and growth processes at the interface in order to enable an effective control of the simultaneous CH₄ production and long-term CO₂ storage in form of hydrate [79].

4. Conclusions

Enthalpy changes of hydrate phase transition is one of the most important properties of clathrate hydrate. However, the data in literature for enthalpy of hydrate formation and dissociation from experiment are lacking in vital information needed for proper understanding and interpretation. Indirect methods of obtaining this significant hydrate property based on the Clapeyron and Clausius-Clapeyron equations also have some limitations. The Clausius-Clapeyron approach for example involves oversimplifications that make results obtained from it to be inconsistent and unreliable. The approach can also not be used for very high-pressure systems. Therefore, we recommend a consistent thermodynamic scheme where every gas hydrate property such as hydrate pressure-temperature equilibrium curves, change in free energy (thermodynamic driving force in kinetic theories), and enthalpy changes involved in hydrate dissociation and formation are obtained based on residual thermodynamics approach. Calculations based on residual thermodynamics enable us to evaluate real gas behaviour with consideration of the thermodynamic deviations from ideal gas behaviour. We have given the overview of the estimates of enthalpy changes of hydrate phase transitions available in literature from experiments, Clapeyron and Clausius-Clapeyron approaches which shows remarkable disagreement in the various estimated values. Our calculations based on our proposed approach, and residual thermodynamics are plotted together. Overview of the available hydration number is also given in this work. The significance of these enthalpy changes of hydrate phase transitions to environmentally friendly energy production from in-situ methane hydrate and simultaneously storing carbon dioxide in form of gas hydrate is also highlighted in this study. Enthalpy changes of hydrate phase transition for CO₂ are between 10–11 kJ/mol of guest molecule more than that of CH₄ within a temperature range of 273–280 K. Kang et al. calculated a difference of 8.4 kJ/mol of guest molecule at 273.65 K, and Anderson calculated it to be 10 kJ/mol of guest molecule at 274 K and 7 kJ/mol of guest molecule at 278 K. And since heat is needed to be supplied from the surroundings during production

of methane from in-situ methane hydrate, injection of CO₂ into the reservoir of in-situ methane which will lead to CO₂ hydrate formation will also provide more heat per guest molecule than the heat per guest molecule needed to dissociate methane hydrate.

Author Contributions: Conceptualization, formal analysis, investigation, writing most parts of the manuscript—original draft, final editing, S.A.A.; Conceptualization, methodology, software, writing part of the manuscript—original draft, and supervision, B.K.; Supervision and review, N.W.; Project administration, review, N.S.

Conflicts of Interest: The authors declare no conflict of interest.

References

1. Collett, T.S. Gas hydrates as a future energy resource. *Geotimes* **2004**, *49*, 24–27.
2. Makogon, Y.F.; Holditch, S.A.; Makogon, T.Y. Natural gas-hydrates—A potential energy source for the 21st Century. *J. Pet. Sci. Eng.* **2007**, *56*, 14–31. [CrossRef]
3. Fu, X.; Wang, J.; Tan, F.; Feng, X.; Wang, D.; He, J. Gas hydrate formation and accumulation potential in the Qiangtang Basin, northern Tibet, China. *Energy Convers. Manage.* **2013**, *73*, 186–194. [CrossRef]
4. Anderson, B.J.; Kurihara, M.; White, M.D.; Moridis, G.J.; Wilson, S.J.; Pooladi-Darvish, M.; Gaddipati, M.; Masuda, Y.; Collett, T.S.; Hunter, R.B.; et al. Regional long-term production modeling from a single well test, Mount Elbert gas hydrate stratigraphic test well, Alaska North slope. *Mar. Petroleum. Geol.* **2011**, *28*, 493–501. [CrossRef]
5. Zhu, Y.; Zhang, Y.; Wen, H.; Lu, Z.; Jia, Z.; Li, Y.; Li, Q.; Liu, C.; Wang, P.; Guo, X. Gas hydrates in the Qilian mountain permafrost, Qinghai, Northwest China. *Acta. Geol. Sin.* **2010**, *84*, 1–10. [CrossRef]
6. Boswell, R. Is gas hydrate energy within reach? *Science* **2009**, *325*, 957–958. [CrossRef]
7. Dunn, C.; Eshbaugh, M. Japan is the second largest net importer of fossil fuels in the world. US Energy Information Association. 7 November 2013. Available online: <https://www.eia.gov/todayinenergy/detail.php?id=13711> (accessed on 7 December 2019).
8. Liu, C.; Ye, Y.; Meng, Q.; He, X.; Lu, H.; Zhang, J.; Liu, J.; Yang, S. The characteristics of gas hydrates recovered from Shenhu Area in the South China Sea. *Mar. Geol.* **2012**, *307*, 22–27. [CrossRef]
9. Lu, Z.; Zhu, Y.; Zhang, Y.; Wen, H.; Li, Y.; Liu, C. Gas hydrate occurrences in the Qilian Mountain permafrost, Qinghai province, China. *Cold Reg. Sci. Technol.* **2011**, *66*, 93–104. [CrossRef]
10. Collett, T.S. Energy resource potential of natural gas hydrates. *AAPG bulletin* **2002**, *86*, 1971–1992.
11. Klauda, J.B.; Sandler, S.I. Global distribution of methane hydrate in ocean sediment. *Energ. Fuel* **2005**, *19*, 459–470. [CrossRef]
12. Milkov, A.V. Global estimates of hydrate-bound gas in marine sediments: how much is really out there? *Earth-Sci. Rev.* **2004**, *66*, 183–197. [CrossRef]
13. Lirio, C.; Pessoa, F. Enthalpy of dissociation of simple and mixed carbon dioxide clathrate hydrate. *Chem. Eng. Trans.* **2013**, *32*, 557–582.
14. Anderson, G.K. Enthalpy of dissociation and hydration number of methane hydrate from the Clapeyron equation. *J. Chem. Thermodyn.* **2004**, *36*, 1119–1127. [CrossRef]
15. Kvamme, B.; Aromada, S.A.; Saeidi, N. Heterogeneous and homogeneous hydrate nucleation in CO₂/water systems. *J. Cryst. Growth* **2019**, *522*, 160–174. [CrossRef]
16. Kvamme, B.; Graue, A.; Aspenes, E.; Kuznetsova, T.; Gránásy, L.; Tóth, G.; Pusztai, T.; Tegze, G. Kinetics of solid hydrate formation by carbon dioxide: Phase field theory of hydrate nucleation and magnetic resonance imaging. *Phys. Chem. Chem. Phys.* **2004**, *6*, 2327–2334. [CrossRef]
17. Kvamme, B.; Qasim, M.; Baig, K.; Kivelä, P.H.; Bauman, J. Hydrate phase transition kinetics from Phase Field Theory with implicit hydrodynamics and heat transport. *Int. J. Greenh. Gas Control* **2014**, *29*, 263. [CrossRef]
18. Kivelä, P.H.; Baig, K.; Qasim, M.; Kvamme, B.R. Phase field theory modeling of methane fluxes from exposed natural gas hydrate reservoirs. *AIP Conf. Proc.* **2012**, *1504*, 351–363.
19. Svandal, A.; Kvamme, B.; Gránásy, L.; Pusztai, T.; Buanes, T.; Hove, J. The phase-field theory applied to CO₂ and CH₄ hydrate. *J. Cryst. Growth* **2006**, *287*, 486–490. [CrossRef]
20. Tegze, G.; Pusztai, T.; Tóth, G.; Gránásy, L.; Svandal, A.; Buanes, T.; Kuznetsova, T.; Kvamme, B. Multiscale approach to CO₂ hydrate formation in aqueous solution: Phase field theory and molecular dynamics. Nucleation and growth. *J. Chem. Phys.* **2006**, *124*, 234710. [CrossRef]

21. Kvamme, B. Kinetics of Hydrate Formation from Nucleation Theory. *Int. J. Off. Polar Eng.* **2002**, *12*, 256.
22. Kvamme, B.; Kuznetsova, T.; Bauman, J.M.; Sjöblom, S.; Avinash Kulkarni, A. Hydrate Formation during Transport of Natural Gas Containing Water and Impurities. *J. Chem. Eng. Data* **2016**, *61*, 936–949. [[CrossRef](#)]
23. Aromada, S.A.; Kvamme, B. New approach for evaluating the risk of hydrate formation during transport of hydrocarbon hydrate formers of sl and sll. *AIChE J.* **2019**, *65*, 1097–1110. [[CrossRef](#)]
24. Kvamme, B.; Aromada, S.A. Risk of Hydrate Formation during the Processing and Transport of Troll Gas from the North Sea. *J. Chem. Eng. Data* **2017**, *62*, 2163–2177. [[CrossRef](#)]
25. Anderson, G.K. Enthalpy of dissociation and hydration number of carbon dioxide hydrate from the Clapeyron equation. *J. Chem. Thermodyn.* **2003**, *35*, 1171–1183. [[CrossRef](#)]
26. Kvamme, B.; Aromada, S.A.; Gjerstad, P.B. Consistent Enthalpies of the Hydrate Formation and Dissociation Using Residual Thermodynamics. *J. Chem. Eng. Data* **2019**, *64*, 3493–3504. [[CrossRef](#)]
27. van der Waals, J.H.; Platteeuw, J.C. Clathrate solutions. *Advan. Chem. Phys.* **1959**, *2*, 1–57.
28. Sloan, E.D., Jr.; Koh, C.A. *Clathrate Hydrates of Natural Gases*; CRC Press: Boca Raton, FL, USA, 2007.
29. Kvamme, B.; Lund, A.; Hertzberg, T. The influence of gas-gas interactions on the Langmuir constants for some natural gas hydrates. *Fluid Phase Equilib.* **1993**, *90*, 15–44. [[CrossRef](#)]
30. Kvamme, B.; Forrissdahl, O.K. Polar guest-molecules in natural gas hydrates. Effects of polarity and guest-guest-interactions on the Langmuir-constants. *Fluid Phase Equilib.* **1993**, *83*, 427–435. [[CrossRef](#)]
31. Kvamme, B.; Tanaka, H. Thermodynamic stability of hydrates for ethane, ethylene, and carbon dioxide. *J. Phys. Chem.* **1995**, *99*, 7114–7119. [[CrossRef](#)]
32. Kvamme, B. Feasibility of simultaneous CO₂ storage and CH₄ production from natural gas hydrate using mixtures of CO₂ and N₂. *Can. J. Chem.* **2015**, *93*, 897–905. [[CrossRef](#)]
33. Kvamme, B. Thermodynamic Limitations of the CO₂/N₂ Mixture Injected into CH₄ Hydrate in the Ignik Sikumi Field Trial. *J. Chem. Eng. Data* **2016**, *61*, 1280–1295. [[CrossRef](#)]
34. Aromada, S.A. New Concept for Evaluating the Risk of Hydrate Formation during Processing and Transport of Hydrocarbons. Master's Thesis, The University of Bergen, Bergen, Norway, 2017.
35. Svandal, A. Modeling Hydrate Phase Transitions using Mean-Field Approaches. Ph.D. Thesis, University of Bergen, Bergen, Norway, 2006.
36. Gibbs, J.W. *The Collected Works of J. Willard Gibbs, Thermodynamics*; Yale university Press: New Haven, CT, USA, 1928; Volume 1, pp. 55–353.
37. Soave, G. Equilibrium constants from a modified Redlich-Kwong equation of state. *Chem. Eng. Sci.* **1972**, *27*, 1197–1203. [[CrossRef](#)]
38. Mu, L.; Solms, N.V. Hydrate thermal dissociation behavior and dissociation enthalpies in methane-carbon dioxide swapping process. *J. Chem. Thermodyn.* **2018**, *117*, 33–42. [[CrossRef](#)]
39. Yang, S.O.; Cho, S.H.; Lee, H.; Lee, C.S. Measurement and prediction of phase equilibria for water+ methane in hydrate forming conditions. *Fluid Phase Equilib.* **2001**, *185*, 53–63. [[CrossRef](#)]
40. Lafond, P.G.; Olcott, K.A.; Sloan, E.D.; Koh, C.A.; Sum, A.K. Measurements of methane hydrate equilibrium in systems inhibited with NaCl and methanol. *J. Chem. Thermodyn.* **2012**, *48*, 1–6. [[CrossRef](#)]
41. Circone, S.; Kirby, S.H.; Stern, L.A. Direct measurement of methane hydrate composition along the hydrate equilibrium boundary. *J. Phys. Chem. B* **2005**, *109*, 9468–9475. [[CrossRef](#)]
42. Adisasmito, S.; Frank, R.J., III; Sloan, E.D., Jr. Hydrates of carbon dioxide and methane mixtures. *J. Chem. Eng. Data* **1991**, *36*, 68–71. [[CrossRef](#)]
43. Gayet, P.; Dicharry, C.; Marion, G.; Graciaa, A.; Lachaise, J.; Nesterov, A. Experimental determination of methane hydrate dissociation curve up to 55 MPa by using a small amount of surfactant as hydrate promoter. *Chem. Eng. Sci.* **2005**, *60*, 5751–5758. [[CrossRef](#)]
44. Nakamura, T.; Makino, T.; Sugahara, T.; Ohgaki, K. Stability boundaries of gas hydrates helped by methane—Structure-H hydrates of methylcyclohexane and cis-1, 2-dimethylcyclohexane. *Chem. Eng. Sci.* **2003**, *58*, 269–273. [[CrossRef](#)]
45. Lievois, J.S.; Perkins, R.; Martin, R.J.; Kobayashi, R. Development of an automated, high pressure heat flux calorimeter and its application to measure the heat of dissociation and hydrate numbers of methane hydrate. *Fluid Phase Equilib.* **1990**, *59*, 73–97. [[CrossRef](#)]
46. Gupta, A.; Lachance, J.; Sloan, E.D., Jr.; Koh, C.A. Measurements of methane hydrate heat of dissociation using high pressure differential scanning calorimetry. *Chem. Eng. Sci.* **2008**, *63*, 5848–5853. [[CrossRef](#)]

47. Fan, S.-S.; Guo, T.-M. Hydrate formation of CO₂-rich binary and quaternary gas mixtures in aqueous sodium chloride solutions. *J. Chem. Eng. Data* **1999**, *44*, 829–832. [[CrossRef](#)]
48. Wendland, M.; Hasse, H.; Maurer, G. Experimental pressure– temperature data on three- and four-phase equilibria of fluid, hydrate, and ice phases in the system carbon dioxide– water. *J. Chem. Eng. Data* **1999**, *44*, 901–906. [[CrossRef](#)]
49. Delahaye, A.; Fournaison, L.; Marinhas, S.; Chatti, I.; Petitot, J.P.; Dalmazzone, D.; Fürst, W. Effect of THF on equilibrium pressure and dissociation enthalpy of CO₂ hydrates applied to secondary refrigeration. *Ind. Eng. Chem. Res.* **2006**, *45*, 391–397. [[CrossRef](#)]
50. Fournaison, L.; Delahaye, A.; Chatti, I.; Petitot, J.P. CO₂ hydrates in refrigeration processes. *Ind. Eng. Chem. Res.* **2004**, *43*, 6521–6526. [[CrossRef](#)]
51. Sabil, K.M.; Witkamp, G.-J.; Peters, C.J. Estimations of enthalpies of dissociation of simple and mixed carbon dioxide hydrates from phase equilibrium data. *Fluid Phase Equilib.* **2010**, *290*, 109–114. [[CrossRef](#)]
52. Ohgaki, K.; Makihara, Y.; Takano, K. Formation of CO₂ hydrate in pure and sea waters. *J. Chem. Eng. Jpn.* **1993**, *26*, 558–564. [[CrossRef](#)]
53. Kvamme, B.; Aromada, S.A. Alternative Routes to Hydrate Formation during Processing and Transport of Natural Gas with a Significant Amount of CO₂: Sleipner Gas as a Case Study. *J. Chem. Eng. Data* **2018**, *63*, 832–844. [[CrossRef](#)]
54. Aromada, S.A.; Kvamme, B. Production of Methane from Hydrate and CO₂ Zero-Emission Concept. In Proceedings of the 10th EUROSIM2019 Congress, Logroño (La Rioja), Spain, 1–5 July 2019.
55. Kang, S.-P.; Lee, H.; Ryu, B.-J. Enthalpies of dissociation of clathrate hydrates of carbon dioxide, nitrogen, (carbon dioxide+ nitrogen), and (carbon dioxide+ nitrogen+ tetrahydrofuran). *J. Chem. Thermodyn.* **2001**, *33*, 513–521. [[CrossRef](#)]
56. Handa, Y. Compositions, enthalpies of dissociation, and heat capacities in the range 85 to 270 K for clathrate hydrates of methane, ethane, and propane, and enthalpy of dissociation of isobutane hydrate, as determined by a heat-flow calorimeter. *J. Chem. Thermodyn.* **1986**, *18*, 915–921. [[CrossRef](#)]
57. Deaton, W.; Frost, E., Jr. *Gas Hydrates and Their Relation to the Operation of Natural Gas Pipe-Lines*; US Bur. Mines Monograph 8; U.S. Department of Energy Office of Scientific and Technical Information: Oak Ridge, TN, USA, 1946.
58. Yoon, J.H.; Yamamoto, Y.; Komai, T.; Haneda, H.; Kawamura, T. Rigorous approach to the prediction of the heat of dissociation of gas hydrates. *Ind. Eng. Chem. Res.* **2003**, *42*, 1111–1114. [[CrossRef](#)]
59. Sloan, E.; Fleyfel, F. Hydrate dissociation enthalpy and guest size. *Fluid Phase Equilib.* **1992**, *76*, 123–140. [[CrossRef](#)]
60. De Roo, J.L.; Peters, C.J.; Lichtenthaler, R.N.; Diepen, G.A.M. Occurrence of methane hydrate in saturated and unsaturated solutions of sodium chloride and water in dependence of temperature and pressure. *AIChE J.* **1983**, *29*, 651–657. [[CrossRef](#)]
61. Roberts, O.L.; Brownscombe, E.R.; Howe, L.S.; Ramser, H. Phase diagrams of methane and ethane hydrates. *Petr. Eng.* **1941**, *12*, 56.
62. McLeod, H.O.; Campbell, J.M. Natural gas hydrates at pressures to 10,000 psia. *J. Pet. Technol.* **1961**, *222*, 590. [[CrossRef](#)]
63. Skovborg, P.; Rasmussen, P. Comments on: Hydrate dissociation enthalpy and guest size. *Fluid Phase Equilib.* **1994**, *96*, 223–231. [[CrossRef](#)]
64. Vlahakis, J. *The Growth Rate of Ice Crystals: The Properties of Carbon Dioxide Hydrate; A Review of Properties of 51 Gas Hydrates*; Washington U.S. Dept. of the Interior: Syracuse University, NY, USA, 1972; Volume 830, p. 14.
65. Galloway, T.J.; Ruska, W.; Chappellear, P.S.; Kobayashi, R. Experimental measurement of hydrate numbers for methane and ethane and comparison with theoretical values. *Ind. Eng. Chem. Fundam.* **1970**, *9*, 237–243. [[CrossRef](#)]
66. Uchida, T.; Hirano, T.; Ebinuma, T.; Narita, H.; Gohara, K.; Mae, S.; Matoto, R. Raman spectroscopic determination of hydration number of methane hydrates. *AIChE J.* **1999**, *45*, 2641–2645. [[CrossRef](#)]
67. Sum, A.K. Measurements of clathrate hydrates properties via Raman spectroscopy. In Proceedings of the 2nd International Conference on Natural Gas Hydrates, Toulouse, France, 2–6 June 1996; pp. 51–58.
68. Bozzo, A.T.; Hsiao-Sheng, C.; Kass, J.R.; Barduhn, A.J. The properties of the hydrates of chlorine and carbon dioxide. *Desalination* **1975**, *16*, 303–320. [[CrossRef](#)]



Graphic design: Communication Division, UIB / Print: Skjipes Kommunikasjon AS



uib.no

ISBN: 9788230868515 (print)
9788230853924 (PDF)